STRATIGRAPHY, SEDIMENTOLOGY, AND ORGANIC GEOCHEMISTRY OF THE LOWER JURASSIC SEDIMENTS FROM THE EASTERN ALBORZ RANGES, NORTH-EAST IRAN, WITH THE STUDY OF THEIR URANIUM CONTENT IN RELATION TO ORGANIC MATTER DISTRIBUTION

BY

FREYDOON KARIMZADEH RAD

B.Sc., M.Sc., D.I.C., F.A.G.I.

A THESIS SUBMITTED FOR THE DEGREE OF
DOCTOR OF PHILOSOPHY IN PETROLEUM GEOLOGY
UNIVERSITY OF LONDON

PETROLEUM GEOLOGY SECTION
DEPARTMENT OF GEOLOGY
ROYAL SCHOOL OF MINES
IMPERIAL COLLEGE OF SCIENCE & TECHNOLOGY
LONDON

DECEMBER 1979

TO MY FATHER

MOHAMMAD KARIMZADEH RAD

ABSTRACT

STRATIGRAPHY, SEDIMENTOLOGY, AND ORGANIC GEOCHEMISTRY OF THE LOWER JURASSIC SEDIMENTS FROM THE EASTERN ALBORZ RANGES, NORTH-EAST IRAN, WITH THE STUDY OF THEIR URANIUM CONTENT IN RELATION TO ORGANIC MATTER DISTRIBUTION

The Lower Jurassic Shemshak Formation is widely distributed in North, Central and East Iran. The outcrops of this Formation in the Eastern Alborz Ranges are studied in detail for the first time. With minor differences the lithostratigraphic units recognised can be correlated approximately with those of the type section in the Central Alborz, about 450 km to the west. The Shemshak Formation was deposited in a complex delta system with an embayed shore-line to the north during Early-Middle Jurassic time. An assemblage of foraminifera, reported for the first time, and other mollusca characterise an interval of shallow marine deposits, but the rest of the Formation is believed to consist of terrestrial and deltaic sediments.

The eastern extension of the Alborz borders the Kopet Dagh range to the north. The differences between the Shemshak Formation in the Alborz and the Kashafrud Formation in the Kopet Dagh suggest that the two regions were probably still separated in the Early Jurassic, following an earlier separation which is believed to have existed during Palaeozoic-Middle Triassic time.

Being of great thickness and regional extent, the Shemshak Formation is probably the most attractive source rock in the Eastern Alborz. A detailed geochemical analysis of outcrop samples from this Formation confirms that it is an immature source rock containing dominantly terrestrial organic matter and huminite kerogen. Nevertheless, the depth of burial of the Shemshak Formation in the Dasht-e Gorgan and the Southern Caspian depression suggests that it might have reached the level of thermal maturity required for the generation of hydrocarbons. Although the hydrocarbon generating potential of the sediments is relatively low, under favourable conditions this Formation could be capable of generating enough crude oil and gas to supply a giant field. The Shemshak Formation is presumably the source rock for the Khangiran gas field and for the Russian oil fields on the eastern coast of the Caspian Sea.

Although the gamma radiation of the Shemshak Formation is mainly due to uranium, the concentration of which averages about 4.5 ppm, there seems to be no relationship between the total organic carbon and uranium content of the rocks. The absence of economic uranium concentrations in the Formation is probably due to a lack of circulation of uranium in solution.

ACKNOWLEDGEMENTS

Above all the writer expresses his gratitude to Professor W.D. Gill for his initial encouragement, for suggesting the topic of my research, and for his supervision and guidance throughout the field and laboratory work.

This research would not have been possible without the encouragement and generous financial support of my father, to whom I remain deeply indebted and to whom this thesis is dedicated.

Substantial support from the Atomic Energy Organisation of Iran (AEOI), both financially and materially, made the field work possible. Within the AEOI, the writer is most indebted to Dr. A. Etemad (former managing director of AEOI) for granting this assistance and to Mr. M. Roohi for organising the field trips. My especial thanks are due to my former colleague Mr. S. Nikpour (geologist of AEOI) for his encouragement, assistance in the field and for compiling previous reports. The drivers Messrs. Tabrizi Nia, Khoddami and George (employees of AEOI) also deserve the writer's thanks for their assistance during the field work.

Special thanks are due to Dr. A. Afshar-Harb (chief geologist of NIOC) for his guidance and advice in the field.

The writer would like to take the opportunity to pay tribute to the people of the Shahpassand and Jajarm areas for their kindness, especially Mr. M. Ghelichlee from the village of Tilabad who provided great assistance during the entire field period.

At Imperial College, the writer is particularly indebted to Dr. R.R.F. Kinghorn for all his advice and guidance. The writer is also grateful to Mr. M. Rahman and Mr. R. Hodgekinson for their technical assistance. Professor R. Stoneley reviewed the text and made useful suggestions. The writer also

benefited from discussion with Dr. R.C. Selley concerning some sedimentological issues.

Among others at Imperial College, who rendered assistance to the writer or contributed to this study: Dr. M.A. Ala, Dr. M. Madani, Dr. M. Al-Gailani and Mr. S. Massoud, Miss G. Davies (Petroleum Geology Section), Mr. A. Brown and Mrs. E. Hin (Drafting team), Dr. C. Peat and Messrs. R. Giddens (from Micropalaeontology Section), R. Chatfield and F. Jones (from Geology Workshop), and Mrs. B. Jaworska; to all of those the writer is deeply grateful.

Professor Donovan of University College, London, identified and dated the ammonites collected, and the writer is sincerely grateful to him. The foraminifera were briefly studied at the Micropalaeontology Department of University College under the direction of Professor T. Barnard.

Mr. G.D. Borholt of the University of London Reactor Centre (the Reactor manager) kindly provided facilities and gave valuble advice on the delayed neutron activation analysis and the writer is also indebted to Mr. J. Herrington of the Atomic Weapon Research Establishment, who carried out uranium and oxygen analyses on a number of samples. Dr. Cooper of the Institute of Geological sciences is also thanked for his useful counsel and discussion concerning the uranium analysis.

Finally, the writer would like to express his sincere gratitude to his wife Shideh K. Rad for her continuous encouragement and patience, as well as for sacrificing her time and effort to type the thesis.

CONTENTS

ABSTRACT..... 3

ACKNOWLEDGEMENTS..... 4

LIST OF FIGURES AND ENCLOSURES..... 11

LIST OF TABLES..... 17

PART I GEOLOGY

Chapter 1 INTRODUCTION..... 19

1.1 Plan of Study..... 21

1.2 Access to the Shahpassand and the Jajarm Areas..... 22
1.2.1 Shahpassand Area 22
1.2.2 Jajarm Area 22

Chapter 2 GEOMORPHOLOGY 23

Chapter 3 REGIONAL GEOLOGY 26

3.1 Summary of Regional Geological History of Iran 27

3.2 Main Geological Zones in Iran 30
3.2.1 Alborz Belt 30
3.2.2 Kopet Dagh 31
3.2.3 Zagros Belt 32
3.2.4 Central Iran 33
3.2.5 Lut Block 34
3.2.6 Eastern Iranian and Makran Ranges 34

3.3 Iran as Part of Gondwanaland 35

3.4 South Caspian High 36

3.5 Some Implications of Plate Tectonic in Northern Iran 36

Chapter 4 STRATIGRAPHY OF THE SHEMSHAK FORMATION 43

4.1 Introduction 43

4.2 Stratigraphic Subdivisions 44
4.2.1 Lithounit 1 "Alternating Shale and Sandstone" 49
4.2.2 Lithounit 2 "Channel Sand Complexes"..... 49
4.2.3 Lithounit 3 "Carbonaceous Sequence"..... 51
4.2.4 Lithounit 4 "Lower Sandstone Member"..... 57
4.2.5 Lithounit 5 "Marine Shale"..... 59
4.2.6 Lithounit 6 "Upper Sandstone Member"..... 59

4.3 Formation Thickness and its Variation..... 60
4.3.1 Vertical Movements..... 60
4.3.2 Compressional Forces..... 62

4.4 Correlation of the Shemshak Formation of the Eastern Alborz with Type Section (Central Alborz)..... 64

4.5 Structural Features Associated with the Shemshak Formation..... 66
4.5.1 Intraformational Deformation..... 66
4.5.2 Faulting..... 69

Chapter 5 SEDIMENTOLOGY..... 72

5.1 Introduction..... 72

5.2 Sedimentology of the Shemshak Formation in the Eastern Alborz Area..... 73
5.2.1 Terrestrial Deposits..... 73
5.2.2 Marine Deposits..... 74
5.2.3 Associated Rocks..... 75

5.3 Palaeoclimate..... 78

5.4 Sedimentary Structures..... 79
5.4.1 Bedding..... 79
5.4.2 Channels..... 80
5.4.3 Cross Bedding..... 80
5.4.4 Current Ripple Marks..... 81
5.4.5 Ball and Pillow Structure (Pseudonodules)..... 81
5.4.6 Cone-in-Cone Structure..... 81
5.4.7 Nodules..... 81
5.4.8 Mud Cracks..... 85

5.5 Biogenic Sedimentary Structures..... 85

5.6 Fossils and Age..... 85
5.6.1 Megafossils..... 87
5.6.2 Microfossils..... 96

5.7 Depositional Environment and the Controlling Factors... 99

5.8 Sedimentary Basin and Palaeocurrents..... 103

PART II ORGANIC GEOCHEMISTRY AND SOURCE ROCK EVALUATION OF THE SHEMSHAK FORMATION

Chapter 1 SOURCE BED CONCEPT AND GENESIS OF PETROLEUM..... 109

1.1 Introduction..... 109

1.2 Characteristics of Source Rocks..... 113
1.2.1 Amount of Organic Matter..... 113
1.2.2 Type of Organic Matter..... 115
1.2.3 State of Maturation of Organic Matter..... 116

1.3 Kerogen and its Convertibility..... 121
1.3.1 Alginite..... 125
1.3.2 Sapropelite..... 125
1.3.3 Huminite..... 126
1.3.4 Inertinite..... 126

1.4 Transformation of Organic Matter in Sediments and Generation of Petroleum..... 127
1.4.1 Diagenesis..... 130
1.4.2 Catagenesis..... 130
1.4.3 Metagenesis..... 130

Chapter 2 FIELD WORK AND LABORATORY EXPERIMENTS..... 133

2.1 Introduction..... 133

2.2 Field Sampling and Preparation of Samples for Organic Geochemical Analysis..... 134
2.2.1 Sample Frequency..... 134
2.2.2 Pulverisation..... 135
2.2.3 Maceration..... 135

Chapter 3 AMOUNT AND TYPE OF ORGANIC MATTER..... 137

3.1 Optical Microscopic Description..... 137
3.1.1 Introduction..... 137
3.1.2 Procedures..... 138
3.1.3 Data..... 138
3.1.4 Results and Interpretation..... 138
3.1.5 Conclusions..... 145

3.2 Quantitative Elemental Analysis..... 149
3.2.1 Introduction..... 149
3.2.2 Procedures..... 152
3.2.3 Data..... 153
3.2.4 Results and Interpretation..... 153
3.2.5 Conclusions..... 158

3.3 Solvent Organic Extraction..... 158
3.3.1 Introduction..... 158
3.3.2 Procedures..... 161
3.3.3 Data..... 162
3.3.4 Results and Interpretation..... 162
3.3.5 Conclusions..... 169

3.4 Fractionation of Bitumen..... 169
3.4.1 Introduction..... 169
3.4.2 Procedures..... 171
3.4.3 Data..... 171
3.4.4 Results and Interpretation..... 171
3.4.5 Conclusions..... 172

3.5 Pyrolysis..... 172
3.5.1 Introduction..... 172
3.5.2 Procedures..... 179

3.5.3 Data..... 180
3.5.4 Results and Interpretation..... 180
3.5.5 Conclusions..... 184

3.6 Gas-Liquid Chromatography and Normal Alkanes Distribution..... 186
3.6.1 Introduction..... 186
3.6.2 Procedures..... 189
3.6.3 Data..... 197
3.6.4 Results and Interpretation..... 197
3.6.5 Conclusions..... 213

Chapter 4 STATE OF MATURATION OF ORGANIC MATTER..... 214

4.1 Pyrolysis-Elemental Analysis..... 214
4.1.1 Introduction..... 214
4.1.2 Procedures..... 217
4.1.3 Data..... 217
4.1.4 Results and Interpretation..... 217
4.1.5 Conclusions..... 217

4.2 Bitumen and its Compositional Fractions..... 218
4.2.1 Introduction..... 218
4.2.2 Procedures..... 219
4.2.3 Data..... 219
4.2.4 Results and Interpretation..... 219
4.2.5 Conclusions..... 225

4.3 Alkanes Distribution and Carbon Preference Index (CPI)..... 225
4.3.1 Introduction..... 225
4.3.2 Procedures..... 227
4.3.3 Data..... 227
4.3.4 Results and Interpretation..... 229
4.3.5 Conclusions..... 241

4.4 Carbonisation of Palynomorphs..... 241
4.4.1 Introduction..... 241
4.4.2 Procedures..... 242
4.4.3 Data..... 242
4.4.4 Results and Interpretation..... 242
4.4.5 Conclusions..... 244

Chapter 5 SUMMARY AND OVERALL CONCLUSIONS..... 251

Chapter 6 PETROLEUM PROSPECTS AND BASIN EVALUATION OF THE EASTERN ALBORZ REGION..... 254

6.1 Evaluation of the Shemshak Formation in the Eastern Alborz..... 257

Chapter 7 CONCENTRATION OF URANIUM IN RELATION TO ORGANIC MATTER DISTRIBUTION..... 260

7.1 Introduction..... 260
7.2 Present Study..... 261
7.3 Experimental..... 263
7.4 Results and Interpretation..... 265
7.5 Conclusions..... 269

REFERENCES..... 270

PERSONAL COMMUNICATIONS..... 281

LIST OF FIGURES

PART I

Fig.	I.1.1 -	Location map.....	20
"	I.1.2 -	River terrace deposits overlying the Shemshak Fm. near the village of Farsian (Shahpassand area).....	24
"	I.3.1 -	Map showing the main geological zones of Iran.	28
"	I.3.2 -	Hypothetical reconstruction of the Palaeo- and Neo-Tethys in Iran during Early-Middle Jurassic time.....	39
"	I.3.3 -	Late Triassic-Early Jurassic reconstruction of Pangaea and Tethys.....	41
"	I.3.4 -	A schematic cross section (XX') showing the subduction of the Palaeo- and Neo-Tethys under Central Iran at Early-Middle Jurassic time.....	42
"	I.4.1 -	Ammonites from the lowermost part of the Dalichai Fm. in the Shahpassand area (Qoznavi Section).....	45
"	I.4.2 -	Sketch cross sections through the Shemshak Fm. in the Eastern Alborz region.....	46
"	I.4.3 -	*Stratigraphic column of the Qoznavi Section...	LE
"	I.4.4 -	*Stratigraphic column of the Rudbar Section....	LE
"	I.4.5 -	*Stratigraphic column of the Jajarm Section....	LE
"	I.4.6 -	*Lithostratigraphic correlation chart of the Shemshak Fm. in the Eastern and Central Alborz	LE
"	I.4.7 -	"Alternating Shale and Sandstone" (Lithounit 1) from the lowermost part of the Shemshak Fm. in the Shahpassand area, north of the village of Qoznavi.....	50
"	I.4.8 -	Two channel sand units separated by a thin shale interval.....	52
"	I.4.9 -	Haematite balls in the "Carbonaceous Sequence" of the Shemshak Fm. (Shahpassand area).....	53
"	I.4.10-	Remnants of a haematite ball after intensive weathering.....	53

Fig. I.4.11- Fossilised plant remains..... 55

" I.4.12- The upper part of the "Carbonaceous Sequence" in the Rudbar Section overlain by the pebbly microconglomerates of the "Lower Sandstone Member" (appear as whitish bands)..... 56

" I.4.13- The upper part of the Shemshak Fm., Shahpassand area..... 58

" I.4.14- Middle-Upper Jurassic sediments in the Jajarm area..... 61

" I.4.15- Diagram showing the compaction effect of compressional stress on beds with different dip angles..... 63

" I.4.16- Sketch cross section between Rudbar and Nargess-Chall showing the basal low angle contact of the Shemshak Fm. with Triassic rocks..... 67

" I.4.17- Sketch cross section through the Shemshak Fm. along the road from Qoznavi to Nowdeh, showing intraformational folding..... 67

" I.4.18- Overturned beds in the basal part of the Shemshak Fm., northwest of the Qoznavi bridge (Shahpassand area)..... 68

" I.4.19- An example of intraformational folding in the Shemshak Fm. (Shahpassand area)..... 70

" I.4.20- Landslide showing a block of limestone slipped down slope over the Shemshak Fm..... 71

" I.5.1 - An iron oxide nodule from the Shemshak Fm..... 77

" I.5.2 - Lamination caused by thin coaly laminae in an argillaceous sandstone interval from Lithounit 2 of the Shemshak Fm..... 77

" I.5.3 - Current (asymmetrical) ripple marks, showing the direction of palaeocurrents to the north, Shahpassand area..... 82

" I.5.4 - Current ripple marks along the Shahpassand-Shahrud Road near the village of Rudbar..... 82

" I.5.5 - Asymmetrical ripple marks on a hand specimen from the Shemshak Fm..... 83

" I.5.6 - Pseudonodules of sandstone in a shale interval of the Shemshak Fm. near Shahpassand..... 83

" I.5.7 - Cone-in-cone structure from a calcareous siltstone horizon in the lowermost part of the Shemshak Fm. near the village of Rudbar..... 84

Fig. I.5.8 - Hand specimen from the basal part of the "Marine Shale" near Jajarm showing worm tracks and burrows..... 86

" I.5.9 - Hand specimen from the Shemshak Fm. showing a worm track..... 86

" I.5.10- Jurassic plant remains from the Shemshak Fm... 88

" I.5.11- Plant fossils collected from the Shemshak Fm.. 89

" I.5.12- Fauna collected from the "Marine Shale"..... 93

" I.5.13- Ammonites collected from the Shemshak Fm. near Jajarm..... 94

" I.5.14- Palynomorphs from the macerated kerogen concentrates of the Shemshak Fm..... 97

" I.5.15- Subenvironments of the subaerial delta deposits of the Shemshak Fm..... 100

" I.5.16- Block diagram illustrating the Shemshak Fm. lithostratigraphic units and the regional current direction..... 101

" I.5.17- Schematic diagram showing embayed delta plain of the Alborz during Early-Middle Jurassic time..... 104

" I.5.18- Development of the Shemshak Fm. under regional subsidence and late-stage marine transgression..... 105

PART II

Fig. II.1.1- The evolution path for different types of kerogen..... 112

" II.1.2- Geothermal evolution criteria..... 117

" II.1.3- n-paraffin distribution in sediments and crude oils..... 120

" II.1.4- Hydrocarbon maturity as shown by gas chromatography of alkanes..... 122

" II.1.5- Correlation of the coal rank and vitrinite reflectance scale with some other maturation indices and zones of petroleum generation..... 120

" II.1.6- Origin of organic sediments..... 124

" II.1.7- Time-temperature of petroleum genesis..... 128

" II.1.8- Origin of petroleum..... 124

" II.1.9- Maturation scheme of organic matter from the time of deposition to metamorphism..... 131

Fig. II.3.1 - Structured humic material from the Shemshak Formation..... 146

" II.3.2 - Oil rim round an organic grain in the macerated organic concentrate of sample no. 166..... 147

" II.3.3 - Fungi filaments in macerated organic concentrates..... 148

" II.3.4 - The kerogen evolution path and related vitrinite reflectance..... 151

" II.3.5 - A plot of the Shemshak Fm. samples showing their early diagenesis (surface and shallow specimens) in the kerogen evolution diagram.. 159

" II.3.6 - Relative composition of the Hydrocarbons generated from the main kerogen types in different basins..... 151

" II.3.7 - Extracted hydrocarbon concentration versus total organic carbon content of the Shemshak Fm. in the Eastern Alborz..... 173

" II.3.8 - Relative variation of C_R and C_T for different types of kerogen..... 176

" II.3.9 - Schematic representation of the pyrogram obtained by pyrolysis of rock samples..... 177

" II.3.10- An example of the pyrogram obtained by the pyrolysis method of Espitalié, et al. (1977). 178

" II.3.11- Total organic carbon before and after pyrolysis showing the average trend of the Shemshak Fm. in the Eastern Alborz..... 181

" II.3.12- The average C_R/C_T trends of the source rocks studied at the Petroleum Geology Section of Imperial College, London..... 182

" II.3.13- Weight percentage of carbon loss versus kerogen initial carbon content..... 185

" II.3.14- Comparison of bitumen composition of different source rocks..... 188

" II.3.15- Pyrograms of different coal macerals..... 190

" II.3.16- Gas chromatograms of the standard mixtures used for identification of the n-alkanes..... 193

" II.3.17- The distribution of n-alkanes in selected samples from the Qoznavi Section (Shahpassand area) and their corresponding CPI values..... 206

" II.3.18- The distribution of n-alkanes in selected samples from the Rudbar Section (Shahpassand

area) and their corresponding CPI values..... 207

Fig. II.3.19- The distribution of n-alkanes in selected samples from the Jajarm Section and their corresponding CPI values..... 208

" II.3.20- Normal C_{18}/C_{22} ratio and kerogen H/C ratio crossplot of the Shemshak Fm. samples from the Eastern Alborz region..... 211

" II.3.21- The pyrograms of the macerated samples, analysed by the pyrolysis-Gas chromatography method..... 212

" II.4.1 - The effect of thermal maturity on pyrogram of source rock and the corresponding production index $(S_1/S_1 + S_2)$..... 216

" II.4.2 - Variation of the hydrocarbon/organic carbon ratios of the Shemshak Fm. samples relative to their corresponding saturates/aromatic ratios..... 220

" II.4.3 - Total organic carbon-soluble extract crossplot showing the average trend of the Shemshak Fm. in the Eastern Alborz..... 222

" II.4.4 - The average trends of the source rock studied at the Petroleum Geology Section of Imperial College, in the organic carbon-soluble extract crossplot..... 223

" II.4.5 - Correlation of the amount of carbon loss as a result of pyrolysis at 500°C of mineral free kerogen concentrates and the quantity of their corresponding soluble organic extract of the immature Shemshak Fm..... 224

" II.4.6 - The distribution of n-alkanes in samples from the Kashafrud Fm. (Kopet Dagh) and their corresponding CPI values..... 230

" II.4.7 - Carbon preference index distribution of the Shemshak Fm..... 231

" II.4.8 - Variation of carbon preference index in the Shemshak Fm. relative to the reciprocal of concentration of saturates..... 232

" II.4.9 - Plot of carbon preference index versus the percentage of solvent organic extract of the Shemshak Fm. samples..... 233

" II.4.10- A comparison of the distribution of CPI in the Qoznavi and Rudbar Sections..... 234

" II.4.11- A comparison of the CPI distribution in the Shahpassand and Jajarm regions..... 236

Fig. II.4.12- Gas chromatogram showing n-alkane distribution in sample no. 133 from the Shahpassand area..... 237

" II.4.13- Gas chromatogram showing n-alkane distribution in sample no. 330 from the Jajarm area..... 238

" II.4.14- Gas chromatogram showing n-alkane distribution in sample no. 256 from the Shahpassand area..... 239

" II.4.15- Gas chromatogram showing n-alkane distribution in sample no. BMM from the Kashafrud Fm. of Kopet Dagh region..... 240

" II.4.16- Comparison of the colour of spores and pollen grains of the Shemshak Fm. at Shahpassand and Jajarm..... 245

" II.6.1 - Temperature gradient in the Gorgan area..... 256

" II.7.1 - Uranium content-total organic carbon (C_T) crossplot of the Shemshak Fm. in the Eastern Alborz region..... 268

LIST OF ENCLOSURES

*GEOLOGICAL MAP A, SHAHPASSAND AREA.....

*GEOLOGICAL MAP B, JAJARM AREA.....

* Loose Enclosures.

LIST OF TABLES

PART I

Table I.5.1 - The flora of the Shemshak Fm. in the Eastern Alborz..... 92

PART II

Table II.1.1 - Principal techniques used for source rock analysis and their degree of efficiency..... 114

" II.1.2 - Conversion factors for estimation of total organic matter from organic carbon content.. 114

" II.3.1 - Microscopic description of the kerogen concentrates..... 139

" II.3.2 - Quantitative elemental analysis results of the rock samples from the Shemshak Fm..... 154

" II.3.3 - Quantitative elemental analysis results of kerogen concentrates..... 156

" II.3.4 - Extraction and fractionation results..... 163

" II.3.5 - Pyrolysis results of the rock powders and kerogen concentrates..... 166

" II.3.6 - Column specification..... 191

" II.3.7 - Operating conditions..... 192

" II.3.8 - Relative concentration of n-alkanes in "A" standard solution..... 195

" II.3.9 - SSCF values for n-C_{15} to n-C_{30}..... 195

" II.3.10- n-alkane distribution data: normalised percentages..... 198

" II.3.11- Analytical GLC results..... 202

" II.4.1 - Carbon preference index..... 228

" II.4.2 - The colour of palynomorphs in relation to the state of maturation of the organic matter..... 242

" II.4.3 - The colour of spores and pollen in the Shemshak Fm. of the Estern Alborz..... 243

" II.7.1 - The uranium content of the Shemshak Fm. specimens..... 266

PART I

GEOLOGY

CHAPTER 1

INTRODUCTION

The mountain ranges of Iran form the Western Asian sector of the Alpine-Himalayan Orogen, connecting the Taurus and Caucasus Ranges to the west with the Hindukush and Himalayan mountain complex to the east. The Alborz Ranges in the north of Iran, form a broad east-west arc (convex to the south) around the Southern Caspian depression. They adjoin the Kopet Dagh mountains to the east and meet the NW end of the Zagros Ranges towards the west. The Kopet Dagh, which covers the boundary region between the northeastern part of Iran and Soviet Turkmanistan, in turn extends from the Alborz and the Caspian Sea in the west to the Afghanistan frontier in the east.

The area studied in this work covers the most eastern part of the Alborz Ranges where they meet the western end of the Kopet Dagh (Fig. I.1.1). As there is no distinct boundary between the two, the area may be regarded as the transition zone between the Alborz and the Kopet Dagh. The aim of this thesis is to clarify the geological relationships between the two ranges through a detailed study of the widespread Lower-Middle Jurassic sediments of the Shemshak Formation in the vicinity of the towns of Shahpassand and Jajarm. A review of their petroleum potential forms an important part of the thesis.

The Shemshak Formation was named after the village and the coal mines of Shemshak in the Central Alborz, by Assereto (1966). The type locality is north of Lazim-Gardaneh in the upper Ruteh Valley, in eastern part of the Shemshak coal mining district. The Shemshak Formation has been studied by different authors* mainly

* Goppert (1862) "Lower Lias Coal Beds"; Tipper (1921) "Jurassic Plant-bearing Series"; Riviere (1934) "Lias"; Beckett (1956) "Coal-bearing Series"; Bozorgnia (1964) "The Lagoonal Continental Lias"; and under the present name by: Lorenz (1964); Dellenbach (1964); Stoklin et al. (1965); Glaus (1965); Barnard (1965); Fantini Sestini (1966). The names are cited from Assereto (1966) and Assereto et al. (1968).

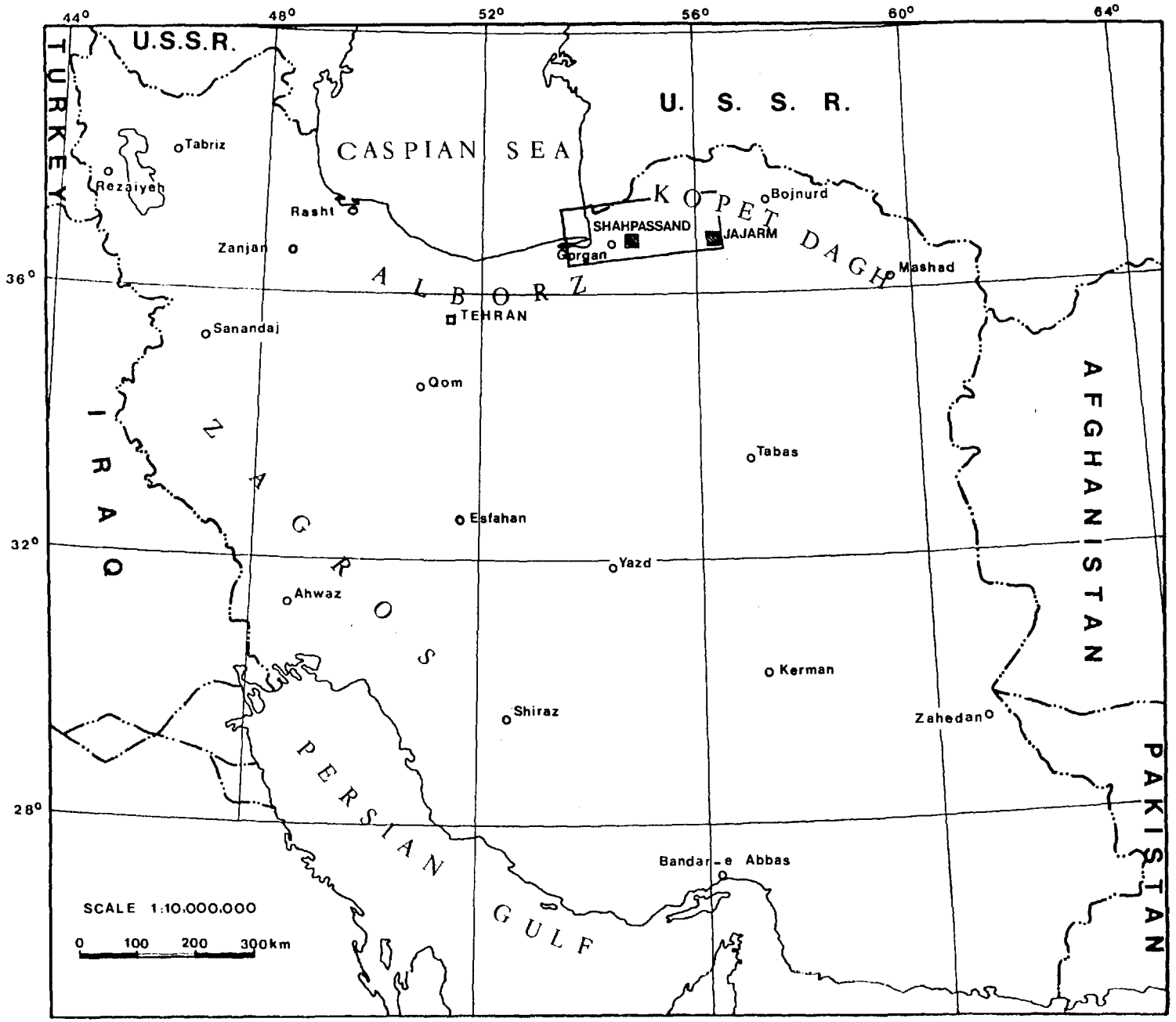


Fig. I.1.1 - Location map. Sections were measured in Shahpassand and Jajarm areas.

because of its economic coal-bearing character.

To the best of the writer's knowledge, no published account exists of the Shemshak Formation in the Shahpassand and Jajarm areas and this study represents the first detailed geological investigation of this formation in the Eastern Alborz region.

1.1 Plan of Study

As a first step, preliminary geological maps of the Shahpassand and the Jajarm areas were prepared, initially on enlarged topographic base maps of the two areas (from 1/250,000 to 1/50,000) and on the writer's geological interpretation of the aerial photographs (scale 1/50,000). These maps were corrected and supplemented by including geological data collected during subsequent field work (see Geological Maps A and B, loose).

Two periods of field work, each of about 2.5 months, were undertaken in the summers 1976 and 1977, during which 4 sections through the Shemshak Formation, and one from the Upper Devonian to Triassic, were measured. For each section, a column was drawn up showing the lithology, sedimentary structures including palaeocurrent indicators, the lateral extent of the beds, and the fossil content of the rocks. A cross-sectional sketch was also prepared. Altogether about 300 rock samples and a number of fossils were collected. A study was made of the larger scale features including the tectonics, structures such as faults and intraformational deformation, the geomorphology and the regional development of the basin. A gamma radiation survey of the area was carried out using a portable scintillometer. The samples collected were studied in more detail in the laboratory, where a brief examination was made of selected thin sections together with a study of grain size and fossil content. The stratigraphic columns were finalised and correlated.

A detailed source rock analysis was made of the samples from the Shemshak Formation. Measurements included the amount, type

and state of maturation of the organic matter by means of solvent organic extraction, fractionation, pyrolysis, elemental analysis, gas chromatography and maceration techniques.

A selection of samples was subjected to delayed neutron activation analysis at the University of London Reactor Centre, to determine their uranium content, in order to examin the possible effect of the organic matter on their uranium concentration.

1.2 Access to the Shahpassand and the Jajarm Areas

1.2.1 Shahpassand Area

Two main roads connect Tehran (the capital city) with the northeast of the country. The Haraz Road leads from the east of Tehran to the northern town of Amol through the Haraz Valley, and from there continues towards the east through the towns of Sari, Gorgan and Shahpassand. The town of Shahpassand is nearly midway between Tehran and the city of Mashad. From Shahpassand a secondary road goes south through the village of Khoshyeilaq to Shahrud. The second road, which is called the old Mashad Road, runs from the south of Tehran, close to the Tehran-Mashad railway along the northern edge of the Great Salt Desert, and passes through the towns of Semnan, Damghan, and Shahrud. The road between Shahpassand and Shahrud provides accessible exposures of sediments of Upper Devonian to Cretaceous age, overlain by Neogene conglomerates.

1.2.2 Jajarm Area

Access to the Jajarm area is by a secondary road which connects the village of Robat-e Gharabil, situated on the main Shahpassand-Mashad Road, with the town of Jajarm. The exposures are located about 15 km northeast of the town.

CHAPTER 2

GEOMORPHOLOGY

The Alborz mountains separate the arid Central Plateau of Iran from the semi-humid hinterland of the Caspian Sea. The northern flanks of the Alborz are mostly covered by dense forests, but across the Alborz from north to south, the vegetation decreases as the aridity increases and the rocks become relatively well exposed.

North and northwest of the town of Shahpassand, which stands at the foot of the northern foothills of the Alborz, extends the flat plain of Dasht-e Gorgan forming the eastern part of the Caspian depression. The whole Dasht-e Gorgan area is covered by the Neogene alluvium of the formerly more extensive Caspian Sea and its elevation ranges from -20m to 123m (topographic map of the area, 1972). The Gorgan River is the only river through this flat land and it flows from the east to the southeast corner of the Caspian Sea. To the north of the Gorgan River, near the Soviet border, old playalakes have left a few patches of salt crust.

Within the survey area the high Alborz mountains rise south of Shahpassand while their northern flanks being covered by dense vegetation. Further to the south across the mountains, as the vegetation decreases, the geology becomes better exposed. The Tilabad River, which rises in the foothills of the Tilabad mountain (east of the village of Tilabad; see Geological Map A, loose), cuts initially through the Upper Palaeozoic and Triassic rocks. The consequent stream pattern, well developed in the Shemshak Formation, provides the main tributaries of the Tilabad River. Here the river has widened its bank in a northwest direction and has left several terraces (Fig. I.2.1). The Shemshak Formation, which is composed mainly of terrestrial deposits, is less resistant to erosional processes than the adjacent rocks. It thus gives



Fig. I.1.2 - River terrace deposits overlying the Shemshak Fm. near the village of Farsian (Shahpassand area).

A) Terrace deposits.

B) Shemshak Fm.

rise to an impressive landscape with a remarkable drainage development and subsequent valleys, as well as landslides and superficial faulting as prominent features. Upper Palaeozoic and Triassic rocks form the elevated northern and southern margins to the outcrops of the Shemshak Formation, and within the basin Upper Jurassic and Cretaceous carbonates also form ridges. The Great Salt Desert of Central Iran laps onto the Palaeozoic exposures farther to the south.

In the Jajarm area (about 120 km east of the Shahpassand area) the geomorphological expression is very similar. The Shemshak Formation is bounded by high ridges of Upper Palaeozoic and Triassic rocks to the south and by ridges of Upper Jurassic-Cretaceous to the north. The quartzose and greywacke beds in the lower part of the Shemshak Formation also stand out as ridges, whilst a big gorge has been cut through the middle marine interval. The hills of the Jajarm area fall away southwards and become buried under the Great Salt Desert of Central Iran.

CHAPTER 3

REGIONAL GEOLOGY

The Iranian Ranges form a part of the Alpine-Himalayan Orogen of Southwestern Asia. Early geological studies in Iran were largely confined to the Zagros mountains because of their petroleum potential, but also extended to the Alborz Ranges because of interest of Mount Damavand, which is an extinct Quarternary volcano in their centre and is the highest mountain in Southwest Asia (5,670 m). The central part of the country, between the Alborz and the Zagros, did not attract much attention from geologists during the early years, partly because of its rather difficult accessibility. However, Stahl (1911) discovered some metamorphic rocks in Central Iran and assigned a Precambrian age to them. The later discovery of the metamorphic complexes along the Zagros Thrust by British Petroleum geologists supported the concept of a Precambrian metamorphic massif in Central Iran. Boeckh et al. (1929) established the idea of a "Median Mass" and the country was thereafter subdivided into three geological zones: the Zagros in the south and west, the Alborz in the north, and the Median Mass in central region. Systematic studies undertaken by the Iranian Oil Company geologists in the 1950s revealed a different tectonic picture of Central Iran and the idea of a Median Mass was rejected. Gansser (1955) and Mostofi et al. (1959) described Central Iran as an intensely folded region having undergone Alpine orogenic movements. This new concept was subsequently confirmed by Huckriede et al. (1962), Stöcklin (1968) and others. The National Iranian Oil Company (1959) summarised these new data on the Geological Map of Iran (scale 1/2,500,000). Later regional studies by geologists of the Geological Survey of Iran (GSI) and the National Iranian Oil Company (NIOC) have revealed the fundamental geological framework of the whole country and have led to a more detailed geological subdivision of Iran.

3.1 Summary of the Regional Geological History of Iran

The oldest known orogenic movements that affected most of Iran are related to the "Assyntic Orogeny" (Stöcklin, 1968), marked by an unconformity between the Precambrian rocks and Infracambrian sediments. Argillaceous-siliceous sediments and metamorphic complexes with local granite intrusions are the main constituents of the Precambrian basement rocks in Iran. They are more or less similar to the Arabian Shield basement rocks and may be considered as their northeast extension. In Northern and Central Iran an Infracambrian sequence of coloured shales and sandstones, massive dolomite and limestone with possible stromatolites overlies the Precambrian basement with unconformity. This laterally persistent sequence includes a saline formation north of Kerman (Stöcklin, 1968) and may be correlated with the Hormuz Salt Formation of Southern Iran.

The distribution of the Hormuz Salt plugs is limited by the "Oman Line" towards the east and by the "Qatar-Kazerun Line" towards the west, both trending north-south, while the northern boundary of these salt diapirs is the "Main Zagros Thrust" striking northwest-southeast (Fig. I.3.1). Thus the structural elements of southern Iran, which are believed to have controlled the distribution of the Hormuz Salt, have been active during Infracambrian time (Stöcklin, 1968). Since the Oman Line and the Main Zagros Thrust Line also had a major structural expression during the Mesozoic and Tertiary orogenic movements, one may speculate that these deep-seated faults originated in the Precambrian Assyntic Orogeny (Stöcklin, 1968) and since then have affected sedimentation and structural developments throughout the eastern and the southwestern parts of the country.

The Infracambrian sequence is transitionally overlain by the arkosic Lalun Sandstone (Assereto, 1963) almost everywhere throughout the country and the adjacent depositional basins. Overlying the Lalun sandstone are fossiliferous Cambrian beds (containing trilobites), and epicontinental, lagoonal, and

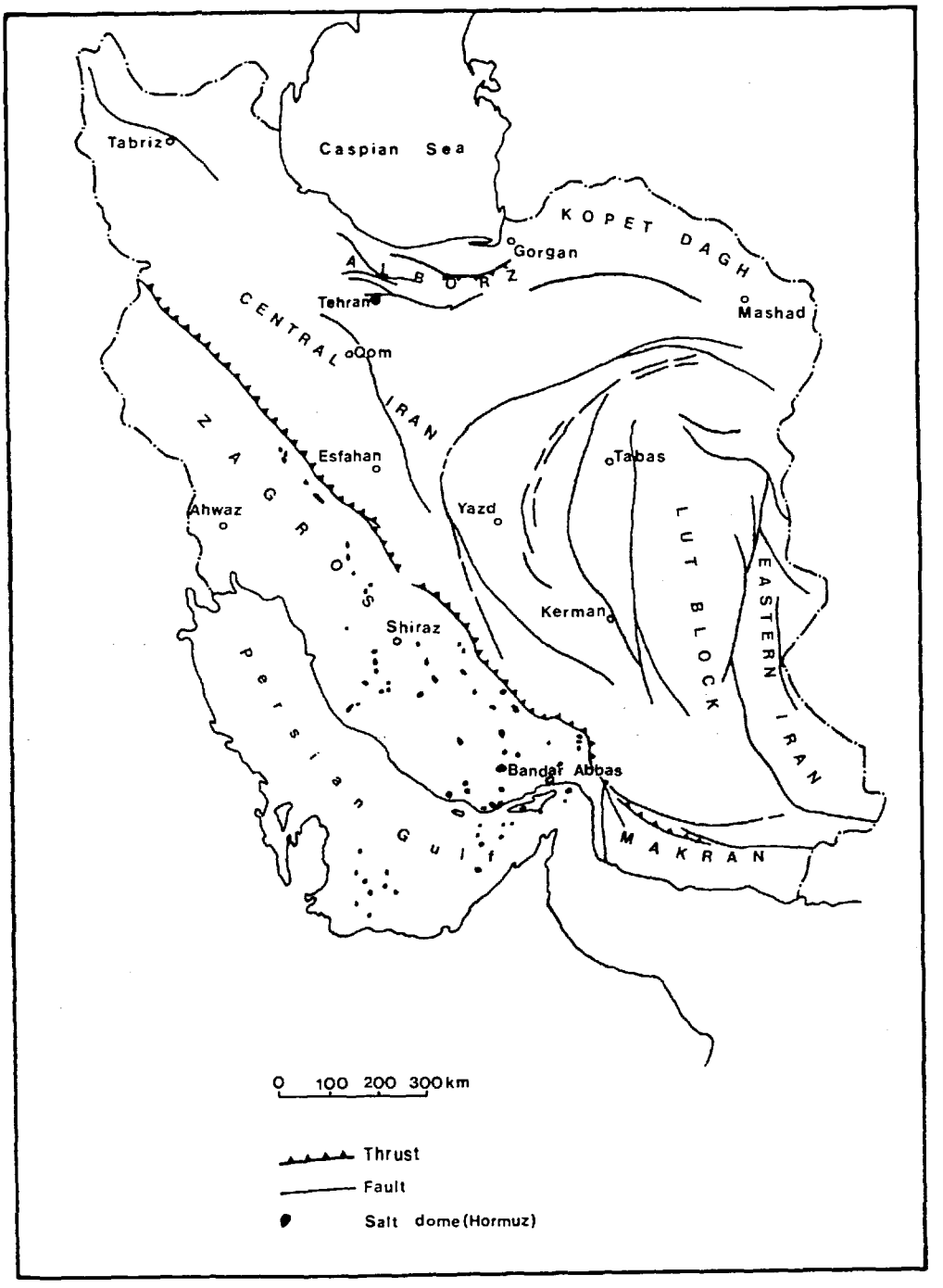


Fig. I.3.1 - Map showing the main geological zones of Iran. The distribution of the Hormuz salt domes is limited by the main Zagros thrust to the north (After GSI, 1970).

terrestrial Palaeozoic deposits. From the Infracambrian up to Middle Triassic time no distinct orogenic movements occurred in Iran (Gansser, 1955; Assereto, 1963; Stöcklin et al., 1964; and Ruttrie et al., 1968) and only epeirogenic movements, possibly an expression of the Caledonian and Hercynian orogenies of adjacent Euro-Asian areas, appear to have been responsible for sedimentary gaps and facies changes.

The first regional tectonic event after this long period of calm was in post-Middle Triassic/pre-Jurassic time (Stöcklin et al., 1971), when mainly epeirogenic movements caused violent thickness variations in the Lower Jurassic sediments. An unconformity/or disconformity, commonly associated with a thin layer of laterite or bauxite, exists between the Triassic and Liassic sediments in Northern and Central Iran. The Late Triassic movements resulted in a regional regression of the Permian-Triassic sea from the area northeast of the Main Zagros Thrust, while shallow marine sedimentation continued in the Zagros trough to the southwest. According to Stöcklin (1968) the most important result of the Late Triassic movements in Iran was the splitting of the Palaeozoic platform along the Main Zagros Thrust.

Late Jurassic and Late Cretaceous to Early Palaeocene tectonic movements caused some folding and faulting with angular unconformities throughout Central Iran, but in the Alborz these disturbances are expressed only as disconformities. Late Jurassic movements were accompanied by granite intrusions and slight metamorphism in some places (e.g. Hamadan phyllites, Stöcklin et al., 1971), whereas Late Cretaceous tectonic disturbances were associated with the formation of ophiolite-radiolarite complexes and flysch-type sediments. In both the Zagros and the Kopet Dagh basins, sedimentation continued without serious interruption until the late Alpine orogenic phases. Widespread volcanic activity in Eocene times affected much of Central, North, and Eastern Iran.

Strong phases of the Alpine Orogeny during the Oligocene, caused strong folding and, thus, a regional unconformity in

Central Iran. Meanwhile elevation occurred in the Alborz and a thick sequence of molasse sediments was deposited in its southern zone. The Zagros trough and the Kopet Dagh basin were less affected by these movements and remained relatively calm until the Miocene. The most important Alpine movements, that eventually affected almost the whole country, occurred during Miocene to Pleistocene times, terminating the miogeosynclinal sedimentation of the Zagros and the Kopet Dagh and virtually outlining the present structure of Iran. The late Alpine tectonism raised the entire Zagros Ranges with considerable crustal shortening along the Zagros Thrust Zone (Falcon, 1967) and formed the present structure of the Kopet Dagh Ranges. Folding, faulting and further elevation represented these movements in the Alborz and Northern Iran. Postorogenic molassic deposits, including conglomerates and freshwater deposits, accumulated in newly formed basins during the Quarternary period.

3.2 Main Geological Zones of Iran

Systematic geological studies in Iran have been carried out by interested oil companies (e.g. NIOC and OSCO), the Geological Survey of Iran, and some academic establishments. Gansser (1955) divided the country into three zones according to their structural trends, Stöcklin (1968) distinguished ten structural zones with different tectonic styles in Iran, and Takin (1972) identified some microcontinental plates in the area. However, as far as available knowledge permits, six main geological zones with different structural and sedimentary histories are recognised in this thesis (Fig. I.3.1).

3.2.1 Alborz Belt

The Alborz Ranges form the most northerly tectonic zone of Iran and display perhaps the most complete stratigraphic succession in the country from Precambrian to Quarternary. Several sedimentary

hiatuses are nevertheless present. The sedimentary sequences are miogeosynclinal; eugeosynclinal elements have not been identified. Structurally and stratigraphically the Alborz, especially near its southern margin, is closely related to Central Iran (Stöcklin, 1968; Gansser, 1969). Compressional deformation can be related to the Precambrian "Assyntic Orogeny" and to Mesozoic-Tertiary "Alpine Orogeny". The "Hercynian" (Variscan) and "Caledonian" orogenies are expressed only by sedimentary gaps in the Palaeozoic sequence, due to epeirogenic movements. The timespan from Infracambrian to Upper Triassic is represented by mainly uniform miogeosynclinal sediments.

The distinctive Precambrian basement rocks of the Gorgan High are probably an expression of a "South Caspian High", which provided the source area for Palaeozoic and Early Mesozoic sediments and was apparently responsible for the east-west trend of the Alborz belt (Stöcklin, 1974a). In the Late Triassic, the sedimentary environment changed when the "South Caspian High" subsided into an east-west trending trough. The Jurassic and Cretaceous deposits of this trough, which occupied the northern flank of the present Alborz belt, are much thicker than the corresponding deposits of the southern area (Stöcklin, 1974a). The Late Cretaceous-Early Palaeocene movements uplifted the Central core of the Alborz belt and were followed by a rapid subsidence of the southern margin and accumulation of a thick sequence of Eocene volcanogenic rocks. The later Middle Oligocene movements led to a further elevation of the central part, as well as to subsidence of both sides of the belt where thick molassic sediments were deposited. The last important tectonic event in the region occurred during the Plio-Pleistocene interval: further elevation and finally Quarternary volcanism (Mount Damavand) completed the present structure of the Alborz.

3.2.2 Kopet Dagh

The Alborz Ranges merge into the Kopet Dagh towards the east with no distinct boundary. Before the discovery of nearly complete

Palaeozoic successions in Robat-e Gharabil, Ghelli and Jajarm by Brice et al. (1973) and Afshar-Harb (1979), the Kopet Dagh was regarded as a Mesozoic-Tertiary basin. These Palaeozoic successions are located along the southern margin of the Kopet Dagh basin where the Mesozoic cover is relatively thin. Some trilobites of Silurian age were found at Robat-e Gharabil and Ghelli by Afshar-Harb in a sequence related to the Niur Formation of East-Central Iran. These rocks are so similar to the Palaeozoic rocks of the Alborz and Central Iran that Afshar-Harb described them under the same formation names (except for the Ghelli Formation). Whether these exposures should be considered as belonging to the Kopet Dagh or to the eastern extension of the Alborz Ranges is an arbitrary issue.

The oldest sedimentary exposures that had previously been reported from the region were some coal- and ammonite-bearing Triassic sediments, underlain by unidentified rocks, in the Aqdarband Uplift in the easternmost part of the Kopet Dagh. Jurassic sediments overlie the folded Triassic at Aqdarband with a sharp angular unconformity (Stöcklin, 1974b; Madani, 1977). A thick succession of Mesozoic-Tertiary sediments was deposited above this unconformity surface in a subsiding trough which was initiated after the Late Triassic movements (Stöcklin, 1974a).

What distinguishes the Kopet Dagh from the Alborz and Central Iran is its more or less continuous sedimentation and lack of volcanic activity during the Mesozoic and Tertiary. The latest Alpine orogenic movements of Plio-Pleistocene age ended the miogeosynclinal sedimentation in the area and uplifted the Kopet Dagh Ranges.

3.2.3 Zagros Belt

The Zagros belt forms the southern margin of the Alpine-Himalayan orogenic system in Iran. The main Zagros Thrust, trending northwest-southeast, has been a major structural feature in the geological history of the Zagros belt. This deepseated

fault zone originated probably in Precambrian time and later, during the Infracambrian, controlled the distribution of the Hormuz Salt (Stöcklin, 1968). The regional stratigraphic evidence suggests a more or less uniform depositional environment throughout the entire coutry from Palaeozoic to Early Triassic time. Since the Late Triassic movements, however, the Main Zagros Thrust has acted as an important tectonic divide between the steadily subsiding trough of the Zagros and Central Iran to the northeast. During later Triassic to Plio-Pleistocene time, sedimentation was nearly continuous in the Zagros trough and disconformities indicate episodes of epeirogenic movements. Nevertheless, from the Late Cretaceous onwards, tectonic movements associated with the line of the Zagros Thrust caused sharp facies and thickness changes in the Palaeocene, Eocene and Oligocene sediments of the inner part of the Zagros belt (James and Wynd, 1965): ophiolite and clastic flysch deposits indicate important Late Cretaceous-Palaeocene movements. The present Zagros Ranges were uplifted by Mio-Pliocene and Plio-Pleistocene orogenic movements, which were associated with a considerable crustal shortening and major underthrusting beneath Central Iran. The salt intrusions of Southern Iran are remarkable structural features, but their role in the formation of the Zagros fold pattern is not exactly known, although the substructure of salt is believed to have acted as a zone of detachment during the folding (Falcon, 1974).

The Sanandaj-Sirjan belt, which occupies the adjacent area of Central Iran to the northeast, is morphologically part of the northwest trending Zagros Range, although the structural history of this belt is much more similar to that of the central and north Iranian tectonic provinces than it is to the Zagros (Stöcklin, 1968), where for example Tertiary volcanism was absent. The geology of this zone, however, is still not fully understood.

3.2.4 Central Iran

The triangular area which is limited by the Alborz, the Zagros, and the Lut Block is referred to as Central Iran. The

geological history of the area is in general similar to that of the Alborz belt, although tectonic activity was higher during Mesozoic and Tertiary times. The Palaeozoic of Central Iran is characterised by epicontinental deposits, like the rest of the country. Since the Late Triassic, Alpine tectonic movements have folded the sediments of this region and have left several angular unconformities, as well as localised ophiolite-radiolarite complexes. The part of the area which subsequently developed into the present Great Salt Desert underwent a rapid subsidence in post- Miocene times and is marked by a thick sequence of both continental and shallow marine deposits.

3.2.5 Lut Block

The Lut Block is a north-south trending rigid mass in Eastern Iran, lying south of the Kopet Dagh region. It is covered mostly by sand dunes, loess, and Palaeogene volcanic rocks (Gansser, 1969). The Lut Block is associated with a conspicuous fault system on its western side which more or less follows the trend of the "Oman Line". This complex fault regime is probably the reason for the stability of the Lut Block, by absorbing the tangential stresses along the fault planes. The main features of this tectonically stable block are a relatively thin Palaeozoic and a thick Mesozoic sedimentary sequence which are subhorizontal and unfolded (Stöcklin, 1968). Overlying these sedimentary rocks are Tertiary volcanics. The possible northward movement of this block, through not fully understood processes, may be the reason for the arcuate structural trends of the Kopet Dagh.

3.2.6 Eastern Iranian and Makran Ranges

The stable structural mass of the Lut Block is bounded towards the east by highly mobile north-south aligned mountain ranges occupying the most eastern part of Iran. The rocks are composed mainly of Upper Cretaceous "coloured melange" overlain

by intensely folded Eocene marine flysch deposits (Stöcklin, 1968). The east-west trending Makran Ranges of the Southwest Iran reveal a very similar character to the eastern ranges. They abut westward against the "Oman Line", which separates them from the Zagros belt. The Eastern Iranian and Makran Ranges converge in the southeast corner of the country and can be considered part of the Baluchistan-Indus Ranges of Pakistan (Stöcklin, 1968).

3.3 Iran as part of Gondwanaland

A review of the literature of Southwest Asia leads to the conclusion that, until the Triassic, Arabia and Central Iran formed a continuous continental block. Isotope data suggest a similar age-range for both the Arabian and Iranian basement rocks, and there is a remarkable uniformity in the Palaeozoic shelf sediments across Iran (Stöcklin, 1974b).

This Arabian-Iranian platform has been regarded as the northern margin of the vast southern continent of Gondwanaland (Takin, 1972). Palaeomagnetic data suggest that it was separated from Eurasia by an elongate ocean, extending across southern Asia (Stoneley, 1974) and referred to as the Palaeotethys, or northern Tethys, ocean.

The evidence further suggests that, following initial fracturing in the Permian, a second ocean appeared in the Triassic within the Arabian-Iranian platform, along the line of the Zagros Thrust Zone. This has been called the Neotethys, or southern Tethys, ocean. Central Iran thus became a separate continental block which was later welded onto Eurasia through the closure of the Palaeotethys. The data of this collision and the position of the line of closure, form one of the objects of the present study and are discussed below. The formation of the Alborz Ranges was a younger, Tertiary, event.

The Neotethys in turn was closed again in the Cainozoic,

through the collision of the Arabian continent with Central Iran, leading to the compression and uplift of Zagros mountain ranges.

3.4 "South Caspian High"

The Infracambrian and the Lower Palaeozoic deposits of Iran wedge out northwards towards the metamorphic basement exposures on the northern flanks of the Alborz (Gorgan High). Here the basement rocks are directly overlain by Upper Palaeozoic or Mesozoic rocks (Stöcklin, 1974b). This important hiatus suggests the existance of an elevated "South Caspian High" during the early geological history of the Alborz. Local Precambrian basement rocks in the northern foothills of the Alborz, such as Gorgan schists, Alamkuh metamorphics and more recently discovered metamorphic rocks southwest of Rasht (Davies et al., 1972), are suggested to be the possible remnants of this reputed "South Caspian High".

If the metamorphic rocks of Southwest Mashad, in Northeast Iran, are Precambrian/or Early Palaeozoic in age as speculated by Stöcklin (1974b), it becomes possible that the "South Caspian High" extended farther eastwards and that it perhaps formed part of the dividing zone between the eastern extension of the Alborz to the south and the Kopet Dagh to the north.

3.5 Some Implications of Plate Tectonics in Northern Iran

The metamorphic rocks of Southwest Rasht and Mashad, suggested to belong to the "South Caspian High", are associated with relatively narrow ophiolite zones (Stöcklin, 1974b). These widely separated ophiolite exposures, and the oceanic crust possibly underlying the thick Mesozoic sediments of the south Caspian depression (Russian seismic data, cited in Stöcklin, 1974b), lead to the speculation that the Palaeotethys ocean, which separated Central Iran from Eurasia, was situated to the

north of the present Alborz Ranges and probably north of the pre-existing "South Caspian High". Stöcklin (as above) suggested that the Late Palaeozoic Palaeotethys closed along this zone in Late Triassic time by northwards subduction beneath the Scytho-Turanian continental plate.

Although the scarcity of surface geological evidence, together with a lack of subsurface data, does not permit the precise identification of the suture(s) or of the ancient continental margins in Northern Iran, some support for the earlier separation of the two continental blocks can be found in the area north of the Alborz.

The Permo-Triassic rocks of the Aqdarband Uplift (east of Mashad), in the eastern extremity of the Kopet Dagh, show some similarity to the post-Hercynian deposits of the Russian "Turan Plataeu" (Stöcklin, 1974b). These rocks are quite different from the Permo-Triassic sequence of the Alborz and the rest of Iran which are mainly shallow marine carbonates. The Jurassic rocks in Aqdarband overlie the Permo-Triassic sequence with a pronounced angular unconformity, as also reported from the Turanian Plate(Stöcklin, 1974b), whilst in the Alborz and the rest of Iran this boundary is a disconfromity. One, may thus conclude that the Kopet Dagh region formed part of the shelf of Eurasia, possibly separated from the Alborz, during Triassic and perhaps Late Palaeozoic time. Stöcklin (as above) supported his suggestion of Palaeotethys closure during Late Triassic by referring to the extension of the Jurassic Asiatic flora throughout northern Iran and the Turan Plate, as noted originally by Assereto et al. (1968). However, the use of flora for such purposes is unreliable and anyway the correlation table given by Assereto et al. does not show the Central Alborz and Turkmenija floras to be identical.

In the Alborz region the Lower-Middle Jurassic Shemshak Formation immediately overlies the Upper Triassic disconformity and is composed predominantly of terrestrial deposits. The Kashafrud Formation in the eastern Kopet Dagh and Aqdarband area

was formerly considered to be the equivalent of the Shemshak Formation, because of its stratigraphic position above the Upper Triassic unconformity and its apparently similar lithology. The sedimentological study of this formation by Madani (1977), however, showed it to be of turbidite facies and proved that the Shemshak and the Kashafrud Formation are not in fact analogous. In addition, the dating of the ammonites from the Kashafrud Formation proved it to be Late Bajocian-Bathonian in age, indicating that, in contrast to the Alborz, no Lower Jurassic rocks (Lias) are present in the Kopet Dagh. Moreover, the Kashafrud Formation starts with a fossiliferous basal conglomerate (Stöcklin, 1971) which is not present at the base of the Shemshak Formation; and two intervals of turbidites indicate a deep marine environment for the Kashafrud Formation (depth of 1,000m; Madani, 1977), whereas deep sea deposits are completely unknown in the Shemshak Formation. Finally, the results of geochemical analyses suggest that the types of organic matter and the thermal histories of the two formations are different (see part II of this thesis and Madani, 1977).

These remarkable differences between the Jurassic sediments of the Alborz and the Kopet Dagh allow one to suppose that the two regions were separated from each other, not only during the Late Palaeozoic and Triassic, but also in the Jurassic and perhaps later. The Late Triassic movements, therefore, although caused the separation of Afro-Arabia from Central Iran along the Zagros Thrust Zone, do not appear to have coincided with the closure of the preexisting Palaeotethys in the north (Fig. I.3.2). The time of closure of this Palaeotethys, which separated Central Iran from Eurasia, is not known precisely, but it appears to have been post-Middle Jurassic, or perhaps even Late Cretaceous, when the Alpine Orogeny is believed to have begun in the Alborz and Central Iran. The oceanic crust of the south Caspian depression might suggest that the ocean did not close uniformly along its length.

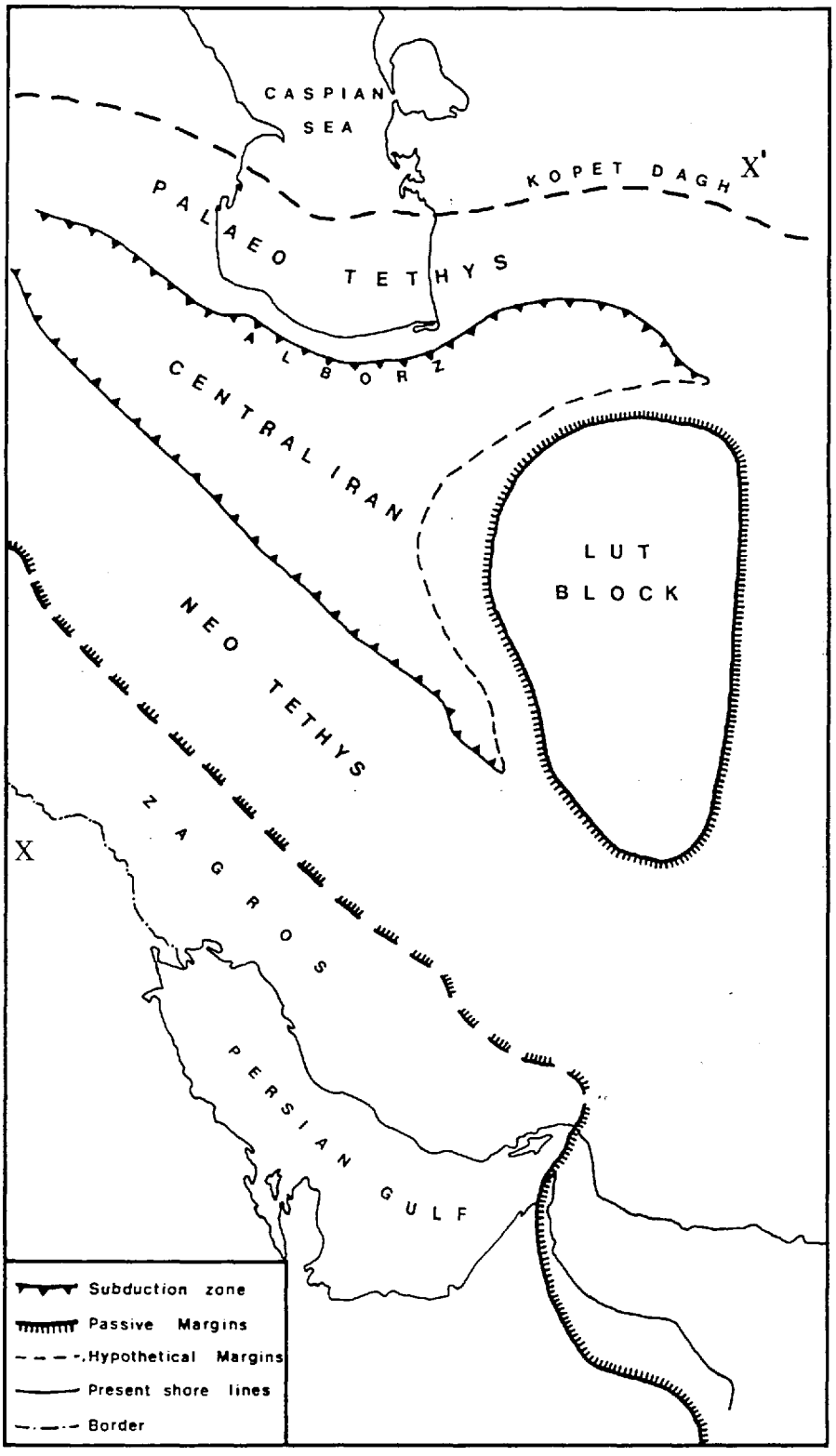


Fig. I.5.2 - Hypothetical reconstruction of the Palaeo- and Neo-Tethys in Iran during Early - Middle Jurassic time. The width of the oceanic troughs are conjectural. X-X shows the line of the section illustrated in Fig. I.5.1.

The supposed post-Middle Jurassic closure of Palaeotethys was probably not accomplished by northwards subduction under the Kopet Dagh and Scytho-Turanian continental plate, as suggested by Stöcklin (1974b), because there is no evidence of regional folding or of compressive deformation in the Kopet Dagh basin between Late Triassic and post Miocene (Afshar-Harb, 1979). This is supported by Şengör's statement (1979), on a regional basis, that the Palaeotethyan orogen was probably north-facing with a south-dipping subduction zone beneath Central Iran (Fig. I.3.3). The Alborz Ranges have steep northwards thrusting on their northern margin (Stöcklin, 1968), illustrated clearly on the recent Geological Map of Iran (NIOC, 1978). This thrust zone may be an expression of part of the suture of the Palaeotethys, which is suggested to have been subducted under the Alborz and Central Iran during its closure.

Acceptance of these suggestions would imply that both the Palaeo- and Neo-Tethys were closed by subduction beneath Central Iran, which also included the present Alborz Ranges, during the general relative movement towards each other of Afroarabia and Eurasia (Fig. I.3.4). Although the closure of the northern ocean was probably completed some time before that of the southern one, this hypothesis could account for the greater mobility of Central Iran as a result of compression from both north and south.

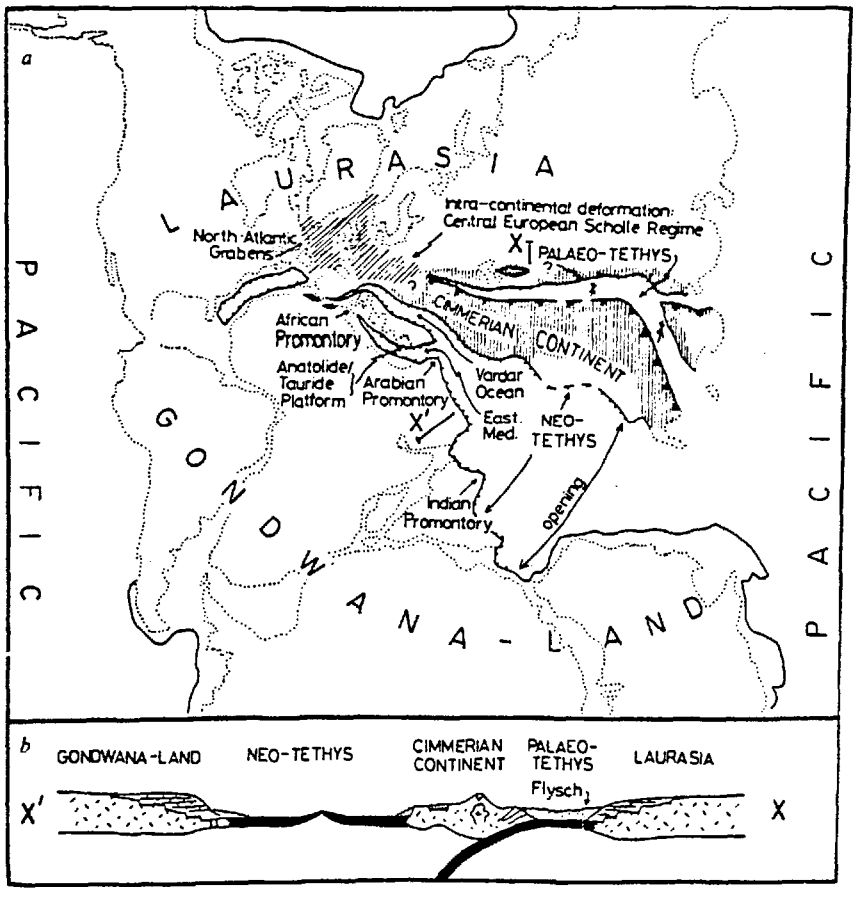


Fig. I.3.3 - Late Triassic-Early Jurassic reconstruction of Pangaea and Tethys. Obliquely ruled areas are regions of complex intracontinental extension inferred to have been partially related to the closure of Palaeo-Tethys. Lines with black triangles are subduction zones with the triangles on the upper plate. Lines with short hachures represent passive continental margins. Dotted lines are the present continental shore-lines put in for reference. XX' indicates the location of the cross section shown in b (after Şengör, 1979).

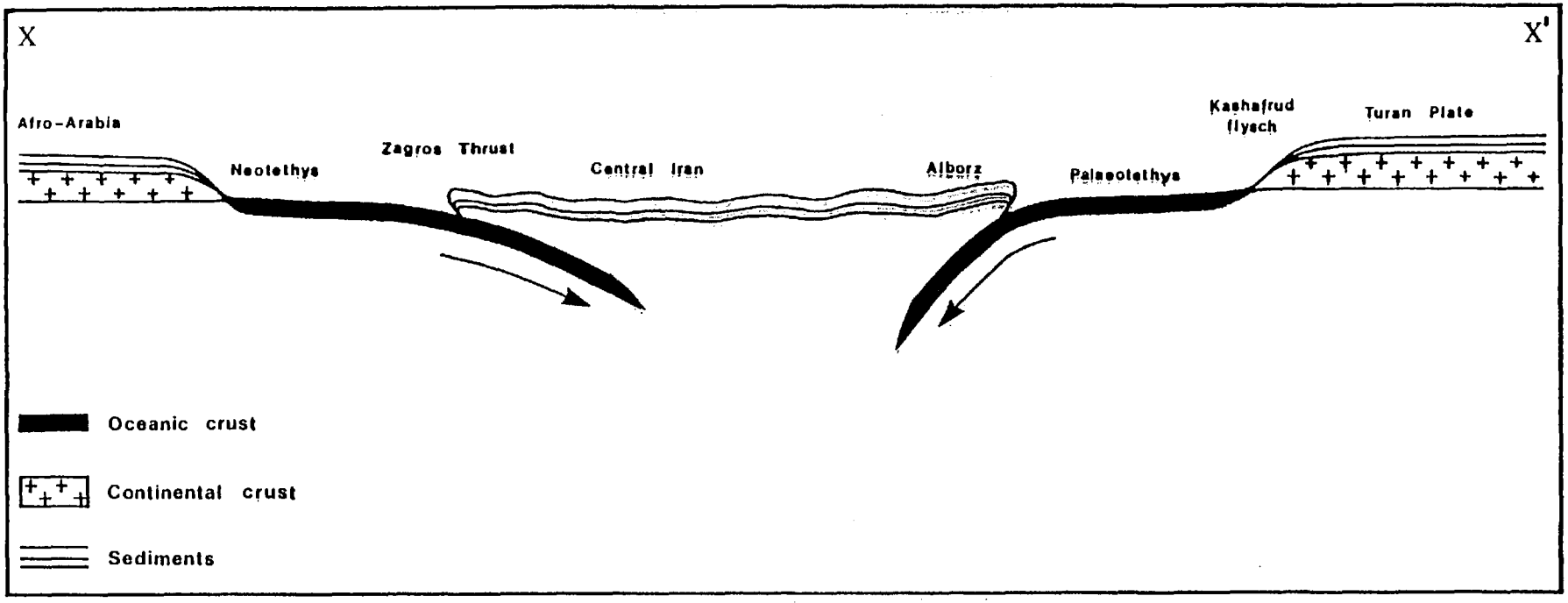


Fig. 1.3.4 - A schematic cross section (X-X') showing the subduction of the Palaeo- and Neo-Tethys under Central Iran at Early - Middle Jurassic time.

CHAPTER 4

STRATIGRAPHY OF THE SHEMSHAK FORMATION

4.1 Introduction

The present study is restricted to the Shemshak Formation of the easternmost Alborz Ranges, where the assumed transition between the Alborz and the Kopet Dagh occurs.

The Shemshak has been described as a persistent (Uppermost Triassic ?) Lower-Middle Jurassic formation (Stöcklin, 1971), extensively developed in North, Central and East Iran. The unique lithological characteristics of this formation and its economic coal reserves have attracted geologists since the start of the geological work in Iran. The formation consists mainly of irregular alternations of sandstone, shale, siltstone and subordinate localised sandy limestone or chalk layers. Some of the shale and siltstone intervals contain coal seams of limited lateral extent. Although the Shemshak Formation is dominated by terrestrial deposits, marine intervals have been reported from different localities by Gansser (1955), Lorenz (1964), Dellenbach (1964), Steiger (1966) and Allenbach (1966). A Middle Toarcian to Early Aalenian age has been agreed upon by most authors for the marine ammonite-bearing part of the formation.

In Northern Iran, the Shemshak Formation rests unconformably on different stratigraphic units, ranging in age from Precambrian to Triassic, mostly with a sharp lithological break (Stöcklin, 1971). The upper boundary of the formation has been reported to be conformable throughout the country (Stöcklin, 1971) although it may be heterochronous in the Alborz (Assereto, 1966).

In the Eastern Alborz region (the studied area) the Shemshak Formation succeeds the Triassic dolomites and limestones with a disconformity. A zone of ferricrete soil deposits (Selley, personal comm.) lies immediately beneath the unconformity surface representing regression of the Triassic sea and subaerial exposure

of the Triassic rocks. Soil horizons within sedimentary sequences are especially characteristic of fluvial and deltaic deposits (Selley, 1976, P. 56-57) and the ferricrete zone underneath the Shemshak Formation is a typical example.

The Shemshak Formation in the Shahpassand area is conformably overlain by the Dalichai Formation of Late Bajocian to Bathonian age, whereas in the Jajarm area the Middle Jurassic Bashkalateh Formation is the succeeding unit. The ammonites collected from the lowermost part of the Dalichai Formation in the Shahpassand area (Fig. I.4.1) are referred to Middle Bajocian-Bathonian (Donovan, personal comm.).

Three stratigraphic sections in the Shahpassand area and one in the Jajarm area were measured for the purpose of this study (Fig. I.4.2). The Shahpassand sections are named Qoznavi Section (east of the village of Qoznavi), Rudbar Section (east of the village of Rudbar), and Nargess-Chall Section (southeast of the village of Nargess-Chall). The Nargess-Chall Section is not described here, because of its close resemblance to the Rudbar Section; the fossils collected from this locality are described in Section 6.6. Figures I.4.3, I.4.4 and I.4.5 (loose) show a detailed description of the studied sections.

4.2 Stratigraphic Subdivisions

Six distinctive lithostratigraphic units (for abbreviation subsequently referred to as lithounits) are distinguished in the Shemshak Formation of the Eastern Alborz. As marker horizons are neither sufficiently common nor regionally persistent, correlation of individual rock bodies is virtually impossible, and the overall characteristics of the lithounits form the basis of the subdivision. They are described from the base upwards (Fig. I.4.6, loose).

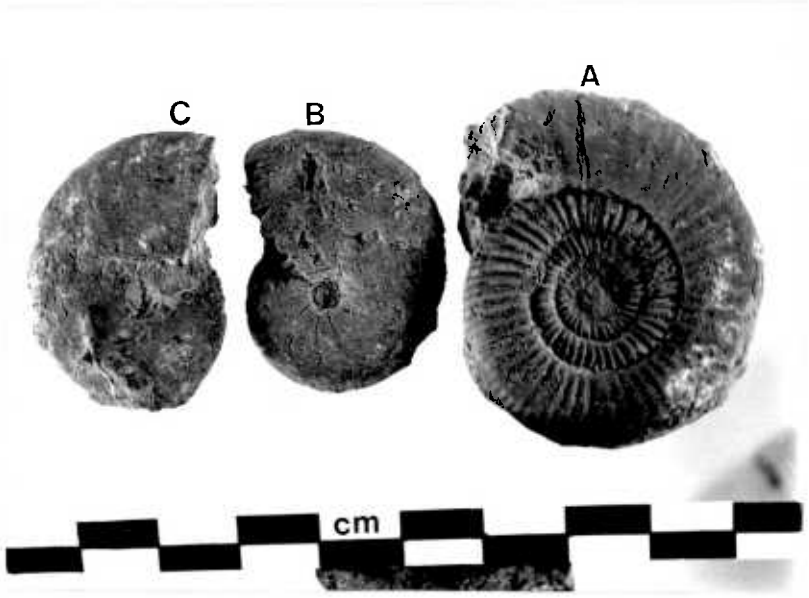


Fig. I.4.1 - Ammonites from the lowermost part of the Dalichai Fm. in the Shahpassand area (Qoznavi Section).

A) Siemiradzkia; near to auri̲gera (oppel); Lower Bathonian.

B) Calliphyllocera; Jurassic.

C) Oppelia (Fam. Oppeliidae); not earlier than Middle Bajocian.

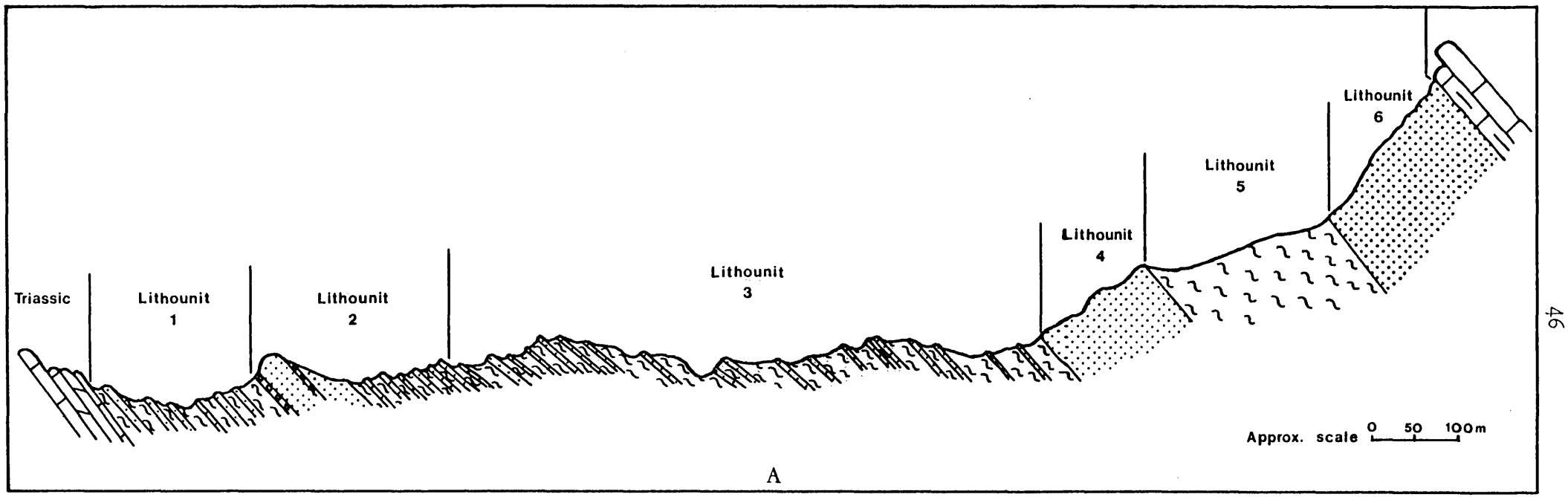


Fig. I.4.2 - Sketch cross sections through the Shemshak Fm. in the Eastern Alborz region.

A) Qoznavi Section (Shahpassand area).

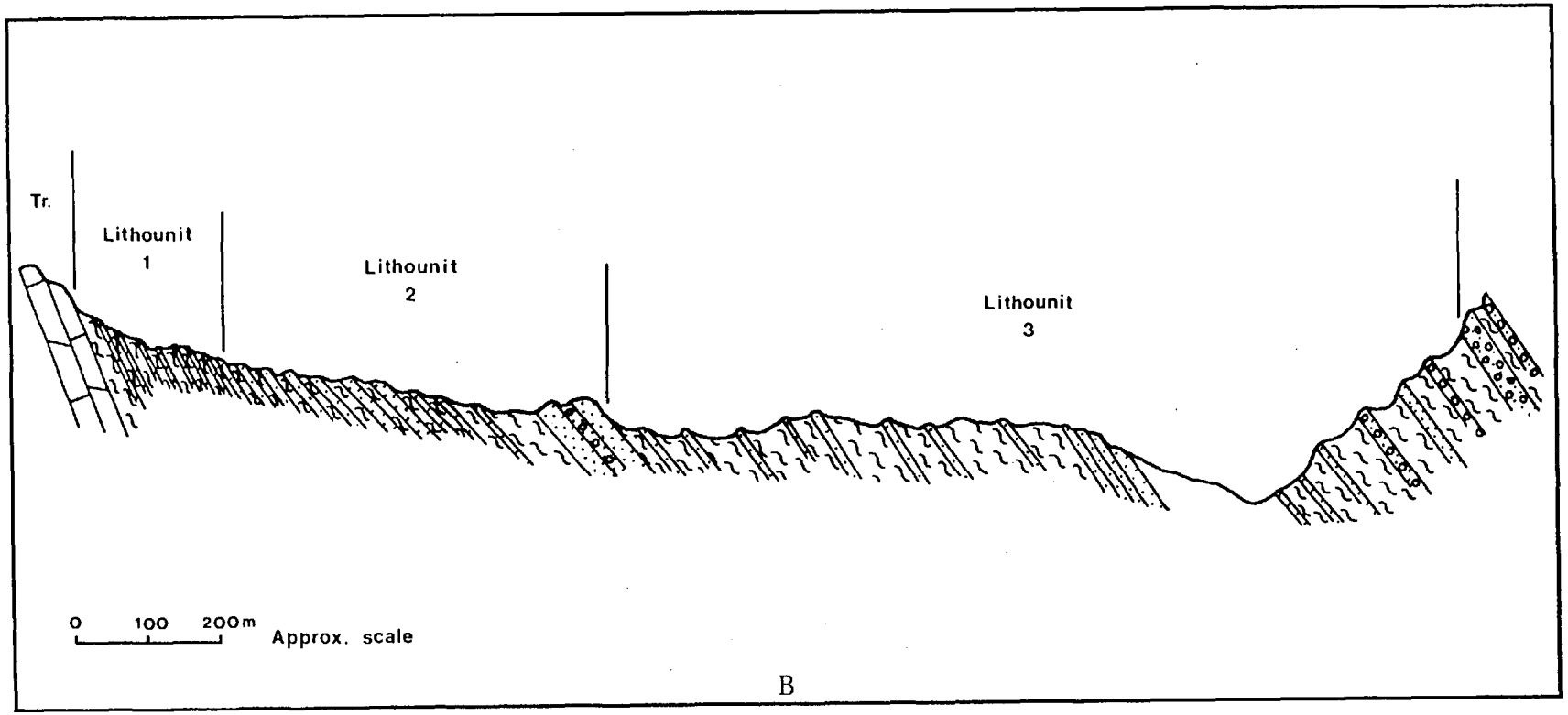


Fig. I.4.2 - Continued.

B) Rudbar Section.

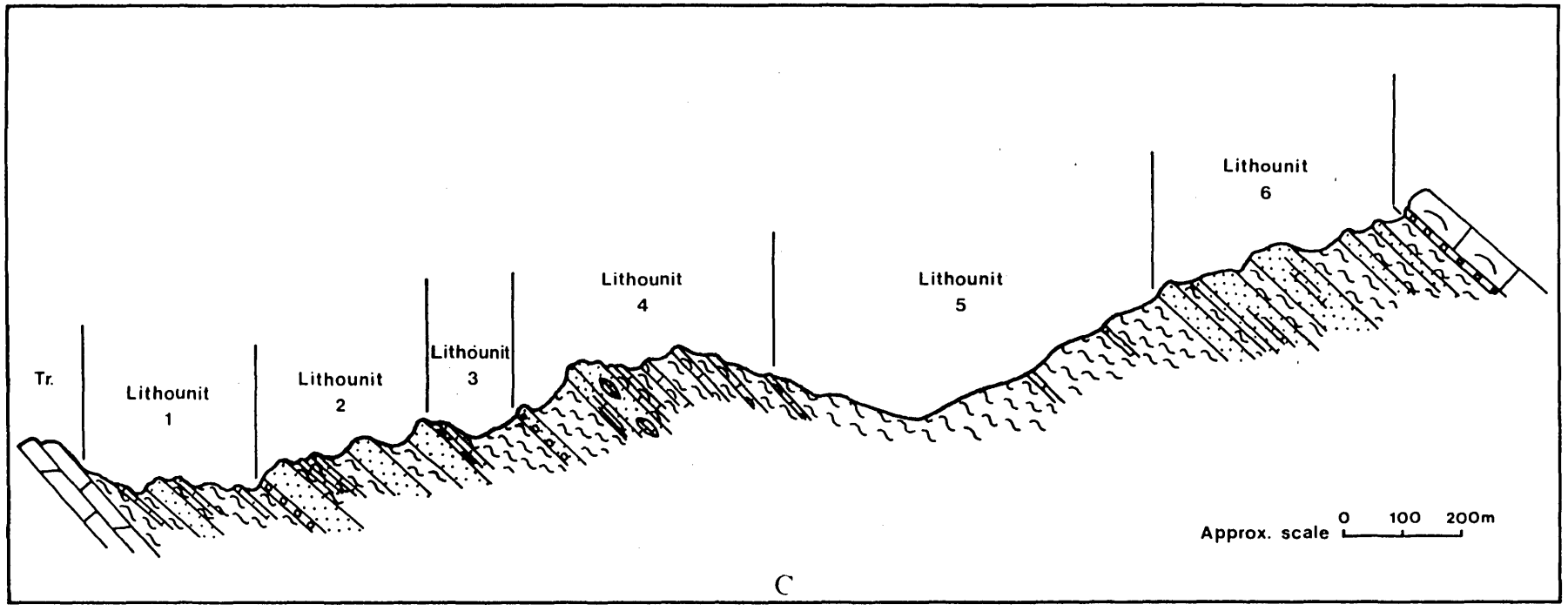


Fig. I.4.2 - Continued.

C) Jajarm Section.

4.2.1 Lithounit (1) "Alternating Shale and Sandstone"

This is the lowermost unit of the Shemshak Formation, overlying the Triassic rocks with a distinct disconformity. It is composed of irregular alternations of ferruginous medium- to fine-grained argillaceous sandstones and sandy shale with a few siltstone layers (Fig. I.4.7). The boundaries between the sandstone and shale beds are transitional, typical of a deltaic sequence. The sandstones contain scattered iron oxide nodules and some carbonised plant remains. They have limited lateral extent and exhibit lamination due to a relatively high quantity of argillaceous and micaceous material. The shales, on the other hand, are blackish gray to green and sandy, sometimes micaceous and laminated, with some plant debris.

Lithounit (1) in the Shahpassand area contains abundant plant remains, both comminuted and larger recognisable forms, and is more carbonaceous than the corresponding unit in the Jajarm area which has two intercolated ironstone beds (80-150m thick). A characteristic bed of yellowish calcareous siltstone, about 30 cm thick and exhibiting "cone in cone" structure at the top, has been recognised at several localities in the Shahpassand area; it may be represented at Jajarm by a bluish claystone layer.

The thickness of Lithounit (1) varies, ranging from 180m in the Qoznavi Section upto 250m in the Jajarm Section (Fig. I.4.6, loose).

The basal part of this lithounit gives the highest gamma radiation counts of the whole Shemshak Formation.

4.2.2 Lithounit (2) "Channel Sand Complexes"

Overlying Lithounit (1) a sequence of channel sand complexes starts with a sudden increase in the size of the sand grains. This unit is characterised by graded channel cycles, each composed of intraformational conglomerates at the base followed upwards by fine-grained sandstones. Scattered iron oxide nodules



Fig. I.4.7 - "Alternating Shale and Sandstone" (Lithounit 1) from the lowermost part of the Shemshak Fm. in the Shahpassand area, north of the village of Qoznavi.

and gray-green sandy shale interbeds are also present.

In the Shahpassand area each channel sand has a restricted lateral extent and discernible thickness variations (Fig. I.4.8), while in the Jajarm area they maintain a more constant thickness (flat channels).

Lithounit (2) has a much higher sand to shale ratio than the underlying Lithounit (1). Remarkable current-bedding and graded-bedding (in festooned troughs), as well as a few coal horizons near the top, are the major sedimentary features in the Shahpassand area. No coal, however, is present at Jajarm, where only carbonised plant remains were found.

The thickness of this unit is 334m, 521m, and 255m in the Qoznavi, Rudbar, and Jajarm Sections respectively.

4.2.3 Lithounit (3) "Carbonaceous Sequence"

The "Channel Sand Complexes" in the Shahpassand area are overlain by a thick sequence of gray-green to black coaly shale and siltstone, interbedded with subordinate argillaceous sands. A sudden decrease of sandstone and a remarkable increase in the carbonaceous content of the sediments distinguishes this unit from the underlying Lithounit (2). Numerous coal seams, ranging in thickness from 15 to 150 cm, are mined near Rudbar village (see Geological Map A, loose). The shale intervals are organic rich, laminated, mostly coaly and ferruginous, and contain well-preserved plant fossils. Haematite balls (about half a metre in diameter) are present either as scattered nodules or semi-continuous horizons throughout this carbonaceous sequence (Fig. I.4.9). A characteristic fracture system commonly develops in these balls due to weathering, breaking them into small pieces with oriented facets. The resultant particles normally scatter down the hillside like a minifanglomerate with the remnants of the original ball at the apex of the fan (Fig. I.4.10). Intervals of lutite (see Fig. I.4.3 and I.4.4, loose), mostly undulating laminae of calcareous siltstone and rarely claystone are also



Fig. I.4.8 - Two channel sand units separated by a thin shale interval. The sand body to the left of the picture increases thickness down the hill, whilst the one to the right pinches out midway down the flank (Lithounit 2, Shemshak Fm., Shahpassand area).



Fig. I.4.9 - Haematite balls in the "Carbonaceous Sequence" of the Shemshak Fm. (Shahpassand area).



Fig. I.4.10 - Remnants of a haematite ball after intensive weathering.

present. They increase rapidly near the top of the unit and seem to have some association with iron oxide content and distribution of the haematite balls. Some of these siltstone layers are replaced locally by chalky and limey horizons.

Among the plant fossils present, upright stems of Neocalamites are interesting as they are in situ suggesting a marsh or swamp environment (Fig. I.4.11).

The sandstone beds of this lithounit are poorly sorted, but exhibit some cyclic grading with mainly coarse-grained sandstone and microconglomerates* at the base fining upwards to very fine-grained sandstones. Cross bedding indicates a current regime directed south to north. Intraformational microconglomerates containing oriented elongate pebbles (pebbly sandstone) and current bedding are developed as flat lenses in the upper part of this carbonaceous sequence and mark termination of the swamp environment.

The thickness of Lithounit (3) is 589m in the Qoznavi Section, but it increases to 1,121m in the Rudbar Section where about 317m of the exposures have been washed away or covered by the bank deposits of the Rudbar stream (Fig. I.4.12).

In the Jajarm Section the thickness of this unit is drastically reduced to 158m. Here the sediments are less carbonaceous and only one low rank coal horizon is present, although carbonised plant remains and the trunks of trees are still plentiful. The sand to shale ratio is higher than at Shahpassand and some of the sandstone beds are well cemented and quartzitic. Ripple marks and current bedding are common syndepositional sedimentary structures, especially in the sandstone beds in the middle part of the unit. The siltstone laminae and their associated haematite balls are absent.

* The term "microconglomerate" is used for a pebble bed in which the clasts are less than 2 Cm in diameter.



A



B

Fig. I.4.11 - Fossilised plant remains.

A) Upright trunks of Neocalamites in the "Carbonaceous Sequence" of the Shemshak Fm., Shahpassand area, indicating a swamp environment.

B) A closer look at a Neocalamites trunk collected from the region.



Fig. I.4.12 - The upper part of the "Carbonaceous Sequence" in the Rudbar Section overlain by the pebbly microconglomerates of the "Lower Sandstone Member" (appear as whitish bands). The Carbonaceous Sequence is partly covered by the deposits of the Rudbar river (see the valley in the middle of the picture).

4.2.4 Lithounit (4) "Lower Sandstone Member"

The upper limit of Lithounit (3) is marked by the appearance of a poorly sorted yellow pebbly sandstone (microconglomerate) belonging to the lowermost beds of the succeeding "Lower Sandstone Member". In the Qoznavi Section of the Shahpassand area, a sequence of medium-bedded to massive, mainly calcareous, sandstones rests on top of the yellow microconglomerate horizon (Fig. I.4.13). A 12m interval of shale and siltstone marks the only interruption of sandstone deposition in this 75m thick lithounit. To the west, in the Rudbar Section, the basal microconglomerate is much thicker but, due to structural deformation and erosion, the rest of this member and the overlying lithounits are missing.

To the east, in the Jajarm Section, this unit is 314m thick. The presence of the basal yellow microconglomerate and a general increase of calcareous cement were the clues to lithological correlation. Three subunits are distinguished:

a) The lowest subunit consists of sandy micaceous shale and argillaceous sandstone over the basal yellow conglomerate. The upper sandstone beds of this subunit display ripple marks and worm tracks which suggest episodes of marine invasion, although some plant debris is still present.

b) The middle subunit is dominantly of shallow marine origin as indicated by limestones and sandstones with lenses of shelly limestone containing ammonites, belemnites, and pelecypods. The ammonites collected from this lacality are dated as Lower Toarcian (Donovan, personal comm.).

c) The highest subunit is composed of alternating sandy marls with extensive iron oxide concretions and ferruginous sandy limestones. The limestone beds contain a large assemblage of molluscs including ammonites, belemnites, pelecypods and gastropods. Remarkable bioturbation marks (e.g. worm tracks) and some plant remains are also present. The ammonites collected from different horizons of this subunit are identified and dated by Donovan (personal comm.) as Upper Toarcian.



Fig. I.4.13 - The upper part of the Shemshak Fm., Shahpassand area.

A) Upper part of the "Carbonaceous Sequence".

B) Lower Sandstone Member.

C) Marine Shale.

D) Upper Sandstone Member.

E) Dalichai Fm.

F) Lar Fm.

4.2.5 Lithounit (5) "Marine Shale"

Overlying the "Lower Sandstone Member" with a sharp lithological boundary in the Shahpassand area are 121m of marine marly shale (Fig. I.4.13) containing foraminifera of uppermost Lias to Bajocian age (Micropalaeontology Section, University College, London, personal comm.). Dating is based on the presence of conical Spinilina in particular, which did not appear until the Middle Jurassic. An appreciable sodium chloride content was discovered during geochemical work on this shale unit and produced an additional clue to the marine origin of the sequence.

Lithounit (5) is much thicker in the Jajarm Section and consists of 470m of sandy micaceous shale and siltstone with a few thin, argillaceous and calcareous sandy layers. The sandstone beds are concentrated mostly near the top and the bottom of the sequence. The iron oxide content of this unit is relatively high, as indicated by aboundant nodules and extensive iron oxide concretions. Copious pelecypods and a few ammonites are the main megafossils of this marine shale interval. Sediments of this lithounit seem to have been more indurated than the corresponding rocks in the Shahpassand area. Correlation of this lithounit with its Shahpassand equivalent is based on the presence of the marine fauna, which shows it to be the only marine shale interval of the Shemshak Formation.

4.2.6 Lithounit (6) "Upper Sandstone Member"

Above the "Marine Shale", a sharp lithological change leads to the uppermost member of the Shemshak Formation. This lithounit in the Qoznavi Section consists of 138m uniform fine-grained calcareous sandstone (Fig. I.4.13). At the top there is a transitional boundary with the Middle Jurassic Dalichai Formation, which starts with a reddish fossiliferous siltstone and then develops upwards into a limestone sequence.

In the Jajarm area, 334m of mainly calcareous sandstone with intervals of sandy shale and two horizons of ferruginous sandy

limestone containing shell fragments are referred to the "Upper Sandstone Member". Here, the Middle Jurassic yellow limestone and shale of the Bashkalateh Formation overlie the Shemshak Formation with a thin basal conglomerate (Fig. I.4.14).

Lithounit (6) of the Shemshak Formation represents the end of arenaceous sedimentation in the Jurassic of the Eastern Alborz region; the succeeding beds are predominantly calcareous.

4.3 Formation Thickness and its Variations

The Shemshak Formation shows considerable thickness variations, even over relatively short distances. The thickness of the type section in the Central Alborz is 1,027m (Assereto, 1966) and it increases northwards to more than 2,000m (Assereto et al. 1968). In the Qoznavi Section, it is 1,491m thick whereas, about 15 km to the west in the Rudbar Section, where the upper units are missing, the thickness has increased to 1,972m. In the Jajarm area it is 1,777m thick.

Formation thickness in a sedimentary basin is controlled by a combination of structural and sedimentary factors. Assereto (1966) ascribed the thickness changes of the Shemshak Formation in the Central Alborz to tectonic dislocations, but all the sections measured for the purpose of this study were stratigraphically continuous and no structural dislocation was seen. The thickness variations in the studied region are considered to be due either to syndepositional vertical movements and different compaction resulting from later compression, or to inequalities of the rate of deposition controlled by sedimentary factors (e.g. distributary channels and interdistributary bays).

4.3.1 Vertical Movements

The Late Triassic movements in the Alborz caused regional uplift and emergence, resulting in a change of the depositional environment from marine to mainly terrestrial. This regional



Fig. I.4.14 - Middle-Upper Jurassic sediments in the Jajarm area.

A) Shemshak Fm.

B) Bashkalateh Fm.

uplift was probably accompanied by the development of numerous horsts and grabens. The resulting unstable blocks were largely responsible for the thickness variation of the Lower-Middle Jurassic sediments and their associated facies changes. An elongate trough, on the present northern flanks of the Alborz, where the Shemshak Formation is several times thicker than the corresponding sequence on southern flanks of the range (Stöcklin, 1974a), was presumably a large subsiding block in the Early Jurassic. The synclinal structure north of Rudbar village (see Geological Map A, loose) was probably also an Early Jurassic basin which, although small, accommodated a thicker sequence of the Shemshak Formation than of at other localities in the Shahpassand area.

4.3.2 Compressional Forces

Gill (1953) noted that thinning of incompetent beds of sedimentary sequences during folding is a factor of compactibility until plastic flow commences. The amount of compaction is, in turn, a function of dip and can reach major proportions, depending on the angle of dip. Full compaction occurs when the beds are vertical and compressive stress is transmitted directly into the incompetent ones. In case of horizontal strata the incompetent beds are protected against laterally compressive compaction by the competent layers, and the net effect of the compressive stress is zero (Fig. I.4.15).

Formation thinning can be calculated using the formula given by Badgley (1959):

$$\text{Thinning} = \text{Normal Fm. thickness for the area} \times \text{Max. thinning \%} \times (1 - \text{Cos dip}) \qquad (1)$$

The percentage of thinning then can be obtained by:

$$K = K_1 (1 - \text{Cos}\alpha) \qquad (2)$$

where K is thinning %, K_1 is the percentage of maximum compression at 90° dip and α is the dip angle. The maximum value for the

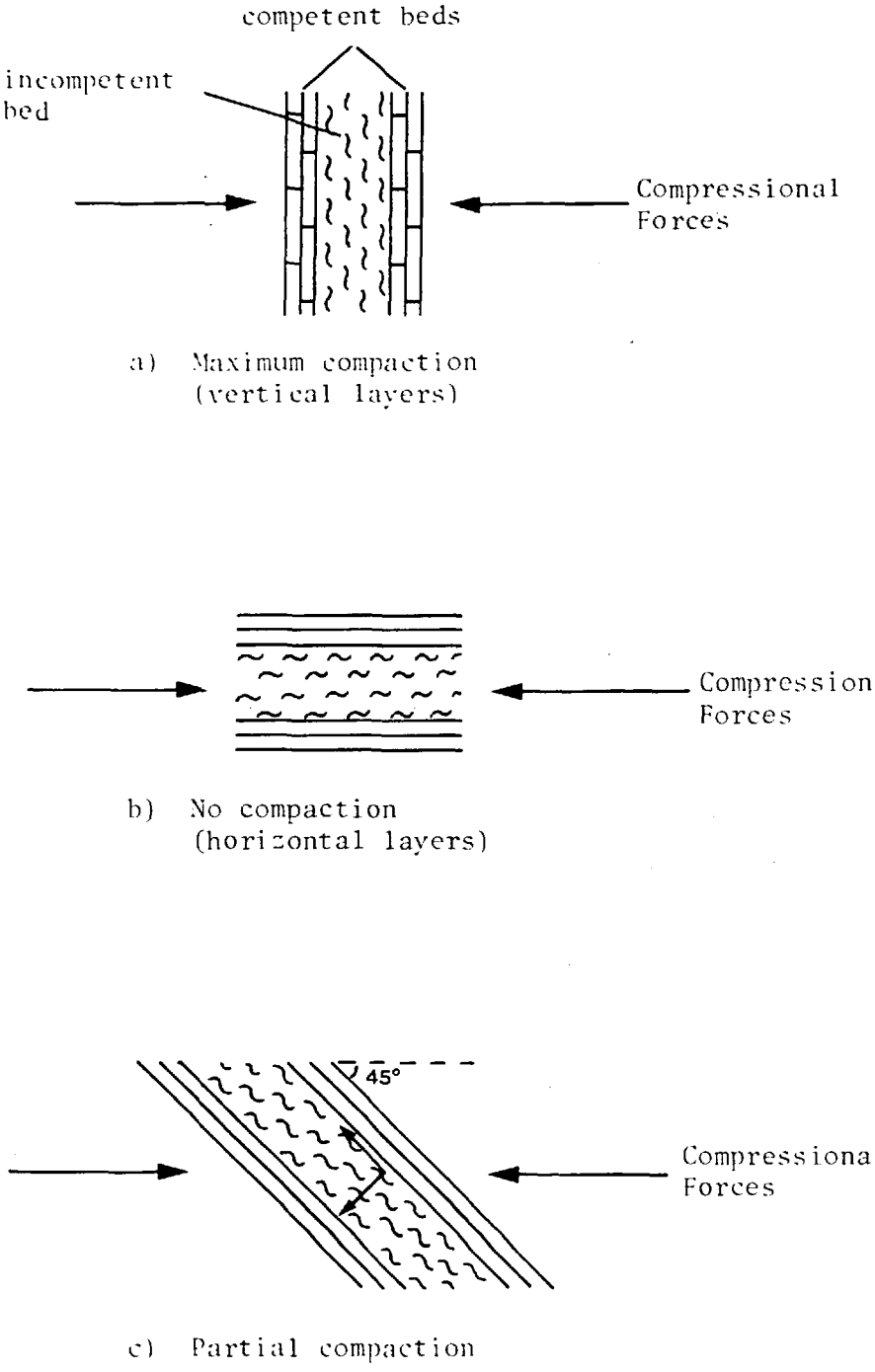


Fig. I.4.15 - Diagram showing the compaction effect of compressional stress on beds with different dip angles.

percentage compressibility of continental deposits, on the basis of field experience, is 30% (Gill, personal comm.). The percentage of thinning of the Shemshak Formation, then, can be calculated by:

$$K = 30\% \ (1 - \cos \alpha) \qquad (3)$$

The difference in the average dip angle of the Shemshak Formation between the Qoznavi Section of Shahpassand (about 50°) and the Jajarm Section (about 37°) is approximately 13 degrees. Thus, the sequence may be compacted to a different amount in the two localities, and about 20% of the difference in formation thickness between the two sections could be accounted for in this manner.

4.4 Correlation of the Shemshak Formation of Eastern Alborz with Type Section (Central Alborz)

An attempt has been made to establish a correlation between the subdivisions of the Shemshak Formation used in the present study and those of the Central Alborz(Fig.I.4.6).

The type locality in the eastern part of the Shemshak coal-mining district (north of Tehran) in the Central Alborz was studied by Assereto (1966). Four lithozones were distinguished (from base to top): Lower Sandstone, Lower Carbonaceous Series, Upper Sandstone, and Upper Carbonaceous Series.

The lowermost 90m of this formation at the type locality consist of alternating shale and sandstone intervals more or less similar to Lithounit (1). This part of the section includes the Lower Sandstone plus about 15m of Lower Carbonaceous Series of the Assereto's subdivision.

The "Channel Sand Complexes" are apparently missing from the type section, but appear towards the east in the Lower Haraz Valley, where they are considered to be part of Lower Carbonaceous Series (Süssli, 1976). It must be pointed out, however, that

lateral discontinuity is a common feature of the channel sand deposits and that the type locality could have been positioned in an interdistributary bay when the channel sands were being deposited in the Haraz Valley and the Shahpassand area.

Overlying the lowest 90m at the type locality are about 580m of mainly siltstone and shale with some intercalated sandstone layers. This sequence includes most of the Assereto's Lower Carbonaceous Series and the basal part of his Upper Sandstone. The corresponding interval in the Eastern Alborz is probably Lithounit (3) (Carbonaceous Sequence), as suggested by its very low sand to shale ratio, the occurrence of several coal seams, and the presence of abundant plant remains. Similar facies also characterise the sediments overlying the Channel Sand Complexes in the Lower Haraz Valley (east of the type locality).

In both the Central Alborz and the Jajarm Section (Eastern Alborz), a sequence of mainly calcareous sandstones containing lamellibranchia and ammonites forms the succeeding interval, although in the Shahpassand area it is much thinner and is unfossiliferous. The ammonites of this sequence are time equivalent in both areas and are Late Toarcian (in Central Alborz by Fantini Sestini, 1966 and in Eastern Alborz by Donovan, personal comm.). Consequently a regional transgression must have occurred throughout the entire Alborz basin during Latest Liassic time.

The unit equivalent to the "Marine Shale" of the studied area is presumably the lower 55m of the Assereto's Upper Carbonaceous Series, which is composed of mainly shale and siltstone. The environment of origin of this unit at the type locality is still unknown as no microfaunal study of the sediments has yet been made.

The "Upper Sandstone Member" (Lithounit 6) has thinned to 25m at the type locality but, the lithology of the rocks is still similar to the Eastern Alborz equivalents. The overlying

Dalichai Formation at the type locality is marked by a rapid change in lithology to ammonite-bearing marly limestone (Assereto, 1966), as is the case in the Shahpassand area.

4.5 Structural Features Associated With the Shemshak Formation

4.5.1 Intraformational Deformation

The Shemshak Formation is structurally more complex than the adjacent formations due to additional intraformational deformation. This is particularly visible in the Shahpassand area where the formation is extensively exposed, whereas at Jajarm the equivalent beds are less complicated. Near the village of Qoznavi and on the southeast flank of the Rudbar Syncline, there is a discrepancy of 5°-10° in the angle of dip between the Triassic strata and the lower beds of the Shemshak Formation, although the contact between them is normally a disconformity (Fig. I.4.16). This could have been caused by gliding of the Shemshak Formation over the more rigid substratum. Along the road from Shahpassand to Shahrud some relatively small scale folds can be recognised in the Shemshak Formation; they appear to die out whithin it and not to continue either downwards into the older rocks or upwards into the younger formations (Fig. I.4.17). The direction and angle of dip often change abruptly, so that the reconstruction of the original structures is impossible. For example at one locality in the Rudbar Section, the beds dip 56° northwest, whereas a few hundred yards away in the Nargess-Chall Section they dip 32° southwest and across the Tilabad River they are nearly horizontal (see Geological Map A, loose). In the basal part of the Qoznavi Section near the Qoznavi Bridge, some of the beds are locally overturned (Fig. I.4.18).

The structural complexity of the Shemshak Formation may be due to the fact that it is a thick sequence of generally

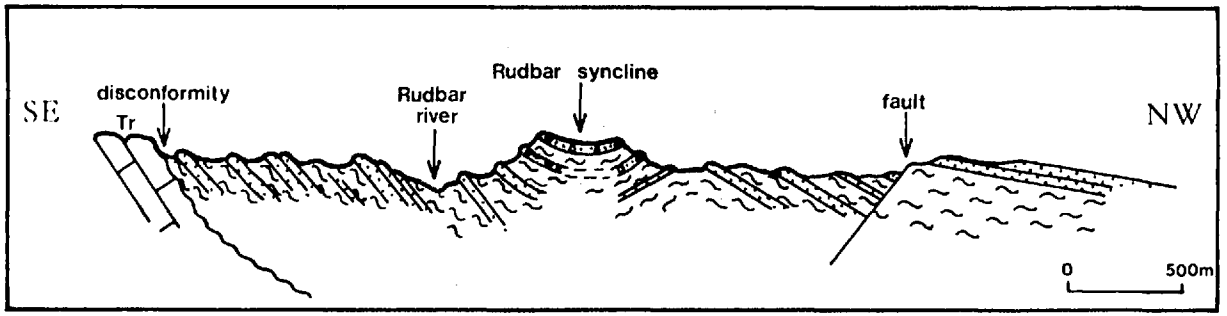


Fig. I.4.16 - Sketch cross section between Rudbar and Nargess - Chall showing the basal low angle contact of the Shemshak Fm. with Triassic rocks. An example of intraformational folding is also illustrated by the Rudbar syncline.

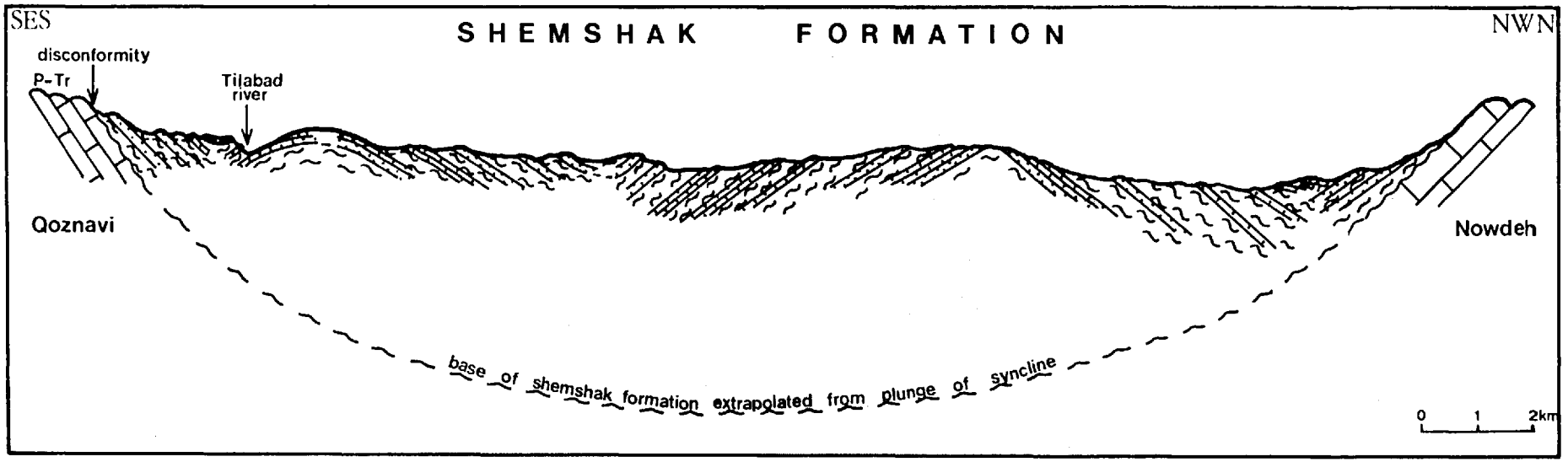


Fig. I.4.17 - Sketch cross section through the Shemshak Fm. along the road from Qoznavi to Nowdeh, showing intraformational folding.



Fig. I.4.18 - Overturned beds in the basal part of the Shemshak Fm., northwest of the Qoznavi bridge (Shahpassand area).

incompetent rocks lying between two competent formations. Consequently it absorbed some of the compressional stress by intraformational deformation. On the other hand, it is possible that some intraformational structures could be the result of slumping due to syndepositional instability while the sediments were still unconsolidated (Fig. I.4.19 and I.4.20).

4.5.2 Faulting

An extensive fault pattern is discernible on the aerial photographs in both the Shahpassand and Jajarm areas. Two groups of faults can be recognised:

Post-depositional faults which cut through the Shemshak Formation and into the adjacent younger (and older) formations. These are major structural features, probably developed during the folding of the Cretaceous and Tertiary. Examples are the NE-SW trending fault north of Tilabad village (see Geological Map A, loose), and the N-S trending fault west of the Jajarm Section (see Geological Map B, loose).

Syndepositional faults which are either restricted to the Shemshak Formation or extend only into underlying rocks. They date from the Late Triassic vertical movements and are believed to have been the main cause of thickness changes in the formation. The NE-SW trending fault between the Rudbar Section and the Nargess-Call Section (see Geological Map A, loose); the fault set which cuts through the upper part of the Qoznavi Section; the diagonal fault system probably originating from shear fractures west of Qoznavi village (see Geological Map A, loose); the dip fault cutting the basal part of the Shemshak Formation in Rudbar which continues southeastwards through the Palaeozoic-Triassic rocks; and the curved fault in Kuh-e Ozom northeast of Jajarm forming a major valley through the Palaeozoic-Triassic rocks and extending into the Shemshak Formation (see Geological Map B, loose) are all examples of such syndepositional faulting.



Fig. I.4.19 - An example of intraformational folding in the Shemshak Fm. (Shahpassand area).



Fig. I.4.20 - Landslide showing a block of limestone slipped down slope over the Shemshak Fm. Compressional forces as a result of this slide might have caused some localised deformation of the underlying strata.

CHAPTER 5

SEDIMENTOLOGY

5.1 Introduction

The Shemshak Formation is not lithologically uniform throughout, but its unique characteristics differentiate it clearly from the adjacent formation. It is widely distributed as evidenced by its outcrops from Northern (Alborz), Central, East-Central and South-Central Iran, and no evidence has yet been reported to arouse doubt that the Shemshak Formation is not continuous underneath younger sediments throughout the whole area of North, East and Central Iran. However, the formation is completely absent from the Zagros region of Southwest Iran, and indeed from the entire area south of the Main Zagros Thrust, where the contemporaneous shallow marine carbonates of the Neyriz and Surmeh Formations were deposited.

The sedimentary structures and lithology indicate that the lowermost part of the Shemshak Formation was deposited in a high energy environment, but they pass upwards into a dominantly shaley interval with numerous coal seams which, although still continental, could have been laid down in a quieter environment such as interdistributary bay. Marine shales overlie the lower continental sediments. Clastic sediments containing plant remains reappear towards the uppermost part of the sequence indicating a return to continental sedimentation.

The sedimentology of the succession was studied partly during the course of the field work including the recognition of lithology, palaeocurrents and sedimentary features, as well as the collection of fossils. A more detailed study of the sediments was made through routine laboratory techniques such as the microscopic examination of the thin sections and palynomorphs, and the identification of plant fossils and microfauna.

5.2 Sedimentology of the Shemshak Formation in the Eastern Alborz Area

5.2.1 Terrestrial Deposits

The great proportion of the Shemshak Formation, particularly in the lower part, consists of terrestrial deposits, mainly sandstone, shale and siltstone. The lowest three lithounits (see Chapter 4, Stratigraphy) of the Formation show no indication of marine sedimentation; samples from different horizons were washed and microscopically examined to make certain that no foraminifera or other marine indicative microfauna were present.

The Sandstones are mostly argillaceous with considerable amounts of iron oxide in the form of nodules (less than 5 cm in diameter) or concretions. Mica is a very common constituent of the matrix in most of the sandstones. Most of the grains are subangular, but a few are subrounded; sorting is rather poor, especially in the "Channel Sand Complexes" where upwards fining cycles ranging from microconglomerates to fine-grained sand are common. The other sandstones throughout the formation are predominantly medium to fine grained.

Most sandstones are medium bedded, although some massive beds also exist in the "Channel Sand Complexes" suggesting deposition by stronger currents*. The sand layers interbedded in shale are highly argillaceous and exhibit well-defined lamination. These layers were probably deposited by comparatively weak currents.

The degree of cementation varies in the sandstones both vertically and laterally, indicating either variation of the cementation processes or fluctuation in the concentration of cementing agents in solution. Although siliceous and calcareous

* The bed thickness is believed to be related to the current competence in clastic sediments. Stronger currents produce thicker and commonly coarser grained beds (Pettijohn et al., 1972).

cements are both present the latter is more common, particularly in the "Lower and Upper Sandstone Members" (see Chapter 4, Stratigraphy). At Jajarm, the sandstones are generally better cemented and thus harder than those near Shahpassand; for example some beds are so well cemented with silica that porosity has been almost completely destroyed.

At outcrops the sandstones are mostly weathered and, where arillaceous, they exhibit lamination. Fretwork weathering is particularly common in the poorly cemented sandstone bodies.

The Shales are commonly sandy, micaceous and sometimes ferruginous. Where they are clearly exposed, they are seen to be laminated, but some are covered by weathering products. The shales contain well preserved plant fossils (e.g. leaves, trunks and seeds), and in the Shahpassand area they are often highly carbonaceous ranging in colour from grey-green to black; some coal seams are present. The carbonaceous content decreases drastically at Jajarm, where the shales are lighter coloured.

The Siltstone laminae are highly carbonaceous, often ferruginous and are associated with haematite balls. They are common near Shahpassand and contain fossilised leaves, which are exceptionally well preserved so that the details of their internal structure are clearly discernible.

5.2.2 Marine Deposits

Marine deposits are represented by uniform grey-green marls and siltstones, with some sandy and/or fossiliferous limestone interbeds. In the Shahpassand area a unit of grey-green marl containing foraminifera is the only proved marine sediment in the Shemshak Formation, although the sandstone units above and below it are uniform calcareous and might have been laid down under some sort of marine influence. At Jajarm, the transgression was seemingly sluggish, as suggested by a gradual transition from continental upwards into marine sediments. This transition began with deposition of a highly calcareous sandstone with large

lenses of coquina limestone and continued upwards into alternating sandy marl and fossiliferous sandy limestone, and finally into a thick interval of mainly sandy marl and siltstone containing lamellibranchia, ammonites, and other marine fauna.

5.2.3 Associated Rocks

Coal- The coal reserves of Iran are largely confined to the Shemshak Formation and to some Middle-Upper Triassic rocks of the Aqdarband area. Coal beds extend eastwards into Afghanistan, where an identical sequence to the Shemshak is exposed (north of Kabul; Afshar-Harb, personal comm.). They indicate a luxuriant vegetation during the Late Triassic and Early Jurassic.

In the Shahpassand area the Shemshak Formation is much more carbonaceous than its Jajarm equivalent. At least 28 different coal horizons were recorded in the Qoznavi Section and 17 in the Rudbar Section, but at Jajarm very few and impure coal seams were found. The coal macerals consist of mainly vitrain and fusain, and their rank is almost as low as lignite. The majority of the coal seams have a limited lateral extent and pass into carbonaceous shale/or siltstone. Their appearance at outcrop is dull and lacking in lustre (possibly due to weathering), but in the mine tunnels of Rudbar the same coals are darker and shiny. The coal seams are mostly in the "Carbonaceous Shale" (see Chapter 4, Stratigraphy) where plant fossils are plentiful, but the sandstones also contain some vitrain and small coaly spots. The coal seems to be of in situ origin, since upright trunks and fossilised roots are preserved in some horizons (Fig. I.4.11).

Iron deposits- Iron, commonly in its oxidised state, is found in the Shemshak Formation as ironstone nodules, concretions and haematite balls: they are to some extent comparable with the Jurassic Minette-type ores of Europe (McInnes et al., 1913). Two layers of shiny, dark green to black sandy ironstone (80-150 cm thick) are intercalated in the lowermost part of the Shemshak Formation near Jajarm. The nodules, ranging from 1 to

5 cm in diameter (Fig. I.5.1), are common throughout the Formation and become abundant in the lower part of it; they are found both in the shales and the sandstones, and sometimes they give a conglomeratic appearance to the rock. They have a concentric structure with a dark-brown or red crust and a yellow-orange core (possibly limonite). On a larger scale, concretions are present in the iron-bearing siltstones, especially in the "Marine Shale" interval at Jajarm (see Chapter 4, Stratigraphy). Iron is also concentrated in haematite balls (about half a metre in diameter), which are here reported for the first time; they consist of rounded heavy ironstone bodies with no concentric structure.

Source of Iron- Subaerial exposure of the Alborz realm in Late Triassic time permitted intense chemical weathering in the region. Surface waters, containing organic acids, dissolved the iron compounds from the preexisting rocks (probably the igneous and metamorphic rocks of the southern margin) and carried them in solution to the basin. Iron was then precipitated in the silts, shales and sandstones under reducing conditions which were possibly caused by the diagenesis of organic matter. The iron may subsequently have been partly remobilised, perhaps as a result of pore water reactions, and then reprecipitated in the form of iron oxide nodules under oxidising conditions due to water table fluctuations. The concentration of iron compounds is closely related to the organic richness of the rocks, especially the humic material; for example, it is higher in the "Carbonaceous Shale" than in the other lithostratigraphic units.

Dykes- Several basaltic dykes about 80 cm wide and dark brown in colour cut through the Shemshak Formation. They have slightly darkened the surrounding sediments which were in direct contact with them, but no sign of metamorphism was recognised. Their intrusion must predate the folding because in places they are bent or truncated. Moreover, the dykes do not continue into the beds which overlie the Shemshak Formation and are in fact



Fig. I.5.1 - An iron oxide nodule from the Shemshak Fm.



Fig. I.5.2 - Lamination caused by thin coaly laminae in an argillaceous sandstone interval from Lithounit 2 of the Shemshak Fm.

restricted to the lower half of it. Thus it may be presumed that they are Middle Jurassic in age.

Basal Soil- The lower boundary of the Shemshak Formation is a disconformity associated with a layer of palaeosol (fossil soil). According to the literature (Selley, 1976) palaeosols commonly occur beneath unconformities and indicate subaerial exposure of the rocks; soils with concretionary iron oxides are called ferricrete and commonly it is the B horizon* that is enriched.

About 2m of ferricrete underlie the Shemshak Formation in the Shahpassand area; they contain some chemically resistant minerals such as quartz, tourmaline and apatite. The quartz grains are deeply corroded, which suggests a period of intense chemical weathering. Iron oxides exhibiting concentric structure are abundantly present as secondary minerals replacing the corroded quartz edges. It is suggested that a reducing alkaline environment controlled the precipitation of the iron oxides (Selley, personal comm.).

5.3 Palaeoclimate

The basal ferricrete, which is overlain by an interval of highly carbonaceous dark shale, suggests that the area was affected by a humid tropical climate soon after the Late Triassic regression, providing ideal conditions for the abundant supply of iron to surface waters. This is because soils that are rich in iron are formed in humid tropical climates (Selley, 1976) and vegetation is believed to be essential for their development (Blatt et al., 1972).

The iron was widely precipitated, commonly as outhigenic

* Soil deposits from bottom to top consist of horizons A, B and C, but generally in palaeosols the upper part of the profile is removed by erosion.

minerals, throughout the Shemshak Formation and its concentration generally increases with increasing humic organic content of the sediments, possibly because the organic acids which are required to mobilise the iron are provided by vegetal remains. This may indicate the existence of a low relief humid area with luxuriant vegetation and periods of seasonal flooding; these conditions led to intense chemical weathering and the supply of water necessary for the circulation of the iron in solution. However, on the basis of mineralogical data, Assereto (1966) inferred that the climate was not tropical during the deposition of the Shemshak Formation, since kaolinite, which is formed abundantly in such a climate, is scarce. Despite the Assereto's belief, there is some additional evidence to indicate a relatively warm climate during some periods of the Shemshak deposition; this includes the presence of prolific molluscs and abundant foraminifera in the marine intervals, enormous amounts of plant debris in the "Carbonaceous Shale" unit, and the localised chalk horizons. Temperature is known to be a controlling factor in the solution of calcium carbonate required for the growth of mollusc shells and in the metabolic rates of plants (Blatt et al., 1972).

5.4 Sedimentary Structures

The sedimentary structures observed in the Shemshak Formation yield useful information on the nature of sedimentation and the depositional environments of the rocks. A wide range of structures, both the primary and secondary, is present throughout the formation.

5.4.1 Bedding*

The Shemshak Formation exhibits a range of thin bedded (1 to

* A bed is described as a sedimentary unit which has been deposited under more or less constant depositional conditions and is separated from the adjacent beds by recognisable bedding planes.

10 cm in thickness) to massive bedded (more than 1m thick) strata. Massive sandstone beds are common in the "Channel Sand Complexes" and the "Lower Sandstone Member" (see Chapter 4, Stratigraphy) probably because of rapid sedimentation. Thin bedded sandstones, on the other hand, are concentrated mainly in the shaley intervals (e.g. the "Carbonaceous Shale"). Lamination is developed in some of the sandstone beds, especially in the fine-grained and micaceous intervals. Lamination due to very small coaly fragments has also been observed (Fig. I.5.2). Of the many variations, medium bedding (10-60 cm thick) is commonest in the sandstones.

The majority of the shale intervals are laminated due mostly to the intercalation of thin silty streaks; some shale units, however, often reaching considerable although variable thickness, are homogeneous throughout (e.g. the "Marine Shale" in the Shahpassand area).

5.4.2 Channels

Channel deposits are well developed in the lower half of the Shemshak Formation (see Fig. I.4.6, loose). Some consist of upwards fining cycles of pebbly (less than 2 cm in diameter) to very fine-grained sandstones. The laterally wedging sand bodies are particularly well seen in the Shahpassand area, where the channels seem to have been steepsided (Fig. I.4.8).

5.4.3 Cross Bedding

Cross bedding is the most common sedimentary feature. It provides evidence of current directions and hence of the source areas of the detrital sediments.

Cross bedding is extensively developed in the Shahpassand area, especially in the "Channel Sand Complexes". Festoon cross bedding is very common and indicates a generally south to north current direction. The Jajarm Section is characterised by a lack of well developed cross bedding.

5.4.4 Current Ripple Marks

Current ripple marks, as opposed to oscillation ripples, are a familiar feature of deltaic sediments and have been used widely as directional indicators for traction currents.

Several horizons of the Shemshak Formation are covered with ripple marks indicating generally south to north directed currents (Figs. I.5.3, I.5.4 and I.5.5).

5.4.5 Ball and Pillow Structure (Pseudonodules)

Pseudonodules are formed in sandstones by internal readjustments, mainly due to gravity (Pettijohn and Potter, 1964). They were seen at one locality near Shahpassand, where a sand body is interbedded in a thick interval of shale (Fig. I.5.6).

5.4.6 Cone-in-Cone Structure

These are calcareous concretionary features comprising a succession of cones, one within another, in an inverted position (apex down) with the axis normal to the bedding planes. They are generally found in more calcareous shales. One instance was seen in the lowermost part of the Shemshak Formation near Shahpassand, where a highly calcareous siltstone horizon exhibits cone-in-cone structure (Fig. I.5.7).

5.4.7 Nodules

Two different types of nodule were identified in the studied sequence: concretionary nodules and silica nodules.

Concretionary nodules are elliptical bodies of iron minerals as described in Section 5.2.3 and are common in the Shemshak Formation (Fig. I.5.1). This kind of nodule is believed to have formed above the water table (Pettijohn et al., 1972) and therefore to indicate continental sedimentation.

Some of the microconglomerate intervals of the Formation

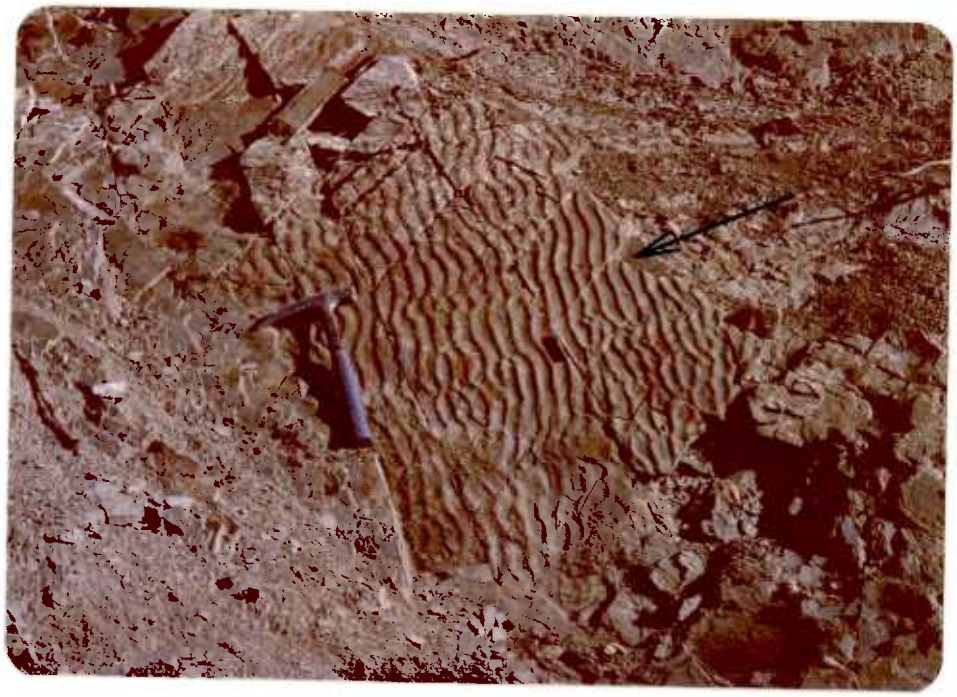


Fig. I.5.3 - Current (asymmetrical) ripple marks, showing the direction of palaeocurrents to the north, Shahpassand area.



Fig. I.5.4 - Current ripple marks along the Shahpassand-Shahrud Road near the village of Rudbar. The arrow indicates palaeocurrents directed to the north.



Fig. I.5.5 - Asymmetrical ripple marks on a hand specimen from the Shemshak Fm. The arrow shows the direction of current.



Fig. I.5.6 - Pseudonodules of sandstone in a shale interval of the Shemshak Fm. near Shahpassand.



Fig. I.5.7 - Cone-in-cone structure from a calcareous siltstone horizon in the lowermost part of the Shemshak Fm. near the village of Rudbar.

contain silica nodules, sometimes together with iron nodules. They average 2-5 cm in diameter and have no concentric structure.

5.4.8 Mud Cracks

Mud cracks are common in terrestrial sediments and indicate subaerial exposure. A few siltstone horizons of the Shemshak Formation exhibit mud cracks filled with ferruginous sandstone.

5.5 Biogenic Sedimentary Structures

Sediments may be disturbed after deposition by living organisms seeking food or housing or involved in the other activities of life. These disturbances produce features known as biogenic sedimentary structures or ichnofossils. The morphology of ichnofossils is believed to be controlled by the animals' behaviour (Seilacher, 1964)or by the environment (Crimes, 1970 and Heckel, 1972); they may therefore be valuable as palaeoenvironmental indicators. Burrows for example are commonly deep and vertical (scolithos) in the littoral zone because of scouring currents and wave action, but they tend to become shallower and horizontal in the deeper water zone.

A few horizons of the Shemshak Formation, especially at Jajarm, have ichnofossils. The lowermost part of the "Marine Shale" contains some vertical burrows and worm tracks (Fig. I. 5.8 and I.5.9).

5.6 Fossils and Age

A study of the flora and fauna, which have been well preserved in the Shemshak Formation, can be a useful contribution to the environmental analysis of the formation. Several beds throughout the formation contain well-preserved plant fossils, especially the "Carbonaceous Shale" (see Chapter 4, Stratigraphy) of the Shahpassand area. The Jajarm Section, on the other hand,

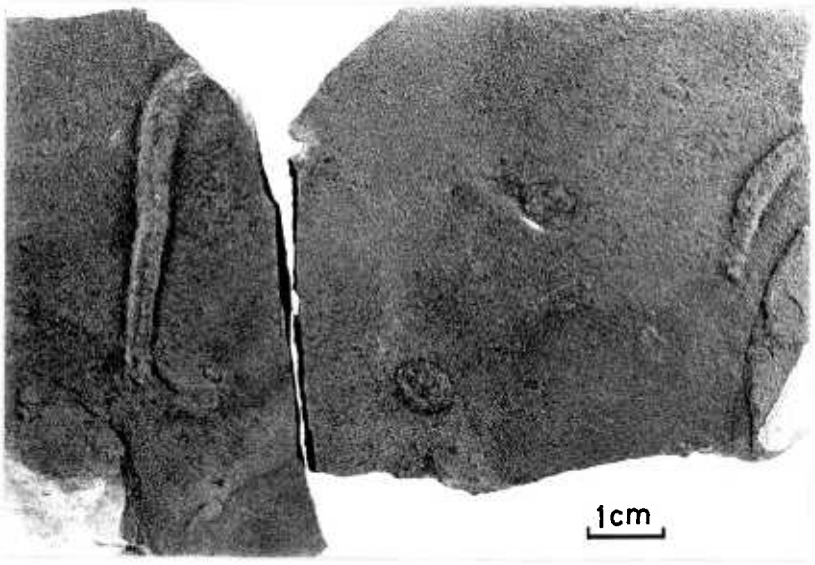


Fig. I.5.8 - Hand specimen from the basal part of the "Marine Shale" near Jajarm showing worm tracks and burrows.

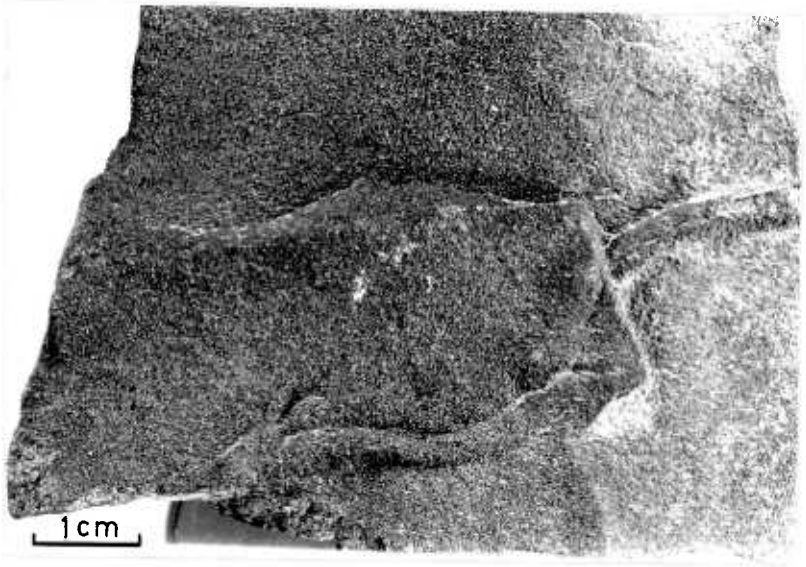


Fig. I.5.9 - Hand specimen from the Shemshak Fm. showing a worm track.

contains prolific ammonite-, belemnite- and lamellibranchia-bearing horizons which are virtually restricted to the "Marine Shale" and the "Lower Sandstone Member".

5.6.1 Megafossils

Flora- Plant fossils are among the most impressive features of the argillaceous beds and include fossilised leaves, trunks, branches and occasionally seeds (Fig. I.5.10). A number of previous authors have studied the plants collected from different localities. The majority have agreed on the Liassic age, but the presence of the Rhaetic is doubtful (Barnard, 1967 and Assereto et al., 1968). Assereto et al. (1968) distinguished three floral zones in the Shemshak Formation of the Central Alborz and also found some evidence to refer the upper part of the formation to the Middle Jurassic.

In the Eastern Alborz, the Shahpassand area is generally more prolific in plant fossils (Fig. I.5.11) than the Jajarm area. The Jajarm collection contained only poor and unidentifiable specimens. Identifications of the plants collected from the studied sections are shown in Table I.5.1; their age is given as Rhaetic (?) to Middle Jurassic (Jones, personal comm.).

Fauna- An assemblage of ammonites, belemnites, lamellibranchia, gastropods and a few echinoids (identified in thin sections) was found in the middle part of the Shemshak Formation near Jajarm (Fig. I.5.12), whereas the Shahpassand area is barren of marine mega-faunas. The fossils are confined to a few horizons of the "Lower Sandstone Member" and the "Marine Shale" (see Fig. I.4.5, loose, for details).

The ammonites have been the most useful organisms for dating purposes. Those collected from the studied area are from the Toarcian Stage of the Jurassic (Donovan, personal comm.), although one collection (JF5) was not precisely datable (Fig. I.5.13). Ammonites from the Central Alborz are, by way of comparison, referred to the Toarcian-Aalenian by Fantini Sestini (1966).

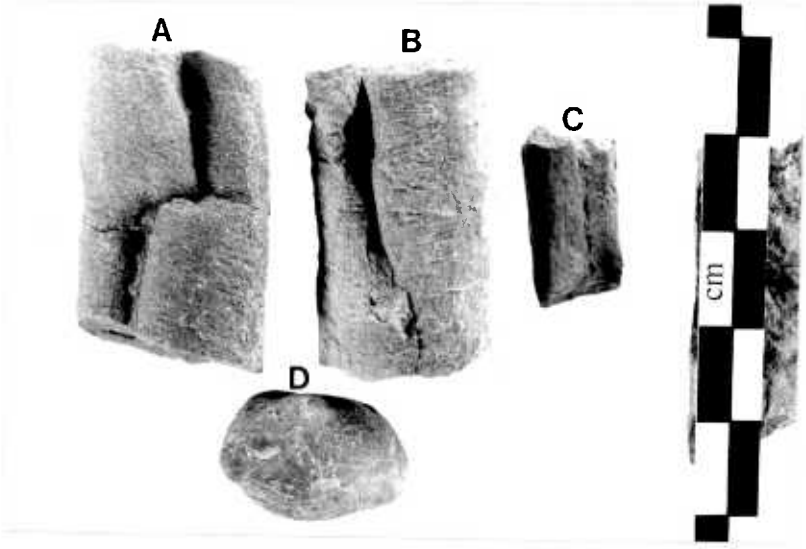


Fig. I.5.10 - Jurassic plant remains from the Shemshak Fm.
A,B,C) Fossilised branches.
D) Fossilised seed.

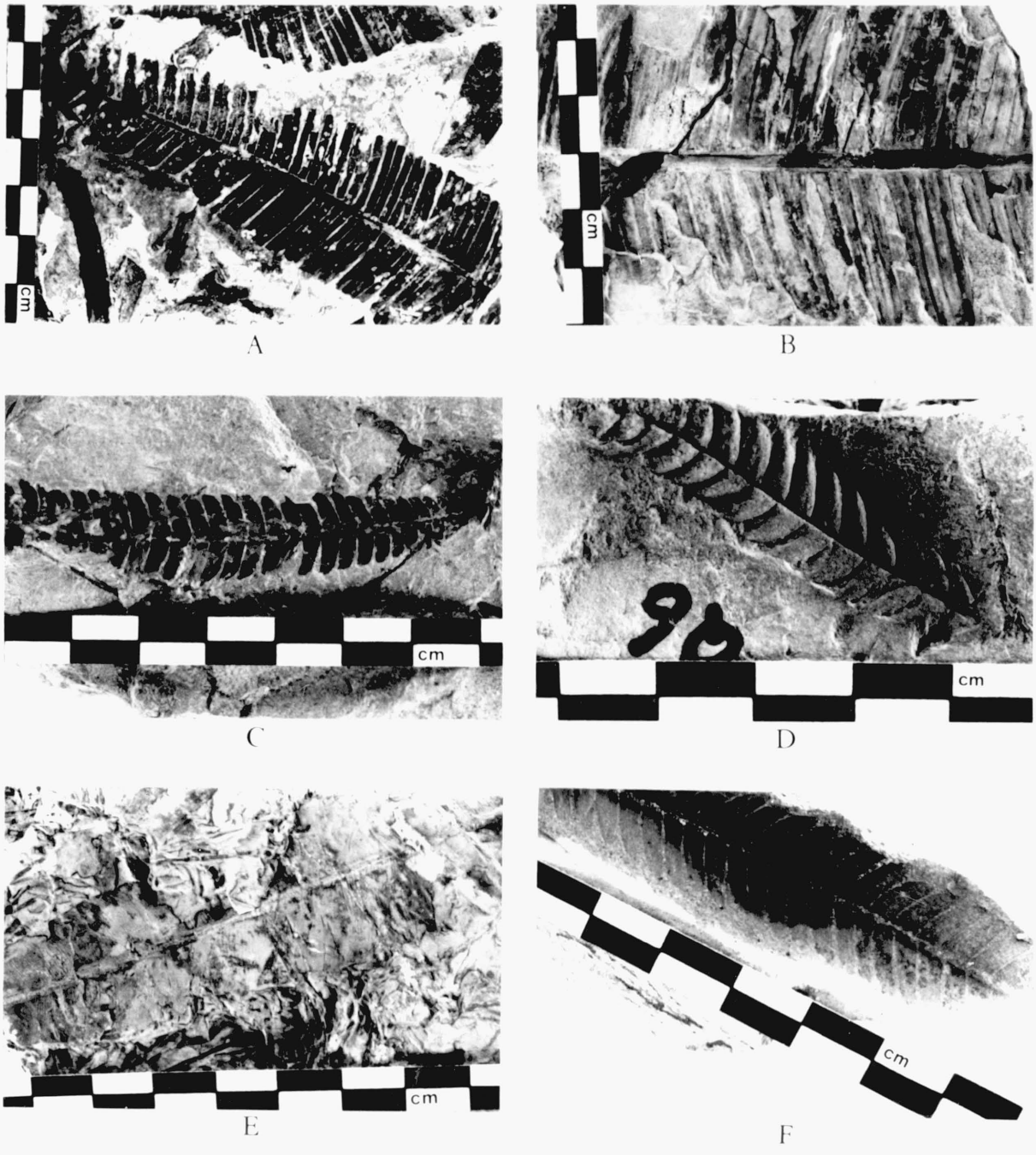


Fig. I.5.11- Plant fossils collected from the Shemshak Formation:

A- Nilssonia compta (Qoznavi Section)
B- Nilssonia cf pseudobrevis (Qoznavi Section)
C- Otozamites ashtarense (Qoznavi Section)
D- Otozamites cf ashtarense Barnard (Qoznavi Section)
E- Nilssonia orientalis Heer (Qoznavi Section)
F- Otozamites cf ptilophylloides (Qoznavi Section)

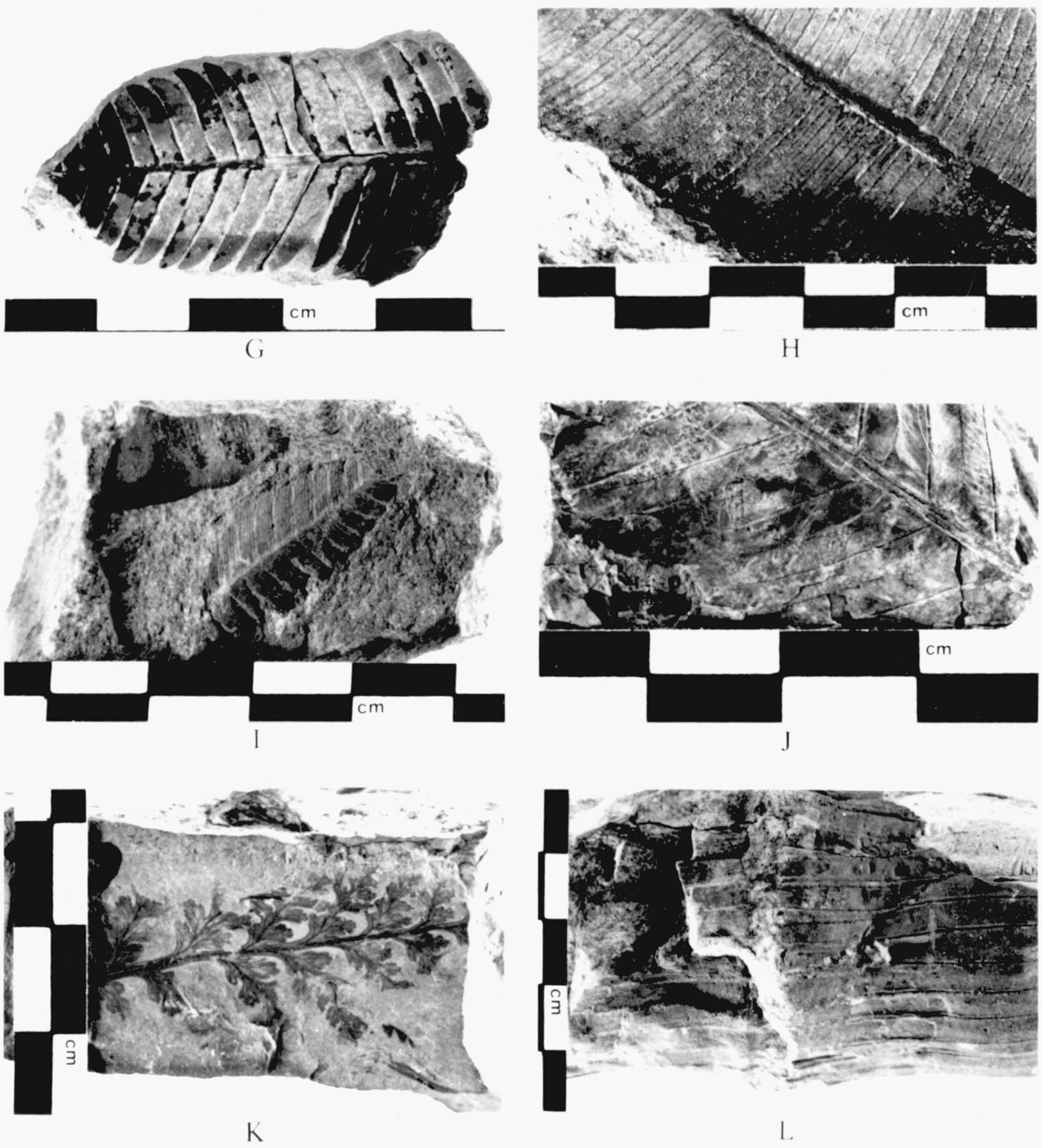


Fig. I.5.11- cont.

G- Nilssonia cf minor (Qoznavi Section)
H- Nilssonia sp. (Qoznavi Section)
I- Nilssonia cf viendalli (Qoznavi Section)
J- Cladophlebis sp. (Qoznavi Section)
K- Sphenopteris sp. (Qoznavi Section)
L- Neocalamites sp. (Qoznavi Section)



M



N



O



P



Q



R

Fig. I.5.11- cont.

M- Cladophlebis denticulata (Rudbar Section)
N- Nilssonia compta (Phillips) Goeppert (Rudbar Section)
O- Cladophlebis nebbensis (Nargess-Chall Section)
P- Cladophlebis nebbensis (Nargess-Chall Section)
Q- Otozamites cf ptilophylloides (Nargess-Chall Section)
R- Cladophlebis nebbensis (Brangniart) (Nargess-Chall Section)

Table I.5.1 - The flora of the Shemshak Formation in the Eastern Alborz.

Qoznavi Section	Rudbar Section	Nargess-Chall Section
Nilssonia orientalis Heer	Nilssonia compta (Phillips) Goeppert	Cladophlebis nebbensis (Brongniart)
Nilssonia compta	Cladophlebis denticulata (Brongniart)	Podozamites distans (Presl) Braun
Nilssonia cf minor		Podozamites sp.
Nilssonia cf viendalli		Nilssonia orientalis (Heer)
Nilssonia cf pseudobrevis		Otozamites cf ptilophylloides Barnard
Pterophyllum lavieri		Marratia cf munsteri (Goeppert)
Otozamites ashtarense		
Otozamites cf ashtarense Barnard		
Otozamites cf ptilophylloides		
Taeniopteris cf pterophylloides		
Neocalamites sp.		
Equisetum sp.		
Cladophlebis sp.		
Sphenopteris sp. (Sternberg)		

The plant fossils were kindly identified and dated by Miss. M. Jones of the University of Reading, England.

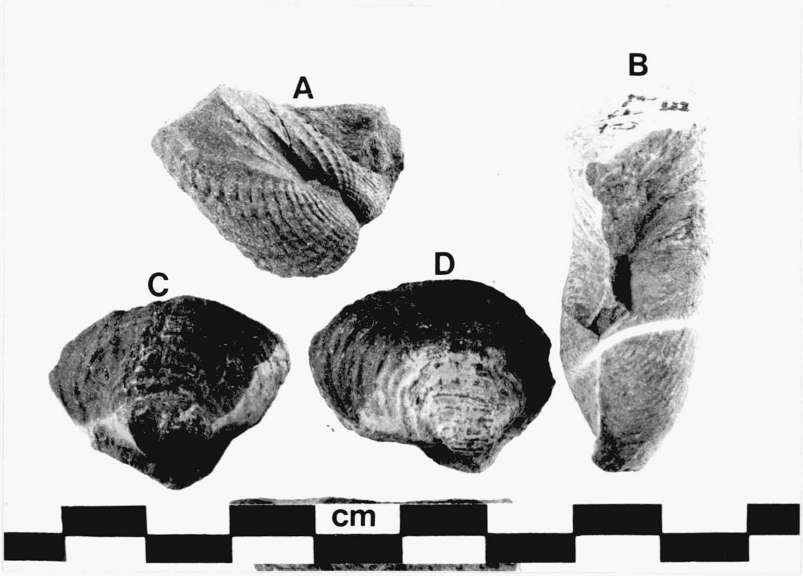


Fig. I.5.12 - Fauna collected from the "Marine Shale" interval of the Shemshak Fm. near Jajarm.

A) Pholadomya (Bucardium) sp.

B) Osteomya sp.

C and D) Unidentified bivalves.

Fig. I.5.13 - Ammonites collected from the Shemshak Fm. near Jajarm.

A)

1,2,3,4) Pleydellia leura (S.S. Buckman); Levesquei Zone, Aslensis Subzone

5) Pleydellia aalensis (Zieten)

B)

1,4) Pleydellia leura (S.S. Buckman); Levesquei Zone, Aalensis Subzone

2,3) Pleydellia aalensis (Zieten)

C)

1) Pleydellia sp.

2) Unidentified belemnite

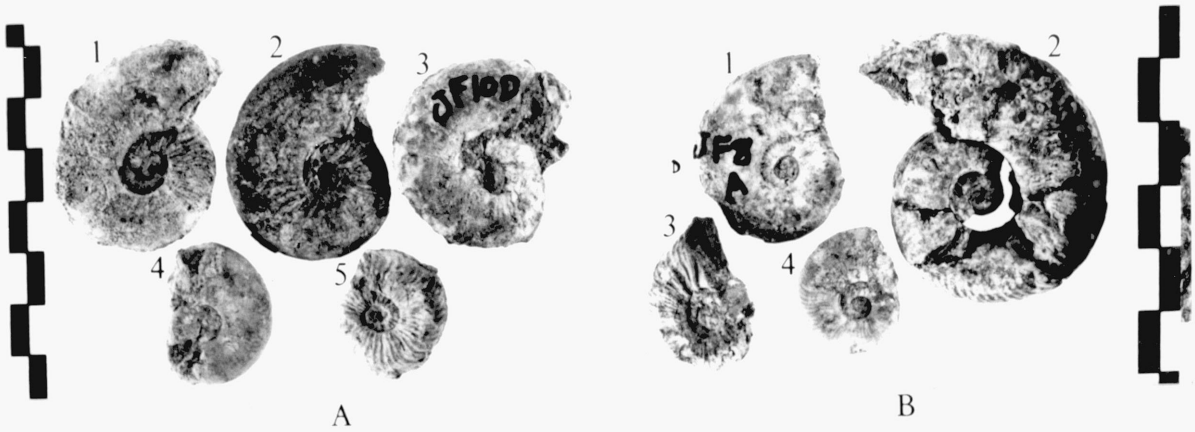
D)

1,2,3) Phlyseogrammoceras dispansum (Lycett); Toarcian: Levesquei Zone, Dispansum Subzone

E) Pseudogrammoceras sp. indet.; Toarcian: Thouarsense Zone, probably Fallaciosum Subzone

F) Haugia or Esericeras sp. indet.; ? Variabilis or Thouarsense Zone

G) Mercaticeras sp.; Lower Toarcian, ? Upper part

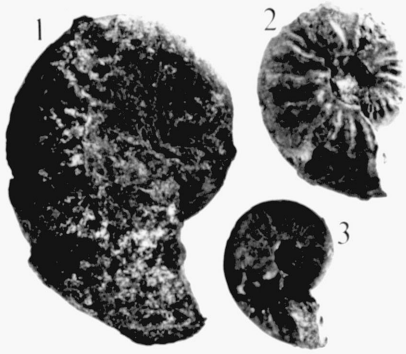


A

B



C



D



E



F



G

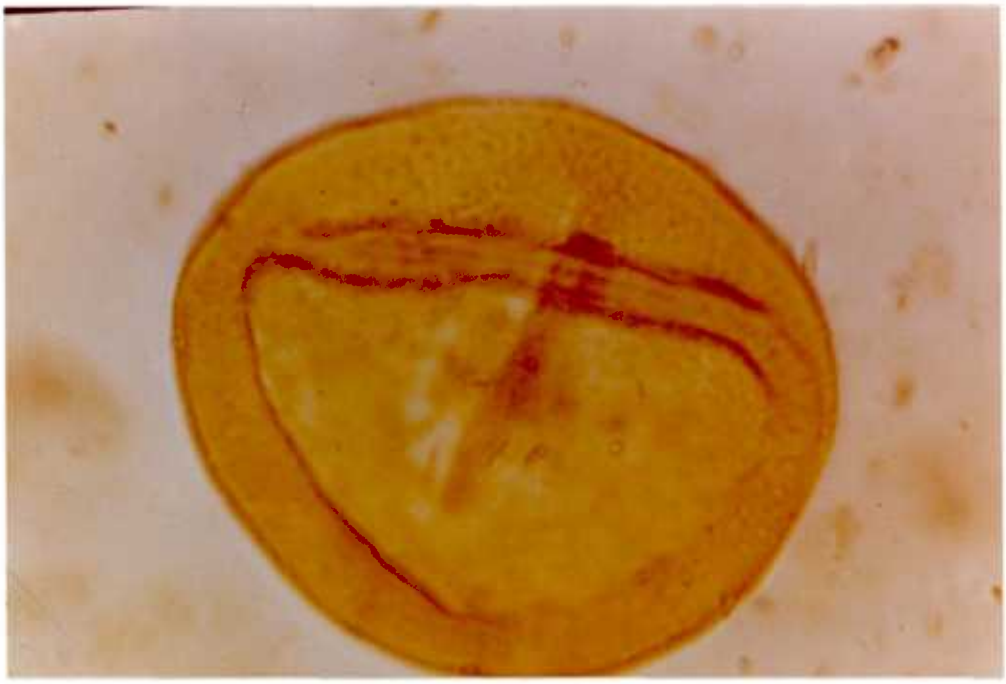
Affinity of the fauna- All of the ammonites identified from Jajarm have also been reported from the Badamu-Kalke Formation of South-Central Iran by Seyed-Emami (1967), and the fossiliferous rocks of Jajarm would appear to correspond in age to the lower part of that Formation. These ammonites are all genera which are common in the Toarcian of Northwest Europe, but no purely Tethyan elements (e.g. Phylloceras, Lytoceras) are present (Donovan, personal comm.).

Ecology- Ammonites and belemnites were pelagic animals and do not give much indication to the sedimentary conditions. Nevertheless, one fauna from the "Marine Shale" of the Jajarm Section (JF7) is accompanied by a number of burrowing bivalves, mainly genera which prefer rather quiet conditions (Donovan, personal comm.). This suggests a low-energy environment.

5.6.2 Microfossils

Foraminifera- Samples from different shale intervals of the Shemshak Formation were selected and processed for microfaunal analysis. All were barren of foraminifera, except those from the "Marine Shale" which yielded an assemblage of foraminifera, here reported for the first time. The assemblage includes: Planularia, Haplophragmiodes, Lagena, Trochammina, Vaginulina, Frondiculina, Lenticulina, Dentalina, Nodosaria, Spillina, Pyralina, Ramulina, Astacolus, Ammobaculites, Marginulinopsis, Polymorphinid, Lingulinopsis, and Ostracoda (Micropalaeontology Section, University College London, personal comm.); it is of Middle Jurassic age (see Chapter 4, Stratigraphy).

Spores and Pollen- Macerated samples of shale and siltstone were examined under the microscope and different types of palynomorphs were seen. They have not been studied in detail, but simple- and decorated-wall species are present including trilete, monolete, mono-sulcate, bi-sulcate, tricolpate or rarely Bisaccate varieties (Fig. I.5.14).



A

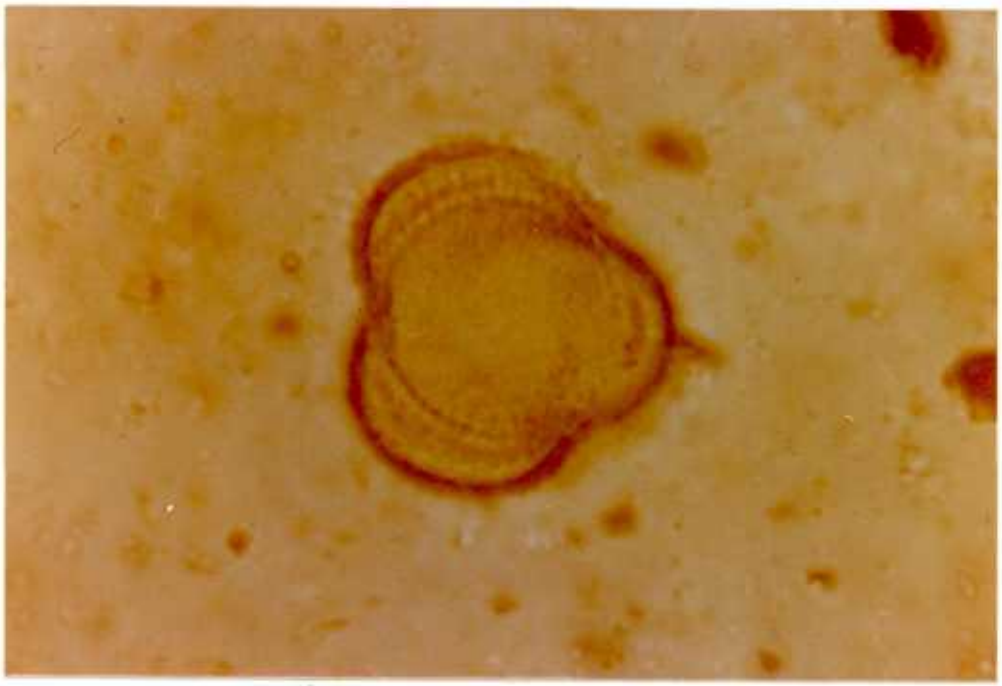


B

Fig. I.5.14 - Palynomorphs from the macerated kerogen concentrates of the Shemshak Fm.

A) Monolete (x 2640).

B) Trilete (x 2590).



C



D

Fig. I.5.14 - Continued.

C) Tricolpate (x 2600).

D) Bisaccate (x 1690).

5.7 Depositional Environment and the Controlling Factors

Although the Shemshak Formation is easily differentiated from the adjacent formations by its unique lithology, a single depositional environment cannot account for its various facies. A study of the lithology, sedimentary structures and fossil content of the formation suggests that a combination of near shore continental and marine environments is represented. The combination of terrestrial terrigenous deposits, plant-bearing shales, littoral sandy limestone containing mollusca, salt-water bearing shale with foraminifera, and several coal horizons suggests a complex delta system. This complex comprised alluvial plain, distributary channels, interdistributary bays, swamp, flood plain, sub-aqueous platform, and marine shelf as its subenvironments (Fig. I.5.15).

The six lithostratigraphic units that have been recognised in the Shemshak Formation of the Eastern Alborz are described in Chapter 4 (Stratigraphy). An attempt is made here to analyse and interpret their depositional environments (Fig. I.5.16). The basal disconformity associated with a zone of soil deposits indicates a period of subaerial exposure. Soon after the area emerged in Late Triassic time, weathering started in the highlands to the south. Newly formed drainage systems carried the weathering products and deposited them in the lowlying and nearshore regions, where they now overlie the basal soil horizon.

The "Alternating Shale and Sandstone" which forms the lowermost lithounit of the Formation represents a period of fluvial deposition. The sandstones were deposited by constructive currents, whereas the intervening shales with plant debris, such as fossilised leaves, accumulated as a result of episodes of flooding, possibly due to some local or regional subsidence.

The succeeding "Channel Sand Complexes", which exhibit a sudden increase of grain size and commonly-developed cross-bedding in festooned troughs, were deposited by strong currents, perhaps in the distributary mouth bars of a constructive delta system.

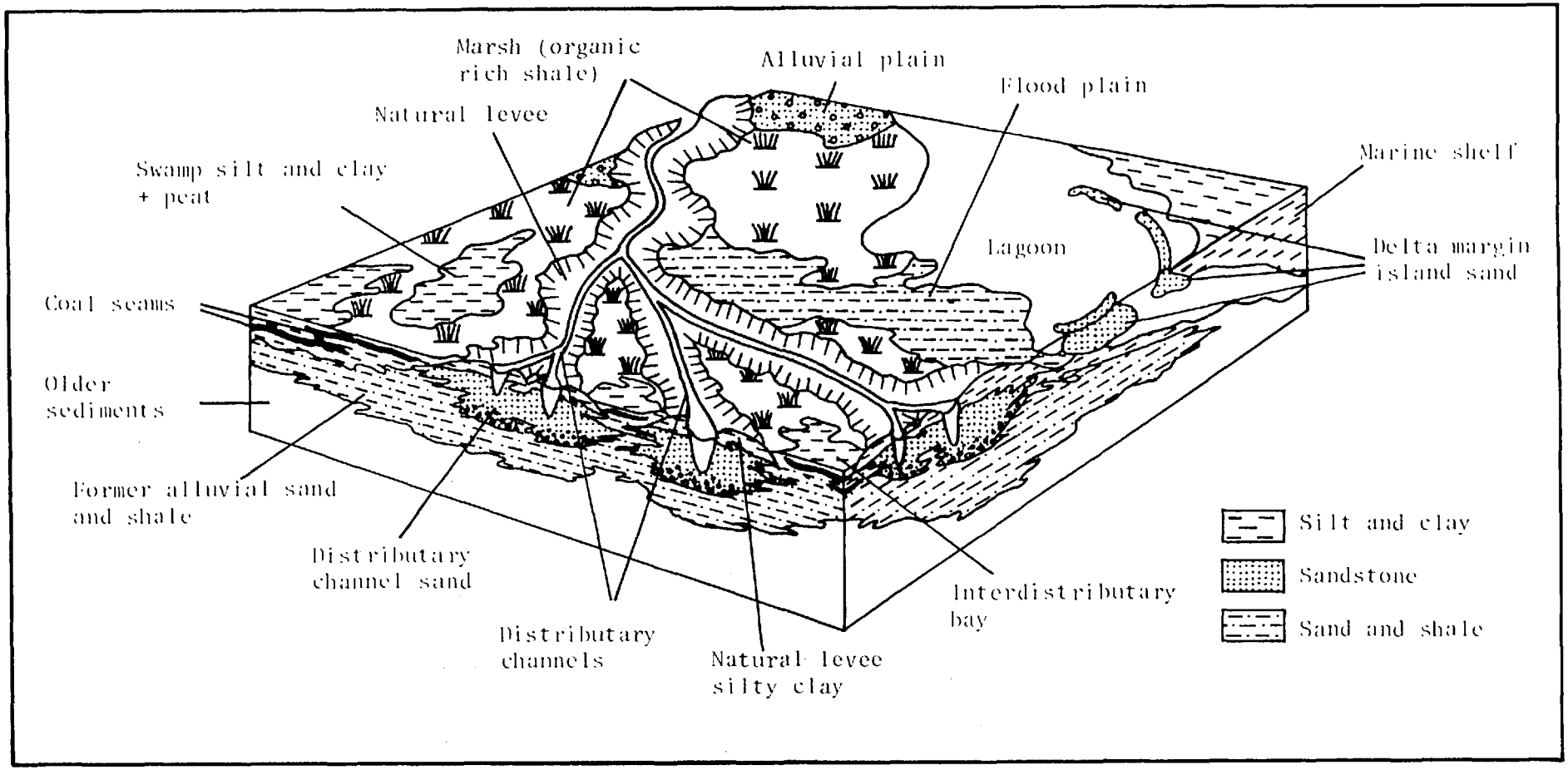


Fig. 1.5.15 - Subenvironments of the subaerial delta deposits of the Shemskah Fm. (modified from Frazier's Mississippi Delta, 1967).

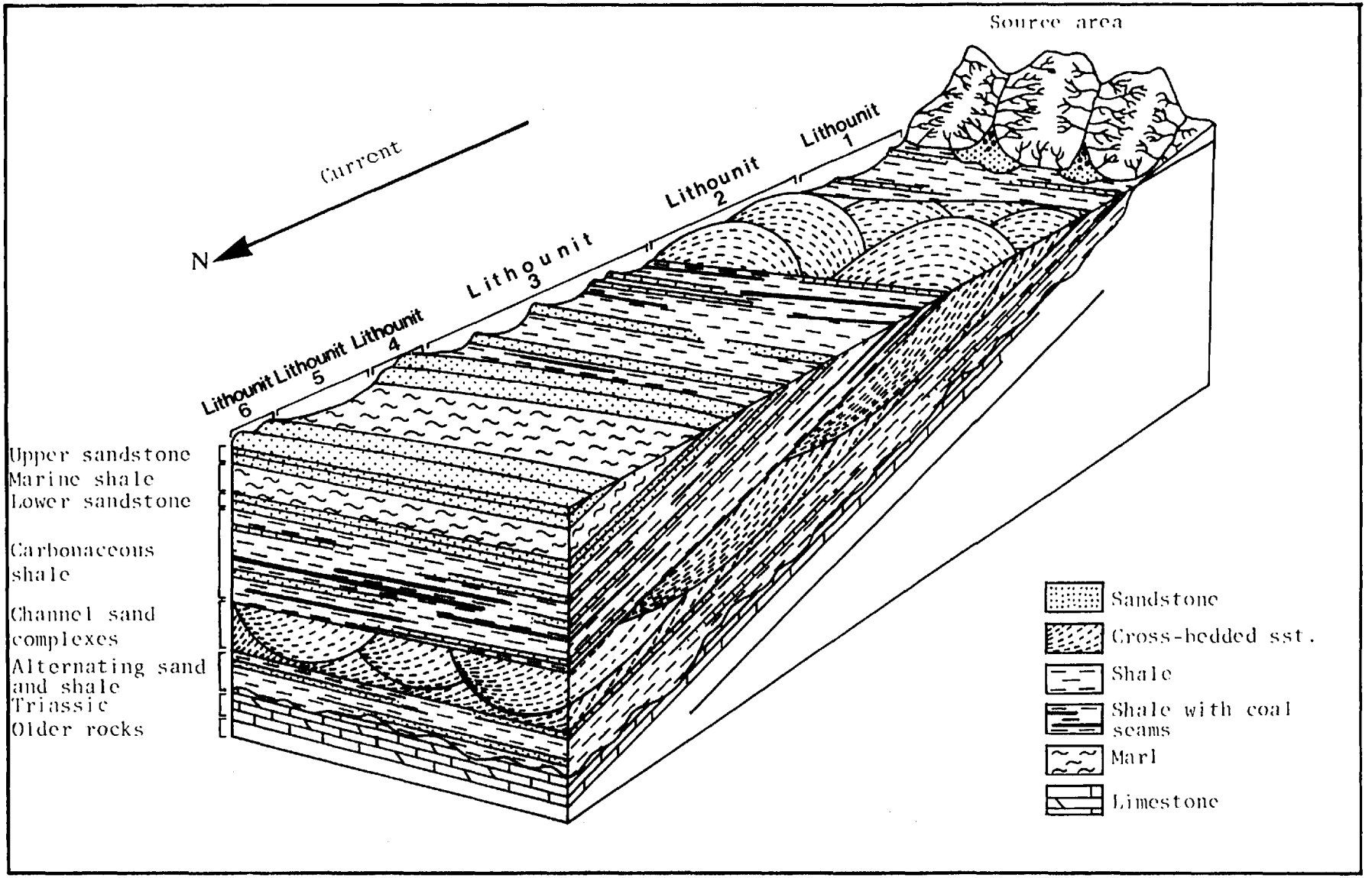


Fig. 1.5.16 - Block diagram illustrating the Shemshak Fm. lithostratigraphic units and the regional current direction.

The cross-sections of the sand bodies resemble big lenses surrounded by fine-grained sandy shale. Lithologically immature sediments and a complete absence of marine fossils, burrowing or other features which might indicate a marine influence (e.g. waves or tides) suggest a fluvial-dominated delta with an immense supply of land-derived materials and rapid deposition. The graded cycles formed by the recurrent shift of distributary channels crevassing their levees. Meanwhile the shale intervals were deposited in the abandoned distributary channels and across the flood-plain (delta plain). The low-lying swamps which apparently developed in some interdistributary bays were probably responsible for the occasional thin coal horizons in this part of the sequence.

The abrupt decrease in sandstone and the abundance of carbonaceous matter, which characterise the fine-grained laminated sediments of the "Carbonaceous Shale", are evidence of a low-energy environment. Numerous coal seams, abundant plant fossils, especially leaves and the upright trunks of Neocalamites, together with layers of laminated calcareous siltstone and claystone that locally change into chalky or limey horizons, all indicate a swamp environment. Several poorly sorted, cross-bedded sandstone beds probably mark the outburst of adjacent channels into the interchannel swamp.

There is no evidence of a marine influence in the Formation until after the deposition of the "Carbonaceous Shale". The marine invasion commenced during the period in which the succeeding "Lower Sandstone Member" was laid down. With a marine shale on the top, this lithounit can be regarded as transitional from continental into marine environments. A transgressive phase is recognisable from a gradual increase in the calcareous cement and other marine elements. Selley (1976) has suggested that, with increasing marine influence, deltas pass gradually into linear barrier islands; thus, with continental biota at the base and marine fossils above, the "Lower Sandstone Member" can be

interpreted as a barrier island in the offshore part of the delta platform. Although this lithounit shows some common features between the Shahpassand and Jajarm areas, important lithological and palaeontological differences exist (see Chapter 4, Stratigraphy). Embayment of the palaeoshoreline, with Jajarm and the Central Alborz representing embayments on either side of the Shahpassand area, was probably responsible for these differences (Fig. I.5.17).

The neritic origin of the "Marine Shale" is indicated by the presence of abundant shallow marine organisms including lamellibranchia, ammonites and benthonic foraminifera. The indications of the burrowing bivalves in the Jajarm Section suggest a low energy environment with little disturbance of the sediments, whilst the presence of sand grains and iron oxides point to some influx from the land.

Sedimentation of the Shemshak Formation in the Eastern Alborz ended with the deposition of the "Upper Sandstone Member" as a nearshore clastic body. A rudimentary regression of the sea was possibly responsible for this, which was then followed by a regional transgression that terminated the Jurassic clastic sedimentation in the area.

5.8 Sedimentary Basin and Palaeocurrents

The area which is now occupied by the Alborz Ranges became an elongated basin after the Late Triassic movements, with a ubiquitous gradual subsidence in the Jurassic during which a thick succession of sediments was accumulated (Fig. I.5.18). The concept of a geosyncline, as has been developed in the Alps, cannot be applied to the Alborz basin, eventhough the Alborz belt is a part of the Alpine-Himalayan Orogen. This is because Jurassic eugeosynclinal elements have not been identified in the Alborz, the whole area of which formed part of an intra- or peri-continental shelf during the Mesozoic.

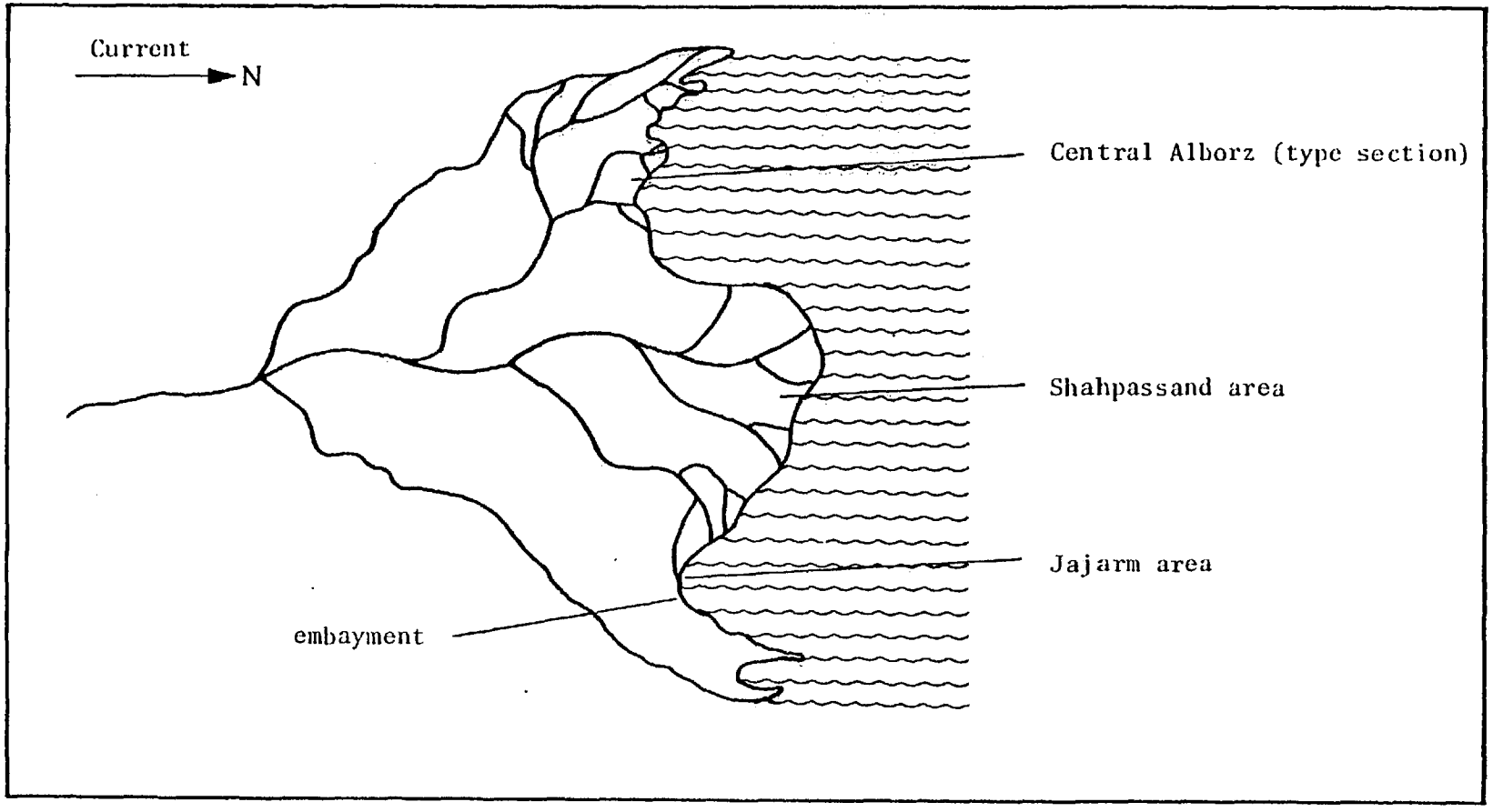


Fig. I.5.17 - Schematic diagram showing embayed delta plain of the Alborz during Early - Middle Jurassic time.

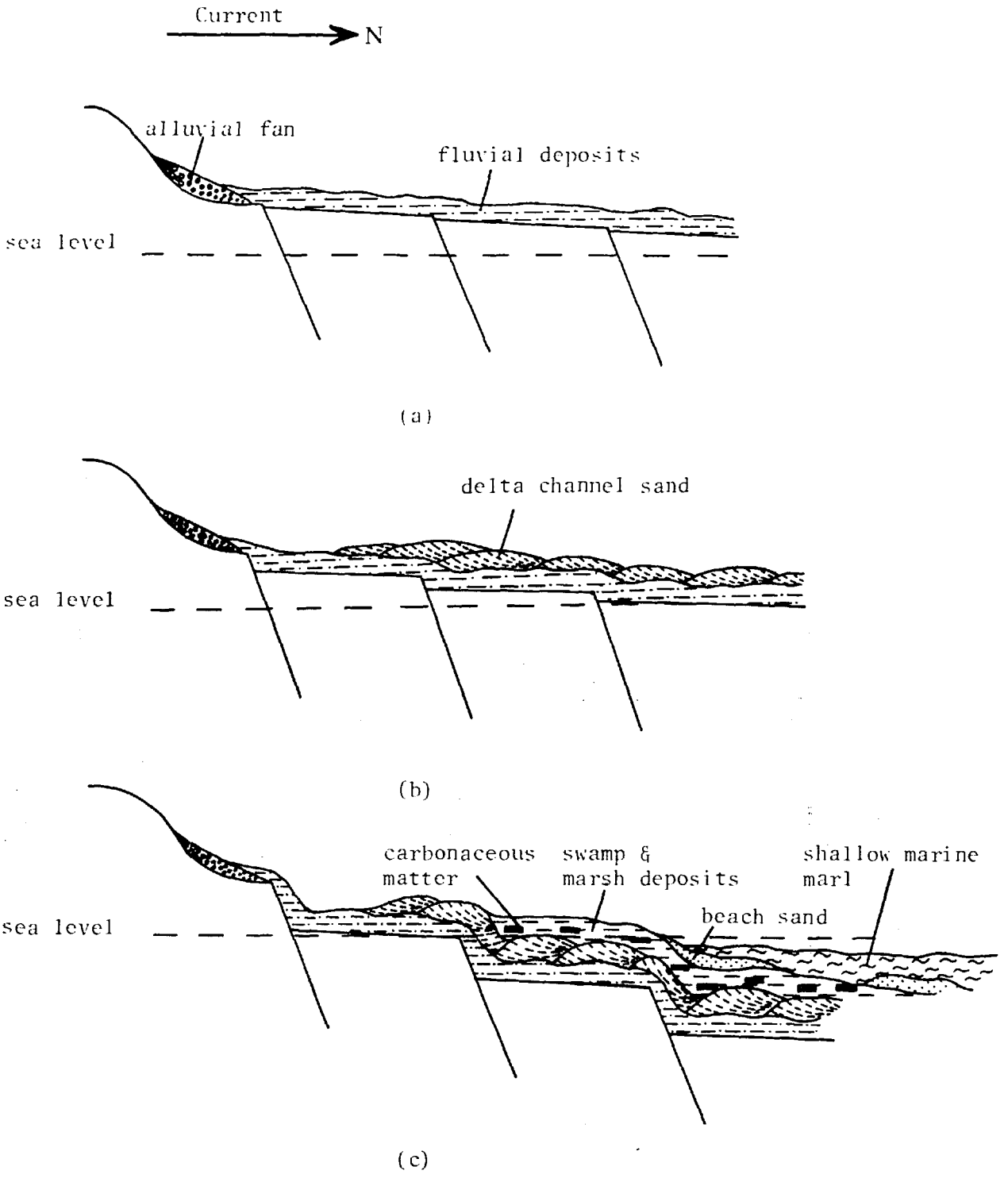


Fig. 1.5.18 - Development of the Shemshak Fm. under regional subsidence and late-stage marine transgression.

Palaeocurrent analysis is an important factor in the study of regional sedimentary models. Currents are slope controlled in fluvial and deltaic environments (Selley, 1976), where the sediments are normally characterised by a unimodal directional pattern. The Shemshak Formation, which is attributed to a deltaic complex, displays directional sedimentary structures indicating current transport predominantly from south to north.

Petrological study has shown that the sandstones of the Formation are immature first cycle sediments, with angular and subangular quartz particles, igneous and metamorphic grains, and locally abundant carbonate rock fragments. This suggests a source area close to the depositional basin, such as the uplifted southern margin of the Alborz which at that time was evidently composed of igneous and metamorphic rocks of possibly precambrian age. Infracambrian and Palaeozoic carbonates could have provided the calcareous fragments and the cementing material of the Shemshak rocks.

Geological data, particularly from the northern margin of the basin are insufficient to allow a complete description of the Alborz basin during the Jurassic. The following synthesis should therefore be regarded as somewhat speculative.

The Late Triassic uplift of the Alborz region resulted in a regional slope leading down from highlands in the south to a basin of sedimentation towards the north. Intensive weathering attacked this newly elevated area and a drainage pattern was established. The weathering products were transported northwards and many of them were deposited in a delta at the edge of the basin to the north. Subsidence of the basin permitted a continuous and rapid accumulation of sediment, particularly towards the north where, on the northern flanks of the Alborz, increased thickness of the Shemshak Formation has been observed (Assereto, 1966). Despite the high rate of sedimentation, a gradual transgression of the sea took place across the Alborz region and shallow marine sediments were deposited during the

Toarcian and Bajocian. Some of the sediment may have been carried further northwards by turbidity currents down the deltafront slope, or through submarine canyons, to be deposited as turbidites on the deep sea floor in what is now the Kopet Dagh region. An incipient regression led to the levelling of the shelf and the subsequent uniform accumulation of shallow-water carbonates across the entire region in the later Middle Jurassic.

PART II

ORGANIC GEOCHEMISTRY AND SOURCE ROCK EVALUATION OF THE SHEMSHAK FORMATION

CHAPTER 1

SOURCE BED CONCEPT AND GENESIS OF PETROLEUM

1.1 Introduction

The theory of an organic origin of petroleum was firmly established at the end of the last century, mainly by Engler and Höfer (Dott and Renolds, 1969, P.23), based on distillation experiments of animal and plant fats. This theory, which was formulated originally by chemists, has now been accepted by virtually all geologists and geochemists.

Fine-grained sedimentary rocks are believed to be the source of most petroleum. Among them shales, clay-shales and marls are the most promising. Andreev et al. (1958) described petroleum source rocks as ordinary sedimentary rocks containing a fraction of a percent to several percent of organic substances. Hunt (1975) specified source beds of petroleum as fine-grained clay or carbonate muds deposited in sedimentary basins under reducing conditions. More recently Tissot and Welte (1978) have generalised that all rocks which are capable of generating petroleum are to be called source rock. Dow (1978) differentiated between source beds and potential source beds. He described "source beds" as units of rock that have generated and expelled oil or gas in sufficient quantities to form commercial accumulations, and "potential source beds" as rock units which are capable of doing so, but have not done so because of insufficient thermal maturation.

Hunt and Jamieson (1956) postulated that practically all shales and carbonates contain indigenous organic matter disseminated in three forms: (1) soluble hydrocarbons, (2) soluble asphalt and (3) insoluble organic matter (kerogen).

Production, accumulation and preservation of undegraded organic matter are believed to be essential for the formation of petroleum source rocks. However, petroleum has originated only from a small fraction of the organic matter deposited in sedimentary

basins, depending on the type of organic material and the geological history of the basin. A certain minimum concentration of organic matter is necessary for a rock to be a potential source.

The organic matter in the source bed is either of allochthonous or autochthonous origin. Allochthonous organic remains are carried into the basin mainly from adjacent sediment source areas and are composed mostly of terrestrial organic debris (humic material); autochthonous organic remains, on the other hand, are *in situ* material and mostly have a marine origin.

The origin of sedimentary organic matter and details of the processes by which petroleum is generated in sediments were controversial issues for a long time. The main question was whether the hydrocarbon forming organic matter was of marine or terrestrial origin. Most earlier authors supported the idea of a purely marine origin and sedimentary strata rich in fish remains were considered as particularly favourable, even by a few later authors (e.g. Hobson, 1954). The contribution of terrestrial organic matter in petroleum generating source beds was also suspected by a number of investigators (Rainwater, 1963; Biederman, 1969), whereas others considered the animal remains to be the only source of petroleum; the plant remains being regareded as the source of coal. Stevens (1956) pointed out that the presence of hemin and chlorophyll porphyrins, which are optically active compounds, in crude oils was convincing evidence that both plant and animal remains were the source materials. This hypothesis was strongly supported by Hedberg (1964), who submitted further evidence in favour of it.

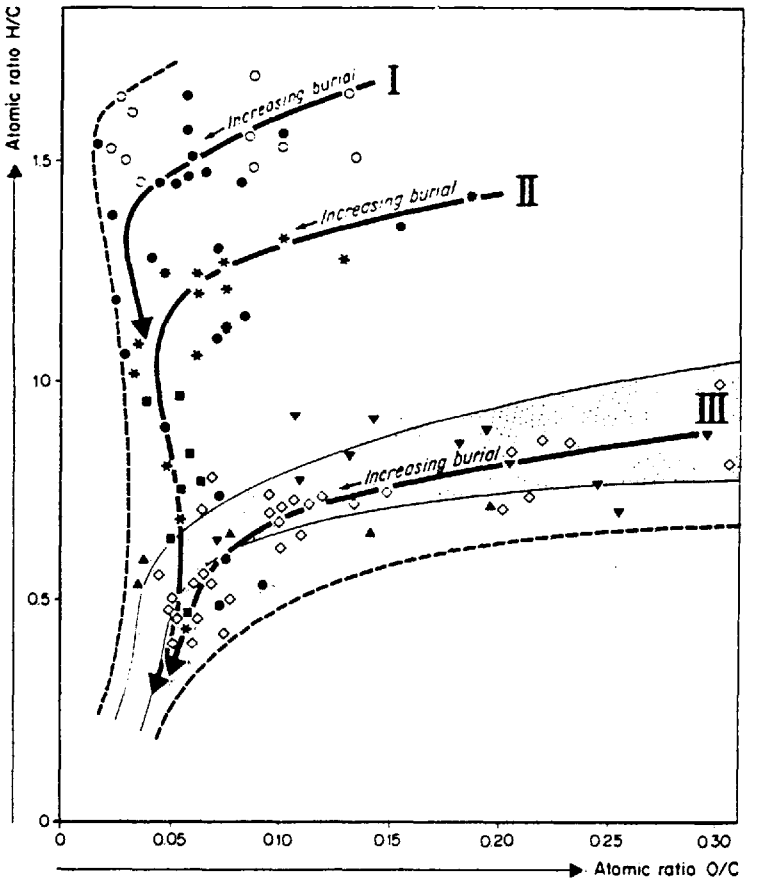
The name "kerogen" was later given to the insoluble organic matter found in source beds regardless of its origin. Two types of kerogen were described, the oily type which is capable of producing oil and the coaly type that generates gas. The more recent geochemical works by Barker (1974) and Tissot et al. (1974) made a big step forward in resolving the problem.

Tissot et al. classified kerogens according to their evolution paths (Fig. II.1.1) and described three types of kerogen: (1) kerogen type I which is rich in aliphatic structures and able to generate oil; (2) kerogen type III with a predominant aromatic structure, mostly from higher plants and terrestrial humic material and; (3) kerogen type II which is an intermediate type with an evolution path between the two former extremes.

Thanks to new approaches to source rock studies made possible by recent improvements in geochemical techniques (e.g. pyrolysis-gas chromatography), it is now clear that both marine and terrestrial organic matter are capable of producing oil and gas, but in different proportions.

Transformation of the organic matter of source beds into petroleum is controlled by numerous factors, mostly related to the geological history of the sedimentary basin. Andreev (1958) and Hedberg (1964) mentioned the significance of a number of these factors including microbial activities, temperature, presence of mineral catalysts, radioactive emanations, etc. The maturation processes of organic matter were divided into three evolutionary stages by Strakhov (1962) as: Diagenesis, Catagenesis, and Metagenesis; this is now accepted by most petroleum geochemists.

The direct genesis of hydrocarbons by organisms was postulated by some authors who believed that nearly all of the hydrocarbons occurring in a crude oil were formed at an early stage of sedimentary diagenesis. This idea was developed after the discovery of petroleum-like hydrocarbons in Recent sediments. However, quantitative and qualitative analyses have now proved that only a minor part of the hydrocarbons in crude oils were more or less directly generated by living organisms (about 10%). The techniques include pyrolysis-gas chromatography (P-GC), combined gas chromatography-mass spectrometry (GC-MS) and vitrinite reflectance (VR); they are now widely utilised in source rock



Main path of humic coals (after Durand et al, 1976)
Boundaries of the field of kerogen
Evolution paths of the principal types of kerogen

Type	Age and /or formation	Basin, country	
I	Green River shales (Paleocene - Eocene)	Uinta, Utah, U.S.A	●
	Algal kerogens (Botryacoccus, etc). Various oil shales		○
II	Lower Toarcian shales	Paris, France; W Germany	✱
	Silurian shales	Sahara, Algeria and Libya	■
	Various oil shales		◆
III	Upper Cretaceous	Douala, Cameroon	◇
	Lower Mannville shales	Alberta, Canada	▲
	Lower Mannville shales (Mc Iver, 1967)	Alberta, Canada	▼

Fig. II.1.1 - The evolution paths for different types of kerogen (after Tissot and Welte, 1978).

studies.

The detailed discussion of the source bed concept and the generation of petroleum is certainly beyond the scope of the present work. A comprehensive study of the subject has been recently published by Tissot and Welte (1978).

1.2 Characteristics of Source Rocks

Shales and marls are the source rocks of most petroleum accumulations, and it is the content and nature of the organic matter in the rock that are the prime factors in their characterisation.

For the recognition and characterisation of a petroleum source bed, determination of three critical factors is necessary. They are the amount, the type and the stage of maturation of the organic matter. Several laboratory techniques, of different degrees of efficiency, are used and they are summarised in Table II.1.1.

1.2.1 Amount of Organic Matter

The amount of organic matter in a rock is normally determined by measuring its total organic carbon content (C_T). Ronov (1958) gave an empirical lower limit of 0.5% organic carbon for a shale to be regarded as a source rock. Dow (1977) suggested that, under the most favourable conditions, a lower limit of about 0.4% organic carbon, which he considered as equivalent to 0.5% total organic matter, is required before significant expulsion can be effected. Tissot and Welte (1978) stressed the need for a conversion factor to estimate the total organic matter from the organic carbon content (Table II.1.2). This factor represents a compensation for presence of the other major elements in kerogen, such as H, O, N, and S, and it varies according to the type and state of maturation of organic matter.

The effective lower limit of organic carbon is believed to

Table II.1.1 - Principal techniques used for source rock analysis and their degree of efficiency (after Tissot and Welte, 1978).

Class of the analysis	Type	Abundance of organic matter	Quality = type of organic matter	Maturation of organic matter	Correlation between source-rock and petroleum
Chemical (on rock)	Organic carbon	●			
Optical microscopy	Transmitted light (Palynofacies, alteration)		●	●	
	Reflected light		•	●	
	Fluorescent light		●	●	
Pyrolysis (on rock)	Rock-Eval	●	●	●	
	C_R/C_T, etc. ...		•	•	
Physicochemical (on kerogen)	Elemental analysis		●	●	
	Infrared spectroscopy Thermal analysis (TGA) Electron microdiffraction		•	•	
	ESR		•	•	
	Carbon isotopes		•		•
Chemical (on bitumen or crude oil)	Amount of HC			●	
	Light HC			●	•
	n-Alkanes		•	●	•
	Isoprenoids		•	•	•
	Steroids, terpenes		•	•	●
	Porphyrins, metals			•	●
Physical (on bitumen, oil or gas)	Carbon isotopes		●	●	●

Efficiency ● Good or excellent ● fair • low or limitations of use

Table II.1.2 - Conversion factors for estimation of total organic matter from organic carbon content (after Tissot and Welte, 1978).

Stage	Type of kerogen			Coal
	I	II	III	
Diagenesis	1.25	1.34	1.48	1.57
End of catagenesis	1.20	1.19	1.18	1.12

be about 0.3% for carbonates. Gill (1978) has given empirical Figures for marine and grey-green shales as commonly 1%, for algal oil shales commonly 5 to 10%, marls rarely more than 2.5% and argillaceous limestones normally less than 1% of organic carbon.

The accumulation and preservation of organic matter in sedimentary rocks are mainly controlled by the environment of deposition. The deposition of sediments rich in organic matter is believed to be restricted to aquatic environments (Tissot and Welte, 1978). Bitterli (1963) asserted that palaeogeographic turning points, which resulted in either transgression or regression, often created favourable conditions for the formation of bituminous sequences. The importance of the deltaic environment was emphasised by Rainwater (1963), who stated that rapid subsidence and sedimentation, and great organic productivity are the requirements for petroleum formation. Depositional areas on continental shelves, such as lagoons, estuaries and basins with limited water circulation, are the most favourable environments for organic rich sedimentation. According to Dow (1978), the continental slopes provide the most favourable depositional environments for the production of aquatic, petroleum-generating organic matter.

1.2.2 Type of Organic Matter

Detailed geochemical studies of the ancient and recent source beds have demonstrated that different types of organic matter have different potentials for the generation of hydrocarbons. Thus, identification of the type of organic matter is essential for source rock evaluation. The origin of organic matter deposited in sediments is either marine or terrestrial. Marine organic matter is described mainly as disseminated and amorphous material, whereas terrestrial organic matter is characterised by angular plant debris and structured tissues. Most sediments, however, contain a mixture of the two, and their relative concentrations

are different for different source rocks.

Atomic H/C ratios of organic matter are considered to be indicative of their hydrocarbon generating abilities. Lijmbach (1975) stated that a high H/C ratio of the source material is indicative of oil and gas generation, while humic material with a low H/C ratio appears to be a source for gas only. Ishiwatari et al. (1978) concluded that terrestrially derived organic matter constitutes a poor source material for hydrocarbons, because of its highly oxidised nature. Harwood (1977) suggested that organic materials (kerogen) with an original atomic H/C ratio above approximately 1.00 are oil (and gas) sources, whereas those with H/C ratios between 0.80 and 1.00 are wet-gas sources; dry gas sources normally have H/C ratios below 0.80. More recently, Larter and Douglas (1978) described the use of low-molecular-weight aromatic hydrocarbons to ascertain the type of organic matter.

In general, aquatic organic matter is deposited in sediments under reducing conditions and is believed to generate both oil and gas, if sufficiently buried, whereas terrigenous organic matter is deposited mostly under oxidising conditions and produces mainly gas.

1.2.3 State of Maturation of Organic Matter

Perhaps the most important requirement for source rock evaluation is a determination of the state of maturation, by the actions of heat and time, of the organic matter incorporated in the rocks. Maturation studies are carried out to resolve whether or not the rock could have generated petroleum.

Many physical and chemical properties of organic remains in a source rock are subject to alteration during their thermal evolution. By means of these properties, the extent of maturation of organic matter can be determined (Fig. II.1.2). Vassoyevich et al. (1969) noticed that the principal phase of

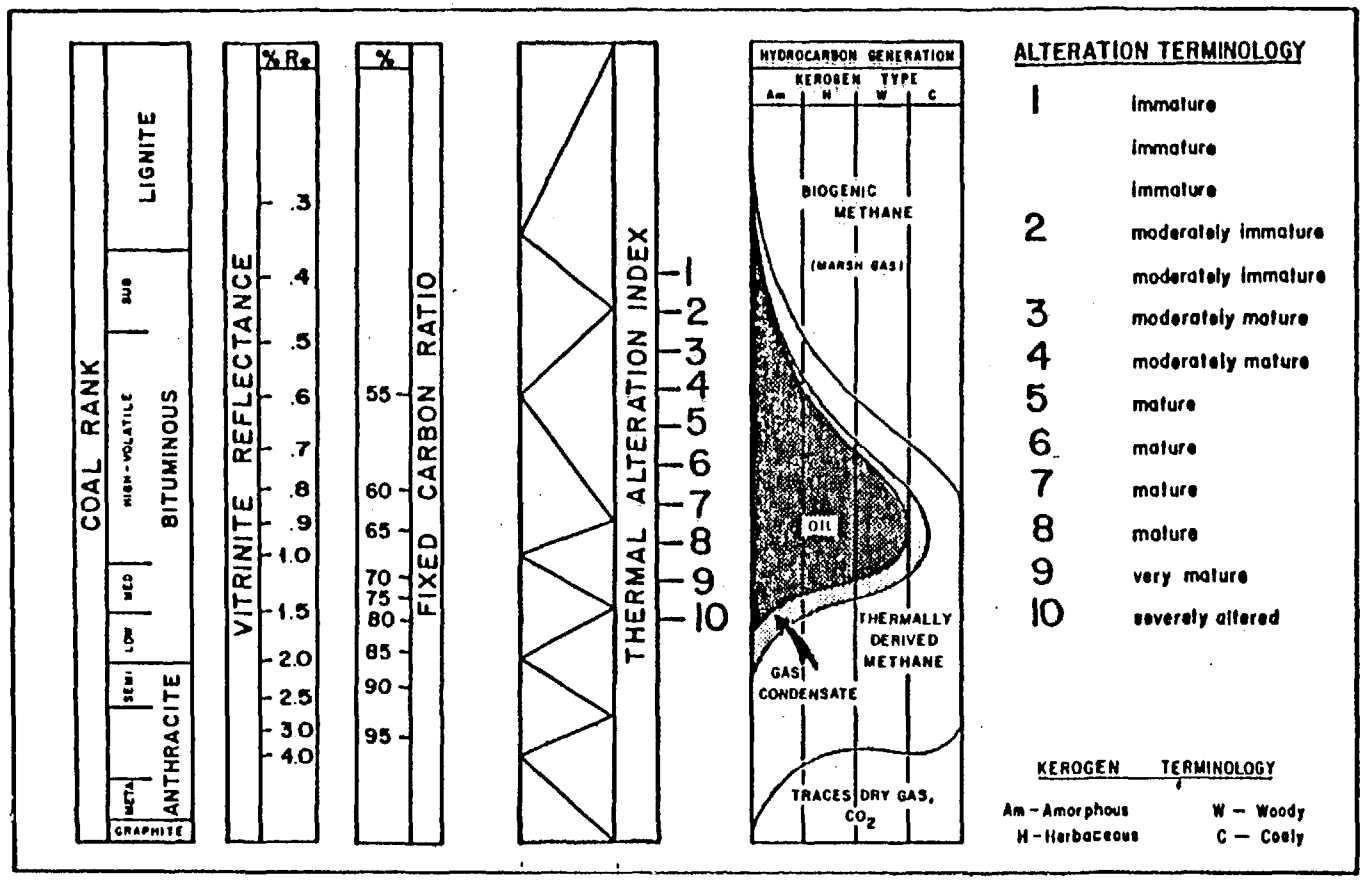


Fig. II.1.2 - Geothermal evolution criteria.

oil formation coincides with a specific carbonisation* jump. But it has now virtually been established that different types of organic matter (kerogen) undergo different thermal evolution paths. Therefore, the changes in composition due to maturation processes will depend on the type of kerogen.

Different optical and geochemical techniques are now being used to measure the degree of maturation. Claypool et al. (1978) studied the organic matter in black shale members of the Phosphoria Formation in the United States and concluded that: (a) thermally immature sediments are characterised by low extractable hydrocarbons relative to organic carbon and bitumen contents, by kerogen of yellow to brown colour, and by atomic H/C ratios greater than 1.1; (b) thermally mature sediments are distinguished by extractable hydrocarbon contents in excess of 1% of the total organic carbon, kerogen of brown to dark brown colour, and atomic H/C ratios in the range of 1.1 to 0.6 and; (c) incipiently metamorphosed sediments have extractable hydrocarbon contents less than 0.2% of the total organic carbon and brownish-black to black kerogen with atomic H/C ratios in the range of 0.6 to 0.4. They also studied the composition of extractable hydrocarbons in samples from the Meade Peak Shales and concluded that there is a preferential loss of aromatic hydrocarbons relative to saturated hydrocarbons with incipient metamorphism.

Pyrolysis techniques have been used widely in petroleum source rock studies. Gransch and Eisma (1966) proposed the C_R/C_T** ratio to evaluate the degree of maturation of a source

* Carbonisation is a thermal process marked by the generation of volatiles relatively rich in oxygen and hydrogen, and by the formation of a kerogen residue increasingly enriched in carbon (Laplante, 1974).

** C_R = total organic carbon after pyrolysis at 900°C.
C_T = total organic carbon before pyrolysis.

rock. C_R/C_T ratios less than 0.6 indicate immature source rocks containing low aromatic kerogen with high genetic potential. In contrast C_R/C_T values more than 0.6 either denote a high potential source rock after maturation or an aromatic-rich kerogen with low genetic potential. Gill (1978) used a plot of C_R against C_T to describe the state of maturation of source beds from different basins.

Pyrolysis studies have shown that in the absence of migration the ratio $HC_p/(HC_p + HC_g)$ increases with increasing temperature (depth of burial), where HC_p is "the amount of hydrocarbon already present in the rock" and HC_g represents "the amount of hydrocarbon generated during pyrolysis". This ratio, which was initially suggested by Barker (1974), can be used as an index of source rock maturation. The $HC_p/(HC_p + HC_g)$ ratio is independant of the type of organic matter during catagenesis and metagenesis (Tissot and Welte, 1978).

The distributions of heavy n-paraffins (C_{15+}) are subject to progressive changes during the thermal maturation of sedimentary organic matter. Study of the organic content of Recent sediments has shown that a strong predominance of odd-carbon-numbered to even-carbon-numbered heavy n-paraffins exists in them. This predominance is believed to disappear gradually with the degredation of kerogen, mainly in the stage of oil formation (Fig. II.1.3). Bray and Evans (1961) gave a formula to indicate the relative predominance of odd-to even-carbon-numbered heavy n-paraffins (carbon preference index):

$$CPI = \frac{1}{2}\left(\frac{C_{25} + C_{27} + C_{29} + C_{31} + C_{33}}{C_{24} + C_{26} + C_{28} + C_{30} + C_{32}} + \frac{C_{25} + C_{27} + C_{29} + C_{31} + C_{33}}{C_{26} + C_{28} + C_{30} + C_{32} + C_{34}}\right)$$

High CPI values (above 1.5) suggest a relatively immature source rock, while low values might indicate higher maturity. The CPI is highly affected by the type of organic matter and is always used in conjunction with other geochemical analyses.

Gas chromatographic analyses of saturated hydrocarbons are also now used widely to describe the type and maturation level

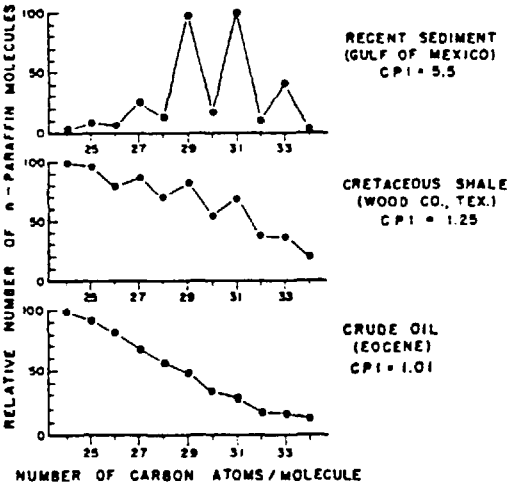


Fig. II.1.3 - n-paraffin distribution in sediments and crude oils (after Bray and Evans, 1965).

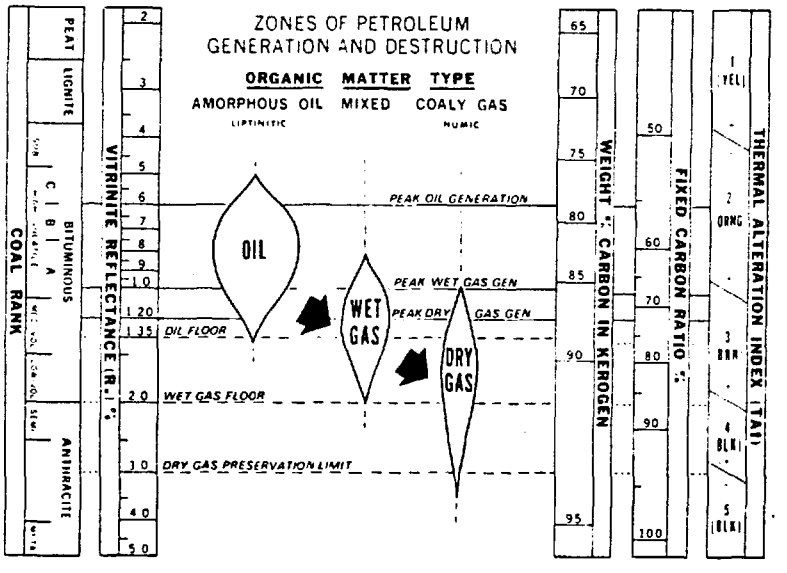


Fig. II.1.5 - Correlation of the coal rank and vitrinite reflectance scales with some other maturation indices and zones of petroleum generation (after Dow, 1977).

of sedimentary organic matter. The thermal cracking of heavier alkanes into lighter compounds is the basis of this method. The chromatogram of the extractable saturated fraction of an immature sample shows a dominance of high molecular weight compounds, whilst a dominance of lower molecular weight compounds can indicate a higher degree of thermal maturation (Fig. II.1.4). The ratio of isoprenoids to n-alkanes is also believed to decrease with depth in all types of organic matter (Rashid, 1979).

Microscopic examination of palynomorphs has shown that their colour progressively changes with increasing thermal maturity. The original colour is light-yellow and it then changes to orange, brown and black (Staplin, 1969).

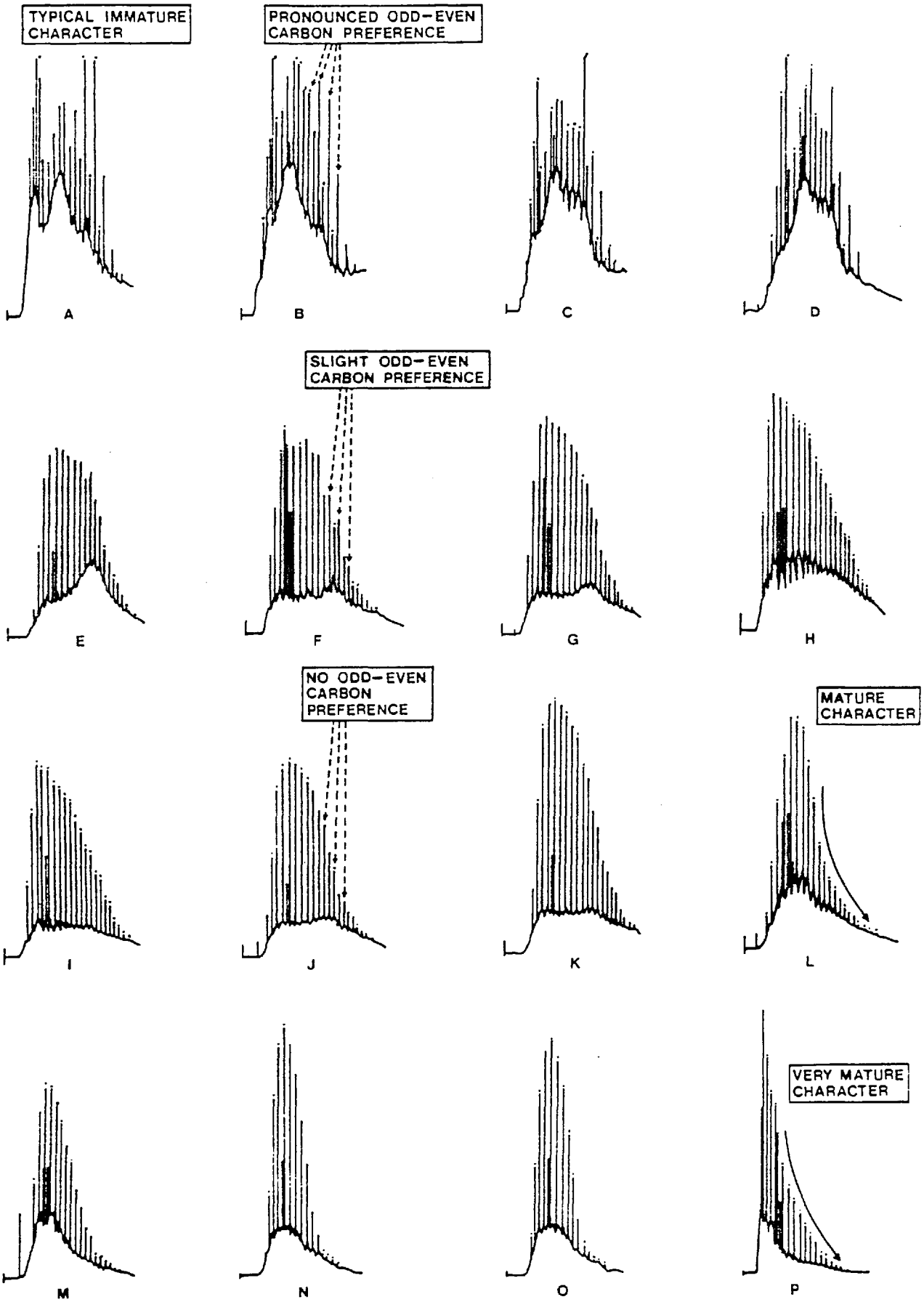
Vitrinite reflectance is now considered as a standard maturation index for kerogen. Vitrinite reflectance is the only maturity measurement which increases exponentially with thermal maturation and it is not affected by the composition of the kerogen (Dow, 1977). The reflectance range of 0.6 to 1.35 represents the principal phase of oil generation, or the "oil window". Figure II.1.5 shows the correlation of the vitrinite reflectance scale with other maturation indices. A linear numerical scale of organic metamorphism, the level of organic metamorphism (LOM) was proposed by Hood et al. (1975).

Other techniques have also been used to measure the degree of maturation of organic matter. They include the use of carbon isotope ratios and electron spin resonance (ESR).

1.3 Kerogen and Its Convertibility

The organic matter in petroleum source rocks is composed essentially of a solvent-extractable fraction called "bitumen" and an insoluble fraction named kerogen. The term kerogen, therefore, is applied to a wide variety of organic mixtures. Coals, kerogen and asphalts all originate from sedimentary organic matter; they reflect differences in source materials,

Fig. II.1.4 - Hydrocarbon maturity as shown by gas chromatography of alkanes.



dispersal, environment of deposition and diagenesis (Hunt, 1975, Fig. II.1.6). Kerogen is essentially the diagenetic product of the original sedimentary organic remains. It has a complex chemical composition, and is believed to be the main source of commercial hydrocarbon reserves. Tissot and Welte (1978) described kerogen as a macromolecule made of condensed cyclic nuclei linked by heteroatomic bonds or aliphatic chains.

Determination of the type of kerogen is essential for source rock evaluation, because the hydrocarbon generating potential is related directly to its chemical composition. Micro-organisms and plant remains are the main contributors to all sedimentary kerogens, and differences in chemical composition may reflect their marine as opposed to terrestrial origin, as well as the extent of their microbial degredation. The environment of deposition is thus a major factor in the hydrocarbon generating potential of the kerogen.

Kerogens can be divided into "sapropelic" and "humic" types according to the physical appearance under the microscope of their constituents. The sapropelic type is composed of finely distributed and amorphous particles, while the humic variety consists of angular and structured particles mainly derived from plant debris.

McIver (1967) emphasised that the amounts of hydrocarbons that a kerogen can generate is a function of its original structure, hydrogen content and to a lesser extent its oxygen content. He added that the coaly type of kerogen may be derived primarily from the carbohydrates, lignin, and humic acids that are the precursors of coal, whereas the oily type consists predominantly of derivatives of lipids. Hunt (1975) noted that the more coaly type of kerogen is derived mainly from nitrogenous and humic residues of both continental and marine plants, whereas the oily type is the amorphous remains of plankton and high lipid residues of spores and pollen.

On the basis of microscopic studies, the subdivisions of

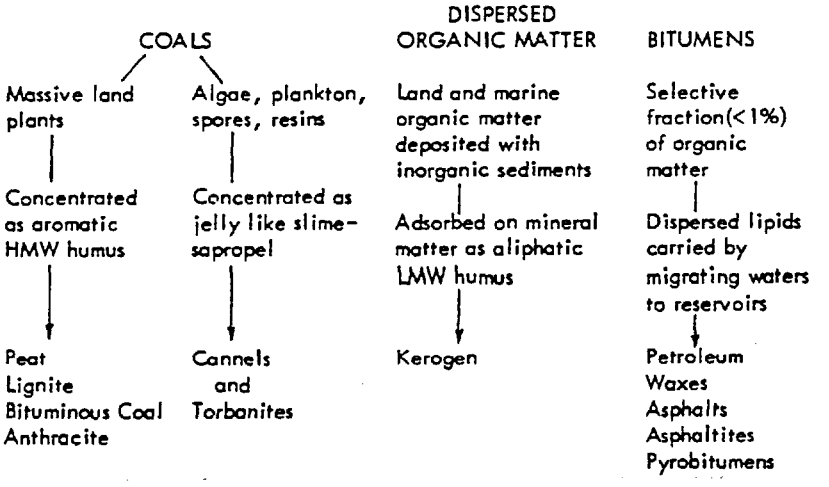


Fig. II.1.6 - Origin of organic sediments (after Hunt, 1975).

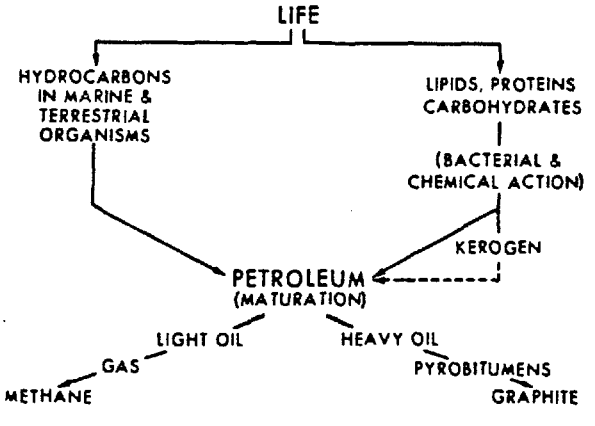


Fig. II.1.8 - Origin of petroleum (after Hunt, 1975).

the coal macerals may be recognised also in sedimentary kerogens, from their similar optical properties and fluorescence. These macerals are liptinite (alginite or sporinite), vitrinite (huminite), and inertinite. The liptinite and vitrinite groups are capable of yielding petroleum, but inertinite has no hydrocarbon generating potential.

Tissot et al. (1974) differentiated three types of kerogen according to the evolution paths shown by changes in their elemental composition. They compared their classification with the one proposed by Van Krevelen (1961), and noted that the evolution paths of their kerogen types I, II, III on the H/C, O/C crossplot diagram resemble the carbonisation paths, reported by Van Krevelen, of alginite, exinite and vitrinite respectively.

The classification of kerogen introduced by Tissot et al. (1974) designates kerogens as type I, type II, and type III, but no geochemical names are proposed for them. The following terminology is suggested by the present writer for kerogen types, augmenting the physiochemical descriptions given by Tissot and Welte (1978): Alginite (type I), Sapropelite (type II), Huminite (type III), and Inertinite (recycled organic debris).

1.3.1 Alginite (type I)

Alginite is composed mainly of structured algal material and organic matter enriched in lipids by microbial activity. This type of kerogen is rich in aliphatic chains, containing very few polyaromatic nuclei and heteroatomic bonds. The initial hydrogen content (H/C) is high (more than 1.0), but the oxygen content is low and it decreases mainly during diagenesis. The hydrocarbon generating potential of alginite is high and represents up to 80% convertibility by pyrolysis.

1.3.2 Sapropelite (type II)

Sapropelite is the most abundant kerogen in petroleum source beds, and is usually composed of autochthonous organic matter of

marine origin which was deposited in a reducing environment. Sapropelite consists mainly of sapropelic organic matter, together with some algal particles and planktonic remains. Minor terrigenous material may also be present. Polyaromatic nuclei and compounds with heteroatomic bonds are more abundant in the chemical structure of this type of kerogen than in the alginite group. Substantial amounts of sulphur are also present. The initial hydrogen content (H/C) is relatively high and the oxygen content (O/C), although more than in alginite, is generally low. The sapropelite group provides commercial sources for oil and gas, and shows up to 60% convertibility by laboratory pyrolysis.

1.3.3 Huminite (type III)

Huminite is derived mainly from allochthonous terrestrial organic matter containing usually higher-plant humic and coaly material. Huminite contains a high proportion of condensed polyaromatic nuclei and oxygen rich heteroatomic compounds with minor amounts of the aliphatic group. The initial hydrogen content (H/C) is low (usually less than 1.0) and the oxygen content (O/C) is relatively high (more than 2.0). This type of kerogen is found especially in deltaic environments, where the high rate of sedimentation permits only limited microbial degredation of the organic matter. Huminite is one of the main sources of gas reserves, but its oil generation potential is low. It has a lower convertibility by pyrolysis (about 35%; Tissot et al., 1974) than alginite and sapropelite.

1.3.4 Inertinite

Inertinite consists mostly of reworked organic residues and coal particles from older sediments. Inertinite is considered as dead carbon, because it shows no convertibility to hydrocarbons by pyrolysis (Dow, 1977). The initial hydrogen content (H/C) is very low, whereas the percentage of organic carbon is very high ($H/C \simeq 0.4$ or less).

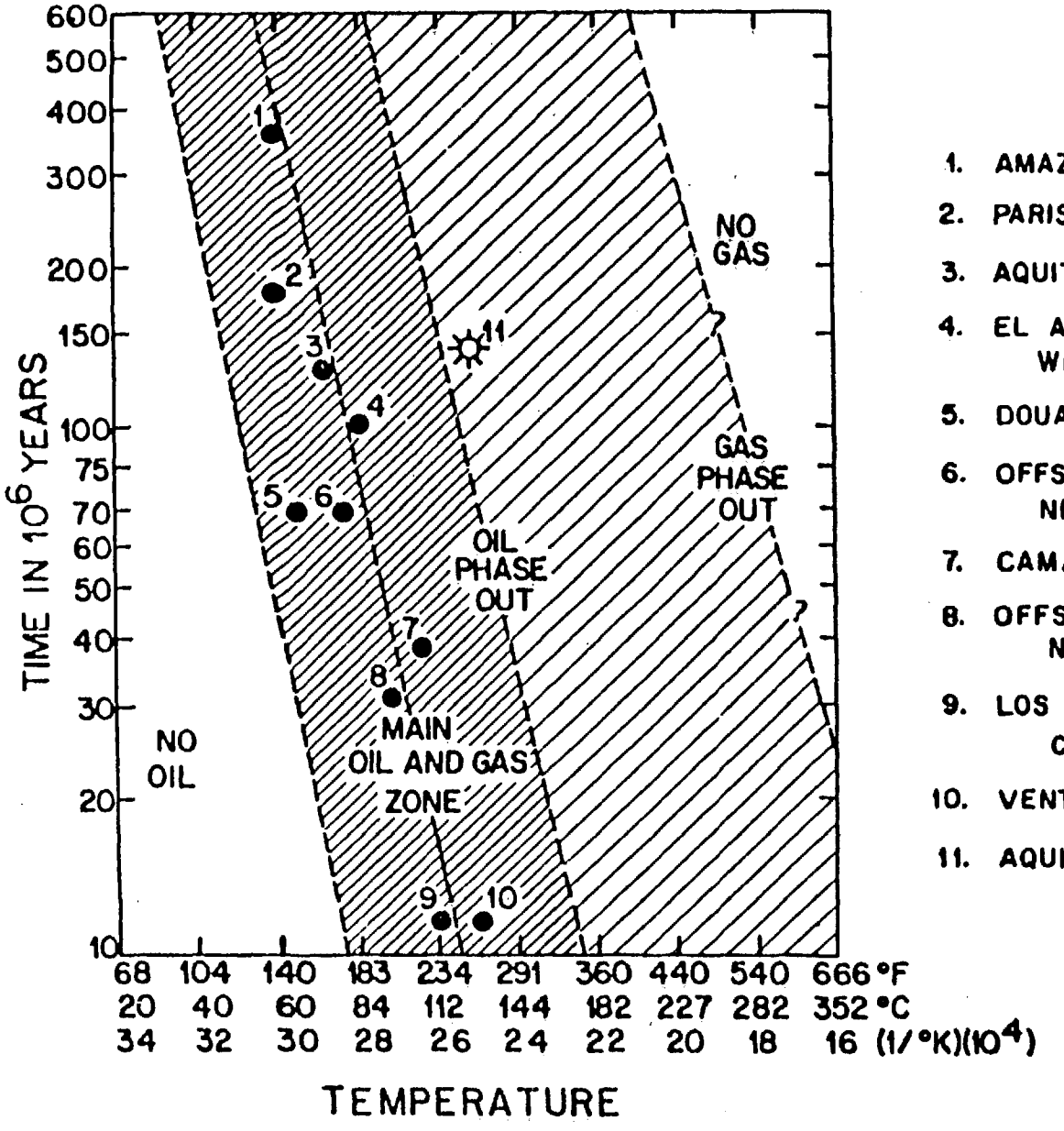
1.4 Transformation of Organic Matter in Sediments and Generation of Petroleum

It is generally agreed in the literature that sedimentary organic matter is converted by microbial action, early in its maturation history into the complex polymer known as "kerogen". The thermocatalic cracking of kerogen into petroleum, as a result of increasing burial (temperature), follows this early diagenetic stage. Further increases in depth of burial and the effects of time cause the destruction of the originally generated petroleum and its conversion into lighter hydrocarbons and, in the final stage, to methane. The transformation of kerogen into hydrocarbons begins gradually beyond a certain threshold and then takes place very rapidly with its thermal breakdown. This period of evolution is termed the principal phase of oil formation (Vassoyevich et al., 1969).

Phillipi (1965) and Laplante (1974) pointed out the importance of time and temperature in generation of oil. The amount of oil generated is believed to increase linearly with time, but exponentially with the absolute temperature (Phillipi, 1965) (Fig. II.1.7). Temperature, time, and pressure are believed to be the major controlling factors in petroleum genesis.

The discovery of petroleum-like hydrocarbons in Recent sediments raised the theory of direct genesis of petroleum from organisms. Hedberg (1964) stated that these hydrocarbons differ significantly from those of crude oil and those extracted from ancient sediments, and it is now clear that less than 15% of the hydrocarbons (Hunt, 1975) were more or less directly derived from organisms incorporated in sediments (Fig. I.4.8). The main fraction of the hydrocarbons found in sedimentary rocks must therefore have been formed by bacterial and chemical processes acting on the original organic matter, and kerogen is the product of the first stage of this conversion. With increasing depth of burial and temperature, the heteroatomic bonds of the kerogen structure break down successively according to its evolution

Fig. II.1.7 - Time-Temprature of petroleum genesis (after Canon, 1974).



CODE

1. AMAZON BASIN, BRAZIL
2. PARIS BASIN, FRANCE
3. AQUITAINE BASIN, FRANCE
4. EL AAIUN AREA, RIO DE ORO, WEST AFRICA
5. DOUALA BASIN, CAMEROON
6. OFFSHORE TARANAKI BASIN, NEW ZEALAND
7. CAMARGUE BASIN, FRANCE
8. OFFSHORE TARANAKI BASIN, NEW ZEALAND
9. LOS ANGELES BASIN, CALIFORNIA
10. VENTURA BASIN, CALIFORNIA
11. AQUITAINE BASIN, FRANCE

path (Tissot et al., 1974). This cracking starts with the carbonyl and carboxyl groups causing a partial removal of the contained oxygen. As the temperature continues to rise, newly generated hydrocarbons, especially aliphatic groups, are released and they increase exponentially as the process continues. Further evolution sees the breaking of C-C bonds and the generation of gas, by the cracking of both the kerogen and the petroleum already formed in the rock. During these transformation processes the residual kerogen becomes more condensed and its carbon content gradually increases (Tissot et al., 1974).

Eisma and Jurg (1967) heated behenic acid mixed with clay minerals (illite) to study the generation of hydrocarbons. They noticed that the total amount of low-molecular-weight hydrocarbons and the percentage of n-alkanes increase as the temperature rises, but that the percentage of unsaturated compounds decreases up to 275°C and then increases very rapidly again above that temperature. Albrecht et al. (1976) studied the organic matter of the Douala basin (Cameroon) and noted that long-chain hydrocarbons are generated preferentially between 1200m and 2200m whilst below 2200m these molecules are cracked mainly into light oils and gas.

Kartsev et al. (1971) remarked that, because the main oil generating constituents are primarily lipoids rich in hydrogen with their polymerides mostly typical of sapropeclic matter that contains more aliphatic and polymethylenic structures, petroleum generation from sapropelic matter develops under lower thermodynamic conditions than that from humic matter. The importance of the hydrogen level, which is higher in sapropelic kerogen than in the humic variety, has also been noted by many others: Laplante (1974) concluded that kerogen having less than 6% hydrogen is principally a source for gaseous hydrocarbons, whereas kerogen with more than 7% hydrogen content satisfies the requirements for an oil source. Demaison (1975) also stated that the principal phase of oil generation is virtually

non-existent, regardless of the thermal regime, if the kerogen undergoing maturation is hydrogen poor.

Transformation of sedimentary organic matter from the time of depoisiton to the stage of incipient metamorphism can be divided into diagenesis, catagenesis, and metagenesis (Fig. II.1.9).

1.4.1 Diagenesis

This is the first stage in the evolution of organic matter and begins in newly deposited sediments. The main agent of transformation during early diagenesis, when temperature and pressure are low, is microbial activity by aerobic and then anaerobic micro-organisms. This biological destruction is followed by polycondensation and insolubilisation of degraded organic matter into kerogen. The most important hydrocarbon formed during diagenesis is methane (marsh gas), whilst CO_2 and H_2O are also given off. The main product of this diagenetic stage is kerogen, and its end is marked by a vitrinite reflectance of about 0.5%.

1.4.2 Catagenesis

The second and most essential stage in the transformation of organic matter to petroleum results from an increase in temperature with depth of burial (50 to 150°C). The thermal degredation of kerogen produces firstly liquid hydrocarbons containing long-chain compounds and then, at later stages, wet-gas and condensates. Significant amounts of methane are also generated by cracking. Catagenesis embraces the principal stage of oil formation (Vassoyevich, 1969) and its end corresponds to a vitrinite reflectance of about 2.0%.

1.4.3 Metagenesis

This is the last stage of organic matter maturation prior to metamorphism and occurs either at great depth of burial or

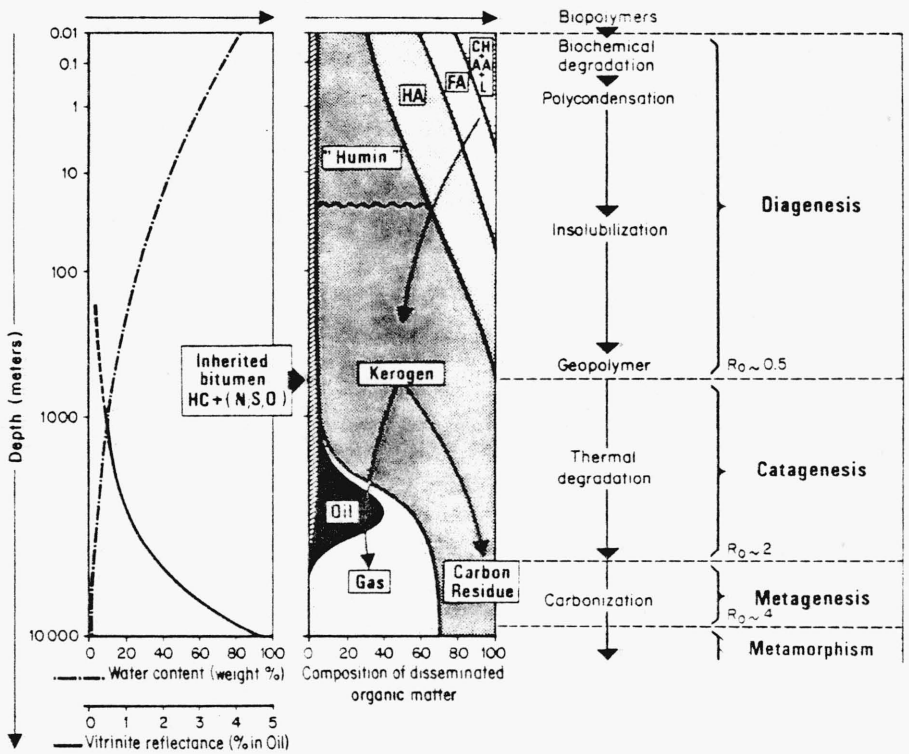


Fig. II.1.9 - Maturation scheme of organic matter from the time of deposition to metamorphism (after Tissot and Welte, 1978). CH: carbohydrates, AA: amino acids, FA: fluvic acids, HA: humic acids, L: lipids, HC: hydrocarbons.

adjacent to local hot spots (e.g. magma intrusions). At this stage mainly methane is formed from the remaining kerogen and, by the cracking of previously generated hydrocarbons, leaving residual carbon. A structural rearrangement of any remaining kerogen also develops. In terms of petroleum generation, the stage of metagenesis is entirely situated in the dry-gas zone (Tissot and Welte, 1978). The end of this stage is marked by a relatively high vitrinite reflectance (about 4%).

CHAPTER 2

FIELD WORK AND LABORATORY EXPERIMENTS

2.1 Introduction

To date, published information of the Alborz basin has been restricted to fundamental studies of the geology of the area, particularly in the Central Alborz; less attention has been paid to the Eastern Alborz region. To the writer's knowledge, no published record of the petroleum prospects or source rock studies of the area is available. The work presented in this thesis is thus believed to be the first detailed organic geochemical analysis of the potential Mesozoic source rocks of the Eastern Alborz region, although a detailed study of the geology of the adjacent Kopet Dagh basin and its regional source rock evaluation has recently been presented by Afshar-Harb (1979).

During the initial field reconnaissance, it became apparent that a few sequences in the studied area were suitable for petroleum source rock analysis. These were the Upper Devonian and Carboniferous shales, and the Shemshak, Bash-Kalateh and Chaman-Bid Formations of Jurassic age.

The Shemshak Formation was selected for geochemical study, because of its great thickness (average 1700m), its uniformity and its wide regional extent. The results of this study may be applied, to some extent, to the developments of the Formation elsewhere in Iran.

Afshar-Harb (1979) concluded that the Chaman-Bid Formation is the most attractive Mesozoic petroleum source rock in the Kopet Dagh region, but he added that his analyses of material from the Shemshak were insufficient for its full evaluation and he recommended a detailed study of it.

2.2 Field Sampling and Preparation of Specimens For Organic Geochemical Analysis

No shallow or deep core samples were available for the purpose of this study and the exploration boreholes drilled by NIOC (one near Gorgan and the other north of Gonbad-e Kavous) reached, but did not penetrate the Shemshak Formation. Samples were, therefore, collected by the writer from surface exposures along the measured stratigraphic sections: 225 were from the Shahpassand area and 42 from Jajarm. They were obtained from fresh exposures at depths of one foot or more in order to minimise the effect of weathering. A few samples suspected to be covered by a weathered crust were scrubbed before crushing.

The removal of organic contaminants by washing samples with distilled water or with organic solvents has been discussed by Davies (1978). Following Degens and Reuter (1962) he concluded that it is impossible entirely to remove organic contaminants without altering the incorporated organic matter. A review of the effects of weathering is also given by Davies (1978). Claypool et al. (1978), in a study of the Phosphoria Formation in the United States, concluded that, despite a slight change in chemical composition of their samples due to weathering, their results were not significantly affected.

2.2.1 Sample Frequency

The organic content of a rock sequence is subject to significant variation, both vertically and laterally, depending on several geological factors: lithology and environment of deposition are the most important. Short sampling intervals are therefore desirable, but time and experimental restrictions sometimes preclude them particularly in thick formations. Although an interval of about 50 metres may be adequate in uniform sequences for source rock identification (Gill, personal comm.), sample frequency must be adjusted to changes in lithology for a meaningful evaluation.

Because the Shemshak Formation exhibits irregular variations in lithology, no uniform sampling interval could be followed for this study. The samples were collected so that each one represented a particular lithological unit and the intervals between them thus varied from 2m to 150m (see Figs. I.4.3, I.4.4 and I.4.5, loose).

2.2.2 Pulverisation

In order to include all disseminated organic particles in the geochemical analyses, rock samples must be crushed and pulverised.

For the present work, a pestle and mortar of cast iron were used to reduce the samples to small grains of approximately 1/5 inch diameter. They were then pulverised in a Raymond Rotary Mill. The resultant powdered rock was composed of particles ranging from 0.104mm (150 Mesh) to less than 0.061mm (200 Mesh). An attempt was made to keep contamination by the particles remaining in the mill after use to a minimum. Such contamination is in fact negligible, considering the volume of each sample prepared.

2.2.3 Maceration

One of the steps in the study of kerogen and palynomorphs is to isolate the organic matter from the rock in such a way that its nature is not significantly affected. Various physical and chemical methods of kerogen isolation have been suggested by different authors, but the destruction of the mineral matter by hydrochloric and hydrofluoric acids (maceration) is most commonly used.

In the present work samples were ground firstly to grains of about 2-4mm in diameter; although a smaller grain size will accelerate the treatment, the palynomorphs are liable to be broken or destroyed. About 200-300 grams of each ground sample were treated with 10% to 20% hydrochloric acid to remove the

calcareous matter. Frankenberg and Giles (1970) noted that 10% HCl generally decreases the carbon content of the samples, and recommended 5% HCl; however, the changes of the organic carbon content, if any, as a result of HCl treatment were found to be negligible. Hydrochloric acid treatment continued for a few days, with fresh acid being added daily after partial decantation, followed by agitation. Later, after complete setting, the liquid was decanted to a minimum level and the samples washed with distilled water.

Hydrofluoric acid treatment in polyethene beakers was carried out in a fume cupboard. 60% acid was used; the sample was stirred and the acid partially replaced each day. The residue was then thoroughly washed to neutrality with distilled water. Finally, to prevent etching of the mounting glass slides by any possible remnant of the acid, a drop of ammonia solution was added to the 250ml sample container to achieve complete neutrality to standard blue litmus.

CHAPTER 3

AMOUNT AND TYPE OF ORGANIC MATTER

3.1 Optical Microscopic Description

3.1.1 Introduction

Microscopic examination methods have been widely utilised in coal petrology for a long time. More recently, similar techniques have been used in petroleum source rock studies by a number of geochemists (Peters et al., 1977; Dow, 1977; Tissot and Welte, 1978; Shibaoka et al., 1978; and others). They can be applied to identify the quality of organic matter (transmitted and fluorescent light) as well as its degree of maturation (reflected light, and translucency). Three optical properties of the organic matter are used: reflectance, transmittance and fluorescence. Under transmitted light the type of organic matter can be identified using a standard polarising microscope. The preparation of samples is the same as for palynological studies, and involves maceration (Sect. 2.2.3) and then mounting the resultant kerogen concentrate on a glass slide.

Correia (1971) differentiated two main groups of organic material from their appearance under the microscope. Lignitic (humic) material has irregular polygonal outlines and clear sharp edges, is often brown but mostly black, and consists of higher plant debris. Sapropelic* material has been homogenised, is generally amorphous, composed of colloidal organic matter and is found mainly in marine sediments: according to Correia, the origin could be either terrestrial or marine. If a kerogen is composed only of the lignitic type, it will under sufficient

* Sapropelic material as described by Correia according to its physical appearance under the microcope does not mean sapropelite, as described in Section 1.3.2, although sapropelite might contain abundant sapropelic material.

thermal matruation produce dry gas, whereas the sapropelic type is capable of yielding different types of hydrocarbons, depending on its degree of maturation: (i) low maturation generates traces of oil or wet gas, (ii) average maturation produces oil or wet gas, (iii) high maturation gives dry gas only, and (iv) very strong maturation results in little gas or nothing. However, the kerogen content of most sedimentary rocks is a mixture of the two types, though their relative proportions are different in different sediments. Despite the amorphous nature of sapropelic organic matter, it must be noted that all amorphous organic materials are not potential sources for petroleum.

Peters et al. (1977) used the colour of kerogen in transmitted light as an index of organic maturity. They heated kerogen from Recent sediments to different temperatures and concluded that the principal zone of oil generation occurs when the colour is between dark-brown and very dark-brown. The description of kerogen under transmitted light has been widely employed, because it is an inexpensive and quick technique.

3.1.2 Procedures

In this study 33 samples, mostly shales, were macerated as described in Section 2.2.3. The kerogen concentrates were then mixed with glycerin jelly and mounted on glass slides, which were examined with a Carl Zeiss polarising photomicroscope.

3.1.3 Data

The samples studied included 23 from the Qoznavi Section in the Shahpassand area and 10 from the Jajarm Section. All of them were from the Shemshak Formation. Detailes are given in Table II.3.1.

3.1.4 Results and Interpretation

Microscopic examination of the kerogen concentrates from the Shemshak Formation of the Shahpassand region shows that the

Table II.3.1 Microscopic desoription of the kerogen concentrates.

Sample No.	Locality	Lithology	Kerogen Description
124	Shahpassand	shale	Mostly fine-grained sapropel as background. High amount of humic particles, some structured, with angular or subangular edges. Abundant membrane cuticles and some black coaly pieces. Poor in palynomorphs. Plant materials are dominant.
129	Shahpassand	shale	Medium to fine sapropelic background. Mainly humic material, mostly black debris with sharp edges. Abundant membrane cuticles and some structured matter. Lots of oil droplets or oil rims (round the particles). Some coaly particles are also present. Rich in palynomorphs. Dominantly humic.
133	Shahpassand	shale	As 129, but particles are slightly finer.
134	Shahpassand	calcareous sandstone	Mainly fine-grained sapropel. Abundant sharp edged black humic debris and coal grains. Some structured matter and tissue cuticles. Poor in palynomorphs.
142	Shahpassand	shale	Mainly fine-grained particles. Some scattered black humic material and coaly grains. Very few structured matter and scarce palynomorphs. Dominantly terrestrial.
149	Shahpassand	shale	As 142; no palynomorph identified.

Table II.3.1 Continued.

Sample No.	Locality	Lithology	Kerogen Description
153	Shahpassand	shale	Mainly fine particles. Abundantly scattered black humic debris with angular or subangular edges. Poor in palynomorphs. Mostly terrestrial.
156	Shahpassand	sandstone	As 153; no palynomorphs, but some structured matter.
158	Shahpassand	shale	Mainly fine-grained particles. Abundantly scattered humic black debris, some are possibly coal grains, with angular or subangular edges. Few structured particles. Some palynomorphs are also present. Dominantly terrestrial.
160	Shahpassand	chalk	Medium- to fine-grained background. Mainly scattered humic matter consist of black particles with angular and subangular edges. Some coal grains, structured material and membrane cuticles. Palynomorphs are also present. Dominantly land derived matter.
166	Shahpassand	shale	Fine-grained background, mainly mixture of humic black particles with sharp edges and structured matter including membrane cuticles. Some grains have yellow-orange oily rims. Palynomorphs are scarce. Dominantly terrestrial matter.

Table II.3.1 Continued.

Sample No.	Locality	Lithology	Kerogen Description
174	Shahpassand	siltstone	Mainly fine-grained matter. Coarser particles are mixture of humic black grains with angular or subangular edges and structured debris. Some membrane cuticles and coal grains are also present. Poor in palynomorphs. Mostly plant debris.
177	Shahpassand	shale	As 174; no palynomorph.
186	Shahpassand	shale	Fine-grained background; mainly structured material and sharp edged brown to black particles. Abundant oil droplets and membrane cuticle, but no palynomorph. Dominantly terrestrial.
190	Shahpassand	limestone	Mainly fine-grained sapropel. Some scattered black organic debris including coaly grains. Little structured matter and tissue. Palynomorphs are rare. Marine invasion (mixture).
191	Shahpassand	shale	Mainly fine sapropel. Very rich in palynomorphs. Abundant humic subangular black debris and structured matter. Some organic tissues, membrane cuticles and coaly grains are also present. Marine invasion (mixture).
199	Shahpassand	shale	As 191.

Table II.3.1 Continued.

Sample No.	Locality	Lithology	Kerogen Description
203	Shahpassand	siltstone	Fine sapropelic background with abundant humic black debris having angular and subangular edges. Some coaly grains and membrane cuticles are incoporated. Structured material is rare. Poor in palynomorphs.
204	Shahpassand	calcareous sandstone	Mainly fine-grained sapropel. Lots of structured material including algal cells and fungi filaments. Some humic black debris and coal grains are also present. Palynomorphs are abundant. Higher marine influence.
205	Shahpassand	marl	Mainly fine-grained sapropel. Abundant structured matter and membrane cuticles. A fair amount of scattered humic debris and coaly grains, but less than the previous ones. Rich in palynomorphs. Dominantly sapropelic kerogen.
209	Shahpassand	marl	Mainly fine-grained sapropel. Some structured material and membrane cuticles are present. Low percentage of humic matter. Some palynomorphs are present. Dominantly sapropelic kerogen.
210	Shahpassand	sandstone	Mixture of sapropel and humic black debris. Abundant algal filaments and cells, as well as fungi. No palynomorph identified.

Table II.3.1 Continued.

Sample No.	Locality	Lithology	Kerogen Description
211	Shahpassand	siltstone	Mainly brown fine-grained sapropel. Some structured material including membrane tissues and acritarch. Plenty of algal and fungi filaments. Some palynomorphs are present. Low amount of black humic debris, but dominantly marine sapropel.
326	Jajarm	shale and siltstone	Mainly sapropel kerogen with a medium grained background. Very small amount of black humic debris. No palynomorph identified.
327	Jajarm	shale	Mainly fine-grained sapropel. Low amount of black humic debris. No palynomorph identified.
336	Jajarm	shale	Mainly sapropel with fine-medium background. Some structured material and tissues are present. Very little humic debris. Kerogen is mostly dark brown to black. Rich in palynomorphs.
339	Jajarm	shale	Mainly sapropel with fine-grained background. Some black sharp-edged humic debris. No palynomorph identified.
344	Jajarm	shale	Mainly dark-brown to black sapropel with a medium-fine background. Some black sharp-edged humic materials are present. A fair amount of palynomorphs.

Table II.3.1 Continued.

Sample No.	Locality	Lithology	Kerogen Description
350	Jajarm	shale	Mainly fine-grained sapropel. Abundant black humic debris and some structured matter and membrane tissues. A few algal/fungi filaments are also present. Rare in palynomorphs. Mixture type.
355	Jajarm	sandy marl	Mainly brown fine-grained sapropel. Larger grains consist of black humic debris and sapropelite. Some structured plant material and membrane tissues are present. Rare in palynomorphs. Dominantly marine.
357	Jajarm	sandy marl	As 355.
361	Jajarm	shale	Mainly fine-grained sapropel. Larger particles are mainly structureless organic aggregates as well as some black sharp-edged humic debris and a few membrane tissues. Very rare palynomorphs. Mixture type.
365	Jajarm	shale	Mainly fine-medium grained particles as background. Abundant black humic debris. Some structured material and membrane cuticles. Rare in palynomorphs. Dominantly terrestrial matter.

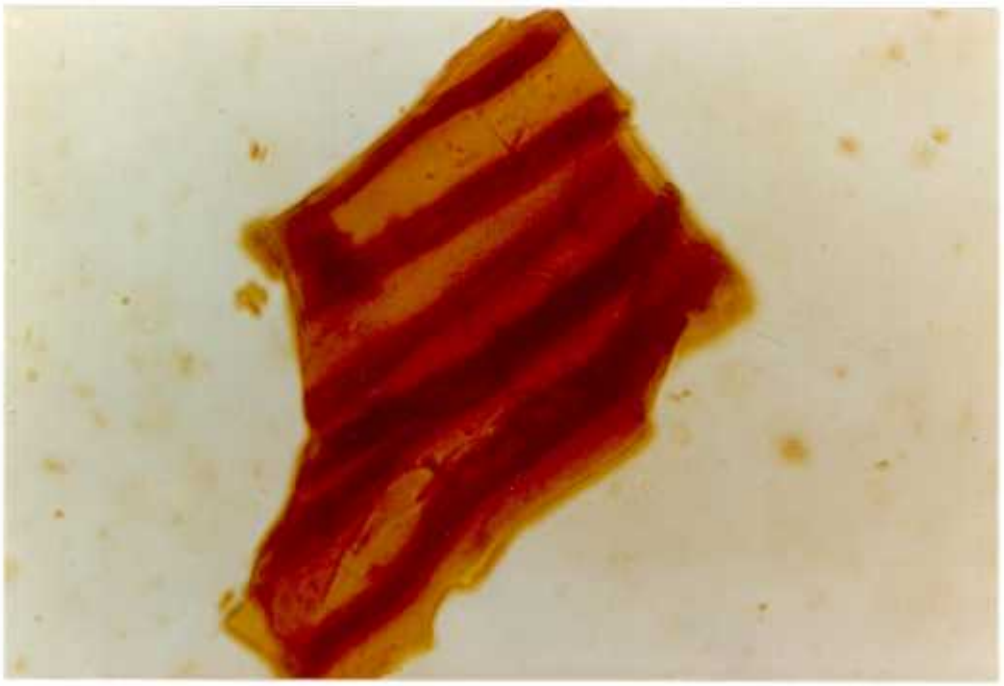
organic matter incorporated in the lower 2/3rds of the Formation is dominantly of terrestrial origin. Black humic particles, having angular or subangular edges, are preponderant throughout this part of the sequence, and the kerogen also includes some structured organic particles (mostly plant debris; e.g. tissues and membrane cuticles, etc.) together with a few lignitic coalgrains (Fig. II.3.1). A most interesting feature is oil droplets seen mainly in conjunction with the humic material (samples: 129, 166 and 186; Fig. II.3.2). This may be evidence that the terrigenous source beds have generated oil.

The marine invasion in the upper 1/3rd of the Formation is reflected in a gradual increase of sapropelic matter and a relative decrease of humic substances (samples: 186 to 203). The highest part of the sequence (samples: 204 to 211) contains predominantly sapropelic kerogen showing algal cells and fungi filaments (Fig. II.3.3), whereas land derived humic matter, although present, is subordinate: the organic matter is mainly of marine origin.

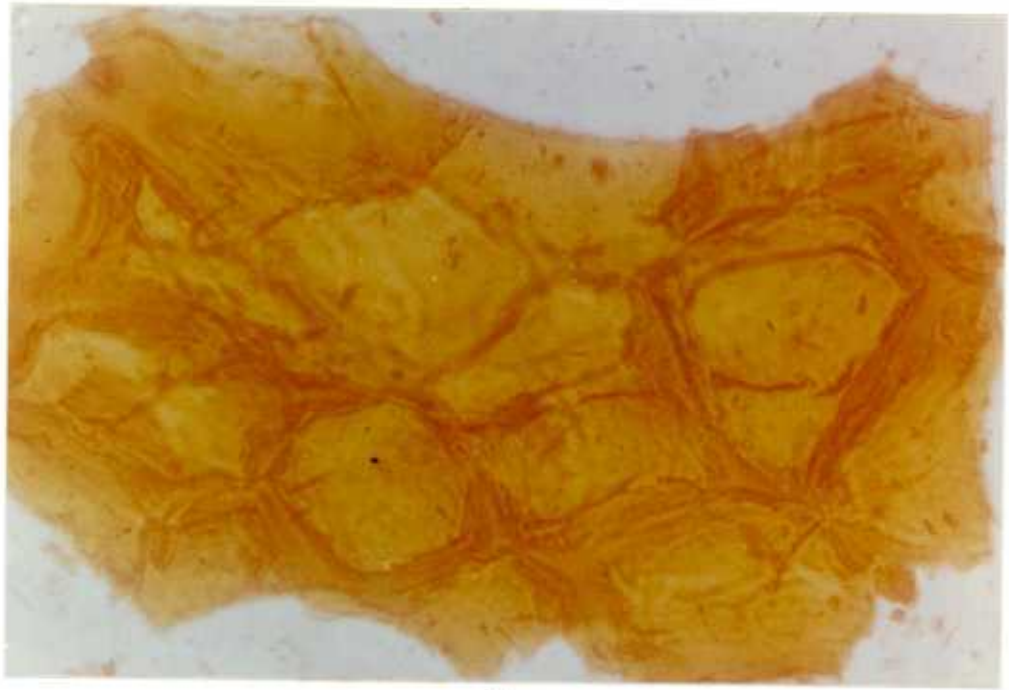
Near Jajarm, the nature of the organic matter is somewhat different. Sapropelic substances predominate almost throughout. Land derived humic material is present, but less abundantly than at Shahpassand. The dominance of material derived from marine organisms is particularly marked in the samples taken from the "Marine Shale" unit (samples: 355 and 357). However, towards the top of the Formation, humic material gradually increases again and in the highest bed studied (sample 365), terrestrial material predominates.

3.1.5 Conclusions

Microscopic examination of the macerated kerogen concentrates has provided useful information about the type of organic matter, and hence about the petroleum generating potential of the source beds in the Shemshak Formation. In the Shahpassand area, the lower 2/3rds of the Formation contain predominantly humic material,



A



B

Fig. II.3.1 - Structured humic material from the Shemshak Fm.
A) Vascular tissue (x 1058).
B) Plant tissue (probably leaf cuticle) (x 992).



Fig. II.3.2 - Oil rim round an organic grain in the macerated organic concentrate of sample no. 166 (x 675).



A



B

Fig. II.3.3 - Fungi filaments in macerated organic concentrates.

A) Sample no. 210 (x 2714).

B) Sample no. 204 (x 2646).

whilst the upper 1/3rd is dominated by sapropelic organic matter. In the Jajarm region the sapropelic matter predominates and humic material is subordinate. The organic matter incorporated in the Shemshak Formation near Shahpassand is dominantly terrestrial, whilst the Jajarm counterpart is mainly marine.

The presence of oil droplets in the kerogen concentrate of a few samples from the Shahpassand region suggests that oil has been generated, at least in some intervals of the Shemshak Formation in the Eastern Alborz.

3.2 Quantitative Elemental Analysis

3.2.1 Introduction

Under favourable conditions, the quantity of petroleum generated in a source bed can be said to be directly proportional to the initial organic content of that bed (Erdman, 1975). Thus, the concentration of organic matter in sediments should be considered a prime factor in assessing the petroleum generating potential of a source bed. This organic matter is composed principally of C, H, O, N and S; and variations in the proportions of these elements will affect the nature of the hydrocarbons generated.

The significance of the total organic carbon content (C_T) has been discussed above and it will be recalled that a minimum of 0.5% is regarded as an essential requirement for a potential source rock: the average organic carbon content of established source rocks, however, has been shown empirically to be 1-2%.

The importance of the hydrogen content of kerogen, when first formed, to the generation of hydrocarbons has been emphasised by many authors. McIver (1967) showed that the amount of hydrogen which a kerogen can generate is a function of its hydrogen and, to a lesser extent, its oxygen content. Kartsev (1971) noted that the main constituents of a kerogen that convert

to oil are lipoids rich in hydrogen. Laplante (1974) suggested that kerogen with a hydrogen level less than 6 percent is principally a source for gas, whereas one containing more than 7 percent hydrogen can generate oil. Hydrogen-poor kerogens, even under sufficient thermal maturation, are virtually incapable of generating significant amounts of oil (Demaison, 1975).

Quantitative elemental analysis is now widely used to identify the kerogen type, based on relative changes in the concentration of the major organic elements. The elemental composition of kerogen in sediments also reflects its state of thermal maturation (Waples, 1979). Maturity of the kerogen, therefore, should be taken into consideration when it is typed on the basis of its elemental composition.

The initial atomic H/C, O/C and N/C ratios of a kerogen can indicate its oil generating potential as well as its origin. Harwood (1977) showed that, for kerogens before the principal phase of hydrocarbon (oil) generation, atomic H/C ratios above approximately 1.00 characterise potential sources of oil (and gas), and are found predominantly in the remains of lower plants and marine animals; atomic H/C ratios between 0.80-1.00 indicate wet-gas source and those below 0.80 dry gas sources. Kerogens derived from higher plant debris and other terrestrial matter are believed to be mainly gas producing. N/C ratios may also indicate the origin of organic matter (Ishiwatari et al., 1978). Phillippi (1977) mentioned that the atomic C/N ratio rises with a proportional increase in the terrestrial organic content of marine sediments.

Perhaps the most significant approach to the determination of kerogen type was the use of a H/C, O/C crossplot by Tissot et al. (1974) who emphasised the importance of hydrogen and oxygen concentrations in the characterisation of kerogen (Fig. II.3.4). However, the typing of highly matured kerogens by this method is rather difficult, since the evolution paths converge closely beyond 1.5 vitrinite reflectance value. The technique

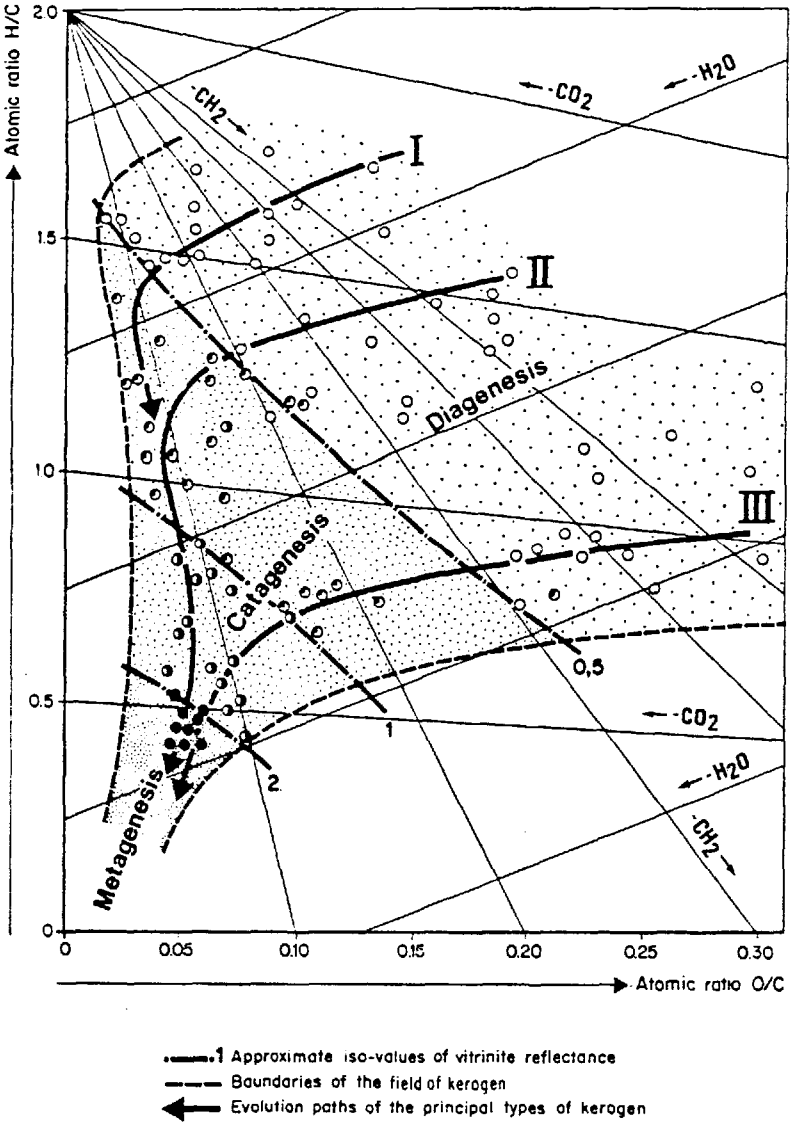


Fig. II.3.4 - The kerogen evolution path and related vitrinite reflectance (after Tissot and Welte, 1978).

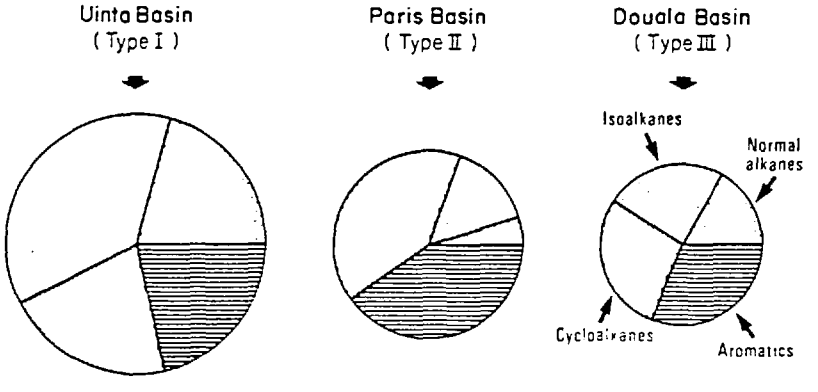


Fig. II.3.6 - Relative composition of the hydrocarbons generated from the main kerogen types in different basins (after Tissot and Welte, 1978).

is also unsuitable for surface and shallow depth samples because of their high oxygen content.

3.2.2 Procedure

All quantitative determinations of C, H and N were carried out with a semi-automatic Perkin-Elmer Model 240 elemental analyser, in conjunction with a Perkin-Elmer Model 56 (1 mv) recorder and a Beckman Model LM 500 microbalance. Oxygen values were measured by the neutron activation technique at AWRE reactor centre at Aldermaston.

2.9 to 5.2 mg (with a few exceptions) of each pulverised rock sample and about 3.0 to 4.0 mg of each kerogen concentrate were used for CHN determinations. Combustion of the samples was carried out in pure oxygen and the resulting products (CO_2, H_2O and N_2) measured by thermal conductivity detectors. Helium was used to carry the combustion products from the combustion train, through the analytical system, to the atmosphere. Samples were weighed within $\pm$ 0.001 mg accuracy (0.1%); accuracy of the analyser to this standard deviation is about 0.3%.

Samples were analysed as follows: The microbalance was first zeroed and calibrated; this was repeated at least after every two weighings.

Pulverised rock samples were carefully weighed in small platinum boats, after they had been homogenised by shaking and stirring. The weighed platinum boats were then stored in a desiccator.

Weighed samples were treated with sufficient 10-20 percent HCl (excepting macerated samples and those for the whole rock analysis) to desolve their carbonates, and then dried in an oven at 50°C for approximately 14 to 16 hours prior to analysis.

The elemental analyser was tested before analysis by measuring its sensitivities with a recommended standard compound (acetanilide: 10.36% N, 71.09% C, 6.71% H). Samples were then inserted into

the analyser by means of a ladle.

The CHN percentages of each sample were calculated relative to the latest measured sensitivities of the analyser (normally measured twice a day).

3.2.3 Data

Analysis was carried out on 74 samples for whole rock composition (without acid treatment) and for total organic composition (after acid treatment), 74 pyrolysed samples at 900°C, 25 pyrolysed samples at 600°C, 15 macerated kerogen concetrates, 10 mineral free kerogen concentrates*, and 10 pyrolysed kerogen concentrates at 500°C. All analytical results are given in Table II.3.2 and II.3.3. A few samples were repeated to check the accuracy of the analyser. A variation of 2.8% was taken as a reproducibility index of the analyser for carbon.

3.2.4 Results and Interpretation

Comparison of the whole rock carbon content (C_W) with the total organic carbon content (C_T) of the analysed samples shows a sharp decrease of the carbon percentage in samples no : 122, 212, 213, 325, and 367 after acid treatment, indicating their high original carbonate content. These samples are in fact from limestone sequences above or below the Shemshak Formation (see Figs. I.4.3, I.4.4 and I.4.5, loose) and they are excluded from the following source rock interpretations. Shemshak Formation samples (except 162, 196, and 346) have inorganic carbon contents in the range zero to 1.6%.

All samples, except 142, 157, 208, 236, 245, 259, 285, 326, 327, 333, 346, 354 and 357, yielded C_T values above the minimum

* After maceration the remaining heavy minerals were removed by floatation and centrifuging in zinc bromide solution.

Table II.3.2 - Quantitative elemental analysis results of the rock samples from the Shemshak Formation.

Sample No.	Whole Rock			Organic Content			Organic Content after Pyrolysis at 900°C			Organic Content after Pyrolysis at 600°C		
	C%	H%	N%	C%	H%	N%	C%	H%	N%	C%	H%	N%
Qomavi Section (Shahpassand area)												
122	11.83	0.29	0.52	0.21	8.02	0.48	0.02	11.72	0.75			
124	1.86	1.65	0.22	1.73	1.90	0.10	0.87	0.51	0.11	1.06	1.32	0.05
125	5.34	1.64	0.23	5.53	4.01	0.23	9.06	0.66	0.21	5.45	1.78	0.13
129	8.02	1.31	0.30	8.55	1.47	0.30	7.23	0.50	0.12	8.10	1.44	0.20
133	0.73	0.53	0.21	1.08	1.18	0.08	0.31	0.23	0.05	0.80	1.79	0.03
138	2.08	1.11	0.17	2.32	1.59	0.14	1.30	0.42	0.04	2.05	3.08	0.06
142	0.23	0.83	0.15	0.16	0.97	0.07	0.01	0.22	0.04	0.02	1.91	0.00
149	0.65	0.79	0.16	0.62	1.14	0.11	0.09	0.25	0.00	0.53	2.26	0.00
150	0.92	0.72	0.11	0.61	1.29	0.09	0.21	0.47	0.00	0.40		1.17
152	38.94	0.51	1.02	39.96	6.35	1.04	48.37	3.01	0.81	47.24	5.03	1.30
157	0.28	0.71	0.19	0.37	1.65	0.12	0.18	1.91	0.00	0.70	2.43	0.05
161	20.76	1.94	0.61	19.55	3.33	0.42	20.96	1.35	0.20	21.30	2.37	0.39
162	2.70	1.03	0.11	0.55	3.88	0.16	0.14	4.44	0.11	0.18	4.52	0.01
166	1.60	0.99	0.15	1.69	3.32	0.17	0.93	0.74	0.04	1.19	2.32	0.03
169	7.54	0.98	0.37	7.17	1.16	0.22	5.90	0.64	0.04	6.45	2.64	0.15
171	4.08	1.05	0.45	4.23	1.30	0.26	3.00	0.93	0.09	3.40	2.45	0.09
173	49.74	3.22	1.49	48.44	2.99	1.18	59.48	2.20	0.76	55.80	4.89	1.36
174	4.20	0.57	0.05	0.52	5.35	0.38	0.76	4.26	0.16	0.39	4.40	0.08
177	1.06	0.87	0.48	1.15	1.35	0.13	0.83	0.87	0.03	1.11	2.45	0.00
179	2.29	1.11	0.41	2.29	1.36	0.24	1.64	0.47	0.04			
184	4.24	1.14	0.12	4.62	1.31	0.19	4.18	5.76	0.13	4.09	4.65	0.28
191	4.84	1.35	0.54	5.40	1.61	0.19	4.35	1.87	0.19	4.61	1.43	0.20
196	45.68	3.03	0.89	29.73	3.32	0.69	28.93	0.58	0.59	30.64	1.99	0.87
197	42.24	3.81	1.05	40.68	3.77	0.87	41.85	0.54	0.87	42.59	3.33	1.09
203	0.62	0.70	0.23	0.73	0.98	0.08	0.35	0.23	0.13	0.52	1.11	0.13
207	0.76	0.57	0.33	0.55	1.44	0.15	0.14	0.79	0.18	0.42	2.80	0.30
208	1.07	0.70	0.48	0.40	1.41	0.13	0.14	0.90	0.10	0.41	2.62	0.16
212	11.36	0.12	0.47	0.17	8.90	0.43	0.00	7.87	0.82			
Rudbar Section (Shahpassand area)												
213	11.26	0.11	0.47	0.12	8.39	0.47	0.02	10.68	0.69			
218	13.88	1.66	0.41	13.53	1.79	0.34	2.38	0.41	0.23			
220	0.68	1.09	0.54	0.68	1.41	0.13	0.12	0.34	0.66			
222	0.81	1.07	2.05	0.86	1.65	0.13	0.47	2.78	0.11			
224	2.32	1.02	0.54	1.30	1.70	0.21	0.95	0.70	0.16			
228	0.59	0.64	0.68	0.66	2.16	0.16	0.20	1.32	0.31			
232	0.90	0.64	0.25	0.76	1.51	0.15	0.23	1.42	0.07			
233	0.80	0.69	0.64	0.61	1.66	0.13	0.16	2.22	0.11			
236	0.35	0.41	0.16	0.41	3.62	0.15	0.05	0.56	0.05			

Table II.3.2 - Continued.

Sample No.	Whole Rock			Organic Content			Organic Content after Pyrolysis at 900°C			Organic Content after Pyrolysis at 600°C		
	C%	H%	N%	C%	H%	N%	C%	H%	N%	C%	H%	N%
238	0.92	0.75	0.19	0.80	2.13	0.15	0.23	0.59	0.06			
242	1.06	0.66	0.20	0.85	1.95	0.14	0.19	0.60	0.09			
245	0.06	0.58	0.13	0.09	1.24	0.43	0.02	0.20	0.06			
249	0.74	0.77	0.17	0.74	1.48	0.14	0.24	0.39	0.03			
251	59.83	3.14	1.27	58.94	3.72	1.08	57.81	0.91	0.87			
253	0.48	0.41	0.58	0.62	0.72	0.06	0.24	0.79	0.04			
254	0.55	0.69	0.65	0.61	1.23	0.11	0.22	1.05	0.03			
256	2.51	1.03	0.66	2.52	1.73	0.19	2.34	1.05	0.11			
257	0.73	0.77	0.77	0.73	1.30	0.12	0.28	0.29	0.04			
259	0.38	0.63	0.59	0.41	1.38	0.10	0.06	0.23	0.71			
260	0.10	0.33	0.59	0.20	1.03	0.08	0.00	0.21	0.45			
261	0.45	0.76	1.04	0.47	1.58	0.18	0.03	0.26	0.69			
262	20.47	1.47	0.94	21.85	2.00	0.93	21.53	2.38	0.99			
265	14.81	1.73	0.90	15.06	8.52	0.88	14.17	0.69	0.66			
271	6.94	1.42	0.70	7.39	1.54	0.70	5.36	0.41	0.57			
276	13.99	1.35	0.68	13.70	1.50	0.77	10.88	1.75	0.81			
282	15.70	1.45	0.62	15.60	2.16	0.82	15.71	0.52	0.66			
285	0.20	0.95	0.59	0.21	1.02	0.56	0.17	0.50	0.53			
				Jajarm Section (Shahpassand area)								
325	12.41	0.09	0.51	0.10	12.32	0.53	0.10	20.47	0.62			
326	0.13	1.26	0.57	0.13	2.19	0.50	0.13	1.70	0.49			
327	0.09	0.52	0.50	0.14	0.95	0.43	0.10	0.50	0.59			
330	0.61	0.61	0.48	0.82	5.18	0.62	0.03	0.35	0.38			
333	0.35	0.51	0.34	0.43	3.96	0.46	0.00	1.01	0.52			
336	3.88	0.92	0.43	3.94	1.26	0.46	2.80	0.33	0.65			
339	0.64	0.34	0.36	0.76	0.61	0.53	0.13	0.51	0.49			
343	0.53	0.73	0.53	0.65	1.54	0.53	0.04	0.31	0.52			
344	3.73	0.80	0.60	4.00	1.57	0.60	2.10	0.50	0.46			
346	6.79	0.33	0.50	0.15	5.14	0.34	0.00	6.26	0.46			
350	0.45	0.59	0.84	0.43	1.43	0.55	0.10	0.23	0.44			
354	0.41	0.46	0.53	0.38	1.20	0.63	0.06	0.47	0.48			
355	0.99	0.35	0.46	0.50	0.94	0.51	0.26	1.20	0.58			
356	0.69	0.51	0.62	0.68	1.09	0.49	0.31	0.77	0.40			
357	0.39	0.49	0.48	0.39	1.02	0.54	0.06	0.73	0.33			
360	1.21	0.56	0.61	1.54	1.54	0.67	0.20	0.77	0.52			
361	0.71	0.80	0.52	0.86	2.06	0.51	0.12	0.53	0.46			
365	0.93	0.64	0.60	1.10	1.91	0.65	0.27	0.75	0.42			
367	10.33	0.16	0.41	0.12	5.36	0.60	0.10	8.50	0.51			
Ave				**5.9**		**0.37**						

Table II.3.3 - Quantitative elemental analysis results of kerogen concentrates.

Macerated kerogen concentrate							
Sample No.	C%	H%	N%	O%	H/C	O/C	N/C
124	48.78	2.49	2.04	31.7	0.61	0.49	0.04
133	12.82	1.61	0.31	28.9	1.51	1.69	0.02
166	36.73	2.03	1.02	30.5	0.66	0.62	0.02
191	23.20	2.26	0.83	28.2	1.17	0.91	0.03
209	5.63	1.27	0.24	30.5	2.71	4.06	0.04
218	66.17	3.43	1.55	24.7	0.62	0.28	0.02
224	31.98	2.71	1.04	24.8	1.02	0.58	0.03
249	9.31	1.50	0.34	28.2	1.93	2.27	0.03
254	7.10	1.41	0.37	29.9	2.38	3.16	0.04
271	50.31	2.85	1.28	29.8	0.68	0.44	0.02
327	1.49	1.30	0.31	32.0	10.47*	16.11*	0.18
336	28.94	1.99	0.61	29.9	0.82	0.77	0.02
344	32.37	2.02	0.56	31.9	0.75	0.74	0.01
355	14.26	1.84	0.40	28.2	1.55	1.48	0.02
365	4.46	0.71	0.15	39.5	1.91*	6.64*	0.03
Average	37.36	1.96			1.31		

* Excluded from interpreted results.

	Mineral free kerogen concentrate					Mineral free kerogen after pyrolysis at 500°C				
Sample No.	C%	H%	N%	H/C	N/C	C%	H%	N%	H/C	N/C
186	41.33	2.71	0.98	0.79	0.02	47.64	1.37	1.35	0.34	0.03
218	45.37	2.82	0.87	0.75	0.02	63.70	1.62	1.50	0.30	0.02
224	41.24	3.29	0.99	0.96	0.02	53.52	1.42	1.31	0.32	0.02
228	21.04	1.48	0.17	0.84	0.03	11.01	0.16	0.00	0.17	0.00
265	42.58	2.81	1.03	0.79	0.02	51.83	1.43	1.52	0.33	0.03
336	39.68	2.91	0.60	0.88	0.01	53.05	1.52	0.88	0.34	0.01
344	34.35	2.50	0.40	0.87	0.01	50.97	1.32	0.88	0.31	0.01
350	6.20	1.69	0.00	3.27	0.00	5.68	0.22	1.10	0.46	0.00
357	12.88	1.74	1.09	1.62	0.006	11.92	0.30	0.10	0.30	0.01
365	56.87	3.51	1.08	0.74	0.02	60.85	1.68	1.26	0.33	0.02
Average	34.16	2.55		0.91		40.03	1.10		0.49	

source rock requirement of 0.5%, although the present C_T values are probably less than the initial amount of organic carbon in the rocks, since some of it might have been incorporated in the hydrocarbons already generated. The average C_T value (ranging from 0.09% to 58.94%) of all samples is 5.9% which is well above the average of established source rocks (1-2%).

Most of the organic nitrogen values are less than those obtained from the whole rock samples, although in a few cases the opposite was found. Organic nitrogen values in general increase variably as C_T values increase. The overall average of the nitrogen contents is 0.37% but, as shown in Table II.3.2, the values are significantly higher in the samples from the Jajarm area (average 0.53%) than in those from Shahpassand (average 0.32%). However, the average atomic N/C ratio of the organic matter from the Jajarm samples is 0.46, much higher than that of the Shahpassand samples, which is 0.04. This may suggest a higher proportion of marine organic matter at Jajarm.

The organic hydrogen content of the rock samples cannot be detected, because of the effects of acid treatment. Table II.3.2 shows that all hydrogen values (except 177 and 197) are higher after acid digestion of the carbonates. The analytical results from the macerated kerogen concentrates provide further information about the type of organic matter in the samples. The hydrogen values of all kerogens (10 are mineral free) are well below the minimum 6% limit for oil generation given by Laplante (1974); they average 1.96% in the macerated kerogen concentrates (ranging from 0.71% to 3.43%) and 2.55% in the mineral free kerogen concentrates (1.48% to 3.51%). These results strongly suggest that the kerogen in the Shemshak Formation is likely to be source of gaseous hydrocarbons.

The atomic H/C ratios of the macerated kerogens averaged 1.31 (ranging from 0.61 to 2.71) and those of the mineral free kerogens 0.91 (0.74 to 1.62, sample 350 being excluded). Atomic H/C ratios of the mineral free kerogens can be used to determine

the kerogen type, as described by Harwood (1977). In the kerogen samples analysed this ratio is below 1.00, except in 350 and 357 (which belong to the marine interval of the Jajarm Section) having an average value of 0.83 (excluding samples: 350 and 357). Assuming the kerogens have not reached the principal stage of hydrocarbon generation, it could be concluded that they are wet-gas sources.

A plot of H/C ratios against O/C ratios of the macerated kerogen concentrates (Fig. II.3.5) shows that the kerogens are of huminite type.

3.2.5 Conclusions

The following conclusions can be derived from the quantitative elemental analyses of samples from the Shemshak Formation: Most samples contain less than 1.6% inorganic carbon.

The amount of organic matter in the sediments is well above the generally accepted minimum requirement of 0.5% for a petroleum source rock.

Atomic N/C ratios suggest that the sediments of Jajarm have a relatively higher proportion of organic matter of marine origin than those near Shahpassand. That they are most likely to be a source of wet-gas as indicated by their hydrogen values and the H/C ratios of their kerogen concentrates. The kerogen is mostly of huminite type (type III), further suggesting that the Formation could be a source for gas.

3.3 Solvent Organic Extraction

3.3.1 Introduction

Extraction of the soluble organic matter from source rocks in order to study the nature of its composition has been practiced by many investigators since the early days of petroleum source rock study. Petroleum source beds have been evaluated on the

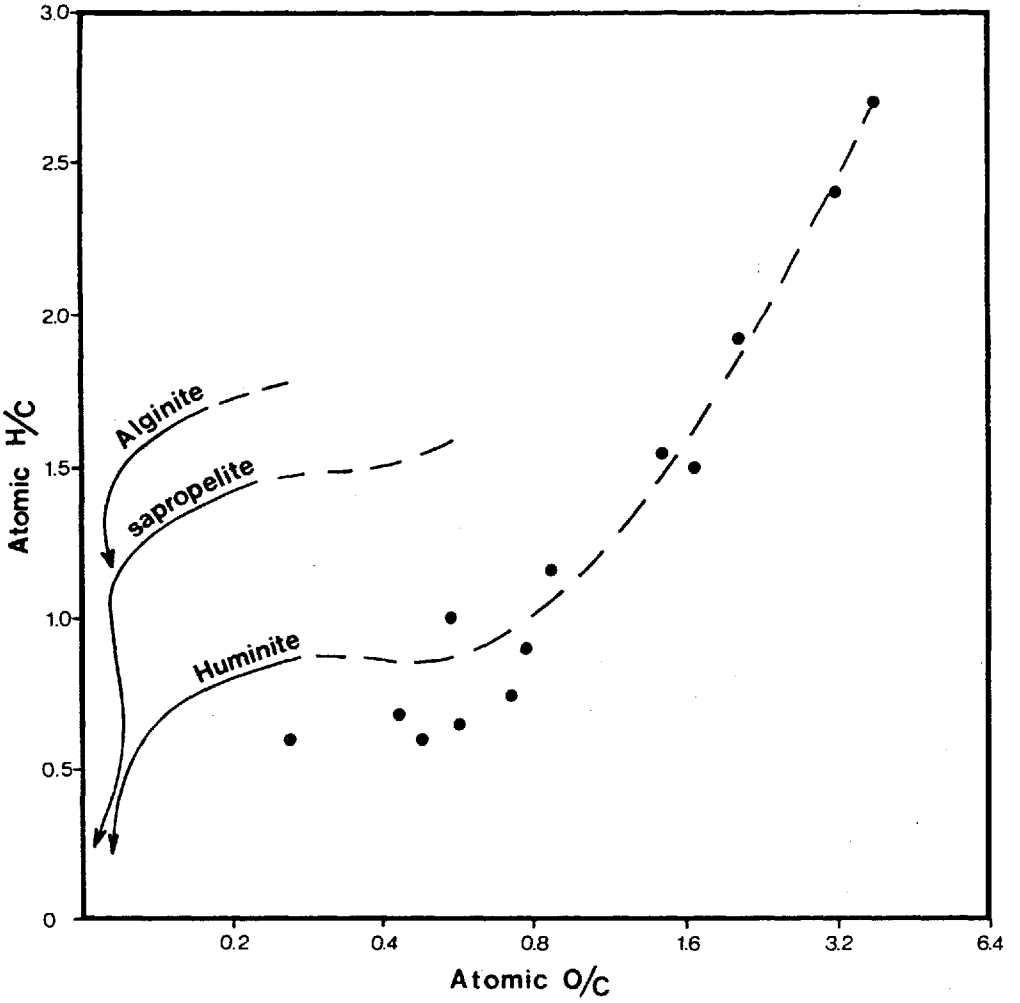


Fig. II.3.5 - A plot of the Shemshak Fm. samples showing their early diagenesis (surface and shallow specimens) in the kerogen evolution diagram (modified after Tissot et al., 1974).

basis of the abundance, composition, and other physiochemical properties of their soluble organic extract (bitumen) by a number of authors, and the composition of the saturated fraction of the bitumen is widely used to characterise a source rock (by gas-liquid chromatography-mass spectrometry techniques).

Bitumen consists of hydrocarbons (saturates + aromatics), resins, and asphaltenes* (non-hydrocarbons). The last two are composed of heavy molecules which are normally precursors of hydrocarbons. Baker (1962) noted that a positive relationship exists between the hydrocarbon content and total organic carbon of the source rocks. In general the amount of bitumen in a source rock increases as its organic content rises, but the rate of this increase depends also on the type of organic matter. This is simply because bitumen is an alteration product of the initial organic matter in the rock. Therefore, a higher bitumen content, which indicates a higher convertibility of initial organic matter, means a better source rock. It should be emphasised, however, that the abundance and composition of bitumens will also depend on the state of maturation of organic matter in the rock.

From the results of Hedberg (1968) and Reed (1969) on high-wax oils, it is reasonable to suggest that bitumens from terrestrial sediments are heavier and more condensed than those from marine deposits. In the absence of migration, the bitumen ratio**(bitumen/total organic carbon) can indicate approximately the type of organic matter in sediments with the same degree of thermal maturity.

However, solvent organic extraction is a highly time

* Resins and asphaltenes are high molecular weight constituents of bitumen which usually also contains N, S, and O compounds.

** Bitumen ratio is the same as E/C_T ratio.

consuming experiment and it needs very careful handling. The extracts, unless they are used for further analysis or unless they are accompanied by the results of other geochemical analyses, can not be used reliably to characterise a source bed.

3.3.2 Procedures

All samples analysed were extracted with a freshly distilled azeotropic mixture of benzene-methanol (approx.3:2) in a soxhelt extraction system. Those samples which were collected during the first field trip (Sect. 2.2) were extracted in a system (referred to as system "a") which was subsequently replaced by a new one (refferred to as system "b"). All samples collected during the second field trip were extracted with system "b". The main purpose of changing the extraction system was to double the number of samples that can be extracted in 24 hours. This was achieved by reducing the sizes of the soxhlets, boiler flasks and heating mantles to make space available for more extraction apparatus to be connected to the whole system. The two systems are believed to have similar efficiencies (Gill, pers. comm.), although the results obtained are not suitable for an accurate quantitative comparison.

As a result of a series of tests carried out by the Petroleum Geology Section of Imperial College, an azeotropic mixture of benzene-methanol was chosen as the solvent, because of its high degree of extraction efficiency (Kinghorn, pers. comm.); Albrecht et al. (1976) also found that a mixture of benzene-methanol (3:1) produces more extracts than chloroform. It must be added that the azeotropic mixture is capable of dissolving some inorganic compounds such as salt (Na Cl) and sulphur. Because of this, samples no. 166 and 169, due to their sulphur impurities, and 207, 208, due to their salt impurities, are excluded from the analytical interpretations.

Extraction experiments were carried out as follows: samples were pulverised as described in Section 2.2.2.

Between 143 and 445 grams of rock powder were weighed into a thimble (175 mm X 60 mm diameter) made of compressed filter paper and then plugged with some glass wool. A further piece of filter paper in the form of a spiral was placed inside each thimble in order to conduct the solvent to the centre of it during extraction.

The thimbles were then placed in soxhlets (capacity = 2320 cc in system "a" and 700 cc in system "b"), which were joined to boiler flasks (5 litres in system "a", and 2 litres in system "b") containing solvent ($\simeq$3500 cc in system "a", and 1200 cc in system "b") and placed in electric heating mantles.

All samples were extracted for a standard 22 hours.

The extract solutions were recovered and then filtered into pre-weighed standard glass tubes.

The samples were then dried in an oven at 50°C to constant weight.

3.3.3 Data

71 samples were extracted for their bitumen content (52 from the Shahpassand area, and 19 from the Jajarm region); a few samples were repeated to check the reproducibility of the system. Table II.3.4 shows the results of the solvent extraction and fractionation experiments.

3.3.4 Results and Interpretation

The solvent organic extracts, expressed as weight percent of the original sample, average 0.41. The E/C_T ratios average 152 mg/g, excluding samples 325, 354, 355, 356, and 367 because of their abnormally high values. In general, the solvent organic extracts and the bitumen ratios of the Jajarm samples are higher than those of the Shahpassand ones (Table II.3.4), suggesting that the former are better source rocks. However, no valid quantitative comparison can be made between the two sets, because

Table II.3.4 - Extraction and fractionation results.

Sample No.	Azeotrope Bitumen%	mg Bitumen / g Organic Carbon x 10	Alkanes% in Bitumen	Aromatics% in Bitumen	Asphatenes% in Bitumen	Hydrocarbon% in Bitumen	Total Hydrocarbon (Alkanes+Aromatics) ppm in rock	Hydrocarbon / Organic Carbon	Saturates / Aromatics
				Shahpassand area					
124	0.04	2.31	25.15	25.92	48.93	51.07	204	1.18	0.97
125	0.16	2.89	21.15	15.18	63.67	36.33	581	1.05	1.39
129	0.40	4.68	10.26	9.71	80.03	19.97	799	0.93	1.06
133	0.06	5.56	25.22	20.72	54.05	45.94	276	2.55	1.22
138	0.69	29.74	20.37	13.37	66.26	33.74	2328	10.03	1.52
142	0.05	31.25	21.49	16.90	61.60	38.39	192	11.99	1.27
149	0.07	11.29	22.04	19.18	58.77	41.22	288	4.64	1.15
150	0.17	27.87	17.38	17.05	65.57	34.43	585	9.59	1.02
152	0.74	1.85	7.83	5.77	86.60	13.40	992	0.25	1.41
157	0.04	10.81	24.44	27.09	48.46	51.54	206	5.57	0.90
161	0.49	2.51	8.12	7.71	84.17	15.83	776	0.40	1.05
162	0.04	7.27	18.51	23.92	57.57	42.43	170	3.08	0.77
166	0.36	21.30	6.55	5.17	88.27	11.73	422	2.50	1.27
169	0.50	6.97	7.22	6.86	85.92	14.08	704	0.98	1.05
171	0.56	13.24	7.44	8.01	84.55	14.45	809	1.91	0.93
173	2.52	5.20	11.94	12.08	75.98	24.02	6053	1.25	0.99
174	0.02	3.85	23.90	22.73	53.37	64.63	93	1.79	1.05
177	0.55	47.83	16.98	21.39	61.63	38.37	2110	18.35	0.79
179	0.32	13.97	8.62	7.77	83.61	16.39	524	2.29	1.11
184	0.14	3.03	14.87	11.10	74.13	25.86	362	0.78	1.34
191	1.38	25.56	11.64	8.28	80.08	19.92	2749	5.09	1.41
196	3.41	11.47	16.73	16.92	66.35	33.64	11471	3.86	0.99
197	6.06	14.90	12.96	11.26	75.77	24.22	14679	3.61	1.15
203	0.04	5.48	31.19	20.79	48.02	51.98	208	2.85	1.50
207	0.52	94.55	17.79	15.15	67.05	32.95	1713	31.14	1.17

Table II.3.4 - Continued.

Sample No.	Azeotrope Bitumen%	mg Bitumen / g Organic Carbon x 10	Alkanes% in Bitumen	Aromatics% in Bitumen	Asphatenes% in Bitumen	Hydrocarbon% in Bitumen	Total Hydrocarbon (Alkanes+Aromatics) ppm in rock	Hydrocarbon / Organic Carbon	Saturates / Aromatics
208	1.35	337.50	6.91	6.27	86.82	13.18	1779	44.47	1.10
218	0.23	1.70	9.81	5.57	84.61	15.38	354	0.26	1.76
220	0.04	5.88	18.56	19.98	61.51	38.54	154	2.26	0.93
222	0.06	6.98	23.38	19.39	57.22	42.78	257	2.98	1.21
224	0.06	4.62	20.33	17.05	62.61	37.38	224	1.72	1.19
228	0.04	6.06	25.03	18.93	56.04	43.96	176	2.67	1.32
232	0.07	9.21	21.31	20.71	57.98	42.02	294	3.87	1.03
233	0.04	6.56	21.66	21.45	56.88	43.12	172	2.82	1.01
236	0.09	21.95	15.03	15.42	69.55	30.45	274	6.68	0.97
238	0.04	5.00	20.93	15.18	63.89	36.11	144	1.80	1.38
242	0.03	3.53	27.42	28.87	43.70	56.30	113	1.99	0.95
245	0.03	33.33	27.41	28.87	43.72	56.28	169	18.78	0.95
249	0.06	8.11	21.72	17.30	60.98	39.02	234	3.16	1.26
251	2.87	4.87	14.72	11.96	73.32	26.68	7542	1.28	1.23
253	0.04	6.45	22.96	17.66	59.37	40.63	162	2.61	1.30
254	0.04	6.56	19.94	18.23	61.82	38.18	153	2.51	1.09
256	0.14	5.56	13.01	20.23	66.75	33.25	465	1.85	0.64
257	0.02	2.74	23.86	28.59	47.55	52.45	105	1.44	0.83
259	0.03	7.32	17.81	17.32	64.87	35.13	105	2.56	1.03
260	0.03	15.00	24.94	28.50	44.60	55.44	166	8.30	0.88
261	0.04	8.51	17.46	11.35	71.18	28.82	115	2.45	1.54
262	0.41	1.88	11.01	11.01	77.98	22.01	902	0.41	1.00
265	0.20	1.33	9.47	9.82	80.71	19.29	386	0.26	0.96
271	0.15	2.03	15.73	11.02	73.24	26.76	401	0.54	1.43
276	0.29	2.12	9.89	7.66	82.45	17.55	515	0.38	1.29
282	0.21	1.35	13.78	8.45	77.76	22.24	467	0.30	1.63
285	0.08	38.10	8.49	13.72	76.79	23.21	186	8.84	0.69
Average		10.40	17.81	16.40		34.22	1264	3.58	

Table II.3.4 - Continued.

Sample No.	Azeotrope Bitumen%	mg Bitumen / g Organic Carbon x 10	Alkanes% in Bitumen	Aromatics% in Bitumen	Asphatenes% in Bitumen	Hydrocarbon% in Bitumen	Total Hydrocarbon (Alkanes+Aromatics) ppm in rock	Hydrocarbon / Organic Carbon	Saturates / Aromatics
				Jajarm area					
325	0.10	100.00	8.58	10.63	80.79	19.21	192	19.20	0.81
326	0.08	61.54	9.00	9.06	81.94	18.06	144	11.08	0.99
327	0.09	64.29	6.16	17.42	76.41	23.59	212	15.14	0.35
330	0.05	6.10	10.06	9.15	80.79	19.21	96	1.17	1.10
333	0.04	9.30	10.46	8.32	81.22	18.78	75	1.74	1.26
336	0.11	2.79	12.73	7.85	79.43	20.57	226	0.57	1.62
339	0.05	6.58	11.63	8.75	79.61	20.38	102	1.34	1.33
343	0.07	10.77	11.35	7.66	80.98	19.01	133	2.05	1.48
344	0.15	3.75	7.38	4.09	88.52	11.48	172	0.43	1.80
346	0.13	86.67	4.85	22.36	72.79	27.21	354	23.60	0.22
350	0.37	86.05	4.95	4.84	90.21	9.79	362	8.42	1.02
354	0.57	150.00	1.59	1.19	97.21	2.78	158	4.16	1.34
355	0.71	142.00	1.62	1.50	96.88	3.12	222	4.43	1.08
356	0.88	129.41	1.34	1.20	97.45	2.55	224	3.29	1.12
357	0.11	28.21	5.45	4.33	90.22	9.78	107	2.74	1.26
360	0.09	5.84	6.99	5.48	87.52	12.47	112	0.73	1.28
361	0.41	47.67	1.82	1.31	96.87	3.13	128	1.49	1.39
365	0.26	23.64	2.82	2.38	94.80	5.19	135	1.23	1.18
367	0.23	191.67	3.14	3.37	93.48	6.51	50	2.48	0.93
Average			6.42	6.89		13.31	174	6.07	
Total Average	0.41	24.71	14.58	13.70	11.72	28.29	955	4.27	

Table II.3.5 - Pyrolysis results of the rock powders and kerogen concentrates.

Sample No.	Rock powder pyrolysed at 900°C C_R/C_T	Rock powder pyrolysed at 900°C $\frac{C_T - C_R}{C_T}$ %	Rock powder pyrolysed at 600°C C_R/C_T	Mineral free kerogen pyrolysed at 500°C %Weight loss	%Carbon loss (per weight of sample)	%Carbon loss (per weight of initial carbon)	%Carbon in pyrolysis products
			Shahpassand area				
124	0.50	49.71	0.61				
125	1.64		0.98				
129	0.85	15.44	0.95				
133	0.29	71.30	0.74				
138	0.56	43.97	0.88				
142	0.06	93.75	0.13				
149	0.15	85.48	0.85				
150	0.34	65.57	0.66				
152	1.21		1.18				
157	0.49	51.35	1.89				
161	1.07		1.09				
162	0.25	74.55	0.33				
166	0.55	44.97	0.70				
169	0.82	17.71	0.90				
171	0.71	29.08	0.80				
173	1.23		1.15				
174	1.46		0.75				
177	0.72	27.83	0.96				
179	0.72	28.38					
184	0.90	9.52	0.88				
186				36.66	11.15	26.99	30.41
191	0.81	19.44	0.85				
196	0.97	2.69	1.03				

Table II.3.5 - Continued.

Sample No.	Rock powder pyrolysed at 900°C C_R/C_T	Rock powder pyrolysed at 900°C $\frac{C_T - C_R}{C_T}$ %	Rock powder pyrolysed at 600°C C_R/C_T	Mineral free kerogen pyrolysed at 500°C %Weight loss	%Carbon loss (per weight of sample)	%Carbon loss (per weight of initial carbon)	%Carbon in pyrolysis products
197	1.03		1.05				
203	0.48	52.05	0.71				
207	0.25	74.55	0.76				
208	0.35	65.00	1.02				
218	0.18	82.41		45.16	10.43	23.00	23.10
220	0.18	82.35					
222	0.55	45.35					
224	0.73	26.92		42.92	10.69	25.93	24.91
228	0.30	69.70		18.37	12.05	65.09	65.62
232	0.30	69.74					
233	0.26	73.77					
236	0.12	87.80					
238	0.29	71.25					
242	0.22	77.65					
245	0.22	77.78					
249	0.32	67.57					
251	0.98	1.92					
253	0.39	61.29					
254	0.36	63.93					
256	0.93	7.14					
257	0.38	61.64					
259	0.15	85.37					
260	0.00	100.00					
261	0.06	93.62					
262	0.99	1.46					
265	0.44	5.91		47.89	15.60	36.56	32.57
271	0.73	27.47					

Table II.3.5 - Continued.

Sample No.	Rock powder pyrolysed at 900°C C_R/C_T	Rock powder pyrolysed at 900°C $\frac{C_T - C_R}{C_T}$ %	Rock powder pyrolysed at 600°C C_R/C_T	Mineral free kerogen pyrolysed at 500°C %Weight loss	%Carbon loss (per weight of sample)	%Carbon loss (per weight of initial carbon)	%Carbon in pyrolysis products
276	0.79	20.58					
282	1.01						
285	0.81	19.05					
Average	0.52	51.20	0.80				
			Jajarm area				
326	1.00	0.00					
327	0.71	28.57					
330	0.04	96.34					
333	0.00	100.00					
336	0.71	28.93		28.73	10.24	14.89	6.52
339	0.17	82.89					
343	0.06	93.85					
344	0.53	47.50		44.51	6.07	17.66	13.64
346	0.00	100.00					
350	0.23	76.74		46.08	3.14	50.60	6.81
354	0.16	84.21					
355	0.52	48.00					
356	0.46	54.41					
357	0.15	84.62		31.69	4.74	36.78	14.96
360	0.13	87.01					
361	0.14	86.05					
365	0.25	75.45		29.30	13.85	24.35	47.27
Average	0.31	69.09					
Total Average	0.47	56.11		37.13	9.80	34.18	26.58

of the change of the extraction system (Sect. 3.3.2) and because of the possibility of prior expulsion or migration of the bitumens.

Heavy and condensed (high-wax) bitumens extracted from the highly carbonaceous samples, particularly the coal specimens, suggest a terrestrial origin for their respective source beds.

3.3.5 Conclusions

The evaluation of source rocks from solvent organic extraction results is ambiguous and speculative, unless further analysis of their bitumen is carried out.

However, the high-wax nature of some of the extracted bitumens points out a terrestrial origin, and the average bitumen ratio suggest that the Shemshak Formation is a good source rock, although this needs to be corroborated by further analysis.

3.4 Fractionation of Bitumen

3.4.1 Introduction

The bitumen content of source rocks is composed principally of hydrocarbons and non-hydrocarbons. Hydrocarbons are generated mainly from the initial organic matter in the rock during its gradual maturation processes, although a minor proportion of them is derived directly from living organisms. Thus the hydrocarbons in bitumen represent the petroleum generating nature of the sedimentary organic matter. In order to study the amount and type of these hydrocarbons, fractionation of bitumen is required to separate them from the non-hydrocarbons.

The most common method of bitumen fractionation in petroleum geochemistry is liquid-phase column chromatography (LPCC) using a mixture of silica gel and alumina as absorbent. A more advanced technique of high performance liquid chromatography (HPLC), that uses a pressured liquid-phase in conjunction with

two UV and RI detectors (Dark et al., 1977), has been developed, mainly for the separation of crude oil into hydrocarbon groups, and is mostly utilised by oil companies. An alternative to LPCC is the thin layer chromatography (TLC) technique which was used for the purpose of this study.

The hydrocarbon fraction of bitumen consists of saturates (n-alkanes, isoalkanes, and cycloalkanes) and aromatics. The relative proportion and composition of these constituents are subject to variation, depending on the type and state of maturation of original organic matter. Tissot and Welte (1978), who compared the sedimentary organic matter of the Uinta basin (alginite), the Paris basin (sapropelite), and the Douala basin (huminite), showed that the hydrocarbons generated by pyrolysis from the Paris basin have the highest and those of Uinta basin the lowest aromatic/saturates ratios(Fig. II.3.6). Hunt (1977) reported that, in Recent sediments, the ratio of C_{15}-C_{40} hydrocarbons to heavier asphaltic compounds is about 1:2 in oxidising environments. Vandenbroucke et al. (1976) showed that in allochthonous terrestrial sediments (Logbaba series, Douala basin) saturated hydrocarbons are more abundant than aromatics, whilst autochthonous marine deposits (Toarcian series, Paris basin) contain equal proportions of the two hydrocarbon fractions. Claypool and Reed (1976) provided an estimate of organic richness for source rock evaluation based on the hydrocarbon content of the rock. They suggested that a limit of 100 ppm extractable heavy hydrocarbons* and 0.5 percent organic carbon (in shales) can be used to separate below- and above-average source rocks, whereas values above 1,000 ppm extractable heavy hydrocarbons and 2.0 percent organic carbon (in shale) indicate an exceptional source bed. Variations of saturated and aromatic hydrocarbons with depth of burial and maturation of organic matter are

* Heavy hydrocarbons in organic geochemistry refers normally to hydrocarbons of $C_{15}+$.

discussed by Alberecht et al. (1976) and Ishiwatari et al. (1977). However, fractionation techniques are used mainly as preparatory treatment for GLC analysis.

3.4.2 Procedures

Standard glass plates (20 cm X 20 cm) were coated with a layer of (approximately 0.5 mm thick) Merck type 60 silica gel and then dried in an oven at 110°C in order to activate the gel. Bitumen samples were dissolved in benzene-methanol (3:2 azeotrope) and the solution applied to the dried plates. Two plates were streaked for each sample. The streaked plates were developed in a tank, using pure n-heptane as the mobile phase. The separated fractions on the developed plates were identified under UV light (3660°A) and marked immediately after developing. All respective fractions were then extracted from silica gel by a technique similar to that described in Section 3.3.2, although the extraction system was smaller (thimble size 80 mm X 25 mm; soxhlet capacity 120 ml). A detailed description of the technique is given by Stock and Rice (1974, 3rd edition). The different fractions were then measured by weight and their percentages calculated.

3.4.3 Data

All 71 extracted bitumens were fractionated and the results are shown in Table II.3.4. Samples no. 166, 169, 207, and 208 are excluded from the analytical interpretations, because of the inorganic impurities described in Section 3.3.2.

3.4.4 Results and Interpretation

The average concentration values are 14.58 percent saturates, 13.70 percent aromatics, and 71.72 percent non-hydrocarbons. The average ratio of non-hydrocarbon/hydrocarbon is 2.54 which is very close to the value given by Hunt (1977) for sediments from oxidising environments (2:1). Thus an overall domination of

terrestrial organic matter is apparent. Table II.3.4 shows that, in the samples from the Shahpassand area, the average proportion of saturated hydrocarbons (17.81) is higher than of aromatic hydrocarbons (16.40), whilst in the Jajarm samples the average percentages of the two fractions (6.42% and 6.89%) are nearly equal. This may indicate that the sediments of the Jajarm region contain a greater amount of autochthonous marine material than those of the Shahpassand area.

An exponential plot of the total organic carbon content versus extracted hydrocarbon concentrations (Fig. II.3.7) shows that the majority of samples fall into the "above-average" and "exceptional" categories.

3.4.5 Conclusions

The organic matter in the Shemshak Formation of the studied region is dominantly of terrestrial origin, as indicated by its average non-hydrocarbon/hydrocarbon ratio. Near Jajarm, however, there is a greater content of autochthonous marine material than at Shahpassand.

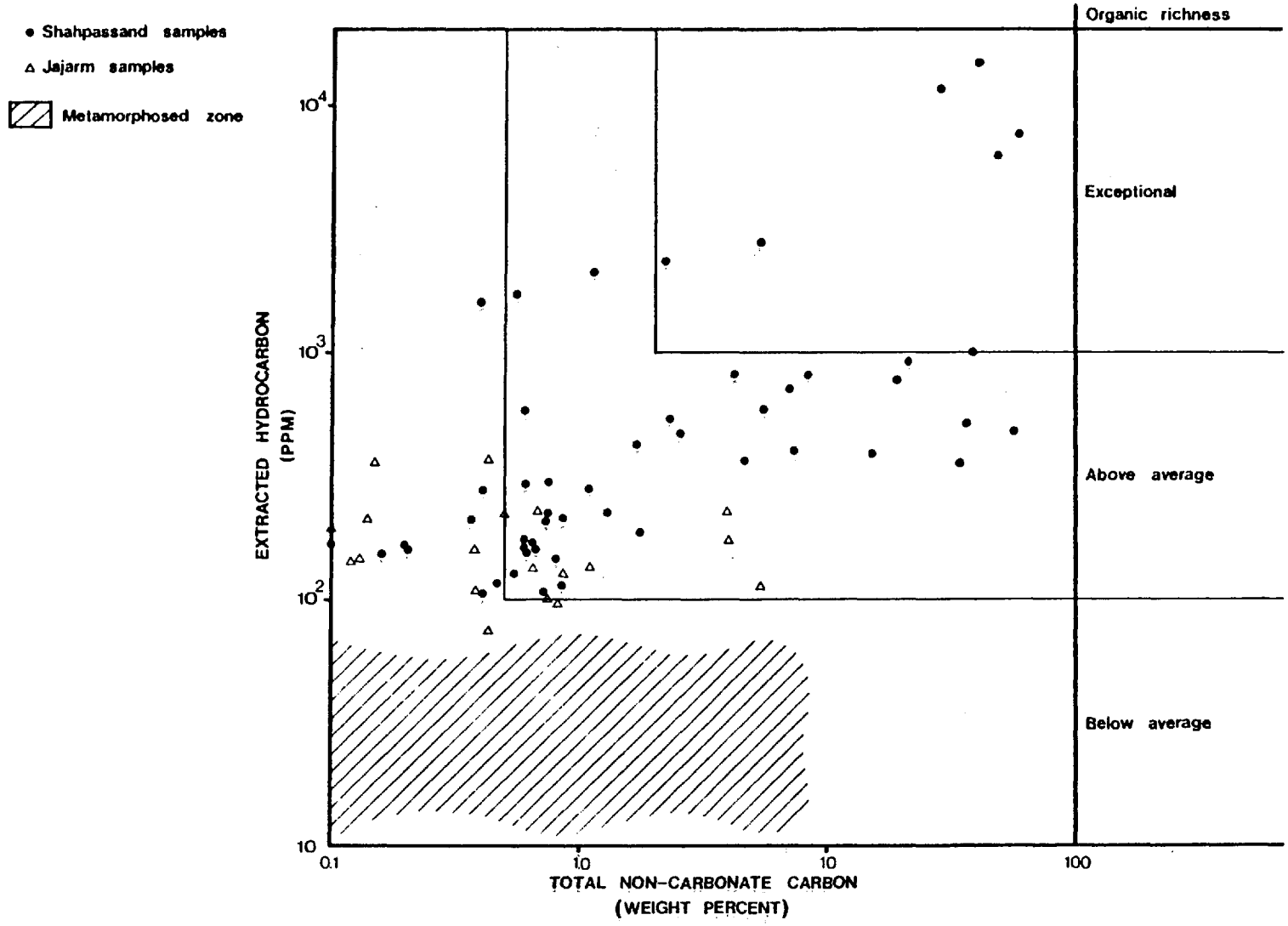
The majority of the samples analysed fall into the above-average or exceptional source rock categories, suggesting that the Shemshak Formation may well be a potential source of hydrocarbons.

3.5 Pyrolysis

3.5.1 Introduction

The transformation of initial organic material into petroleum depends primarily on temperature and time. Pyrolysis techniques have been introduced to source rock studies in order to simulate the temperature dependent processes over a short period of time, and thus to characterise the organic matter in the sedimentary rocks. This is done by using temperatures higher than those

Fig. II.3.7 - Extracted hydrocarbon concentration versus total organic carbon content of the Shemshak Fm. in the Eastern Alborz (crossplot modified after Claypool et al. 1978).



reached naturally in the earth. Temperature increase has an exponential effect on transformation rate whereas the effect of time is linear (Phillippi, 1965). Experimental heating can therefore be made to compensate for time.

Although some deviations from natural conditions occur, experimental pyrolysis has been proved to produce results analogous to natural transformations of organic matter (Harwood, 1977; Tissot and Welte, 1978). The pyrolysis results from shallow or outcrop samples can thus be used to assess the nature and level of maturation of the organic matter in more deeply buried areas of a sedimentary basin.

Pyrolytical analysis of source rocks can be made on either: (i) the separated kerogen concentrates, or (ii) the rock powder.

Analysis of the separated kerogen involves pyrolysis with subsequent examination of the generated products by gas chromatography (PGC) and mass spectrometry (MS). This method is used to determine the type of kerogen, based on relative amounts of generated hydrocarbons and carbon dioxide. Harwood (1977) has shown that the proportion of CO_2 generated by pyrolysis is higher for huminite (kerogen type III) than for alginite (kerogen type I) and sapropelite (kerogen type II). He also showed that during pyrolysis there is a much greater loss of carbon from oil-type kerogens than from gas-type kerogens. Vandenbroucke et al. (1976) concluded that terrestrial organic matter (Logbaba series, Douala basin) mainly gives rise to paraffinic hydrocarbons, whilst marine organic matter (Toarcian series, Paris basin) yields mainly naphtheno-aromatic hydrocarbons. However, this method is rather lengthy due to the kerogen isolation procedures.

The pyrolytical analysis of rock powder is quick and can provide valuable information about the type and maturity of organic matter in the rock. Gransch and Eisma (1966) introduced the carbon ratio "C_R/C_T" for the characterisation of kerogen, where C_R is the percentage residual carbon after pyrolysis. C_R,

in fact, also represents the abundance of polyaromatic nuclei in the kerogen (Tissot and Welte, 1978) that do not break down by pyrolysis. Gransch and Eisma suggested that the thermal maturation of humic coaly matter starts with a C_R/C_T ratio of approximately 0.6, in contrast to 0.2 or less for non-coaly organic matter: the carbon ratios of all kerogens tend to approach unity with continued thermal maturation. Thus, if the state of maturation is known, the C_R/C_T ratio can, to some extent, be used to identify the type of organic matter: C_R variations relative to C_T can be illustrated in a crossplot (Fig. II.3.8), which can be used to determine the type of kerogen if thermal maturity is low.

Barker (1974) developed a temperature programming pyrolysis technique in which the generated hydrocarbons are detected through a flame ionisation detector (FID). By using a suitable temperature programme two peaks can be detected (Fig. II.3.9). Peak I represents mainly the hydrocarbons already present in the rock (distilates) and peak II the hydrocarbons generated by thermal breakdown of the kerogen content of the rock (cracking products). He also concluded that the generated hydrocarbons already in the rock are released at temperatures lower than those needed to crack the kerogen. Claypool and Reed (1976) used a plot of peak I against peak II to define the generating potential of organic matter. More recently Espitalié et al. (1977 and 1978) introduced a more advanced and quick pyrolysis method for the evaluation of source rocks. They developed a device known as "Rock-eval", which can give a general idea of the type, generating potential, and state of maturation of organic matter in the source rock. In this method, two peaks identical to those of Barker (1974), are detected through an FID, as well as a third peak which represents the amount of CO_2 generated during pyrolysis (Fig. II.3.10). The second peak is referred to as the hydrogen index (mg HC/g organic carbon) and the third peak as the oxygen index (mg CO_2/g organic carbon).

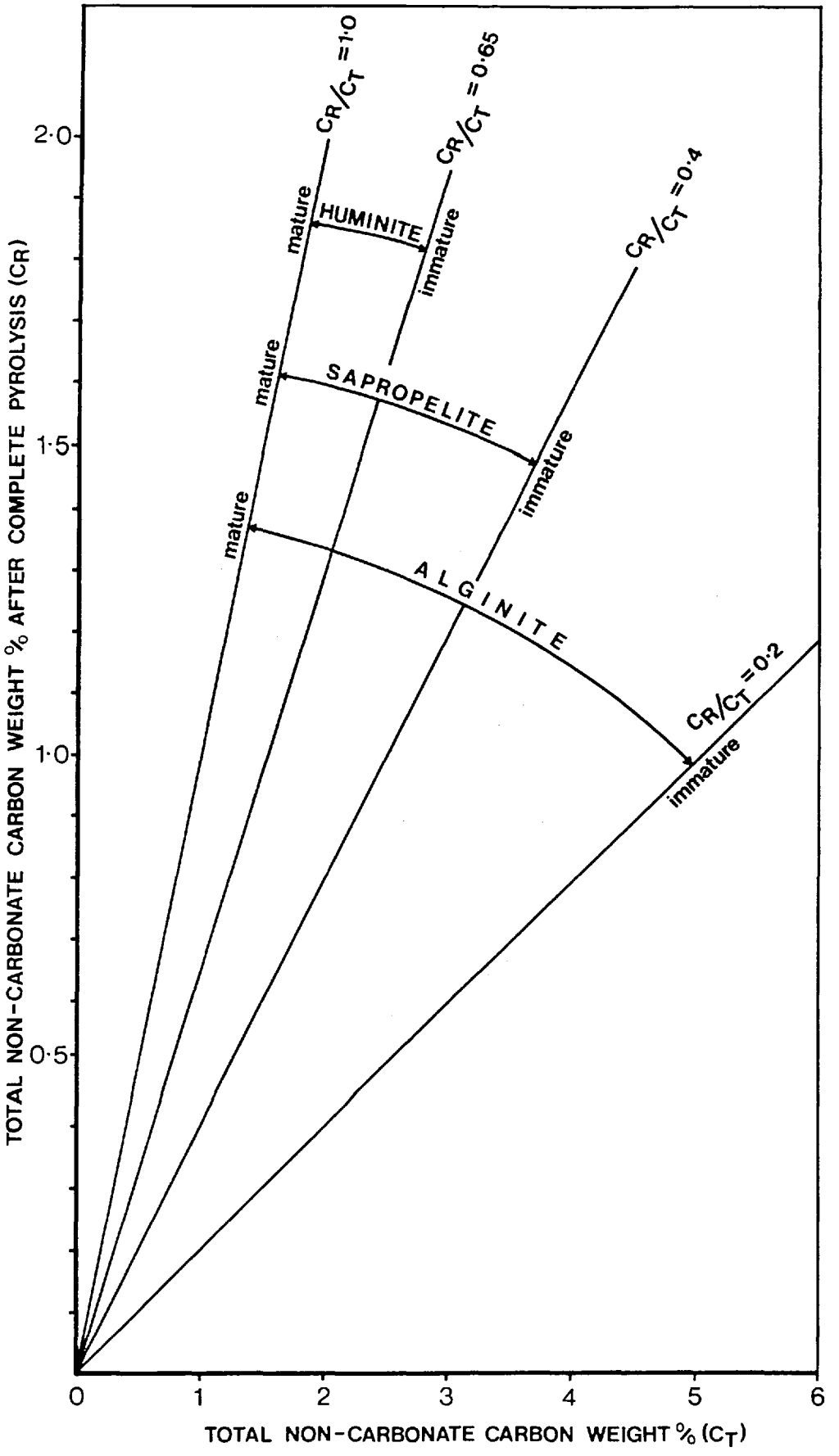
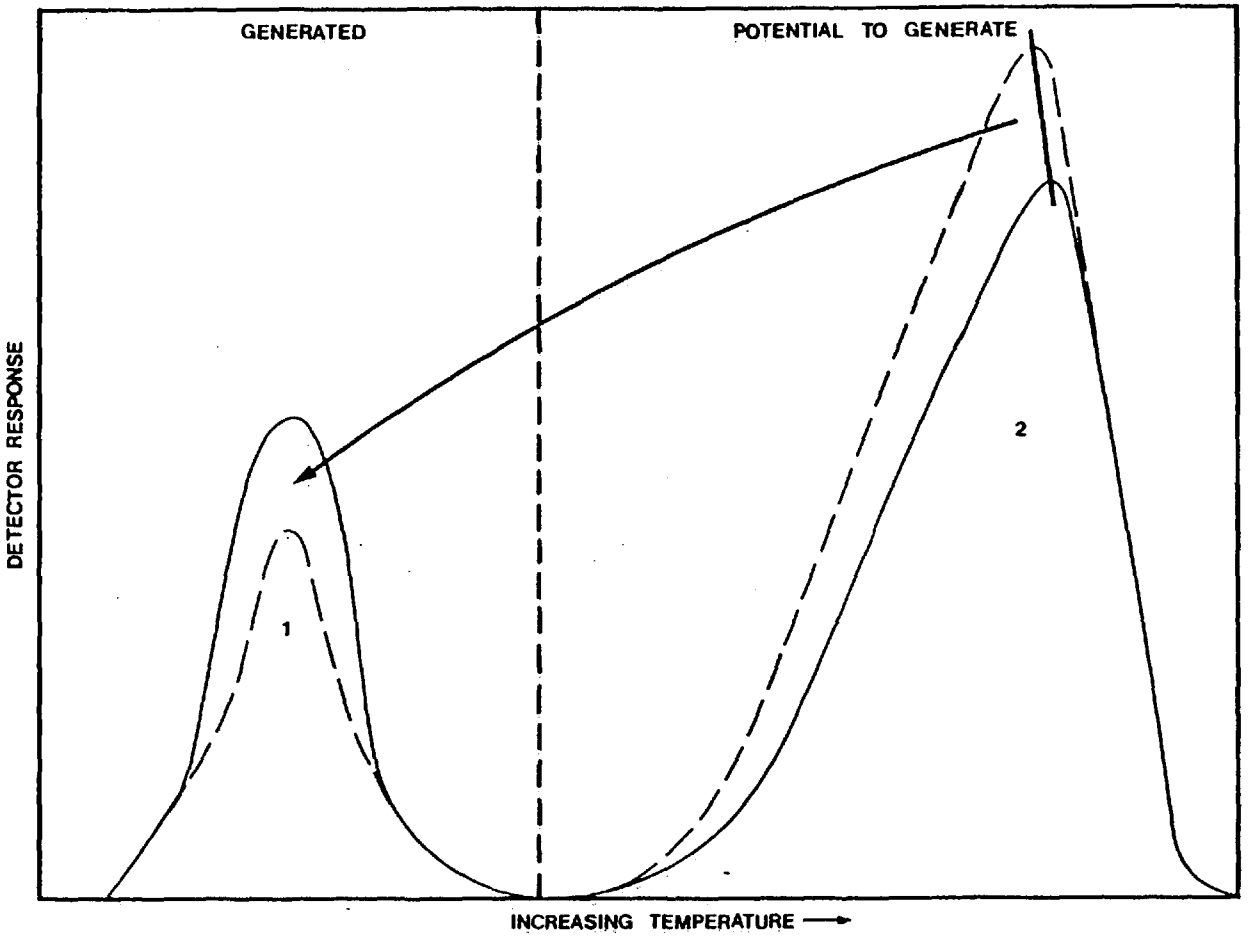


Fig. II.3.8 - Relative variation of C_R and C_T for different types of kerogen.

Fig. II.3.9 - Schematic representation of the pyrogram obtained by pyrolysis of rock samples. Dashed line: response for shallow sample; solid line: response for deep sample (after Barker, 1974).



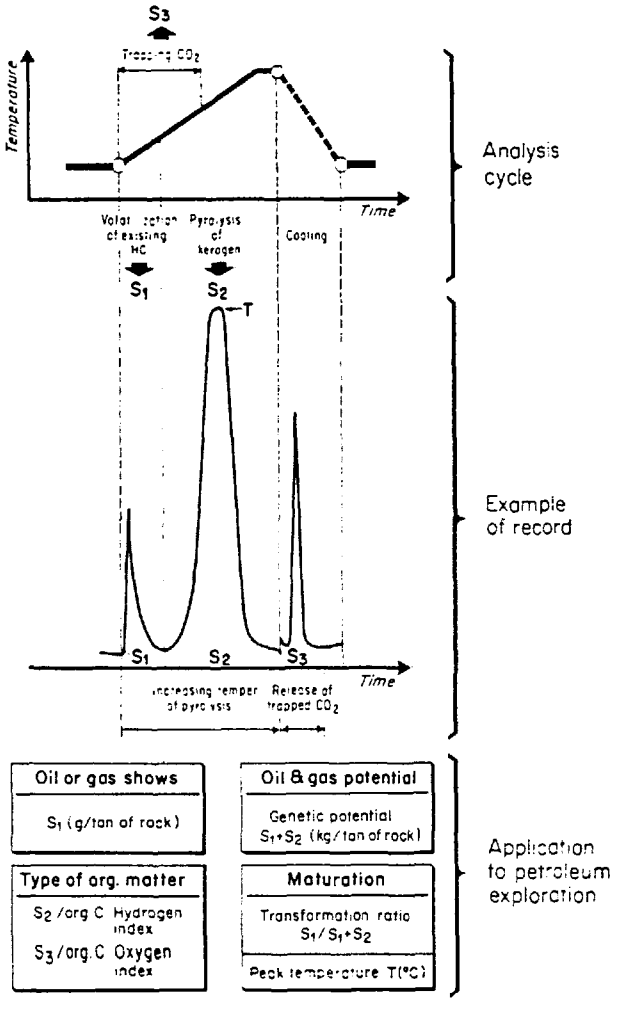


Fig. II.3.10 - An example of the pyrogram obtained by the pyrolysis method of Espitalié et al. (1977). From Tissot and Welte, 1978.

These indices are then used as substitutes for atomic H/C and O/C ratios respectively in determining the kerogen type. However, it must be pointed out that the oxygen index does not fully represent the organic oxygen content of the sample, because the oxygen-rich heteroatomic compounds of kerogen mostly break down at higher temperatures than those of the selected CO_2 trapping range. Moreover, there is a high possibility of interference by the inorganic CO_2 from carbonates, which can however be tested by carbon isotope analysis. In the case of highly calcareous samples, it is probably better to digest their carbonate contents in HCl before pyrolysis. The Rock-eval technique is, in fact, more suitable for the determination of the generating potential and maturity of organic matter rather than its kerogen type. Rock-eval does have the advantage that it can be utilised at a well site, to select proper samples for detailed geochemical analyses.

In the present writer's opinion, the best pyrolysis technique would be to trap the temperature programmed pyrolysis products in a mixing flask by means of a pressured carrier gas at different temperature ranges. These pyrolysis products can then be injected into a GC-MS system to identify the components and determine their relative abundances. The results could determine the type and maturity of the organic matter. Details of the use of alkanes distribution are given in Sections 3.6 and 4.3.

3.5.2 Procedures

For direct pyrolysis, pulverised samples were pyrolysed in a platinum tray under nitrogen at 900°C for about 1½ hours. A further batch was pyrolysed under identical conditions at 600°C. The total organic carbon contents of these samples were then measured with an elemental analyser as described in Section 3.2.2.

Alternative samples were macerated, as described in Section 2.2.3, and then treated, for standard heavy mineral separation,

in concentrated zinc bromide solution. The resulting mineral free kerogens were then pyrolysed for 24 hours in a small platinum boat under nitrogen at 500°C. Elemental analysis of the kerogen was carried out before and after pyrolysis.

3.5.3 Data

74 samples from the studied Sections were pyrolysed at 900°C and 25 samples from the Qoznavi Section were also pyrolysed at 600°C. 10 mineral free kerogens, representative of both the Shahpassand and Jajarm regions, were pyrolysed at 500°C and their weight losses measured. All analytical results are shown in Tables II.3.2, II.3.3 and II.3.5.

3.5.4 Results and Interpretation

C_R/C_T ratios after pyrolysis at 900°C averaged 0.47 (less than 0.6) and, following Gransch and Eisma (1966), would indicate organic matter favourable for the generation of hydrocarbons. The mean value of the C_R/C_T ratios is 0.52 for the Shahpassand samples and 0.31 for the Jajarm samples showing that the latter have a higher generating potential than the former. These C_R/C_T results exclude samples 125, 150, 173 and 174, because of their abnormal values (more than and/or equal to 1.1). A plot of C_R against C_T (Fig. II.3.11) shows that a direct relationship exists between the two. Figure II.3.12 gives a comparison of the Shemshak Formation with other source rocks studied at RSM (on a diagram similar to Fig. II.3.8): this suggests that the immature Shemshak Formation kerogen (see Chapter 4) is dominantly of huminite type. It must be admitted, however, that Gransch and Eisma (1966) obtained their results from rocks from which their bitumen had previously been extracted, whereas untreated rock powders were used in this study. During the present work, examination of extracted samples revealed that, even after lengthy drying, some solvent remains in the samples possibly adsorbed by polar organic matter or by swelling clay minerals.

Fig. II.3.11. Total Organic Carbon before and after pyrolysis. Showing the average trend of the Shemshak Formation in the Eastern Alborz (excluding samples: 125, 152, 161, 173, 196, 197, 218, 251, 262, 276, 282).

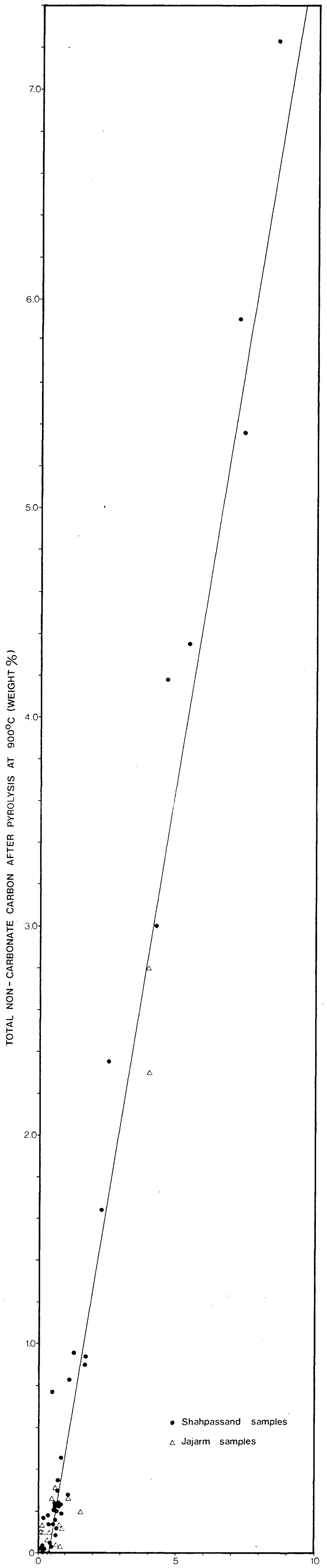
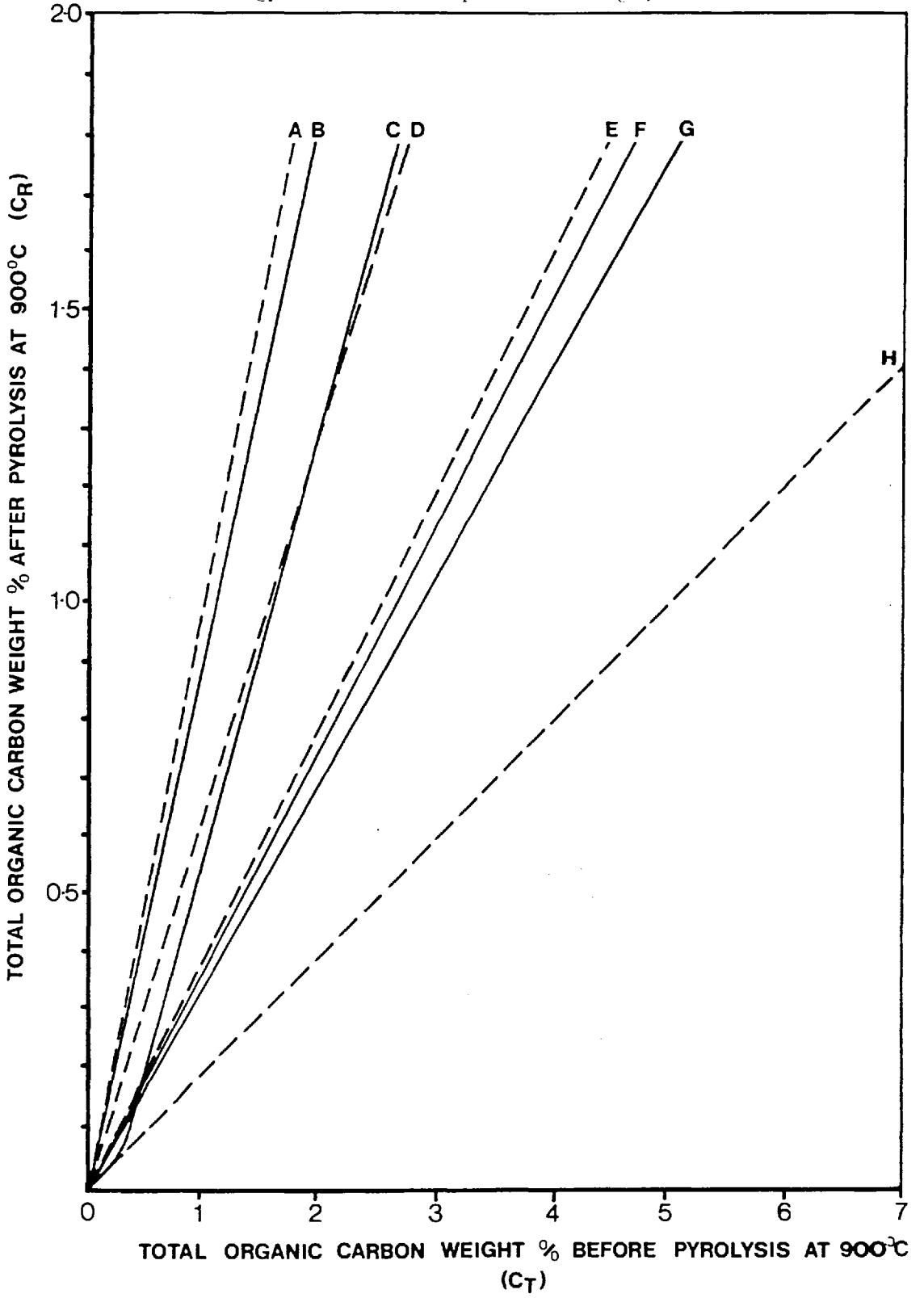


Fig. II.3.12 - The average C_R/C_T trends of the source rocks studied at the Petroleum Geology Section of Imperial College, London.



A - No conversion (Lower limit)
B - Senile Kashafrud Fm. (Average convertibility 8%)
C - Immature huminite (Convertibility 35%)
D - Immature Shemshak Fm. (Dominantly huminite)
E - Immature sapropelite (Convertibility 60%)
F - Immature Kimmeridge Clay (Av. convertibility 64%, dominantly sapropelite)
G - Reasonably mature Kazhdumi Fm. (Av. convertibility 65%, dominantly alginite)
H - Immature alginite (Upper limit – convertibility 80%)

However, the amount of organic carbon corresponding to bitumen is normally less than 0.2% of the total organic carbon (Tissot and Welte) and does not affect the overall conclusions.

Some of the samples showed a C_R value higher than their C_T (C_R/C_T more than 1), particularly those from coaly horizons. This is due to the loss of pyrolysis products other than hydrocarbons, such as CO_2 and H_2O. Tissot et al. (1974) showed that the pyrolysis products of terrestrial organic matter (huminite) contain over 50 percent $CO_2 + H_2O$. Therefore, the higher percentage weight loss due to oxygen than to carbon can cause an increase in the percentage of residual carbon (C_R) after pyrolysis. It should be noted that $C_T - C_R$ does not exactly represent the amount of carbon lost, as has been assumed by some authors: for example, an increase of carbon percentage after pyrolysis, as is the case for a few of the samples studied here, does not mean an actual increase in the total amount of carbon, but an increase of the amount of carbon relative to the rest of residual constituents of the pyrolysed samples. The amount of the carbon loss during pyrolysis can be measured either from the quantity of generated bitumen + gaseous hydrocarbons + CO_2 or by the following equation:

$$\text{Amount of carbon loss} = (\text{initial weight} \times C_T) - (\text{weight after pyrolysis} \times C_R)$$

In this study the values of carbon loss are calculated for pyrolysed kerogen from the above equation. A similar formula can be used for the calculation of carbon loss percentages in experiments involving rock powder pyrolysis. A general formula is suggested as:

$$\% C_L = \frac{(W_i \times C_T) - (W_p \times C_R)}{(W_i \times C_T)} \times 100$$

where C_L is the amount of carbon loss, C_T is total organic carbon before pyrolysis, C_R is organic carbon after pyrolysis, and W_i and W_p the weight of sample before and after pyrolysis respectively.

A comparison of the pyrolytical results of 900°C and 600°C shows that, in coaly samples, the percentage of residual carbon (C_R) rises with increasing pyrolysis temperature (maturation) due to a gradual graphitisation of their kerogen.

In the case of mineral free kerogen concentrates, the average weight loss after pyrolysis at 500°C was 37.13%. This is very close to the average value of 35% given by Vandenbroucke et al. (1976) for the terrestrial organic matter deposited in a deltaic environment in the Douala basin. The average carbon loss ratio (C_L/C_T%) is 34.18%, indicating a huminite kerogen (average convertibility = 35%). Increase in carbon percentages after pyrolysis (except 228 and 357) relative to initial carbon is evidence that significant amount of non-hydrocarbons (CO_2 and H_2O) were lost during pyrolysis, pointing to a huminite kerogen.

Figure II.3.13 shows that the amount of carbon loss due to pyrolysis of kerogen concentrates increases with their initial carbon content, although the average trend of the samples is still below the huminite threshold.

3.5.5 Conclusions

The Shemshak Formation contains organic matter dominated by huminite (as indicated by the C_R, C_T diagram), but still favourable to the generation of hydrocarbons (average C_R/C_T less than 0.6).

The Jajarm sediments have a higher generating potential than the Shahpassand counterparts.

Pyrolytical results of mineral free kerogen concentrates show an average of about 35 percent convertibility which also suggests that the kerogen is predominantly huminite.

A relative increase in the carbon percentages after pyrolysis is due to loss of non-hydrocarbon products such as CO_2 and H_2O again indicating huminite kerogen.

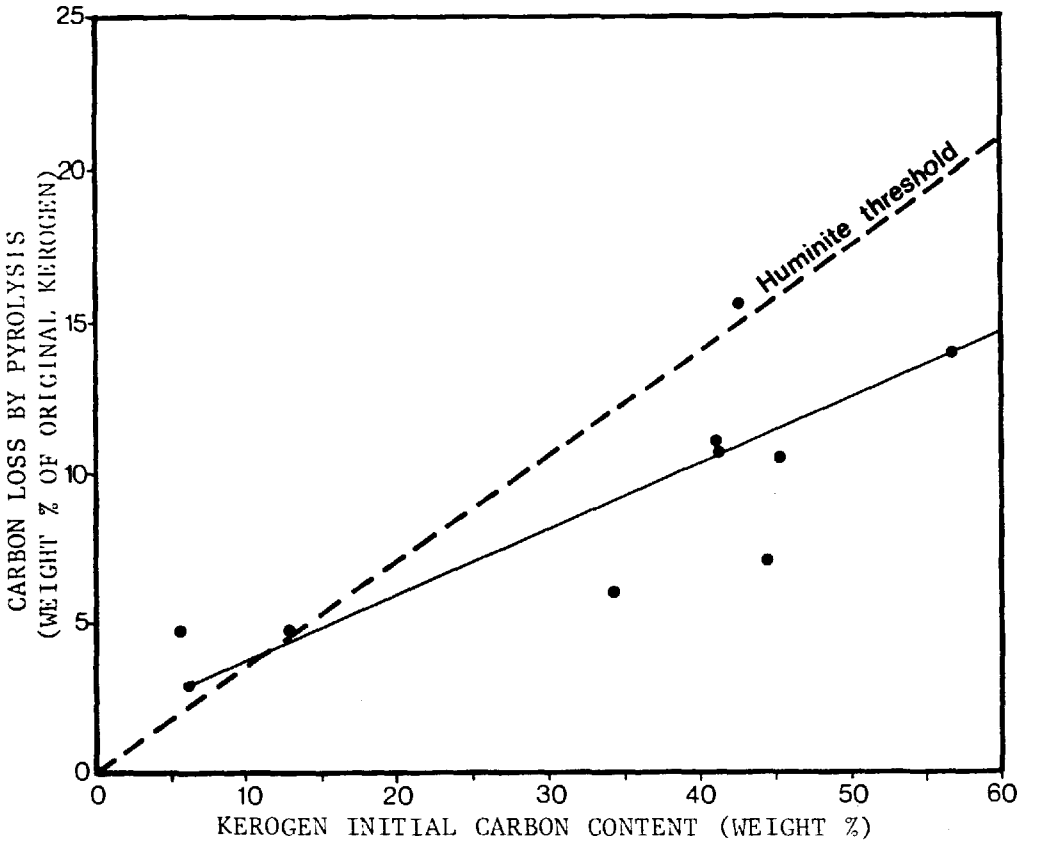


Fig. II.3.13 - Weight percentage of carbon loss versus kerogen initial carbon content. The majority of the Shemshak Formation samples fall below the huminite threshold.

3.6 Gas-Liquid Chromatography and Normal Alkane Distribution

3.6.1 Introduction

Gas chromatography (GC) is a method of separating out the individual components of a mixture of volatile compounds, in order to identify them and to determine their relative abundance. Gas-liquid chromatography (GLC) was introduced in 1952 by James and Martin (Littlewood, 1970) and is recognised to be the best separation technique available (Ettre and McFadden, 1969). It has been widely utilised in organic geochemistry, particularly in typing crude oils and source rocks and in determining states of maturation.

GLC techniques are commonly used for the analysis of soluble organic matter (bitumen), thus providing valuble information about the petroleum generating potential of source rocks. The GLC of alkanes can be systematised more precisely than that of any other group of organic compounds (Littlewood, 1970), because they boil off almost without decomposition.

The n-alkanes* found in a source rock were in part deposited with the original organic matter and in part generated during the processes of maturation. Thus if the effect of maturation can be minimised, as in Recent or only slightly heated sediments, then a knowledge of the relative abundances of the alkanes can provide a clue to the nature of the organic matter and hence to the environment of deposition (Douglas and Henderson, 1972). Harwood (1977) found that the extracts from source rocks with oil or wet-gas type kerogen usually have a high proportion of n-alkanes in C_{16}-C_{20} range, whilst those of dry-gas type contain a higher proportion of C_{20}-C_{24} n-alkanes. Tissot and Welte (1978) confirmed that continental organic matter has a high alkane content, dominated by heavy n-alkanes with an odd carbon

* n-alkanes = normal paraffins.

number predominance, and a low content of isoprenoids. In contrast, marine organic matter contains smaller amounts with a preference for low to medium weight n-alkanes, and abundant isoprenoids (Fig. II.3.14). Thus, whilst normal alkanes in the range of C_{25} to C_{31} with a marked odd carbon predominance were derived from terrestrial plant material, the $n\text{-}C_{13}$ to $n\text{-}C_{21}$ range represents either the original marine microorganisms (Amit, 1978) or other types of organic matter that have been subjected to thermal maturation. $n\text{-}C_{17}$ is believed to be dominant in brown benthonic algae (Hobson and Tiratsoo, 1975); a similar predominance in source rocks is thus taken as evidence that algal material formed a large proportion of the original organic content.

Phillippi (1974) proposed the ratio $(C_{21} + C_{22})/(C_{28} + C_{29})$ as an environmental indicator of source rocks. He found that the n-paraffins are characterised by abnormally low $(C_{21} + C_{22})/(C_{28} + C_{29})$ ratios of 0.6-1.2 in source beds rich in terrestrial plant matter, whilst those with a dominantly marine origin have a ratio in the 1.5-5.0 range. A relation between the C_{18}/C_{22} peak-height ratios and the initial H/C ratios of mineral free kerogens has also been suggested by Harwood (1977) as a means of distinguishing oil-generating from gas-generating kerogens.

The distribution of the isoprenoids, particularly pristane ($C_{19}H_{40}$) and phytane ($C_{20}H_{42}$) because of their higher concentrations, is believed to be influenced by the depositional environment of the source material: high ratios of pristane to phytane may reflect a terrestrial origin (Powell, 1973 and 1976). Lijmbach (1975) mentioned that oils from source rocks deposited under peat-swamp conditions are relatively rich in pristane and poor in phytane, and Rashid (1979) also showed that the pristane/phytane ratios increase with increasing terrigenous organic content. He calculated a mean value of 1.12 ± 0.54 for dominantly marine organic matter and an average of 1.61 ± 1.00 for those dominated by terrestrial material.

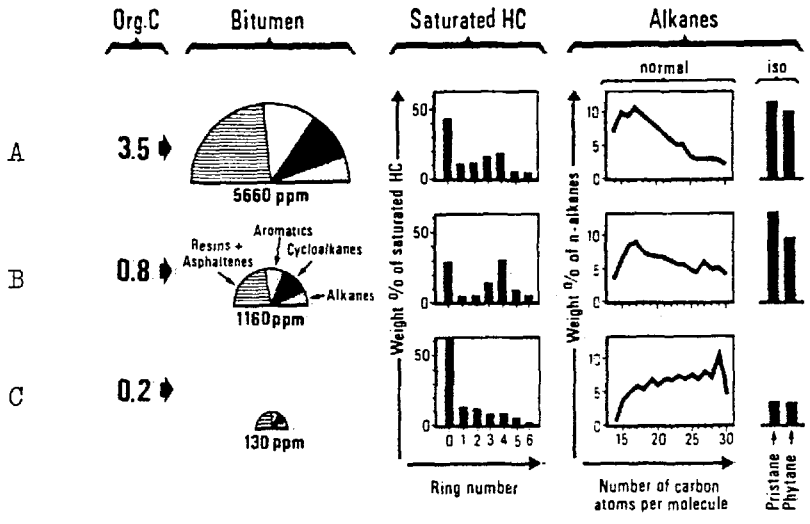


Fig. II.3.14 - Comparison of bitumen composition of different source rocks.

A and B) Organic rich shales contain mostly marine and autocthonous material.

C) Organic lean shale contains mostly terrestrial matter derived from higher plants.

(after Tissot and Welte, 1978).

More recently a method of pyrolysis-gas chromatography was used by Larter and Douglas (1977) to identify the type of organic matter based on the relative proportion of straight chain hydrocarbons to aromatic components generated from laboratory pyrolysis (Fig. II.3.15).

3.6.2 Procedures

A Perkin-Elmer model F 30 gas chromatograph equipped with flame-ionisation detectors (FID) and a SGE glass support coated open tabular (SCOT) capillary column was used in this study. The specifications of the column and operating conditions are given in Table II.3.6 and II.3.7 respectively. All samples were run under the instrumental conditions shown on these Tables, although the sample size (0.03 to 0.08 μl) and attenuation of the detector response (20 to 320) were adjusted to produce comparable chromatograms.

Two standard mixtures (A: n-C_{15} to n-C_{22}; B: n-C_{15} to n-C_{36}) were made and run at least once a day to check the reproducibility of the instrument and the identification of the n-alkane components in the samples (Fig. II. 3.16). Under the operating conditions shown on Table II.3.7 a final time of 48 minutes was needed for the elution of n-C_{36} in the B standard. The relative concentrations (by weight) of the components in the A standard mixture are given in Table II.3.8.

Qualitative analysis- Identification of the n-paraffin components was carried out by comparison with chromatograms of the standard mixtures based on their retention times. As is shown in Figure II.3.16, the alkanes are separated in order of their boiling points, because of the non-polar stationary liquid phase (silicone oil) of the column.

Quantitative analysis- The basic equation for quantitative analysis, given by Littlewood (1970), is:

$$W_i = \frac{A_i/S_i}{\sum_k (A_k/S_k)} \qquad (1)$$

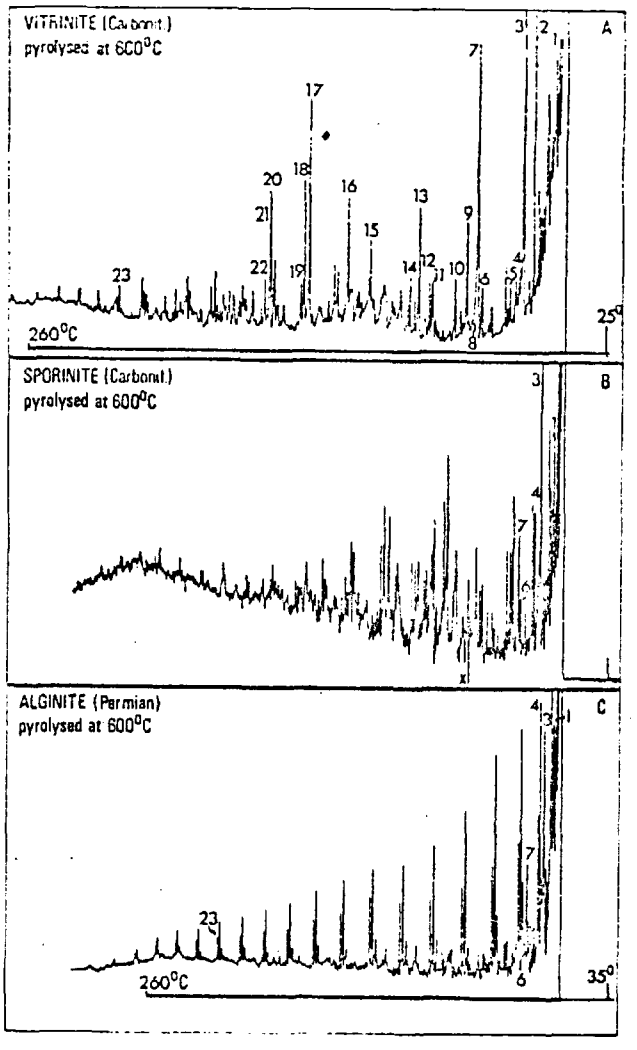


Fig. II.3.15 - Pyrograms of different coal macerals (after Larter and Douglas, 1977).

Table II.3.6 - Column specification.

Type - SGE glass SCOT coated with SF-96

Length - Approximately 40 metres (grade C)

O.D. - 1 mm

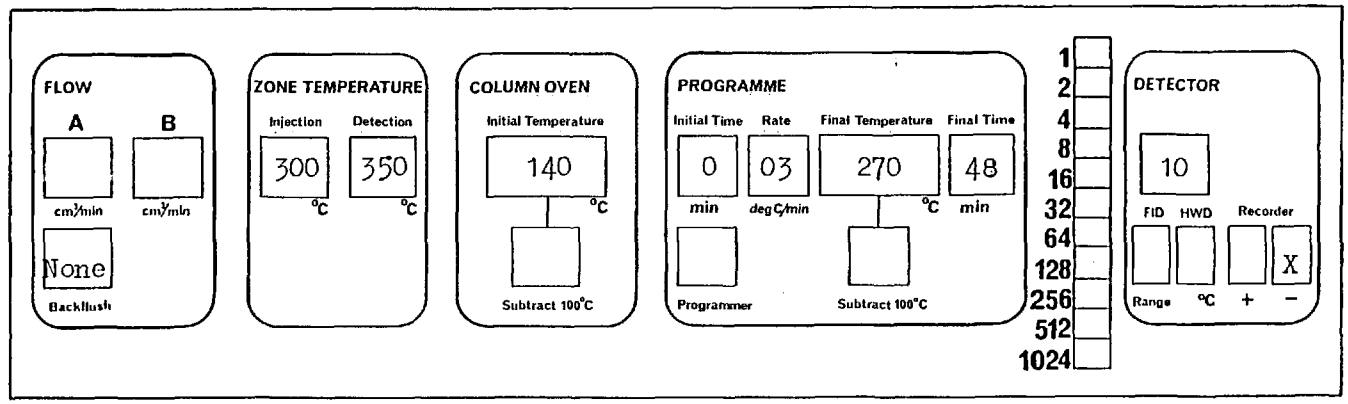
I.D. - 0.5 mm

Liquid phase - SP 2100 (silicone oil, equivalent to SE 30, OV 101)

Efficiency - 30-40,000 effective plates

Operating temperature - 30 to 275°C

Table II.3.7 - Operating Conditions.



COLUMN: length 40m o.d. 1.0mm i.d. 0.5mm * delete where appropriate metal/glass/WCOT/SCOT /packed Glass SCOT

stationary phase Silicone Oil support mesh ratio

SAMPLE: size 0.03 to 0.08 l split ratio None *manual/capsule

CARRIER: Nitrogen pressure 60kn/m^2 flow/pressure control Pressure Hydrogen pressure 18 lbf/in^2 Air pressure 24 lbf/in^2

RECORDER: Modle 56 span 1mv chart speed 5mm/min integrator sensitivity

COMMENTS:

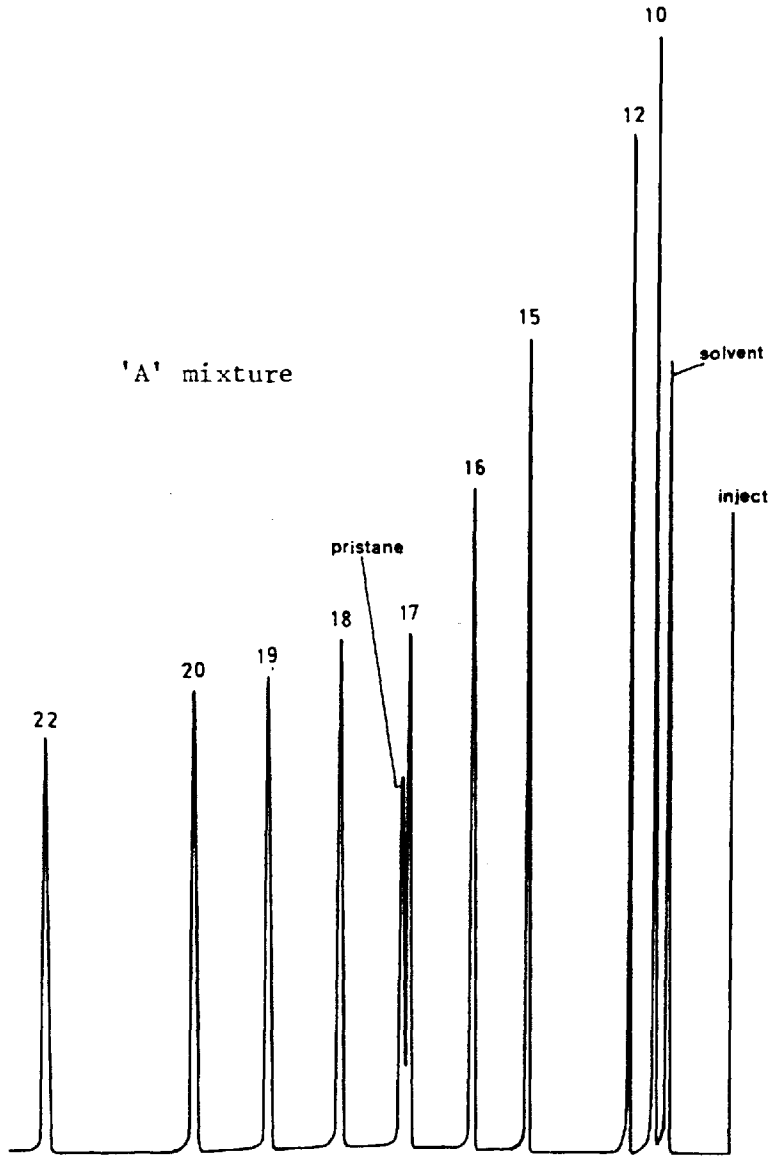


Fig. II.3.16 - Gas chromatograms of the standard mixtures used for identification of the n-alkanes.

A) Gas chromatogram of standard 'A' mixture (n - C_{15} to n - C_{22}).

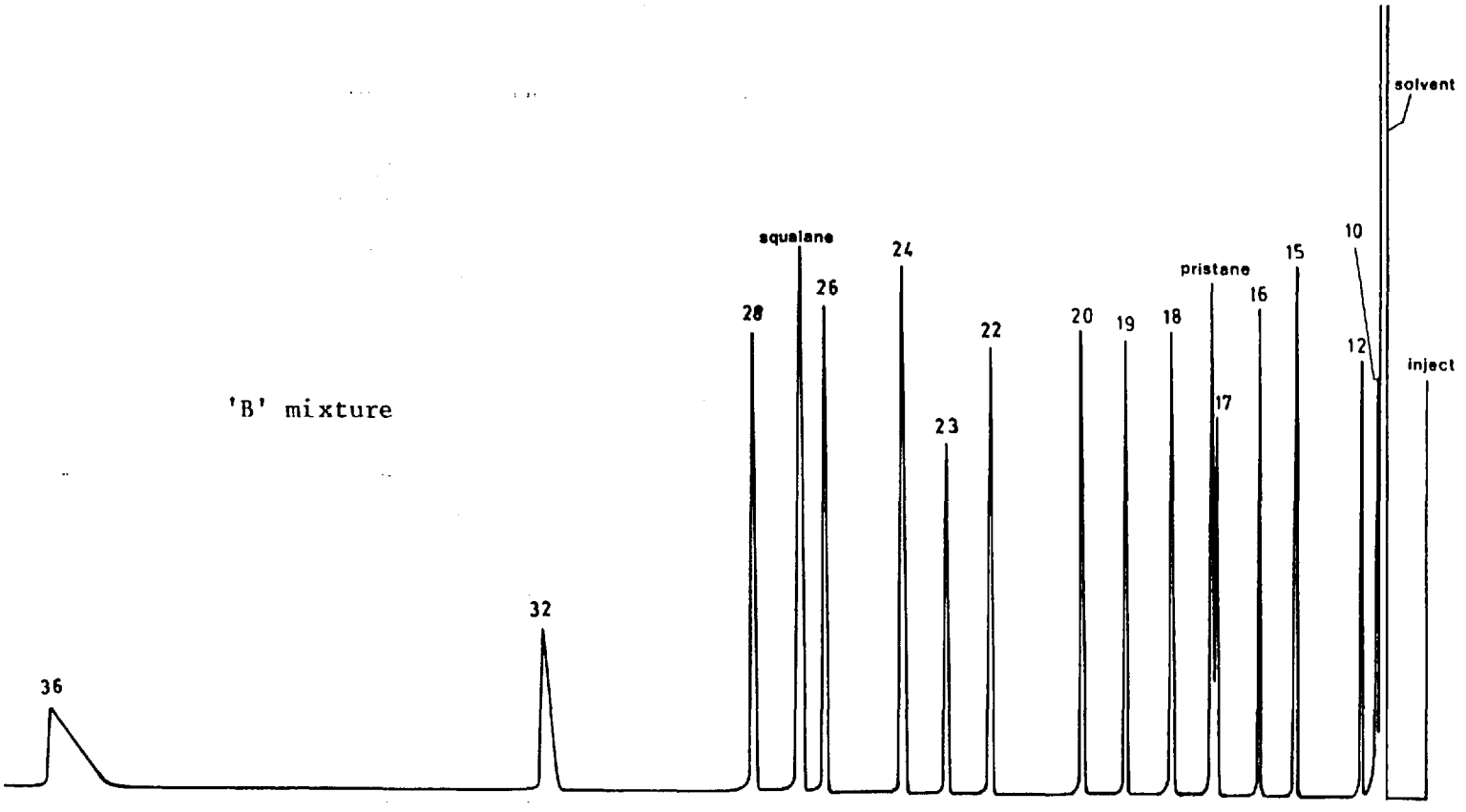


Fig. II.3.16 - Continued

B) Gas chromatogram of standard 'B' mixture (n - C_{15} to n - C_{36}).

Table II.3.8 - Relative concentration of n-alkane in "A" standard solution.

n-alkane	Weight% in Solution
$C_{10}H_{22}$	5.84
$C_{12}H_{26}$	5.84
$C_{15}H_{32}$	8.90
$C_{16}H_{34}$	9.54
$C_{17}H_{36}$	10.73
$C_{18}H_{38}$	12.12
$C_{19}H_{40}$	13.73
$C_{20}H_{42}$	15.60
$C_{22}H_{46}$	17.68

Table II.3.9 - SSCF values for n-C_{15} to n-C_{30}

n-alkane	SSCF
$C_{15}H_{32}$	1.178
$C_{16}H_{34}$	1.177
$C_{17}H_{36}$	1.176
$C_{18}H_{38}$	1.176
$C_{19}H_{40}$(and pristane)	1.175
$C_{20}H_{42}$(and phytane)	1.175
$C_{21}H_{44}$	1.175
$C_{22}H_{46}$	1.174
$C_{23}H_{48}$	1.174
$C_{24}H_{50}$	1.174
$C_{25}H_{52}$	1.173
$C_{26}H_{54}$	1.173
$C_{27}H_{56}$	1.173
$C_{28}H_{58}$	1.173
$C_{29}H_{60}$	1.172
$C_{30}H_{62}$	1.172

where W is the mass flow (weight/time) of the separated substance, A is the area under its peak, and S is the sensitivity of the detector to that substance.

In this study the relative concentration of each component was calculated by the formula:

$$W_i = \frac{h_i \cdot f_i}{\sum_k h_k} \times 100 \qquad (2)$$

in which W is the weight percentage of the component, h is its peak height, and f is the substance-specific correction factor (SSCF). An additional correction factor of 1.5 was calculated and used for the n-C_{30} peak height, as it elutes after the temperature programme has been completed. The peak heights were used for quantitative analysis, because measurement of the peak height is considered to be more accurate and, at the same time, simpler than the area measurement, particularly when the peaks are relatively high and narrow (Guiochon and Pommier, 1973; Stock and Rice, 1974).

FID is the most precise detector for quantitative analyses in GC (Kaiser, 1963) and the results are independent of temperature and of the carrier gas. Kaiser (1963) proposed a formula for the approximation of SSCF in the case of FID as:

$$f_i = \frac{M_i}{n \times 12} \qquad (3)$$

f_i = Approximate SSCF for substance i
M_i = Molecular weight of substance i
n = Number of carbon atoms is substance i
The calculated SSCF values (f_i) for n-C_{15} to n-C_{30}, which have been used for quantitative analysis through Formula (2) in this study, are given in Table II.3.9.

Five samples from the Shahpassand area were also analysed by PGC in the University of Newcastle-Upon-Tyne, following procedures described by Larter and Douglas (1977).

3.6.3 Data

71 saturated fractions, including 52 samples from the Shahpassand area and 19 samples from Jajarm, were analysed by GLC for distribution of n-alkanes in the C_{15}-C_{30} range. Hydrocarbons with carbon number below C_{15} were not included in the analysis because a significant proportion of them were expected to boil off during sample drying in the oven at 50°C (see Sections 3.3.2 and 3.4.2). Those alkanes with carbon number above C_{30} are also excluded, because their elution occurs during the final time (Table II.3.7) and therefore their peaks are not sharp and symmetrical. A close reproducibility of chromatograms was achieved for a few samples which were repeated for solvent extraction, fractionation and GLC (samples 152 R, 218 R and 271).

PGC analysis was carried out on 5 macerated kerogen concentrates from the Shahpassand area at the University of Newcastle-Upon-Tyne (solli, personal comm.).

The GLC results are shown in Tables II.3.10 and II.3.11.

3.6.4 Results and Interpretation

The distribution of n-alkanes, as well as of the isoprenoids pristane and phytane, as determined from the selected samples, are presented in Figures II.3.17, II.3.18 and II.3.19.

In general, two ranges of n-alkanes can be differetiated in the majority of studied specimens. The n-C_{22} to n-C_{30} range represents alkanes derived mainly from humic material. This range, which usually culminates at n-C_{25} or n-C_{26}, dominates the saturates fraction in all samples from highly carbonaceous horizons. In samples 152, 161, and 262, which were taken from the coal seams, the dominance of n-C_{22} to n-C_{30} is clear. The other range of distribution is n-C_{15} to n-C_{21} which has a non-humic origin, probably derived from sources other than higher plant material.

Table II.3.10 - n-alkane distribution data: normalised percentages.

Sample No.	n-C_{15}	n-C_{16}	n-C_{17}	n-C_{18}	n-C_{19}	n-C_{20}	n-C_{21}	n-C_{22}	n-C_{23}	n-C_{24}	n-C_{25}	n-C_{26}	n-C_{27}	n-C_{28}	n-C_{29}	n-C_{30}
							Qoznavi Section									
124	1.37	1.43	5.08	8.45	10.28	10.02	6.92	7.24	5.56	5.69	13.77	5.50	4.83	5.12	4.34	4.41
125	1.97	6.95	13.94	12.95	8.21	6.75	3.06	3.78	2.81	4.21	18.05	3.74	3.22	5.13	2.62	2.60
129	2.00	5.50	10.80	8.20	8.00	6.70	5.50	6.60	4.90	4.90	10.80	3.30	3.00	2.40	1.50	2.60
133	1.60	3.80	8.80	10.50	9.90	9.10	5.80	8.40	4.50	4.00	7.40	3.80	3.80	3.50	3.20	2.60
138	1.58	1.73	3.56	6.34	8.21	9.26	6.16	7.58	6.25	6.13	12.27	5.70	7.65	5.05	5.74	6.81
142	0.90	2.00	8.30	5.40	5.00	4.20	2.70	3.00	3.30	6.20	11.30	10.40	9.60	8.40	6.00	5.30
149	0.91	1.57	6.70	10.11	10.18	9.88	8.60	12.81	5.69	5.65	10.16	3.95	3.86	3.37	3.61	2.97
150	2.05	6.53	12.53	11.83	8.77	7.99	4.30	5.32	3.80	5.73	13.43	3.88	3.65	4.73	2.83	2.63
152	0.00	0.40	4.10	3.50	5.30	6.70	7.50	7.80	10.30	9.20	11.40	6.60	8.50	3.50	3.90	5.60
157	7.30	7.30	24.60	9.60	9.20	9.90	1.90	10.20	2.00	2.20	7.30	2.60	1.60	1.70	1.40	1.10
161	0.20	0.30	4.40	4.00	4.70	6.10	5.80	7.00	7.00	7.10	13.60	12.30	8.50	5.10	4.80	4.30
162	2.30	4.00	18.10	9.70	8.70	8.00	3.90	6.60	3.00	3.00	5.80	3.00	2.60	2.40	2.00	1.80
166	0.54	0.69	1.13	1.15	0.74	0.69	0.24	0.54	0.24	0.22	27.04	31.98	22.85	8.57	1.54	1.84
169	0.29	0.59	0.93	0.59	0.68	0.59	0.34	0.68	0.39	0.37	27.03	33.00	23.60	8.77	1.51	0.29
171	0.57	1.24	1.75	1.91	1.61	1.21	0.87	0.90	0.94	0.84	24.43	29.68	22.42	8.97	1.84	0.84
173	0.13	0.17	0.33	0.44	0.55	0.57	0.41	0.59	0.59	0.72	24.23	28.76	25.54	13.07	3.29	0.61
174	3.90	6.90	12.10	12.00	9.80	9.30	4.20	7.90	2.50	2.50	7.30	2.60	2.40	2.30	2.00	1.70
177	4.30	5.60	12.50	7.70	6.30	6.90	1.70	7.00	2.50	4.90	9.50	7.30	5.50	4.80	3.20	2.90
179	0.80	3.60	7.00	7.10	6.70	5.00	3.90	3.60	4.20	4.90	11.90	7.10	9.10	5.90	5.50	5.60
184	3.00	4.70	8.70	8.10	7.40	8.60	4.70	7.50	3.70	4.30	9.00	8.80	5.40	3.60	3.10	2.40
191	0.90	1.90	4.60	4.80	4.00	4.90	3.70	4.50	6.20	6.80	21.20	6.20	12.60	4.90	5.00	2.90
196	0.00	0.17	0.44	0.69	0.81	0.49	0.49	0.54	0.76	0.76	24.95	29.74	25.91	13.08	3.17	0.59
197	0.26	0.64	1.05	1.24	1.48	0.88	1.02	0.97	1.59	1.24	23.57	27.37	23.71	11.38	2.61	1.00

Table II.3.10 - Continued.

Sample No.	n-C_{15}	n-C_{16}	n-C_{17}	n-C_{18}	n-C_{19}	n-C_{20}	n-C_{21}	n-C_{22}	n-C_{23}	n-C_{24}	n-C_{25}	n-C_{26}	n-C_{27}	n-C_{28}	n-C_{29}	n-C_{30}
203	2.40	4.00	11.60	11.30	9.00	8.00	4.70	7.60	4.00	3.60	10.90	3.00	2.80	2.20	1.90	1.50
207	0.17	0.64	0.81	0.58	0.35	0.58	0.92	1.30	1.33	1.59	24.56	30.21	23.92	10.00	2.01	1.04
208	0.15	0.60	0.89	0.99	1.12	1.27	1.30	1.39	1.45	2.05	24.07	27.27	21.50	9.58	2.35	1.63
							Rudbar Section									
218	1.00	1.00	2.61	6.69	9.22	10.33	8.56	8.13	11.09	7.10	10.50	7.40	6.06	4.41	3.26	2.64
220	3.06	4.59	12.16	8.31	7.29	7.86	2.79	6.57	3.50	3.76	17.47	6.20	5.40	4.71	3.80	2.54
222	4.41	6.47	13.71	6.85	5.40	5.88	1.67	5.08	2.35	3.19	15.20	13.16	7.93	3.39	3.35	1.94
224	1.70	4.50	6.40	4.80	3.00	3.30	2.50	3.00	3.80	6.50	11.70	12.60	10.60	8.80	6.20	5.60
228	1.69	4.14	10.53	6.73	5.72	5.54	2.46	4.60	3.77	6.40	11.03	10.64	9.24	7.82	5.17	4.48
232	2.16	5.70	10.01	7.40	5.84	5.25	3.05	3.92	3.66	6.02	11.98	10.35	8.67	6.99	4.91	4.09
233	1.70	4.20	8.60	8.60	6.30	6.80	4.40	5.40	4.40	5.50	8.70	7.90	6.30	5.30	4.00	3.50
236	0.16	0.88	1.60	2.19	2.13	1.91	1.56	1.47	1.28	1.31	23.28	28.43	22.18	9.06	1.87	0.69
238	4.50	7.10	12.70	9.70	7.80	8.40	2.60	7.00	2.90	3.70	5.90	5.60	4.40	3.90	2.80	2.70
242	1.57	4.14	8.29	7.71	6.19	6.40	4.61	4.67	4.63	6.02	10.44	12.86	7.35	6.00	4.86	4.27
245	4.40	6.28	11.37	8.07	6.38	7.19	2.48	6.31	3.41	5.35	9.31	8.79	6.75	5.92	4.19	3.80
249	1.71	1.89	7.80	5.93	4.10	3.76	2.54	3.06	3.27	5.60	18.05	15.06	9.58	7.21	5.38	5.04
251	0.30	0.76	1.45	1.91	2.05	2.11	2.06	1.99	1.92	1.81	29.64	20.68	18.92	10.00	2.97	1.43
253	2.20	6.30	8.00	6.40	4.00	4.10	3.20	3.50	3.80	5.80	9.20	9.30	8.20	7.10	5.20	5.10
254	1.20	2.40	5.30	4.80	3.70	3.30	2.60	3.20	4.30	8.20	12.40	12.90	10.80	8.70	6.20	5.50
256	0.50	0.70	1.30	2.90	4.50	5.60	5.40	5.90	6.60	8.50	13.70	11.70	10.80	8.50	6.20	6.00
257	6.30	7.10	11.50	9.90	9.90	9.80	3.40	7.80	3.10	3.60	5.60	4.40	3.70	3.10	2.20	1.80
259	1.50	3.40	7.20	6.60	5.10	4.80	2.70	3.50	3.70	6.50	11.60	11.00	9.40	7.20	4.90	4.10
260	2.42	6.35	11.81	8.75	6.24	5.75	4.34	4.12	3.49	3.78	13.22	13.03	8.24	3.41	2.72	2.35
261	0.60	1.30	4.60	5.10	5.30	5.10	3.50	4.10	4.10	7.00	11.20	12.20	10.70	9.00	6.10	5.30

Table II.3.10 - Continued.

Sample No.	n-C_{15}	n-C_{16}	n-C_{17}	n-C_{18}	n-C_{19}	n-C_{20}	n-C_{21}	n-C_{22}	n-C_{23}	n-C_{24}	n-C_{25}	n-C_{26}	n-C_{27}	n-C_{28}	n-C_{29}	n-C_{30}
262	0.80	2.20	3.60	3.70	3.50	2.80	2.50	2.10	1.90	1.40	19.10	20.70	15.80	6.60	2.10	1.20
265	0.32	1.24	2.03	2.31	2.40	2.21	2.37	2.29	2.59	2.13	20.43	23.68	21.00	10.77	2.81	1.42
271	1.80	4.60	7.20	7.90	7.80	6.50	6.40	6.80	7.00	5.60	10.90	4.40	6.60	2.40	1.90	3.20
276	1.90	4.70	7.50	7.90	8.20	6.10	5.90	6.30	6.70	6.40	11.20	6.10	6.50	2.90	2.70	2.30
282	0.40	1.10	1.80	2.00	2.20	1.60	1.60	1.60	1.70	1.50	22.60	25.90	21.20	9.80	2.30	0.80
285	0.97	1.42	5.97	10.72	11.51	9.98	6.76	6.86	5.06	4.47	12.87	8.76	6.40	3.81	2.45	1.69
							Jajarm Section									
325	0.42	2.15	4.45	4.77	3.72	2.54	1.62	1.81	1.36	1.20	22.50	25.64	18.69	6.98	1.36	0.78
326	0.80	3.10	6.20	6.70	2.60	3.70	2.30	2.60	1.80	1.60	20.40	19.70	14.20	5.60	1.00	1.20
327	2.16	9.73	16.41	14.42	9.48	6.65	3.98	4.52	3.27	2.97	8.76	5.52	4.61	3.30	2.49	1.72
330	0.71	5.22	11.37	11.91	8.88	6.52	3.87	6.35	2.96	2.54	12.57	12.33	8.54	3.22	1.75	1.26
333	1.60	5.50	11.60	11.00	8.40	6.60	3.90	6.00	2.40	1.80	9.40	9.40	7.00	2.70	1.80	1.20
336	2.17	9.13	16.76	16.71	12.88	9.97	5.58	4.95	2.73	1.93	7.68	1.54	4.67	1.88	0.80	0.63
339	2.00	5.40	10.40	12.10	10.80	9.00	5.40	8.50	3.70	2.90	7.70	6.00	3.70	1.50	1.30	0.70
343	2.11	3.66	7.68	9.32	7.99	7.08	3.38	5.11	2.88	2.46	18.05	14.86	9.71	3.37	1.41	0.96
344	2.97	7.04	9.49	9.07	6.83	5.49	3.96	3.35	2.65	2.11	16.29	15.97	10.20	3.37	0.78	0.43
346	1.30	3.50	5.80	5.80	4.50	3.80	2.20	2.50	1.80	1.60	18.90	20.40	14.40	5.20	1.60	0.90
350	0.20	1.27	2.43	2.70	1.96	3.21	0.92	0.72	0.57	0.47	15.97	28.80	21.42	8.34	1.47	0.32
354	1.10	7.10	12.70	11.90	9.00	6.90	4.60	3.80	3.00	2.40	9.00	8.50	6.20	2.30	1.70	1.20
355	4.80	12.30	14.50	12.30	8.70	5.70	3.70	2.80	2.40	1.70	6.70	6.30	5.00	2.10	0.50	0.90
356	6.60	13.20	14.60	12.20	9.00	7.00	4.90	4.20	3.60	3.00	5.40	3.40	2.50	1.60	1.10	0.80
357	1.40	7.40	13.40	13.20	11.00	8.90	6.00	5.20	4.20	3.40	6.00	3.30	2.90	2.10	1.70	1.20
360	2.80	8.20	12.50	12.20	10.50	8.20	6.30	5.40	4.70	4.30	6.10	4.50	3.30	2.10	1.40	0.90

Table II.3.10 - Continued.

Sample No.	n-C_{15}	n-C_{16}	n-C_{17}	n-C_{18}	n-C_{19}	n-C_{20}	n-C_{21}	n-C_{22}	n-C_{23}	n-C_{24}	n-C_{25}	n-C_{26}	n-C_{27}	n-C_{28}	n-C_{29}	n-C_{30}
361	3.80	9.60	13.00	11.20	8.80	6.90	5.00	4.30	3.40	2.80	7.60	6.50	4.70	2.10	1.40	0.90
365	2.93	6.39	7.70	6.83	7.55	5.05	3.73	3.20	3.03	2.75	14.87	16.24	11.48	6.30	1.08	0.84
367	1.10	7.60	11.50	8.60	5.80	4.60	3.10	2.80	2.70	2.30	11.60	13.30	9.60	3.80	1.60	1.10
Kashafrud Fm. (Kopet Dagh)																
BMM	0.20	0.20	0.80	2.10	3.70	5.20	5.60	6.10	7.50	11.30	13.20	13.80	11.30	9.30	5.20	4.50
28MM	0.20	1.60	5.60	6.90	7.50	8.30	8.70	8.40	7.20	7.00	6.90	6.80	5.80	5.00	3.70	3.60
MM118	1.00	1.10	1.40	2.80	6.30	11.30	9.90	10.3	7.70	7.50	9.70	7.70	6.90	5.80	4.40	4.40

Table II.3.11 - Analytical GLC results.

Sample No.	%Pristane	%Phytane	Pristane/n-C_{17}	Pristane/Phytane	$(C_{21} + C_{22})/(C_{28} + C_{29})$
			Shahpassand area		
124	3.31	4.19	1.53	0.79	1.50
125	7.50	5.00	0.54	1.50	0.88
129	10.00	3.10	0.93	3.19	3.11
133	4.50	4.90	0.51	0.91	2.13
138	2.43	2.65	0.68	0.91	1.27
142	5.30	2.50	0.64	2.07	0.40
149	4.00	5.50	0.60	0.74	3.07
150	6.90	4.97	0.55	1.39	1.27
152	4.10	1.60	1.00	2.63	2.05
157	12.40	1.50	0.50	8.26	3.87
161	3.20	1.60	0.72	1.98	1.29
162	11.30	3.90	0.62	2.87	2.39
166	0.66	0.24	0.58	2.71	0.08
169	0.49	0.29	0.52	1.67	0.10
171	2.15	0.80	1.23	2.67	0.16
173	0.26	0.17	0.80	1.50	0.06
174	6.00	4.60	0.50	1.32	2.85
177	5.60	1.80	0.45	3.13	1.10
179	4.80	3.30	0.68	1.45	0.50
184	4.50	2.60	0.52	1.74	1.83
191	2.80	1.90	0.62	1.49	0.83
196	0.64	0.20	1.44	3.24	0.06
197	1.90	0.38	1.82	5.00	0.14
203	6.20	5.20	0.54	1.21	2.96

Table II.3.11 - Continued.

Sample No.	%Pristane	%Phytane	Pristane/n-C_{17}	Pristane/Phytane	$(C_{21} + C_{22})/(C_{28} + C_{29})$
207	0.40	0.20	0.50	2.00	0.18
208	1.04	1.04	0.58	1.00	0.22
218	1.15	1.42	0.44	0.81	2.18
220	6.47	2.95	0.53	2.19	1.10
222	6.50	1.90	0.47	3.40	1.00
224	3.10	1.90	0.49	1.62	0.36
228	5.60	2.30	0.53	2.43	0.54
232	5.60	3.16	0.56	1.77	0.58
233	4.30	4.10	0.50	1.05	1.05
236	1.00	1.00	0.63	1.00	0.28
238	5.60	2.70	0.44	2.09	1.44
242	4.30	3.90	0.52	1.10	0.85
245	5.37	2.57	0.47	2.09	0.87
249	4.00	2.50	0.52	1.60	0.44
251	1.60	0.44	1.10	3.61	0.31
253	5.00	3.50	0.63	1.43	0.55
254	2.60	1.80	0.49	1.43	0.39
256	0.70	1.10	0.59	0.68	0.77
257	4.50	2.40	0.39	1.85	2.12
259	3.90	2.80	0.54	1.41	0.51
260	6.33	5.26	0.54	1.20	1.38
261	2.50	2.40	0.54	1.04	0.50
262	8.50	1.70	2.39	5.10	0.53
265	2.85	0.84	1.40	3.39	0.34
271	6.80	2.10	0.94	3.25	3.03
276	5.00	1.70	0.67	2.85	2.16

Table II.3.11 - Continued.

Sample No.	%Pristane	%Phytane	Pristane/n-C_{17}	Pristane/Phytane	$(C_{21} + C_{22})/(C_{28} + C_{29})$
282	1.50	0.40	0.83	3.34	0.26
285	4.00	5.50	0.54	0.71	2.17
Average			0.72	2.11	1.15
			Jajarm area		
325	2.77	1.73	0.62	1.61	0.41
326	4.10	2.50	0.64	1.64	0.73
327	8.30	6.10	0.50	1.35	1.47
330	5.50	5.00	0.49	1.11	2.06
333	5.30	4.30	0.46	1.23	2.20
336	5.93	4.10	0.35	1.44	3.94
339	5.20	3.90	0.50	1.36	4.94
343	3.83	2.88	0.50	1.33	1.77
344	3.14	2.30	0.33	1.36	1.76
346	3.40	2.20	0.59	1.54	0.69
350	1.04	0.84	0.43	1.24	0.17
354	4.90	3.80	0.38	1.27	2.12
355	5.60	3.90	0.39	1.44	2.53
356	4.20	2.70	0.29	1.57	3.31
357	4.70	4.00	0.35	1.18	2.93
360	4.30	2.40	0.34	1.76	3.38
361	4.70	3.30	0.36	1.40	2.68
365	2.90	1.90	0.37	1.50	0.94

Table II.3.11 - Continued.

Sample No.	%Pristane	%Phytane	Pristane/n-C_{17}	Pristane/Phytane	$(C_{21} + C_{22})/(C_{28} + C_{29})$
367	5.50	3.40	0.48	1.62	1.11
Average			0.44	1.42	2.05
Total Average			0.64	1.93	1.39
			Kashafrud Fm. (Kopet Dagh)		
BMM	0.60	1.20	0.77	0.50	0.80
28MM	3.30	3.50	0.59	0.94	1.95
MM118	0.80	1.00	0.60	0.86	1.99

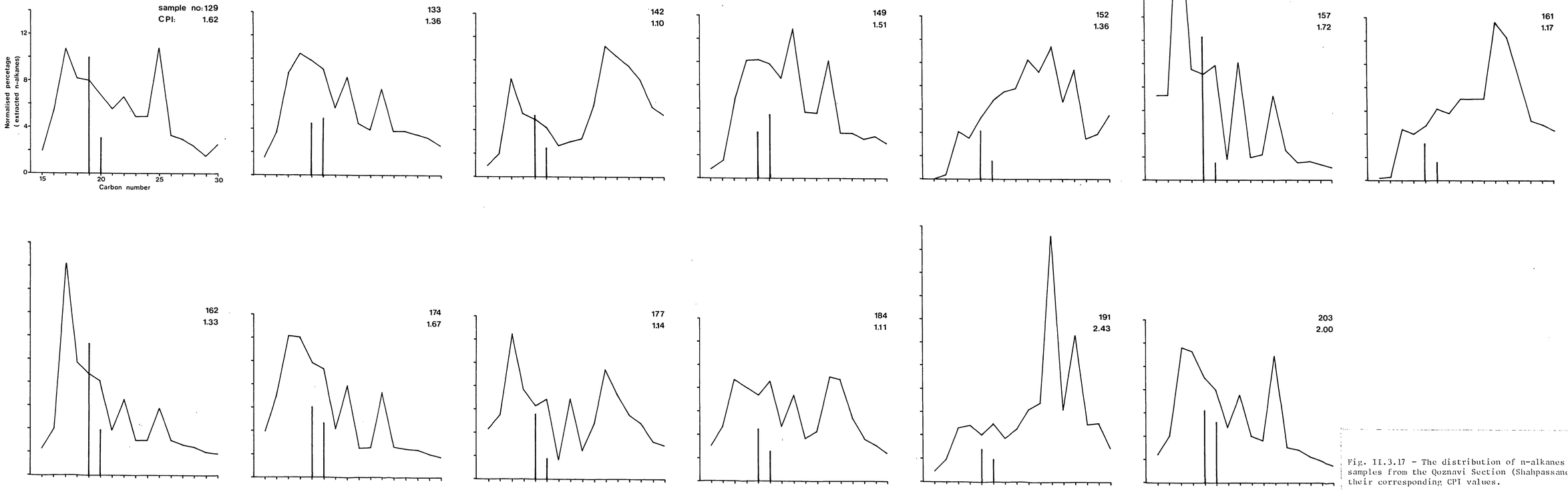


Fig. II.3.17 - The distribution of n-alkanes in selected samples from the Qoznavi Section (Shahpassand area) and their corresponding CPI values.

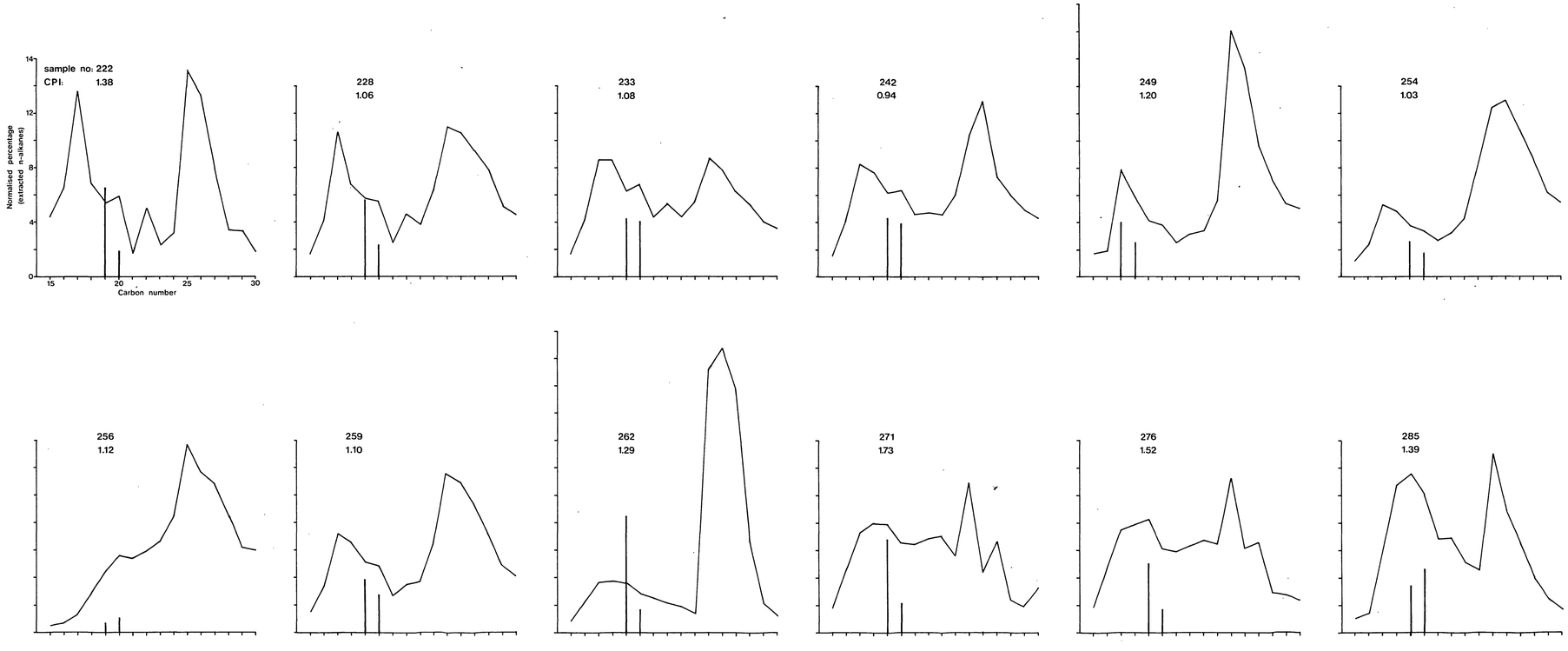


Fig. II.3.18 - The distribution of n-alkanes in selected samples from the Rudbar Section (Shahpassand area) and their corresponding CPI values.

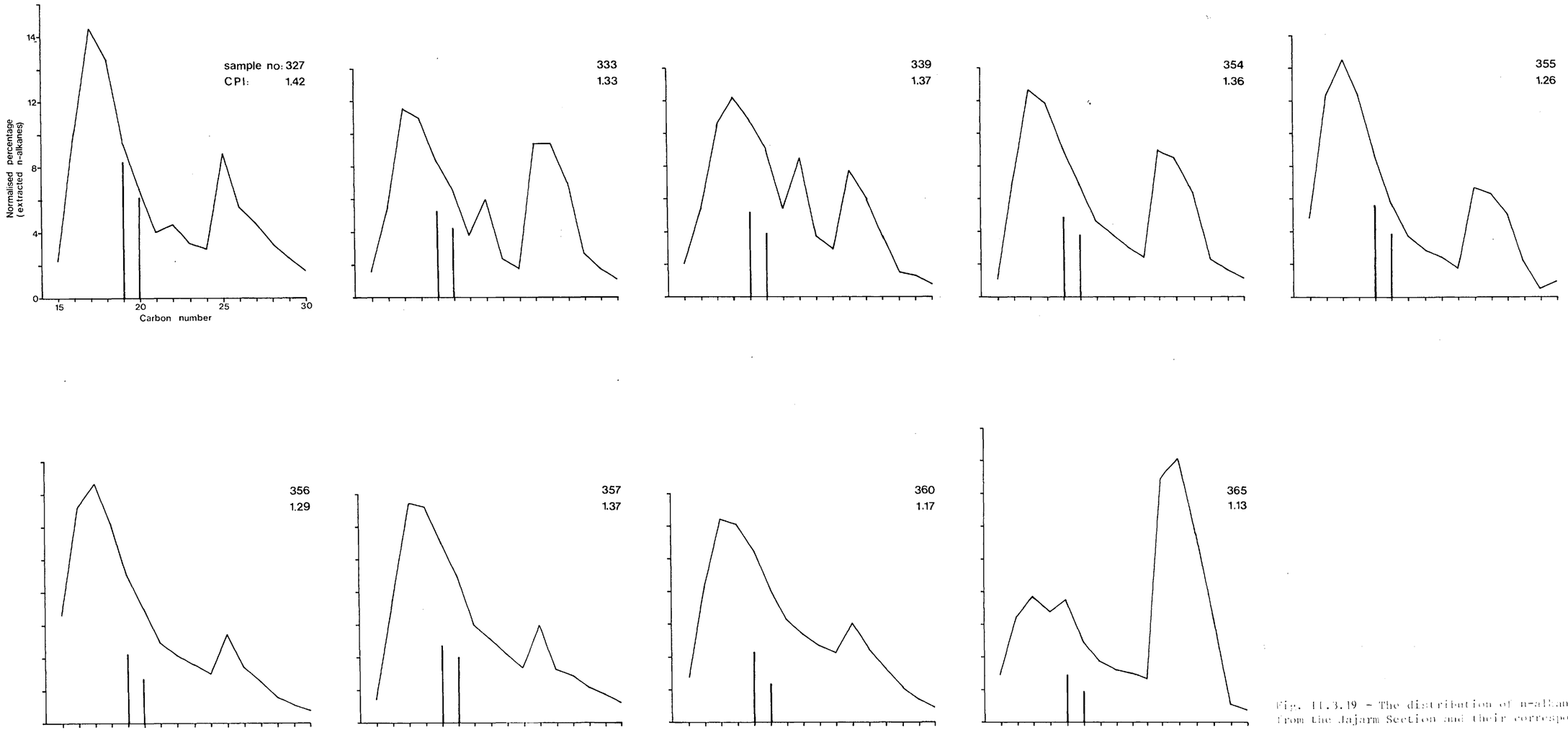


Fig. II.3.19 - The distribution of n-alkanes in selected samples from the Jajarm Section and their corresponding CPI values.

In the Qoznavi Section of the Shahpassand area, samples from the lower part of the Shemshak Formation show a mixture of the two ranges of n-alkanes (samples: 129, 133, 142, and 149). Upwards through the Section, this mixture changes as the n-C_{15} to n-C_{21} range becomes dominant (samples: 157, 162, and 174). The samples 157 and 162 (Fig. II.3.17) probably contain some algal remains because of their high n-C_{17} alkane. In the overlying beds, the "Carbonaceous Shale" unit, the n-C_{22} to n-C_{30} range increases gradually and reaches its maximun towards the top (samples: 177, 184, and 191). The uppermost part of the Section, particularly the "Marine Shale" unit, contains saturates dominated again by the n-C_{15} to n-C_{21} range (sample 203). Viewing the formation as a whole, the GLC results indicate a dominantly wet-gas type kerogen.

In the Rudbar Section of the Shahpassand area, variations of the n-alkane spectrum are less than in the Qoznavi Section (Fig. II.3.18). Here, the saturated fractions are mostly dominated by the n-C_{21} to n-C_{30} range (samples: 222 to 285), although in some of the samples, the n-C_{15} to n-C_{21} range alkanes are significant (samples: 222, 233, and 285). The Shemshak Formation at this locality contains mainly dry gas type kerogen.

In the Jajarm region (Fig. II.3.19), samples from the lower part of the Section yielded saturated fractions containing a mixture of the two n-alkane ranges, with a slight predominance of n-C_{15} to n-C_{21} (samples 327, 333, and 339). The proportion of plant derived alkanes (n-C_{22} to n-C_{30}) gradually decreases upwards and consequently causes a strong dominance of the n-C_{15} to n-C_{21} range in the upper part of the "Marine Shale" lithounit (samples: 354, 355, 356, 357, and 360). Towards the top of the Section, plant derived alkanes (n-C_{22} to n-C_{30}) increase again to dominate the saturated fractions (sample: 365). The kerogen of the Shemshak Formation here is primarily of wet-gas type.

The $(C_{21} + C_{22})/(C_{28} + C_{29})$ ratios average 1.15 for samples from the Shahpassand area which, following the values given by

Phillippi (1974), would indicate a source rock rich in terrestrial plant matter. In contrast, these ratios average 2.05 in the Jajarm samples signifying a dominantly marine origin. It is, however, interesting to notice that samples 157, 162, and 174 from the Shahpassand area, which in contrast to the rest of samples from this locality contain a high percentage of $n\text{-}C_{17}$, also had $(C_{21} + C_{22})/(C_{28} + C_{29})$ ratios in the range given by Phillippi (1974) for marine derived source beds.

A plot of H/C of the mineral free kerogens against the $n\text{-}C_{21}/n\text{-}C_{22}$ ratios of the extracts, in a diagram similar to that suggested by Harwood (1977), is given in Fig. II.3.20. It shows that the samples are of both dry-gas and wet-gas types.

In 64 samples out of 71 the percentage of pristane is higher than that of phytane (Table II.3.10). The mean value of pristane /phytane ratio is 2.11 for the Shahpassand samples, but it decreases to 1.42 for those from Jajarm. This may again indicate that the Shemshak Formation near Shahpassand contains a higher proportion of source material of terrestrial origin than its Jajarm equivalent. An average value of 1.93 was calculated for all 71 samples, which is in the range of mean values given by Rashid (1979) for organic matter dominated by terrestrial derivatives. The quantity of pristane in 63 samples out of 71 is less than the amount of $n\text{-}C_{17}$ alkane with a mean ratio of 0.64. A low proportion of isoprenoids as compared with n-paraffins is to be expected in terrestrial organic matter (Fig. II.3.14).

Figure II.3.21 shows the pyrograms of the 5 macerated samples analysed by the PGC method. Pyrograms of samples 124, 205, 218, and 233 all show less straight chain hydrocarbon material in relation to the aromatic components, and are comparable with vitrinite pyrogram of Larter and Douglas (1977). Among these, sample 233 is very humic and has the lowest potential for the generation of hydrocarbons; sample 218, although of huminite type, has a better generating potential than the others. The pyrogram of sample 186 is slightly different with a relatively weak high-

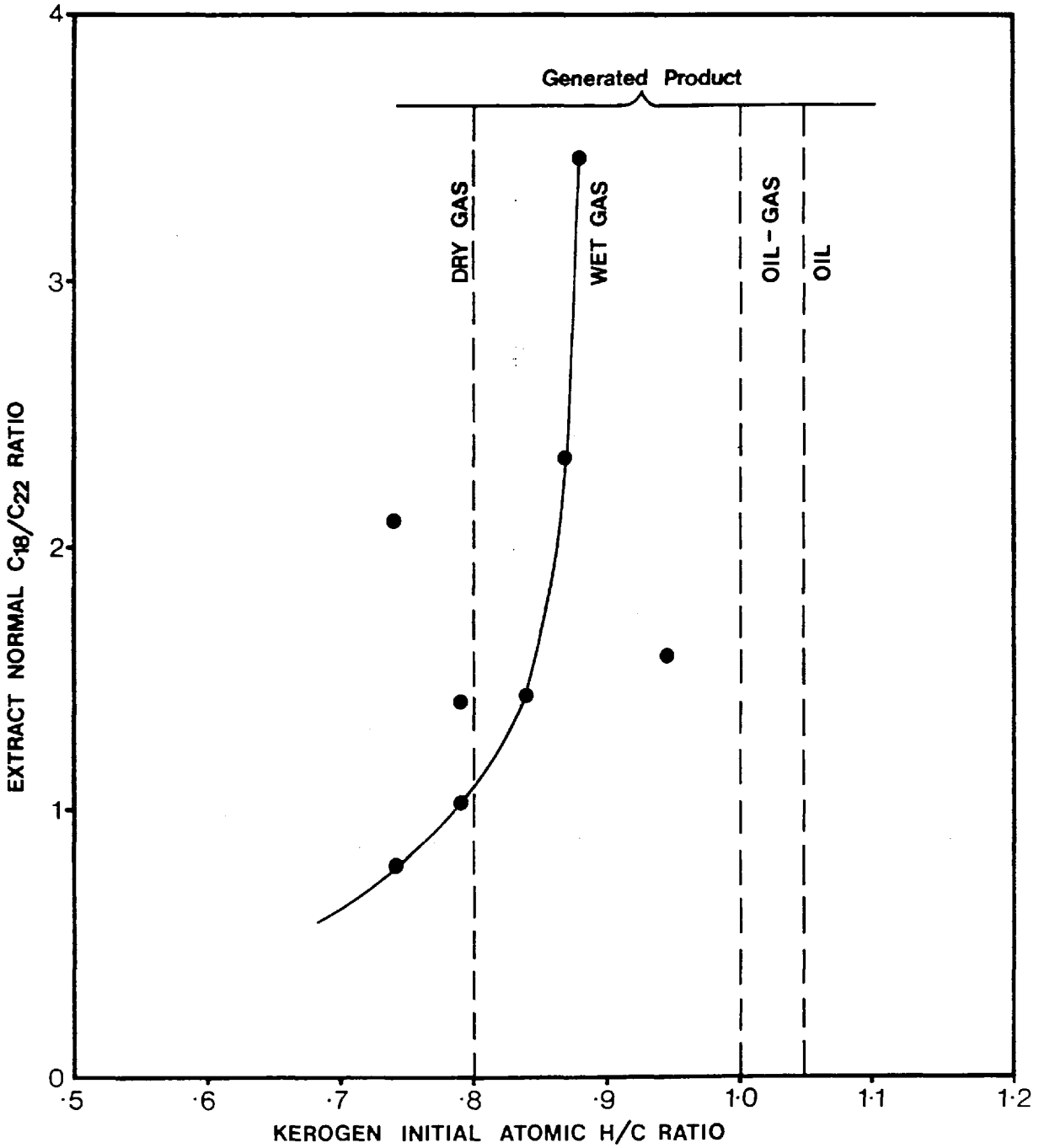
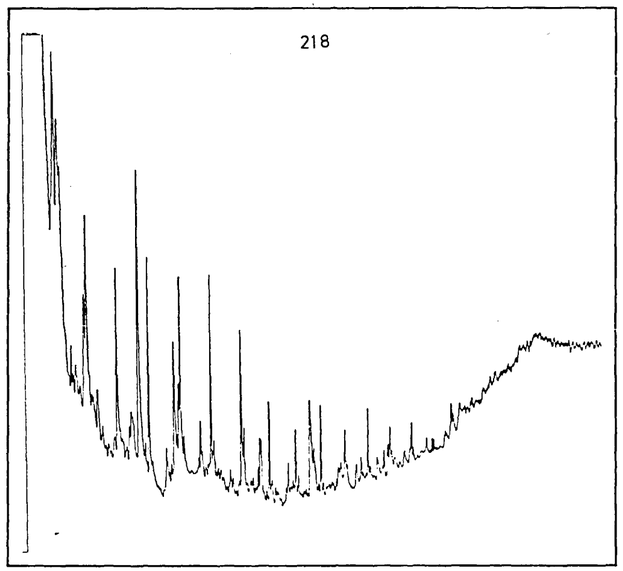


Fig. II.3.20 - Normal C_{18}/C_{22} ratio and kerogen H/C ratio crossplot of the Shemshak Fm. samples from the Eastern Alborz region (determined from mineral free kerogens). The rocks are capable of producing dry and wet gas only (excluding samples 350 and 357). (Crossplot after Harwood, 1977).



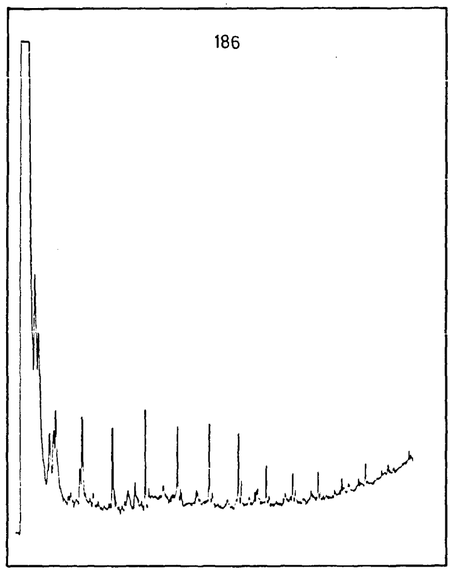
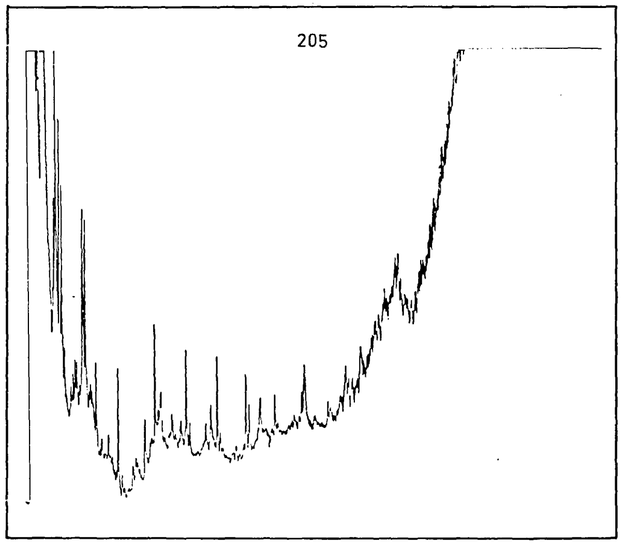
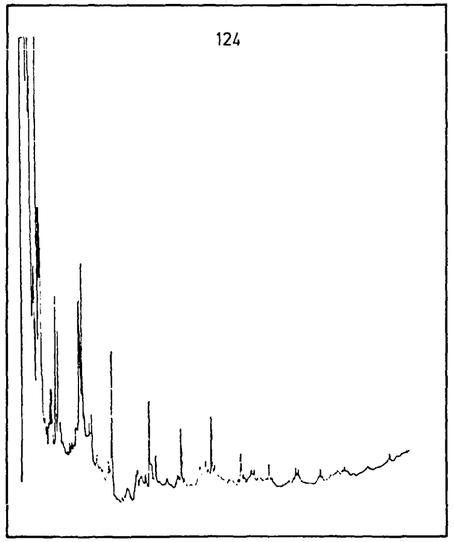
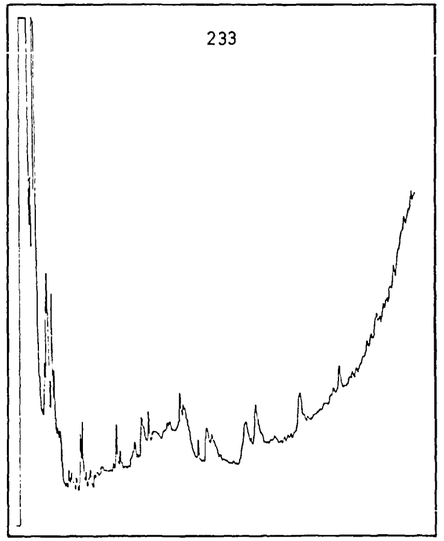


Fig. II.3.21 - The pyrograms of the macerated samples, analysed by the pyrolysis - Gas chromatography method. They are comparable with the vitrinite pyrogram in Fig. II.3.14.







molecular-weight aromatic background: the rock has generated more straight chain hydrocarbons in relation to the aromatic components than the rest of the samples. Its better potential is possibly due to the presence of some algal material.

A spurious peak, mostly massive, is present between n-C_{19} and n-C_{20} in all chromatograms. The same peak was reported by Davies (1978) and has also been eluted in chromatograms of samples from the Kashafrud Formation of Kopet Dagh. It is believed to originate from some sort of contamination in the experimental processes.

3.6.5 Conclusions

The n-C_{22} to n-C_{30} range alkanes dominate the saturated fraction of samples from highly carbonaceous horizons.

In general, the Shemshak Formation in the regions studied contains a dominantly wet-gas type of kerogen, as shown by the distribution of normal alkanes in the sediments, although those from Jajarm seem to have a higher potential for generating liquid hydrocarbons than the Shahpassand counterparts.

The average $(C_{21} + C_{22})/(C_{28} + C_{29})$ ratio indicates that the Shemshak Formation of the Shahpassand area is a source rock rich in terrestrial plant matter, whereas that of the Jajarm region is dominantly of marine origin.

Similarly the mean pristane/phytane ratios also point to a higher proportion of terrestrial source material at Shahpassand than at Jajarm.

A H/C, n-C_{21}/n-C_{22} crossplot for most mineral-free kerogens shows that they are wet-gas and dry-gas types.

Pyrograms of macerated samples generally show less straight chain hydrocarbons than aromatic components; they are comparable with the pyrogram of vitrinite maceral.

CHPTER 4

STATE OF MATURATION OF ORGANIC MATTER

4.1 Pyrolysis-Elemental Analysis

4.1.1 Introduction

Temperature and pressure increase as a function of depth of burial. The maturation of the organic matter incorporated in sedimentary rocks, which causes the generation of hydrocarbons, depends mainly on temperature and geological time (Cannon, 1974). The quantity and composition of the generated hydrocarbons are controlled also by the type of the organic matter initially deposited in the source bed.

Pyrolysis techniques have been used widely in source rock studies, in order to determine the type and the state of maturation of organic matter in sediments. A combination of pyrolysis and elemental analysis can provide useful information on the degree of maturation. But it must be pointed out that organic matter in sediments passes through the primary diagenesis stage, especially microbial degredation, before it becomes capable of generating hydrocarbons by thermal maturation.

A pyrolysis method was introduced by Barker (1974) (Sect. 3.5.1), based on the idea that the source rocks contain the hydrocarbons already generated together with the organic matter which has reacted incompletely. Later a more extensive use of this method was established by Espitalié et al. (1977) through a commercial apparatus known as "Rock-eval" (see Section 3.5.1). It is believed that the temperature marking the maximum elution of the cracking peak indicates the state of maturity for a given type of organic matter (Barker, 1974; Claypool and Reed, 1976; Espitalié et al., 1977). This temperature is shown to increase with the degree of maturation, because the more thermally stable part of the organic matter remains in the rock at relatively

higher levels of thermal maturity. Another way of defining maturity by this technique is through the production index, defined as the ratio $S_1/(S_1 + S_2)$ (Fig. II.3.10); where S_1 is the area under the distilates peak and S_2 the area under the cracking peak. This ratio increases with increasing depth of burial and can be used as an index of maturity (Fig. II.4.1).

A pyrolysis-elemental analysis method, similar to that introduced by Gransch and Eisma (1966) and described in Sect. 3.5.1, is introduced here using a plot of C_R versus C_T to determine the level of maturation of the organic content of source rocks. Figure II. 3.8 illustrates the variations of C_R relative to C_T for different types of organic matter. When the type is known* the average trend of the C_R, C_T crossplot can indicate the degree of maturation more accurately than other available pyrolysis methods. A plot of the average trends of other source beds studied at the Petroleum Geology Section of Imperial College is illustrated in Figure II.3.12: the type and maturation state of the organic content of these source beds agree with the results of other geochemical methods.

Many researchers prefer to analyse the kerogen concentrates of the rocks in order to obtain more reliable results than those from the rock itself. Tissot et al. (1974) carried out a series of evolution tests on kerogens and proposed a diagram with three evolution paths for different types of kerogen based on their elemental composition. This diagram can give an indication of maturity if the kerogen is not highly cooked.

The carbonisation level of kerogen concentrates increases with increasing maturity. A carbonisation level of about 74-76 percent carbon was designated by Laplante (1974) as the threshold of significant hydrocarbon generation. This limit given by

* Organic matter in sediments are composed usually of a mixture of two or more types of kerogen. The type of organic matter is usually referred to its dominating kerogen type.

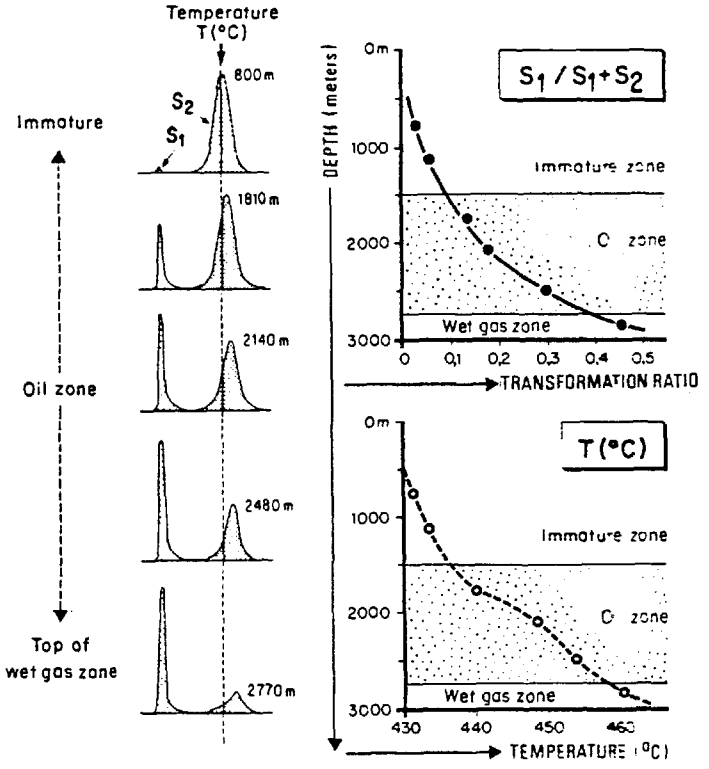


Fig. II.4.1 - The effect of thermal maturity on pyrogram of source rock and the corresponding production index $(S_1/S_1 + S_2)$. After Espitalie et al. (1977).

Harwood (1977) is 81-85 percent for huminite (type III).

4.1.2 Procedures

All samples were analysed as described in Sections 3.2.2 and 3.5.2.

4.1.3 Data

As given in Section 3.2.3 and 3.5.3.

4.1.4 Results and Interpretation

A plot of C_R against C_T values indicates a direct relationship between the two with a general trend as shown in Figure II.3.11. This trend more or less coincides with the trend of immature huminite (Fig. II.3.12). The type of kerogen was found to be dominantly huminite as discussed in Chapter 3, and the samples are thus shown to be thermally immature.

An atomic H/C with O/C crossplot for macerated kerogen concentrates in the evolution paths diagram also indicates a highly immature source rock (Fig. II.3.4). In the case of mineral free kerogens the average percentage of carbon loss relative to initial organic carbon is 34.18 which is very close to the level of convertibility for immature huminite (35%). The percentage of initial carbon in the mineral free kerogen concentrates is well below the carbonisation level of 81% given by Harwood as the starting level for the catagenesis stage. This implies that the source rock studied has not yet reached the catagenesis stage and is thermally immature.

4.1.5 Conclusions

The Shemshak Formation at the localities studied is an immature source rock, as indicated by its average trend in the C_R, C_T diagram.

The kerogen content of the Formation is also shown to be immature by H/C, O/C crossplot.

The average percentage of the carbon content and the carbon loss of mineral free kerogen concentrates confirm the state of immaturity.

4.2 Bitumen and its Compositional Fractions

4.2.1 Introduction

The amount and composition of the bitumen in source rocks depend on the nature of the original organic matter and the extent of thermal maturation of the rock. The amount of generated bitumen and its related hydrocarbons increase with increasing depth of burial to a maximum where the principal stage of oil formation occurs and then gradually decrease below this point (Fig. II.1.9). Tissot et al. (1974) showed variations of the oil and gas generated in source rocks with depth of burial. Albrecht et al. (1976) who studied the sediments of Douala basin (West Africa) realised that the ratios of soluble organic extract to organic carbon (bitumen ratios) and hydrocarbon to organic carbon (hydrocarbon ratios) change with depth of burial. They also showed that the amount of soluble organic extract of the rocks rapidly increases between 1500 and 2200 m depth, mainly due to a sudden increase of the saturated hydrocarbons. The E/C_T* ratios were also used by Amit (1978) to define the state of maturation of organic matter. However, the bitumen and hydrocarbon ratios are highly affected by migration and should be interpreted carefully. Powell (1978) found that a hydrocarbon content of extract less than 30% signifies the immature stage.

Claypool et al. (1978) demonstrated that incipiently metamorphosed rocks are consistently low in extractable hydrocarbons at all levels of organic content, whereas

* E = Soluble organic extract.

unmetamorphosed sediments generally show a positive correlation between the two. They also showed that unmetamorphosed source rocks have saturated/aromatic hydrocarbon ratios less than 2 and a wide range of hydrocarbon/organic carbon ratios, whilst saturated/aromatic hydrocarbon ratios greater than 2 and hydrocarbon/organic carbon ratios of less than 1% represent incipiently metamorphosed rocks. High saturated/aromatic ratios of overcooked source rocks are due to a preferential loss of aromatic hydrocarbons relative to saturates. Gill (1978) used a plot of C_T against total soluble organic extract to show the state of maturation of organic matter.

4.2.2 Procedures

All samples were analysed according to the procedures described in Section 3.3.2 and 3.4.2.

4.2.3 Data

As given in Sections 3.3.3 and 3.4.3.

4.2.4 Results and Interpretation

As all the samples were collected from outcrop, variations of the amount and composition of bitumens with depth of burial cannot be studied. However, the average hydrocarbon content of the extracts is 28.29% (less than 30%) suggesting an immature stage for the organic content of the rocks.

Figure II.3.7 illustrates a log-log plot of the extractable hydrocarbon concentrations versus total organic carbon values in a diagram similar to the one by Claypool et al. (1978, Fig. 4). All analysed samples fall within the unmetamorphsed zone and exhibit a generally positive correlation between the two sets of values. Additionally the hydrocarbon concentration values, which are mostly moderate even in samples with a high organic carbon content (Fig. II.3.7), can indicate immaturity of the source rock.

An identical diagram to that of Claypool et al. (1978, Fig. 5) is also depicted in Figure II.4.2. Again, all of the samples are

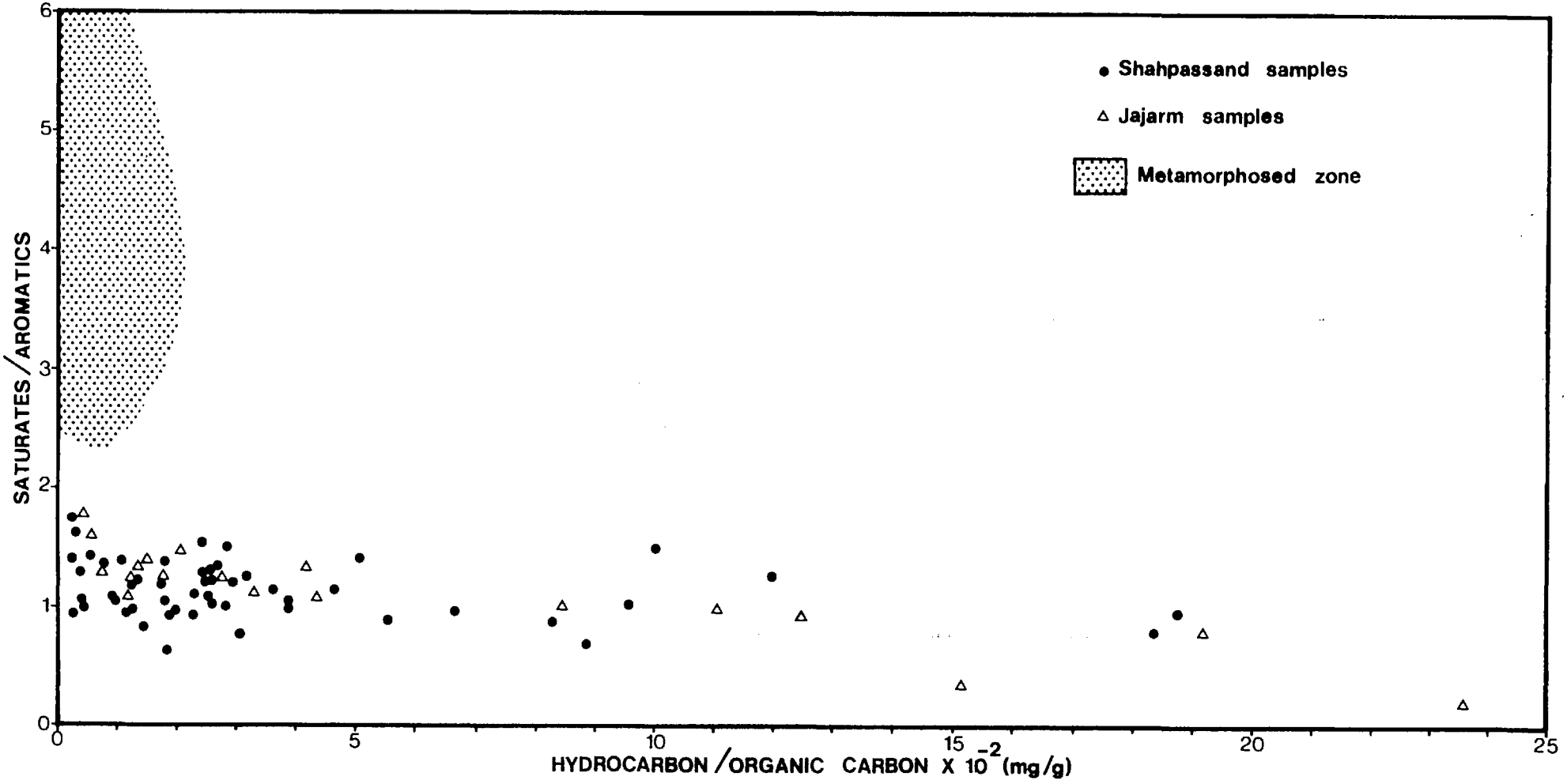


Fig. 11.4.2 - Variation of the HYDROCARBON/ORGANIC CARBON ratios of the Shemshak Fm. samples relative to their corresponding SATURATES/AROMATIC ratios (excluding samples 207 and 208). Crossplot modified after Claypool et al. (1978).

shown to be unmetamorphosed by their saturated/aromatic ratios less than 2 and a wide range of hydrocarbon/organic carbon ratios.

Except in 7 samples (124, 157, 203, 242, 245, 257, and 260), the hydrocarbon contents of the extracted bitumens are less than those of the non-hydrocarbons. The average amount of non-hydrocarbons is in fact over 2.5 times the average quantity of hydrocarbons. This suggests immaturity, by comparison with the highly mature Kashafrud Formation of the Kopet Dagh basin which contains a low asphaltic fraction and extracted bitumens dominated by saturates (Madani, 1977).

A plot of C_T against soluble organic extract is given, together with the average trend, in Figure II.4.3. Samples placed in the shaded area are probably contaminated, because of their abnormally high bitumen content. The average trend of the samples shown in this diagram shows that the quantity of extract is relatively low with respect to the organic carbon content of the rocks and suggests immaturity of the source rock. The average trend of the immature Shemshak Formation, which is now known to be dominantly a gas source (see Chapter 3), lies between the trends of the senile Kashafrud Formation and the immature Kimmeridgian Shale, believed to be dominantly an oil source (Fig. II.4.4).

Figure II.4.5 presents a new diagram using a crossplot of the percentages of kerogen carbon loss and soluble organic extract to verify the state of maturity. The carbon loss values are calculated as described in Section 3.5.4. This diagram can only be applied to the kerogen concentrates from which their original rock samples were not solvent extracted before maceration. However, it clearly indicates immaturity of the Shemshak Formation.

In general a paucity of soluble organic extracts and low bitumen ratios (E/C_T) of the Shahpassand samples relative to

Fig. II.4.3 - Total organic carbon - soluble extract cross-plot. Showing the average trend of the Shemshak Fm. in the Eastern Alborz. The shaded area covers the contaminated samples (excluding samples 152, 161, 173, 191, 196, 197, 218, 251, 262 and 265).

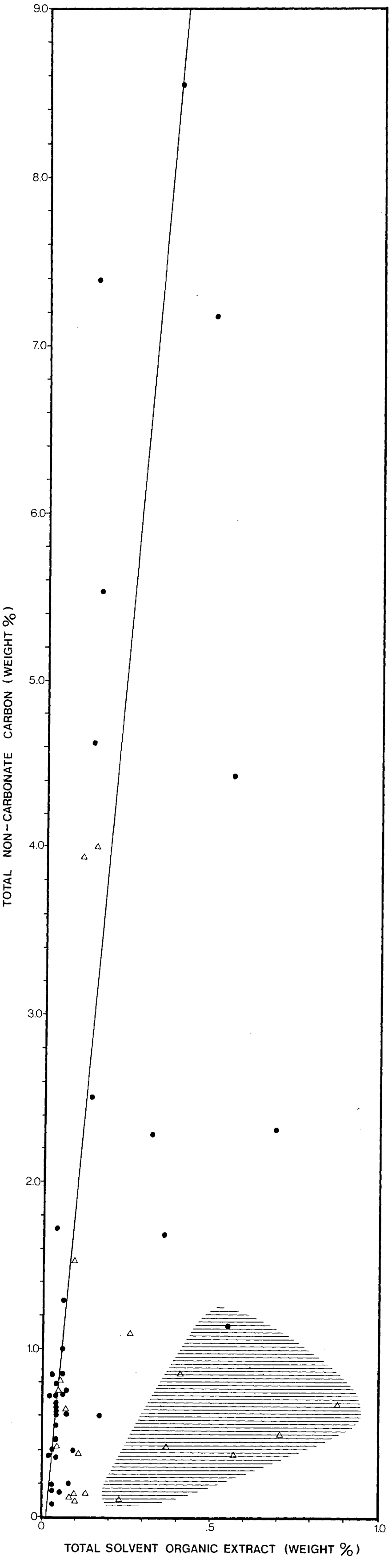
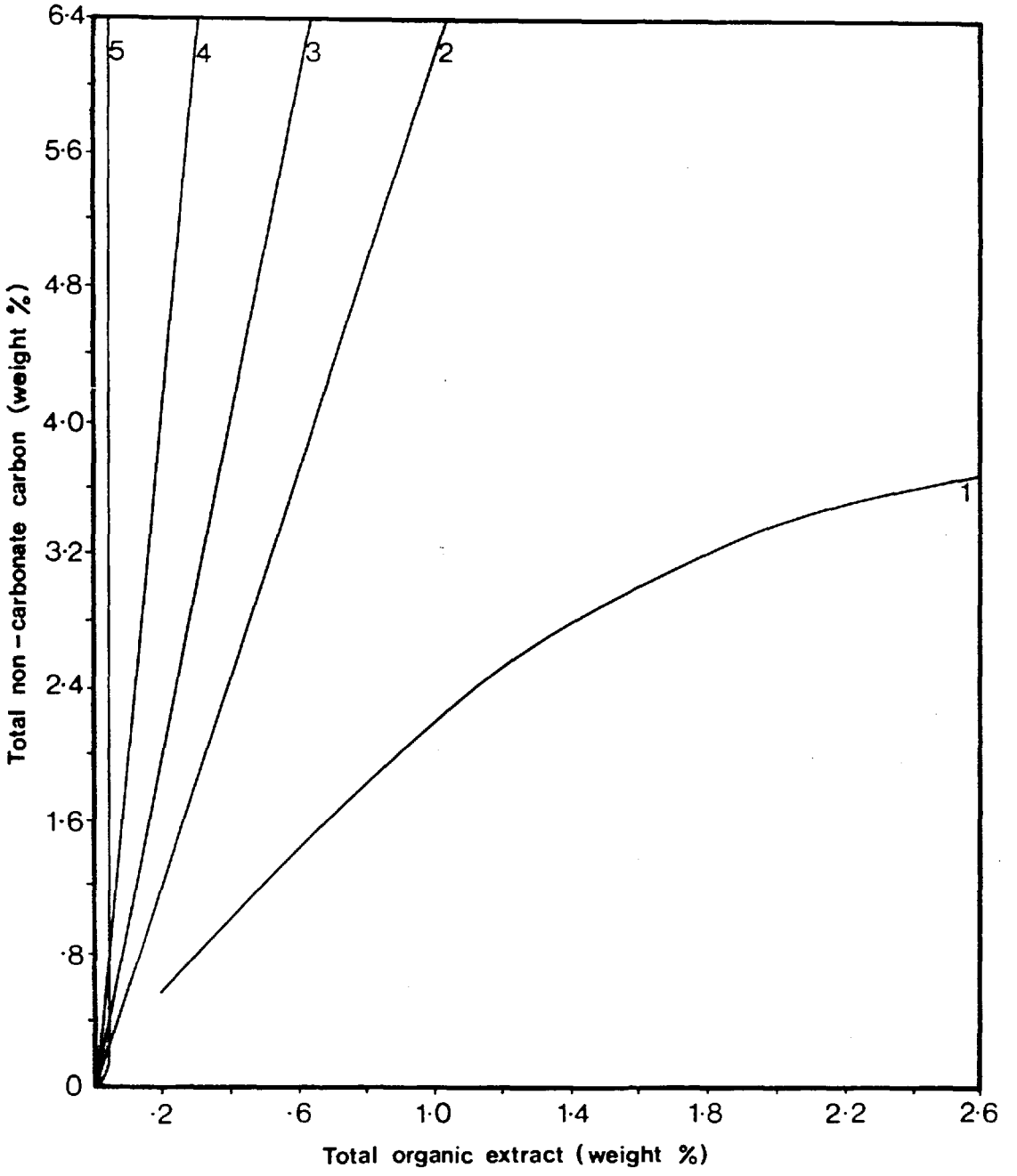


Fig. II.4.4 - The average trends of the source rock studied at the Petroleum Geology Section of Imperial College, in the organic carbon-soluble extract crossplot.



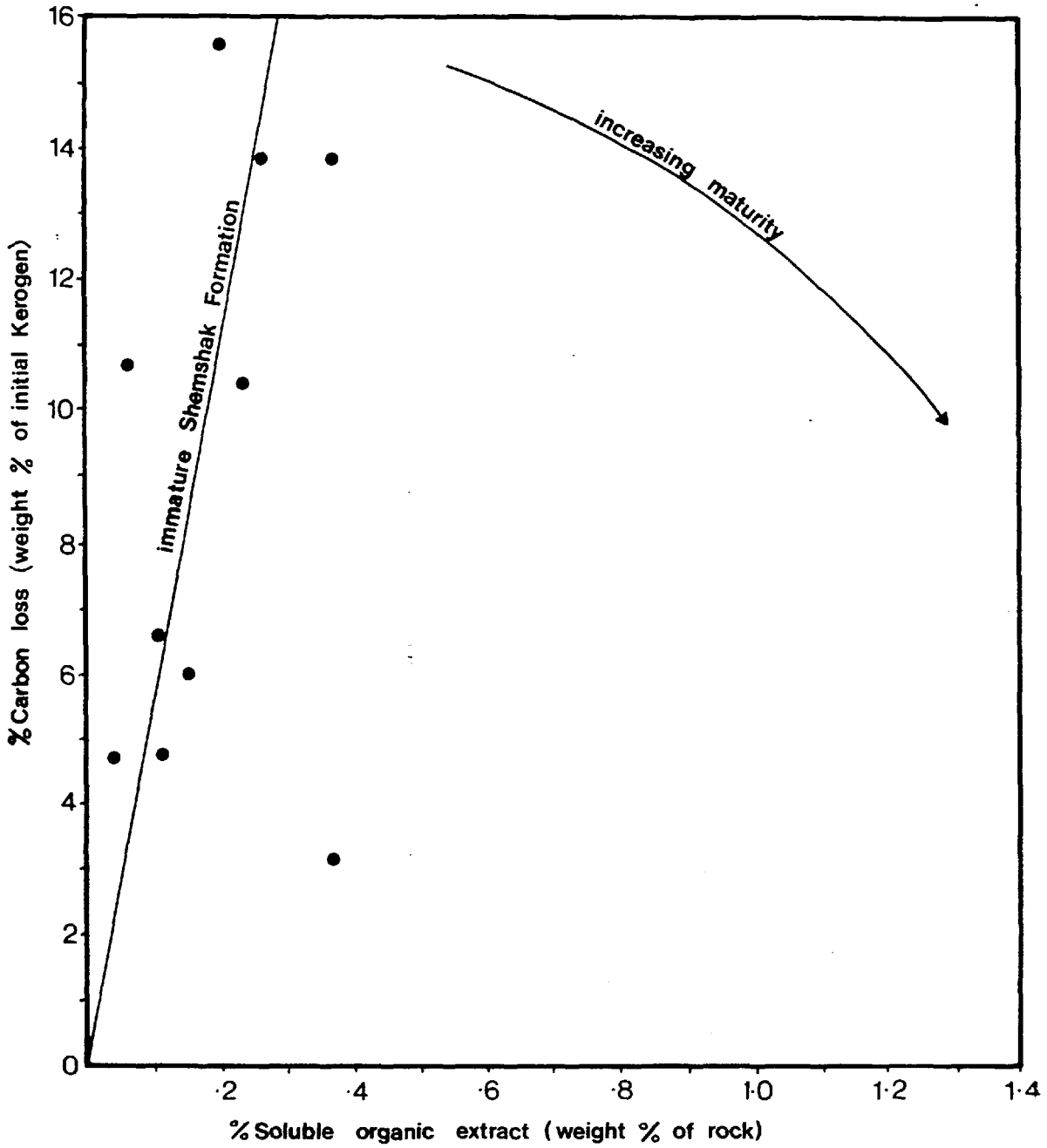
1 Unexpelled source rock (micro reservoir; Gurpi sequence, Kuh-e Bangestan)

2 Expelled mature source rock (Kazdhumi Fm.)

3 Immature oil-type source rock (Kimmeridgian Shale)

4 Immature gas-type source rock (Shemshak Fm)

5 Senile source rock (Kashafrud Fm.)



Formula used for calculation of the amount of carbon loss (C_L).

$$C_L = \frac{(W_i \times C_T) - (W_p \times C_R)}{(W_i \times C_T)} \times 100$$

C_L – Carbon loss	W_i – Initial weight of sample
C_T – Total organic carbon	
C_R – Organic carbon after pyrolysis at 500°C	W_p – Weight of sample after pyrolysis at 500°C

Fig. II.4.5 – Correlation of the amount of carbon loss as a result of pyrolysis at 500°C of mineral free kerogen concentrates and the quantity of their corresponding soluble organic extract of the immature Shemshak Fm. The arrow shows the direction of increasing maturity. N.B. Samples were not extracted before maceration.

those of Jajarm suggest a slightly higher degree of maturation of the latter; the types of the initial organic matter in the two areas, however, must also be taken into consideration.

4.2.5 Conclusions

While the Shemshak Formation is categorised as unmetamorphosed in the hydrocarbon versus C_T and saturated/aromatic versus hydrocarbon/C_T diagrams, the moderately low concentration of hydrocarbons, even for samples with high C_T values, suggests immaturity of the source rock.

The average ratio of non-hydrocarbons/hydrocarbons also implies immaturity, when compared with that of highly mature Kashafrud Formation of the Kopet Dagh basin.

The trend shown by the Shemshak Formation in the C_T versus E crossplot also indicates immaturity, as do the percentages of carbon loss in respect to the soluble organic extracts of the kerogens.

4.3 Alkanes Distribution and Carbon Preference Index (CPI)

4.3.1 Introduction

The distribution of alkanes in source beds is subject to extensive variations depending mainly on the type of the organic matter and the geothermal history of the source rock. Long chained n-alkanes with odd carbon numbers predominate in the saturated fraction of most young sediments, particularly those with a terrestrial origin: with increasing depth of burial and age the odd/even predominance progressively disappears by dilution with newly generated petroleum-like* n-alkanes (Phillippi, 1965; Eisma and Jurg, 1967; Albrecht et al., 1976). In contrast, no

* Petroleum-like n-alkanes are referred to those with no odd/even predominance similar to crude oils (Bray and Evans, 1965).

odd carbon predominance is found in the alkanes from purely marine organisms (Koons et al., 1965). Vandenbroucke et al. (1976) noted that the distribution of n-alkanes in autochthonous (marine origin) sediments at shallow depth is comparable to that of highly mature samples of terrestrial origin. Thus, the distribution of alkanes in a source bed depends both on those initially present in the rock and on the quality and quantity of alkanes generated through maturation of its kerogen content.

The predominance of odd/even carbon numbered n-alkanes can be assessed by CPI (Bray and Evans, 1961) or R_{29} (Phillippi, 1965) or OEP (Scalan and Smith, 1970). The CPI is the most commonly used as an index of maturity. CPI, which is mostly high for immature sediments, gradually decreases with increasing thermal maturity and subsequently approaches unity (similar to crude oil). However, low CPI values do not necessarily indicate maturity, since an immature source bed with predominantly algal organic content might also exhibit a low CPI (Vandenbroucke et al., 1976).

As the odd/even carbon predominance disappears with increasing maturation, the distribution maxima of the n-alkanes shifts to lower carbon numbers, due to a preferential generation of shorter chain alkanes (Powell, 1975; Tissot and Welte, 1978). Demaison (1975) noted that this shift takes place mainly at the threshold of intense oil generation, from the C_{23}-C_{29} range to the C_{13}-C_{19} range; intermediate bimodal distributions are however, often observed. Allan and Douglas (1977) studied the distribution of n-alkanes in coal maceral concentrates and found that a fairly consistant relationship exists between the maximum reflectance of vitrinite and CPI (the CPI decreases with increasing vitrinite reflectance).

Nevertheless, gas chromatograms of the saturated fraction of extracted bitumens can provide a good indication of maturity. For immature rocks, the spectrum of the saturates shows a dominance of high molecular weight (HMW) alkanes (C_{25}-C_{29} range)

with a strong odd to even carbon preference (high CPI). As the degree of maturation increases, the domination of HMW alkanes gradually disappears, due to the generation of lighter (LMW) alkanes, and CPI values decrease correspondingly. The gas chromatograms of highly mature rocks are in fact similar to those of crude oils. At this stage the gas chromatograms exhibit a dominance of the C_{15}-C_{19} range and CPI values are close to 1.0. Powell (1978) showed that a pronounced hump in the base line of the gas chromatograms in the C_{26} to C_{30} region, which indicates the presence of large amounts of branched and cyclic alkanes, is a sign of immaturity. Purcell et al. (1979) noted that the gas chromatograms from the immature zone of the Scotian basin are characterised by a bimodal base line (naphthenic envelope).

Powell and McKirdy (1973) realised that oils derived from immature terrestrial organic matter have low pristane/phytane ratios. Rashid (1979) showed that the pristane/phytane ratios increase with increasing depth of burial and rise of the level of organic maturation. He also noticed a significant reduction in phytane during the thermal evolution of organic matter. The pristane/n-C_{17} ratios are also reported to decrease with increasing thermal maturity, because branched alkanes are less thermally stable than n-alkanes (Ishiwatari et al., 1977).

4.3.2 Procedures

All samples were analysed according to the procedures described in Section 3.6.2.

CPI values were calculated from the formula:

$$CPI = \frac{2\,(C_{25} + C_{27} + C_{29})}{C_{24} + 2C_{26} + 2C_{28} + C_{30}}$$

The same formula was used by Vandenbroucke et al. (1976) and Harwood (1977).

4.3.3 Data

The CPI values are listed in Table II.4.1 and other data

Table II.4.1 - Carbon Preference Index.

Sample No.	CPI
Qoznavi Section	
124	1.46
125	1.94
129	1.62
133	1.36
138	1.49
142	1.10
149	1.51
150	1.56
152	1.36
157	1.72
161	1.17
162	1.33
166	1.24
169	1.24
171	1.23
173	1.25
174	1.67
177	1.14
179	1.45
184	1.11
191	2.43
196	1.24
197	1.25
203	2.00
207	1.22
208	1.24
Average	1.44
Rudbar Section	
218	1.19
220	1.90
222	1.38
224	1.04
228	1.06
232	1.14
233	1.08
236	1.23
238	1.03
242	0.94
245	1.05
249	1.20
251	1.59
253	1.04
254	1.03
256	1.12
257	1.13
259	1.10
260	1.24
261	1.02
262	1.29
265	1.22
271	1.73
276	1.52
282	1.25
285	1.39
Average	1.23
Jajarm Section	
325	1.26
326	1.33
327	1.42
330	1.31
333	1.33
336	2.80
339	1.37
343	1.46
344	1.32
346	1.30
350	1.32
354	1.36
355	1.26
356	1.29
357	1.37
360	1.17
361	1.31
365	1.13
367	1.21
Average	1.38
Total Average	1.35
Kashafrud Fm. (Kopet Dagh)	
BMM	0.96
28MM	0.96
MM118	1.09

are given in Section 3.6.3. The saturated fractions of three samples from the Kashafrud Formation of the Kopet Dagh were also analysed for comparison with the Shemshak Formation (Fig. II.4.6).

4.3.4 Results and Interpretation

The mean value of the CPI for all of the studied samples is 1.35. This figure is appreciably higher than the value of 1.15 given by Bray and Evans (1961) as the upper limit for sediments with petroleum-like n-alkanes (no significant odd carbon predominance). Thus it can be concluded that the Shemshak Formation of the area studied has not reached the principal stage of oil formation* and is consequently immature. Figure II.4.7 shows that over 75 percent of the samples have CPI values greater than 1.15, whereas the values calculated for the three analysed samples from the highly mature Kashafrud Formation are all very close to unity (0.96, 0.96 and 1.09) and average 1.00. By way of comparison, it may be noted that the immature Kimmeridge Clay of Dorset (England) showed average values of 1.3 (Davies, 1978).

The CPI values of the samples analysed are independent of their alkane concentrations and amounts of solvent organic extracts, as illustrated in Figures II.4.8 and II.4.9. This may suggest that the quantities of alkanes (bitumens) formed by thermal maturation of the kerogens are insufficient to control the CPI values, since this type of kerogen (dominantly huminite, see Chapter 3) is capable of generating adequate alkanes if sufficiently heated.

In the Shahpassand area the CPI values from the Qoznavi Section average 1.44, whilst in the Rudbar Section the average is only 1.23. A comparison of the two (Fig. II.4.10) shows that the Rudbar Section provides a higher percentage of samples having

* At the principal stage of oil formation copious quantities of hydrocarbons with no odd carbon predominance are generated.

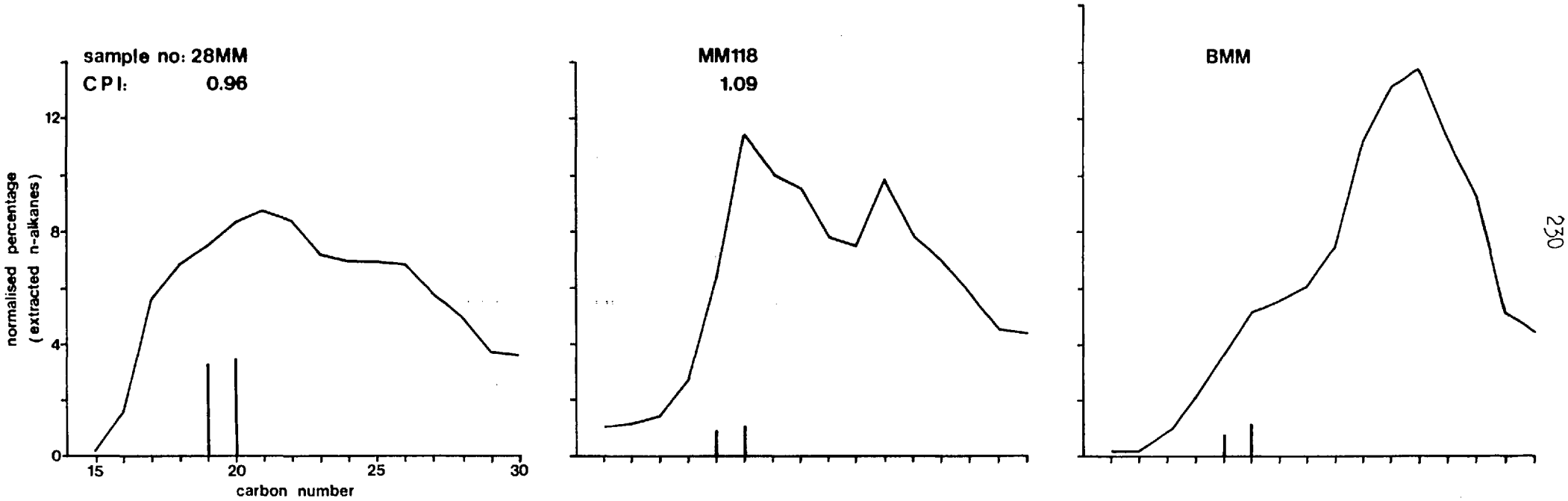


Fig. II.4.6 - The distribution of n-alkanes in samples from the Kashafrud Fm. (Kopet Dagh) and their corresponding CPI values.

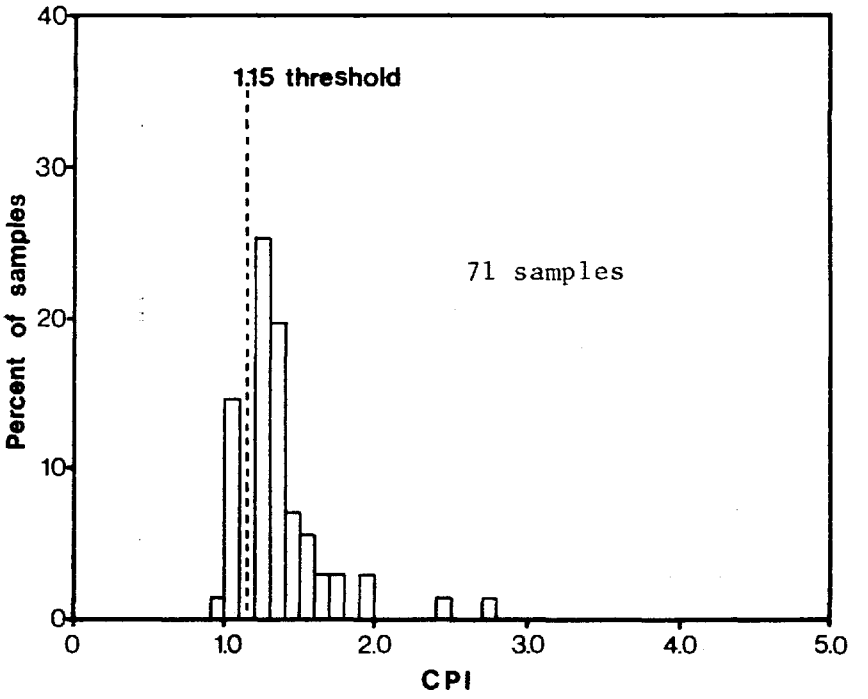


Fig. II.4.7 - Carbon preference index distribution of the Shemshak Fm. Over 75% of the samples have CPI more than 1.15.

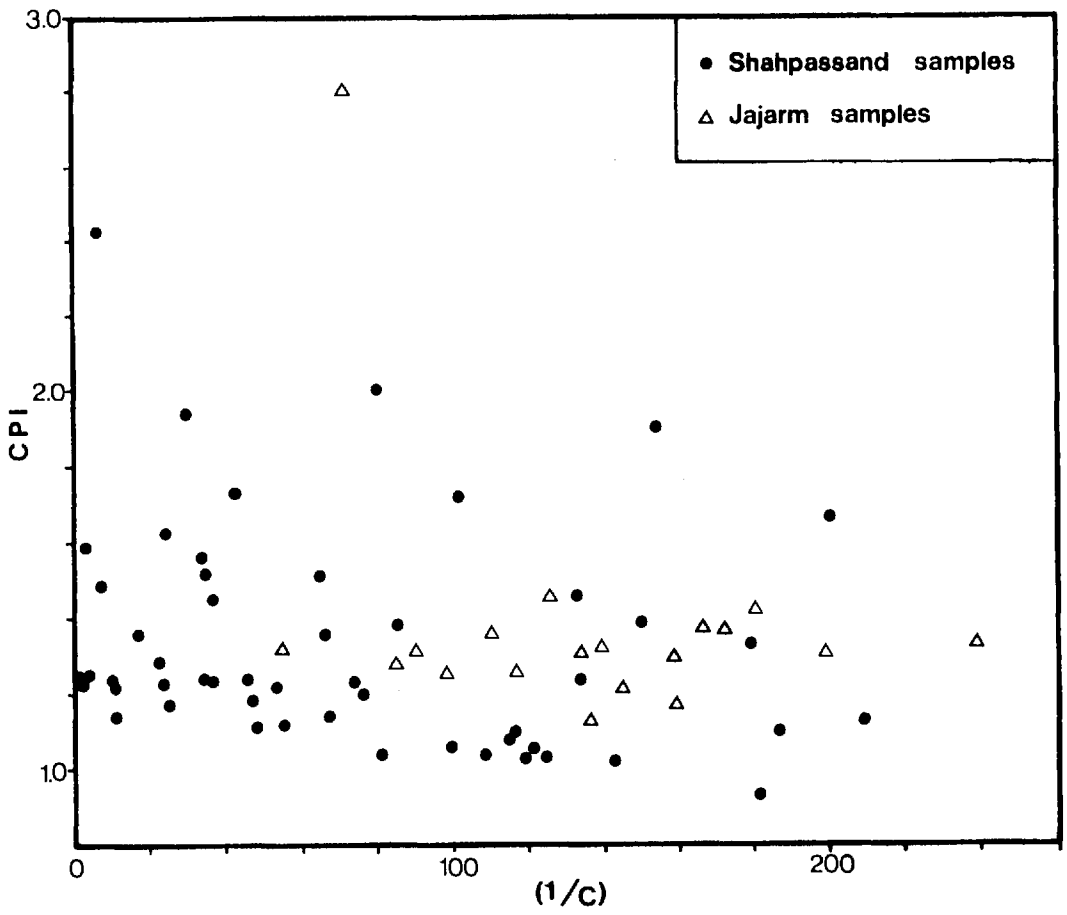


Fig. II.4.8 - Variation of carbon preference index in the Shemshak Fm. relative to the reciprocal of concentration of saturates. CPI is independent of alkanes concentration.

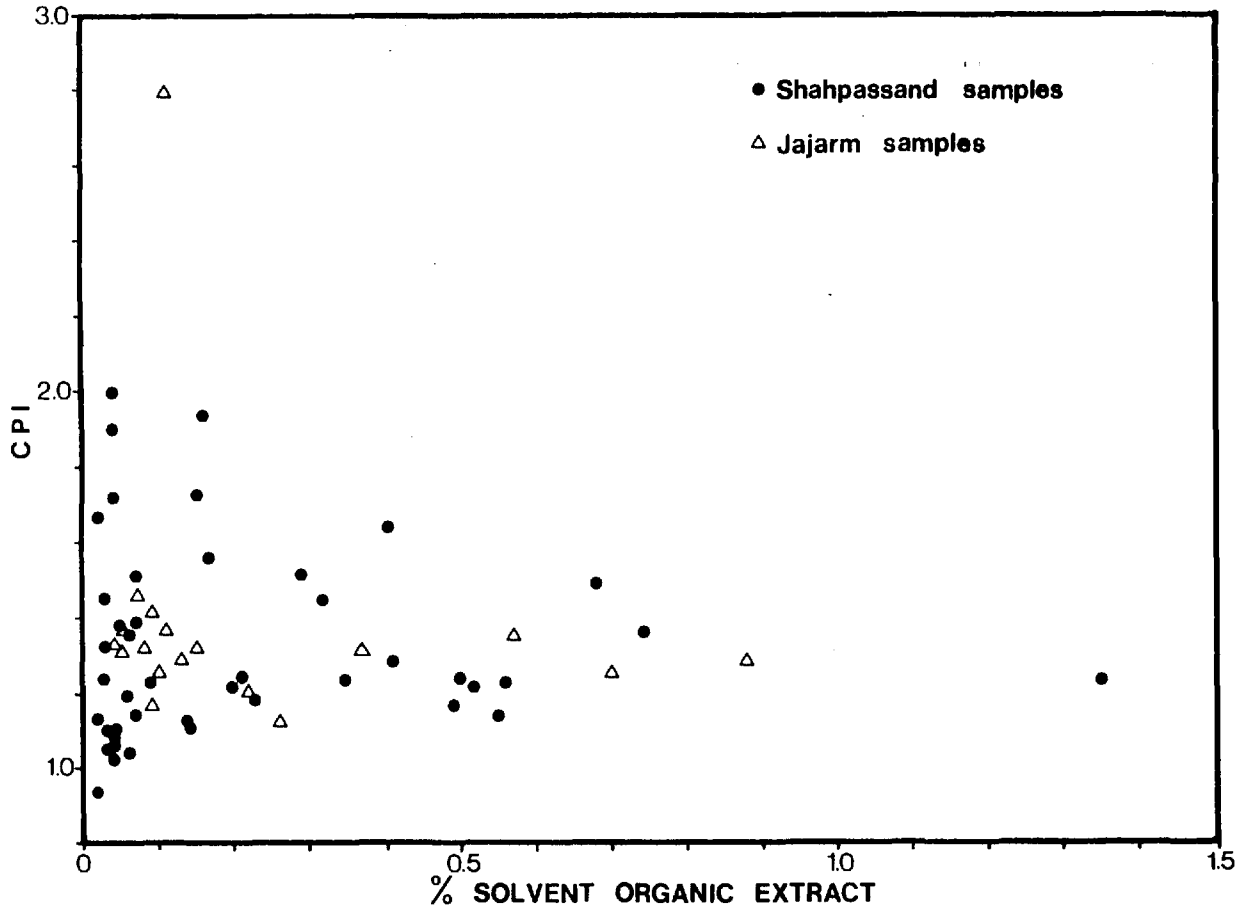


Fig. II.4.9 - Plot of carbon preference index versus the percentage of solvent organic extract of the Shemshak Fm. samples. CPI is independent of solvent extract.

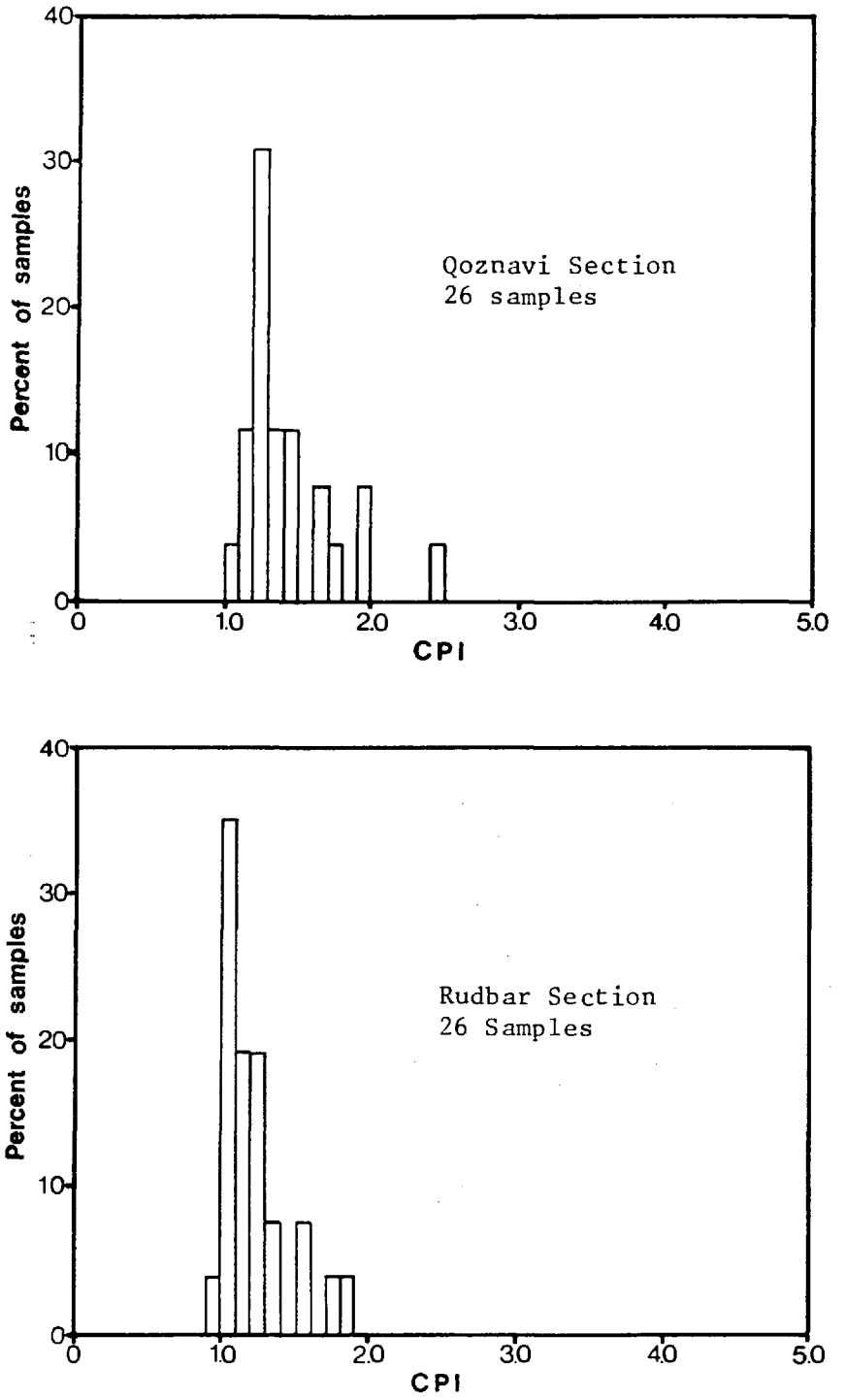


Fig. II.4.10 - A comparison of the distribution of CPI in the Qoznavi and Rudbar Sections. The latter has a higher percentage of samples with petroleum like n-alkanes.

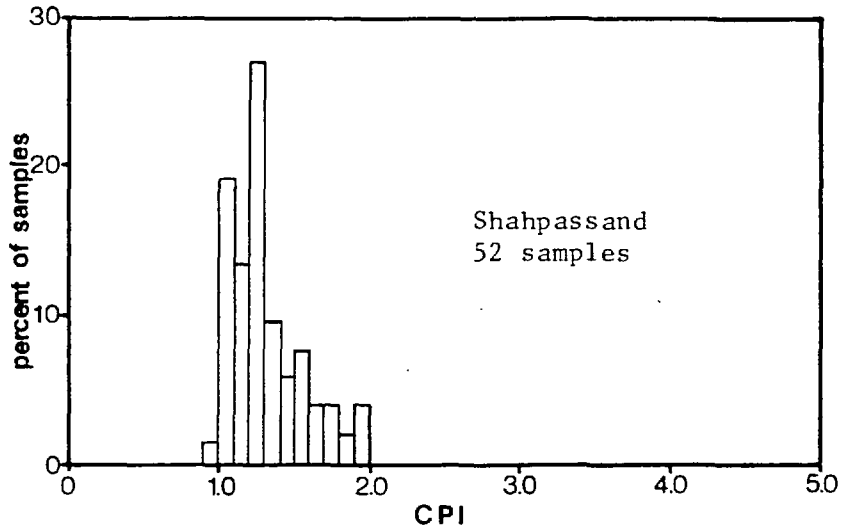
petroleum-like n-alkanes (CPI less than 1.15) as well as a narrower range of CPI distribution. These differences might suggest that the Rudbar area is the more mature, and it should also be noted that a number of samples from this Section have saturated fractions strongly dominated by C_{23}-C_{29} range n-alkanes: this is regarded by some authors as a sign of immaturity, but the predominance of HMW n-alkanes at Rudbar may also reflect the high contribution of coaly material.

A comparison of the CPI distributions between Shahpassand and Jajarm is illustrated in Figure II.4.11. Although the Jajarm spectrum is dominated by values between 1.2 to 1.3, its very narrow range of distribution might suggest a higher maturity than at Shahpassand with its wider range of CPI distribution.

The n-alkane distributions vary widely throughout the sequence and, although a mostly bimodal configuration exists, the bias fluctuates between the HMW and LMW regions (Figs. II.3.12, II.3.13 and II.3.14). These fluctuations arise mainly from relative changes in the type of organic matter present, rather than in the degree of maturation. However, all of the gas chromatograms show a naphthenic envelope, which is mostly bimodal and typical of immature rocks. In contrast, samples from the highly mature Kashafrud Formation show a very low unimodal naphthenic envelope (Fig. II.4.15).

The overall average of the pristane/phytane ratios is relatively low (1.93) and typical of immature source rocks. Since this ratio is highly affected by the type of organic matter (Rashid, 1979), no comparison of the pristane/phytane ratios is made between the Shahpassand and the Jajarm samples.

The average pristane/n-C_{17} ratio of all the samples analysed is 0.64, also clearly indicative of immaturity; however, the average value of the Jajarm samples (0.44) is slightly lower than that of the Shahpassand ones (0.72) and possibly suggesting somewhat higher degree of maturation.



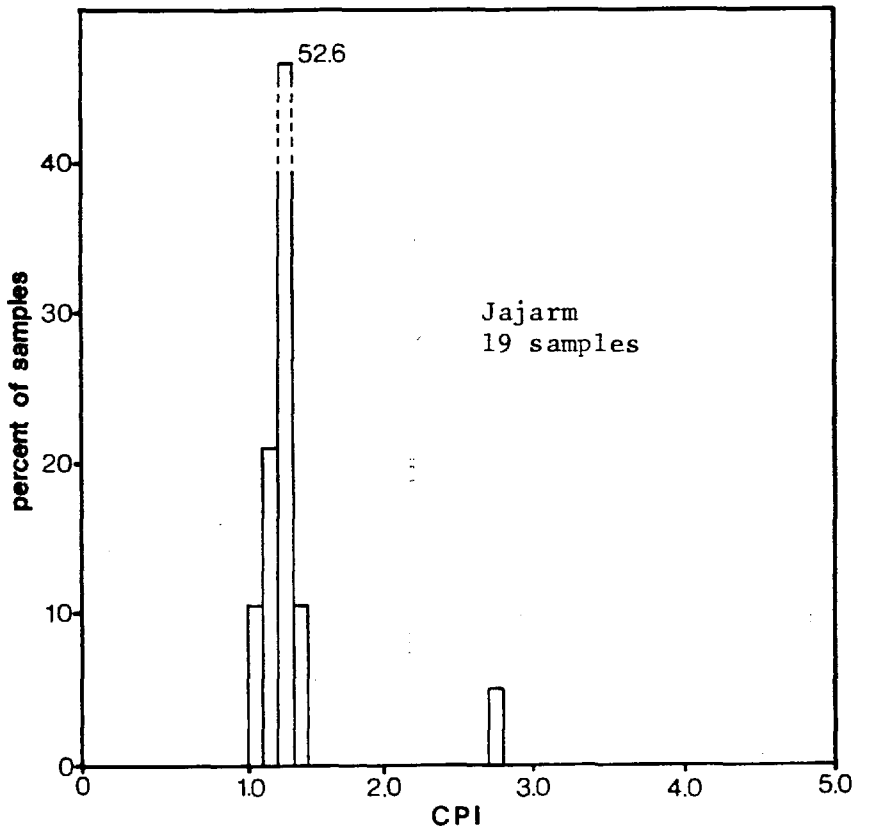


Fig. II.4.11 - A comparison of the CPI distribution in the Shahpassand and Jajarm regions. The latter shows a narrower range of distribution.

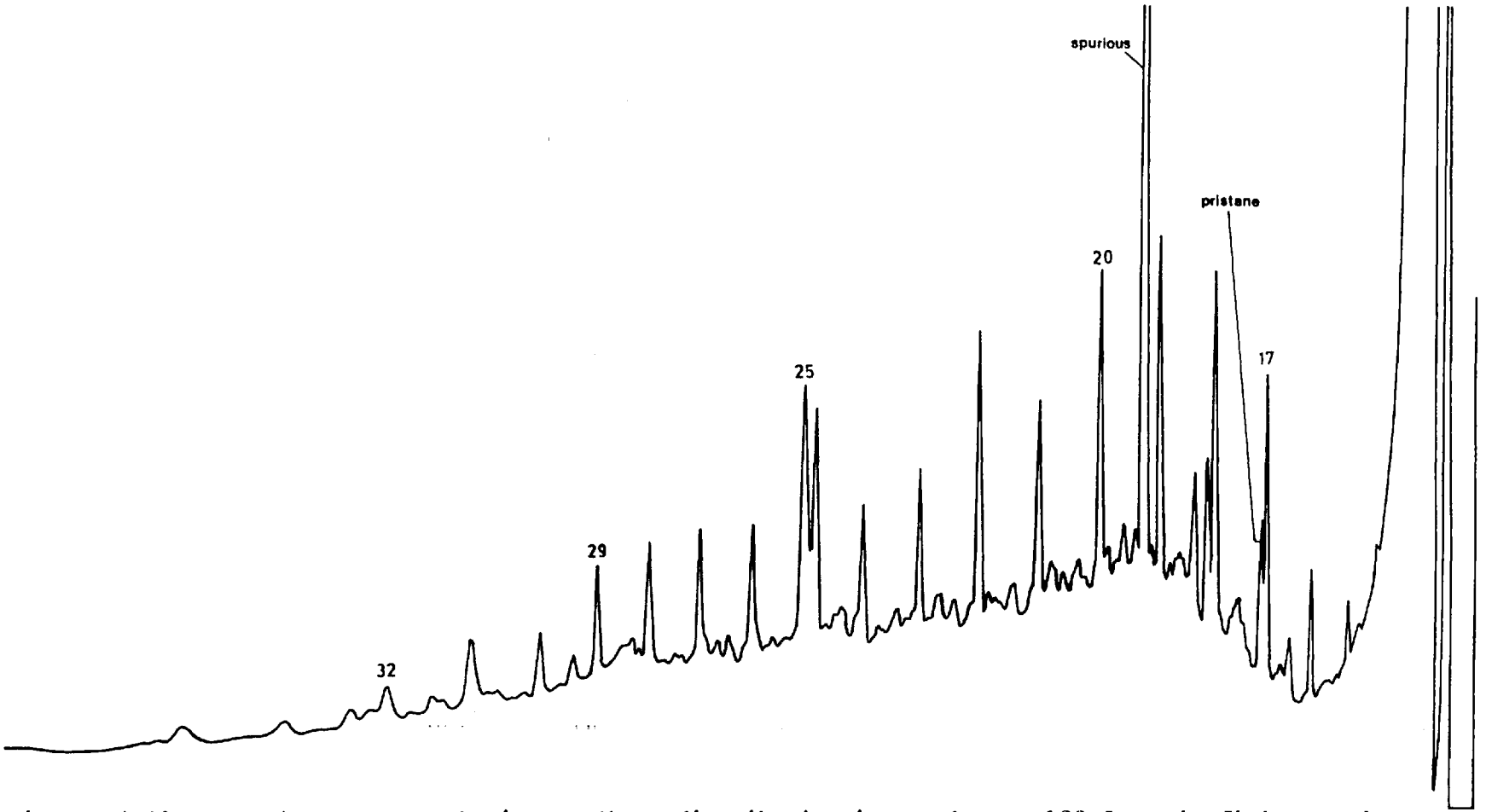


Fig. II.4.12 - Gas chromatogram showing n-alkane distribution in sample no. 133 from the Shahpassand area. The bias is in the LMW (C_{17} - C_{20}) region.

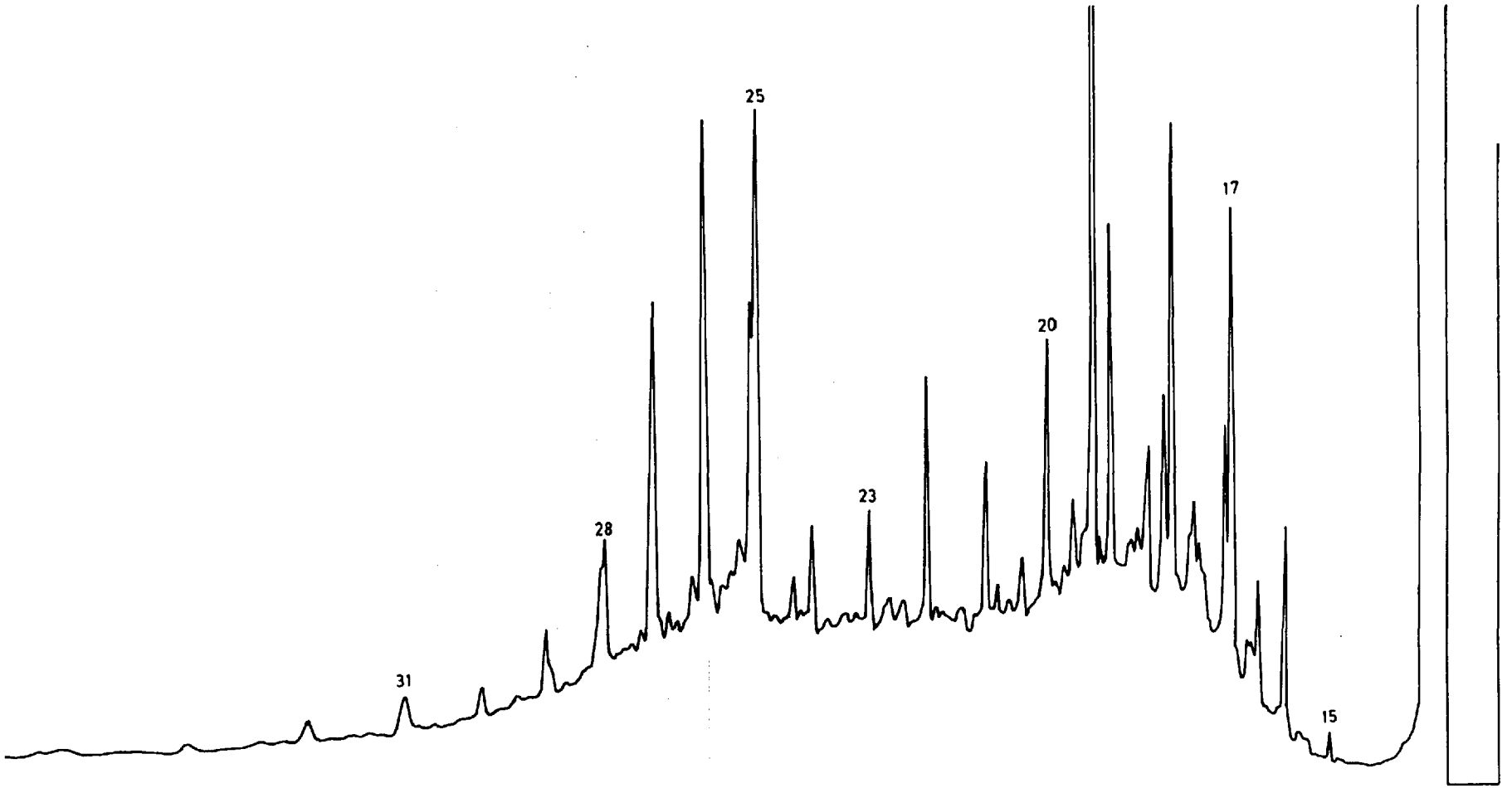


Fig. II.4.13 - Gas chromatogram showing n-alkane distribution in sample no. 330 from the Jajarm area. A bimodal configuration is discernible with maxima on C_{18} and C_{25} peaks.

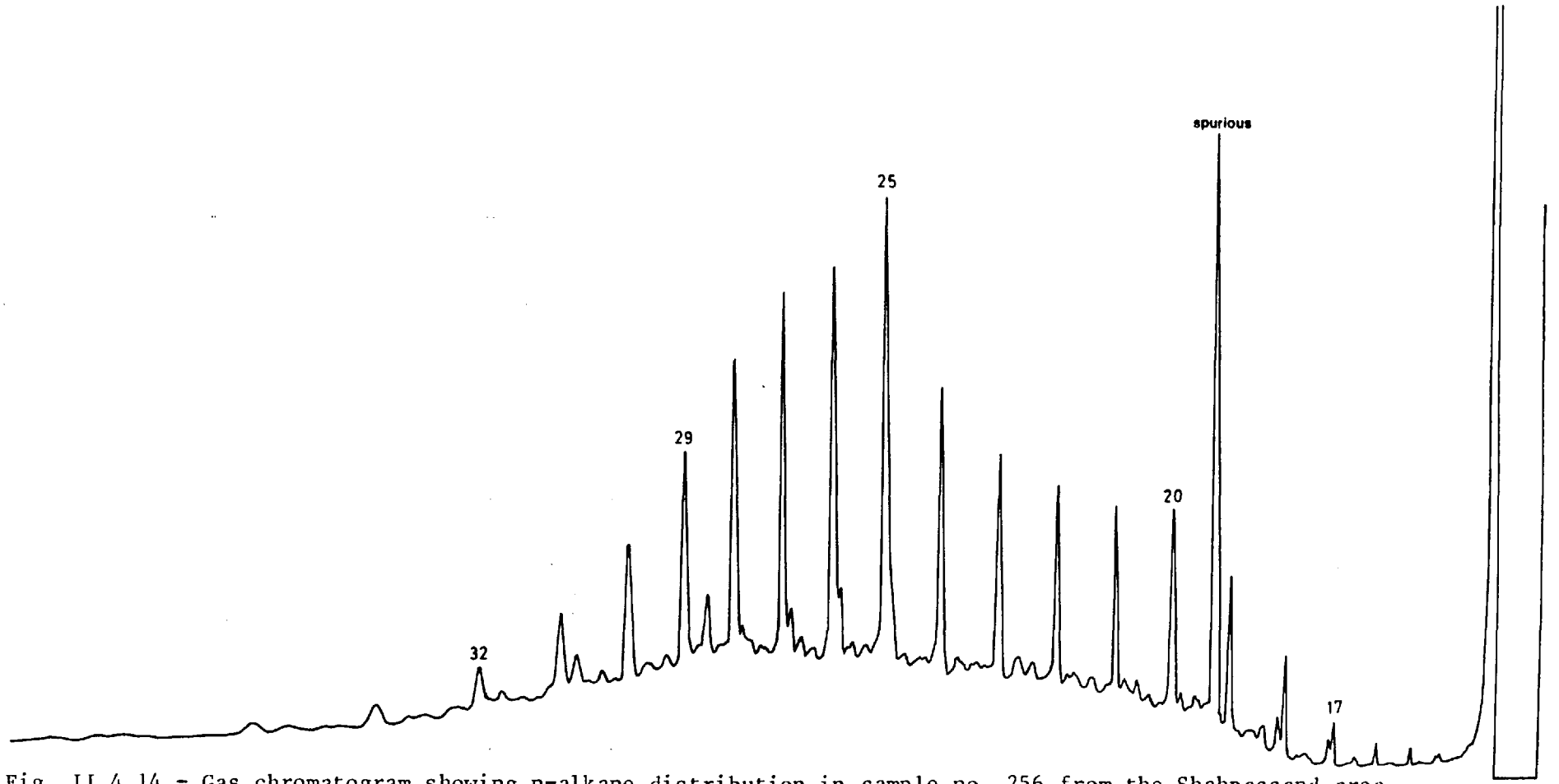


Fig. II.4.14 - Gas chromatogram showing n-alkane distribution in sample no. 256 from the Shahpassand area. The bias is in the HMW (C_{25} - C_{29}) region.

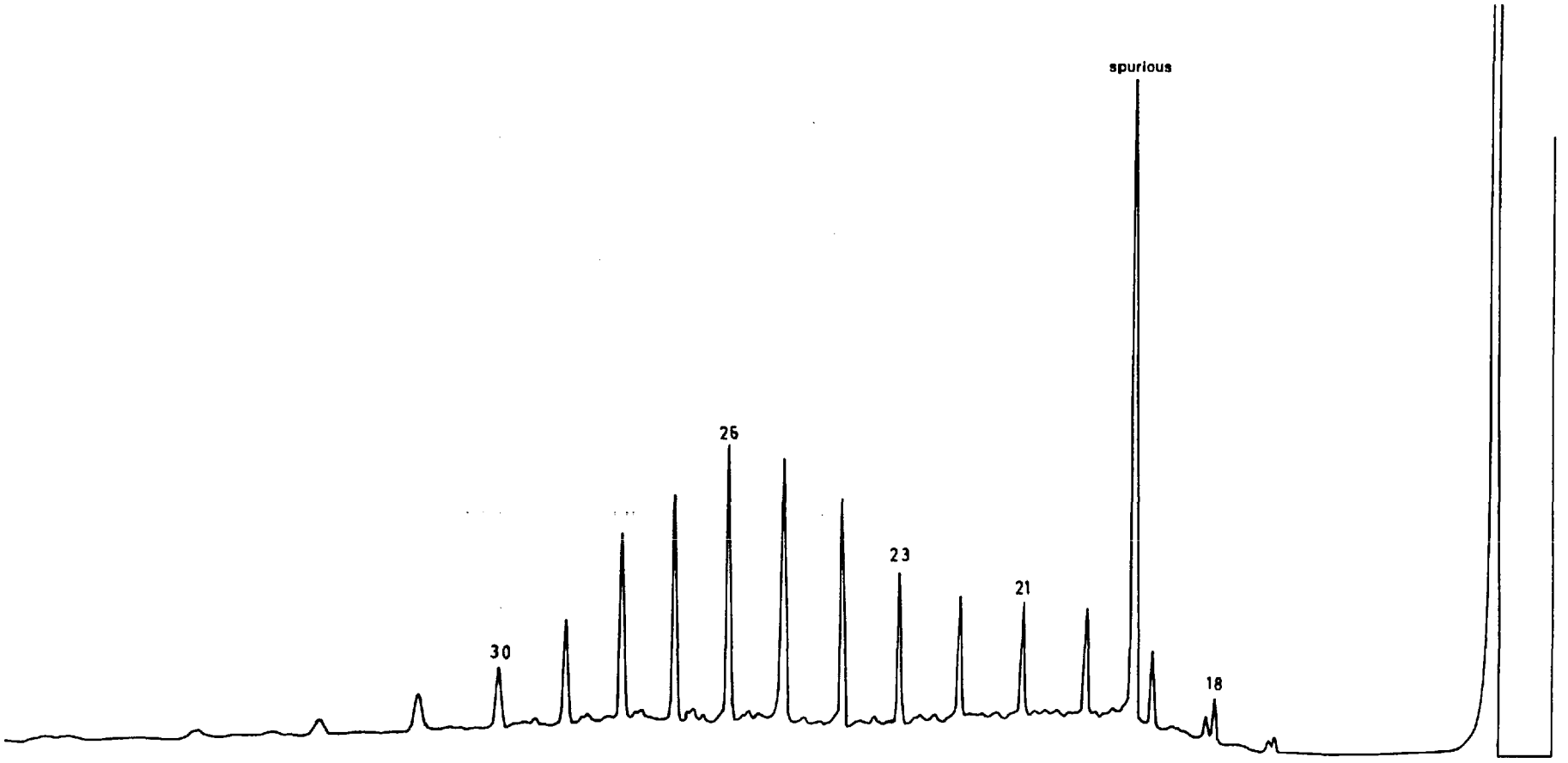


Fig. II.4.15 - Gas chromatogram showing n-alkane distribution in sample no. BMM from the Kashafrud Fm. of Kopet Dagh region. The low naphthenic envelope indicates maturity, whilst the bias in the HMW region suggests humic matter.

4.3.5 Conclusions

The Shemshak Formation has not reached the principal stage of oil formation and is thus immature. This was shown by its high average CPI value, and confirmed by: independence of the CPI values in relation to alkane and bitumen concentrations; bimodal naphthenic envelope of gas chromatograms; low pristane/phytane ratios.

A comparison of the samples from the Qoznavi and Rudbar Sections on the basis of their CPI distribution and average values suggest a higher degree of maturation of the latter.

A slightly higher level of maturity can also be detected in the Jajarm samples, relative to the Shahpassand area, from their CPI distribution spectrums.

4.4 Carbonisation of Palynomorphs

4.4.1 Introduction

Carbonisation is a process of thermal destruction or decomposition of organic material (Gray and Boucot, 1975) synchronous with a gradual increase in its relative carbon content. Different organic substances respond differently to this process, although the end products are usually graphite or anthracite. During the carbonisation process, the organic particles progressively become more opaque and darker in colour. In general, their colours change successively from yellow to orange, red, reddish brown and finally to black (Correia, 1971). Among the organic particles, spores and pollen grains are the most sensitive indicators of thermal maturity, because their external membranes are constructed from sporopollenin* (Correia,

* Sporopollenin is more susceptible to thermal maturation than the constructional substances of other organic particles such as: acritarchs and chitinozoa (Correia, 1971).

1971). Gutjahr (1966) used their light-absorption value as a measure of carbonisation, but emphasised that this method is unsuitable for extremely carbonised zones.

The degree of carbonisation can be measured by: (i) colorimetry in transmitted light, (ii) translucency, or (iii) fluorescence under UV light. In this study the first methd is used in conjunction with Table II.4.2.

The regional plotting of the colour of spores and pollen is widely used to determine the state of maturation of sedimentary organic matter, and consequently to predict the possibility of the occurrence of hydrocarbons in a sedimentary basin.

4.4.2 Procedures

All samples were prepared as described in Section 3.1.2.

4.4.3 Data

The colour descriptions of palynomorphs in the samples studied are given in Table II.4.3.

4.4.4 Results and Interpretation

As is shown in Table II.4.3, the Shahpassand samples range in colour from pale-yellow to orange whereas the Jajarm samples

Table II.4.2 The colour of palynomorphs in relation to the state of maturation of the organic matter.

Colour of spores and pollen	State of maturation of organic matter
yellow orange	immature
light-brown brown	mature
dark-brown black	metamorphosed

Table II.4.3 - The colour of spores and pollen in the Shemshak Formation of the Eastern Alborz.

Sample No.	Locality	Colour of spores and pollen
124	Shahpassand	pale yellow-orange
129	"	light yellow-yellow
133	"	light yellow-orange
134	"	yellow-orange
142	"	pale yellow
149	"	(no palynomorphs)
153	"	pale yellow
156	"	(no palynomorphs)
158	"	yellow-orange
160	"	yellow-orange
166	"	yellow
174	"	yellow
177	"	(no palynomorphs)
186	"	(no palynomorphs)
190	"	yellow-orange
191	"	yellow-orange
199	"	yellow-orange
203	"	pale yellow-orange
204	"	yellow-orange
205	"	yellow-orange
209	"	yellow-orange
210	"	(no palynomorphs)
211	"	pale yellow-orange
326	Jajarm	(no palynomorphs)
327	"	(no palynomorphs)
336	"	orange-light brown
339	"	(no palynomorphs)
344	"	yellow-orange-light brown
350	"	yellow-brown
355	"	orange-light brown
357	"	orange-light brown
361	"	light brown
365	"	orange-light brown

are, in general, slightly darker in colour, ranging from yellow to light brown (Fig. II.4.16). The Shahpassand samples all indicate immaturity (Table II.4.3), but the Jajarm specimens show some indications of higher maturation (early mature). It must also be stated that the Jajarm samples, although showing a slightly higher degree of maturation in comparison with those of the Shahpassand area, are still immature (e.g. yellow and orange palynomorphs). This slight difference between the two areas in the colour range of their palynomophs may also reflect the heterogeneity of the spores and pollen, but the general lack of carbonisation of the palynomorphs denotes an overall immaturity.

Although the Shemshak Formation average 1700m in thickness no relationship exists between stratigraphic depth and degree of carbonisation of the palynomorphs.

4.4.5 Conclusions

The lack of carbonisation and the light colour of the palynomorphs both indicate a general state of immaturity for the Shemshak Formation.

While the colour of palynomorphs in the Shahpassand samples suggests an overall state of immaturity of the sediments, the Jajarm samples exhibit a slightly higher degree of thermal maturation as indicated by a darker colour of their spores and pollen.

No relationship exists between the stratigraphic depth and level of carbonisation of the palynomorphs.



A (x 1685)

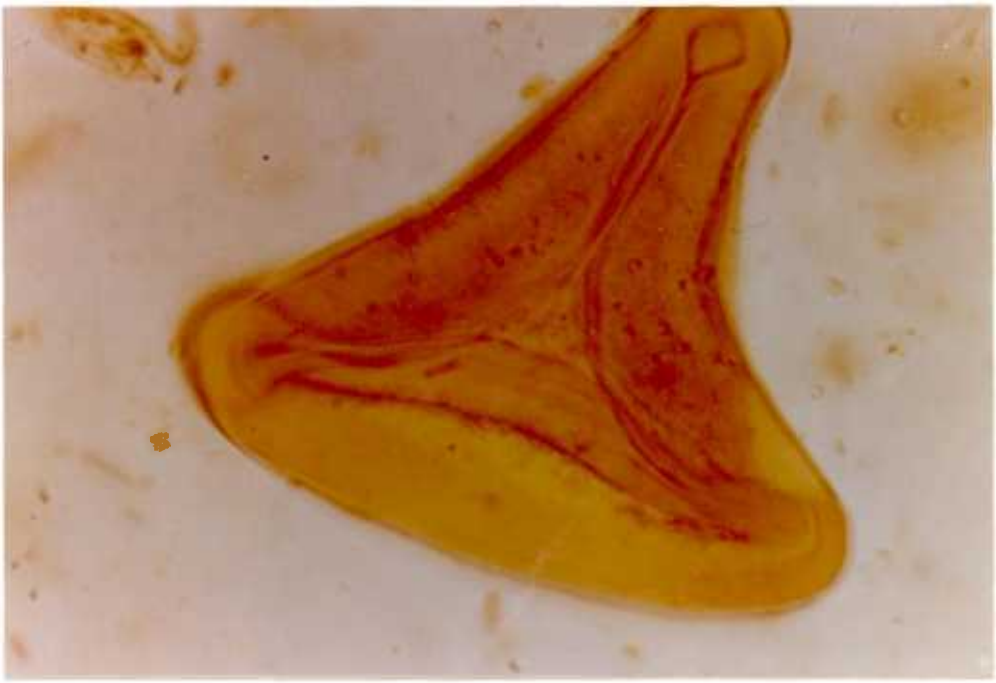


B (x 1655)

Fig. II.4.16 - Comparison of the colour of spores and pollen grains of the Shemshak Fm. at Shahpassand and Jajarm.

A,B,C,D,E,F,G) Shahpassand specimens, mainly yellow to orange suggesting immaturity.

H,I,J,K,L) Jajarm specimens, mainly orange to light-brown suggesting a higher degree of thermal maturity than the Shahpassand equivalents.



C (x 2071)



D (x 2602)

Fig. II.4.16 - Continued.



E (x 2100)

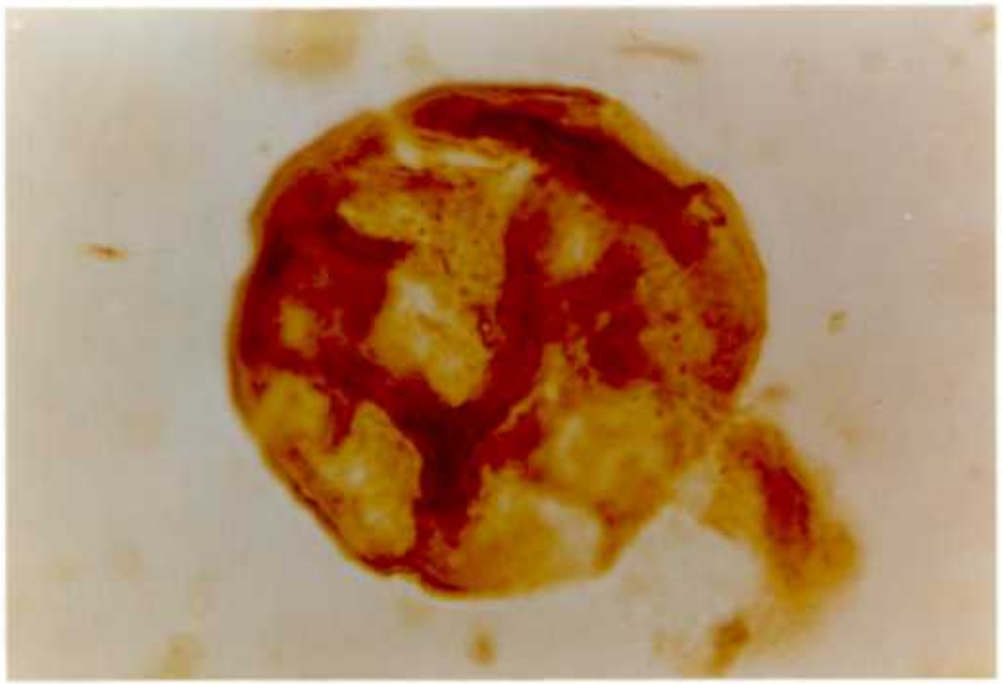


F (x 2075)

Fig. II.4.16 - Continued.

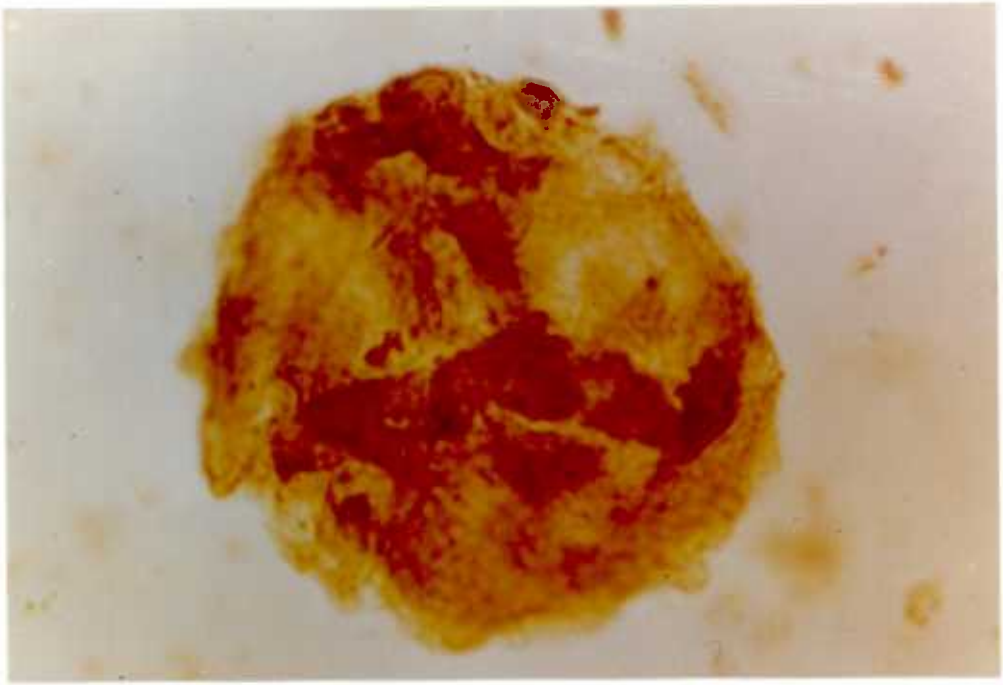


G (x 2600)

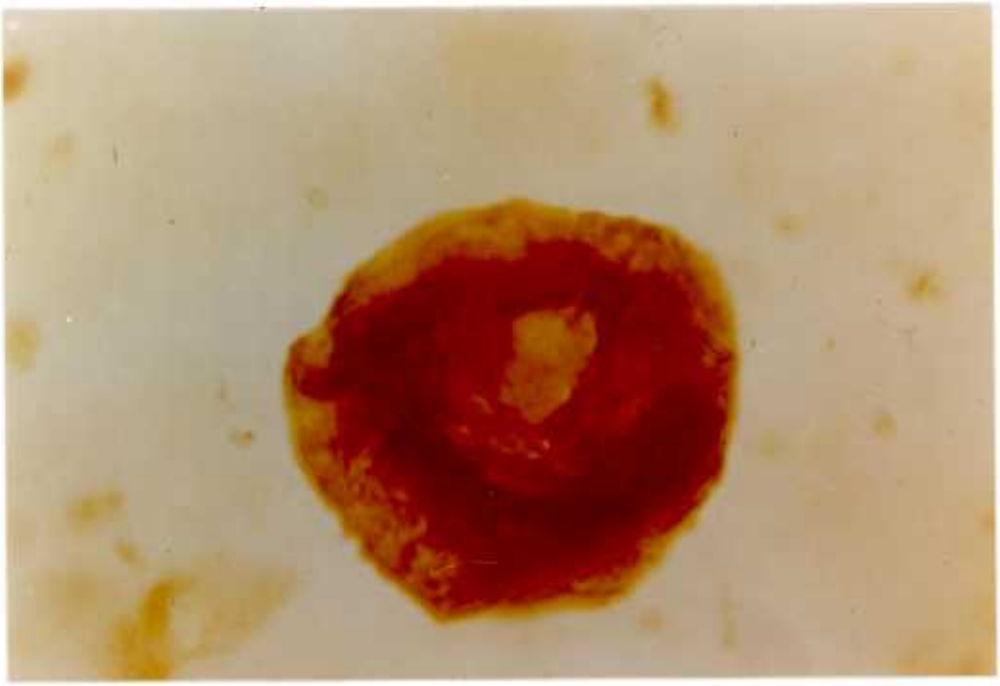


H (x 2625)

Fig. II.4.16 - Continued.



I (x 2655)



J (x 2655)

Fig. II.4.16 - Continued.



K (x 2062)



L (x 2620)

Fig. II.4.16 - Continued.

CHAPTER 5

SUMMARY AND OVERALL CONCLUSIONS

As far as petroleum source rock potential is concerned, the Shemshak Formation is probably the most attractive part of the succession in the Eastern Alborz region. Source rock studies and geochemical analyses of possible source rocks have hitherto received rather little attention in Iran, particularly in the Alborz basin. No published records of geochemical studies are yet available, although a number of Palaeozoic and Mesozoic formations are highly prospective source rocks. The evaluation of the Shemshak Formation in the Eastern Alborz is thus an important factor in assessing the petroleum potential of the region.

As detailed a geochemical analysis of the Formation as permitted by the departmental facilities, was carried out to determine the three critical elements which normally characterise a source rock. These are the amount, the type and the state of maturation of the organic matter in sediments. For this purpose, microscopic examinations under transmitted light, elemental analysis, solvent organic extraction and fractionation, pyrolysis and gas-liquid chromatography techniques were employed.

A new terminology is proposed for kerogen types: alginite (type I), sapropelite (type II), huminite (type III) and inertinite (recycled). A new pyrolysis technique is also introduced to work out the carbon loss of kerogen during its thermal evolution.

Microscopic examinations suggest a mixture of marine and terrestrial organic matter in the sediments studied, although terrigenous material predominates particularly in the Shahpassand area. The lack of carbonisation and light colour of the palynomorphs indicate a state of immaturity, although conspicuous oil droplets, found in conjunction with the humic debris, indicate the capacity of the rocks (at least in some intervals)

to generate oil. In general, the Jajarm sediments were found to have a higher content of marine organic matter and a slightly higher degree of maturation than the corresponding beds near Shahpassand.

A combination of pyrolysis and elemental analysis has provided the most useful information. The Shemshak Formation could become a source rock, since its organic content is mainly above the generally accepted minimum of 0.5%. However, the elemental composition and convertibility of the kerogen content shows that the formation is dominantly huminitic and an immature source. The average trend of the Formation in the C_R/C_T diagram more or less coincides with that of immature huminite. The studied sediments are most likely to be a potential wet-gas source. The elemental composition of the organic matter in sediments also suggests a higher contribution of organic matter of marine origin in the Jajarm sediments than the Shahpassand equivalent.

Although solvent organic extraction and fractionation methods can provide some indications of the type and the degree of maturation of organic matter in sedimentary rocks, the results need to be corroborated by further analytical results. While the majority of the samples from the Shemshak Formation fall into the above-average or exceptional source rock categories, the high-wax nature of some of the extracted bitumens and the average non-hydrocarbon/hydrocarbon ratio indicate a terrestrial origin of most of the organic matter. Likewise, the average trend of the Shemshak Formation in the C_T versus E diagram, a moderately low concentration of the hydrocarbons even for samples with high C_T values, and the percentage of kerogen carbon loss with respect to the corresponding soluble organic extracts all denote immaturity of the source rock, although the Jajarm sediments are likely to contain a greater proportion of autochthonous marine material than their Shahpassand equivalents.

On the basis of the distribution of n-alkanes from GLC

analysis, two ranges were differentiated. The n-C_{22} to n-C_{30} range with a culmination usually at n-C_{25} or n-C_{26} represents alkanes derived mainly from humic material, whereas the n-C_{15} to n-C_{21} range probably has a non-humic origin. A general view of the n-alkane distributions points to the Shemshak Formation as a wet-gas source, and the pyrograms are comparable with those of vitrinite macerals. The dominantly high CPI values and their independence of the alkane concentrations, the bimodal naphthenic envelopes, and the relative distribution of isoprenoids also indicate that the Shemshak Formation is rather immature and has not reached the principal stage of oil formation. There is again some evidence that the Shahpassand succession contains a higher proportion of source material of terrestrial origin and that it is in a slightly lower stage of thermal maturation than the corresponding sequence near Jajarm.

CHAPTER 6

PETROLEUM PROSPECTS AND EVALUATION OF THE EASTERN ALBORZ REGION

The literature indicates that less attention has hitherto been paid to the petroleum prospects of the Alborz basin than to the prolific Zagros region. The widespread igneous activity of mainly Eocene age, the tectonic complexity of the area and the scarcity of seepages were probably the main reasons for this, although the igneous activity diminishes significantly towards the north and east.

Several intervals of possible source rock are developed as seen in the exposures of the Eastern Alborz. Potential reservoir rocks (e.g. porous limestone, and sandstone) and effective cap rocks (impermeable shale and siltstone) are also present. However, no meaningful evaluation of the petroleum prospects of the basin was previously possible since no geochemical data were available. The contribution of the present work is to show that, under suitable geothermal conditions, the Shemshak Formation could be an important source rock interval.

As already discussed, the Shemshak Formation of the Eastern Alborz is an immature source rock (as far as surface exposures are concerned) containing dominantly terrestrial organic matter and huminite kerogen. Sediments of this kind are known generally to have a low potential for the generation of oil, but this could be offset by the great thickness and regional extent of the Formation (see Sections I.3.2 and I.4.3). The generation of even a very low quantity of oil per unit volume of the rock could supply enough crude for a giant oil field, and the Shemshak Formation would undoubtedly be a prolific source of gaseous hydrocarbons if it reached a sufficient level of maturity.

An essential problem to be solved is thus to find out whether, anywhere in the basin, the Shemshak Formation has reached the required level of thermal maturation. Unfortunately,

the data required for this purpose are lacking, and the writer had recourse only to the Geological Maps and Sections of Iran (NIOC, 1978).

In the exposures to the southern part of the basin (e.g. Shahpassand and Jajarm regions) the Shemshak Formation is overlain by only a few hundred metres of Middle-Upper Jurassic sediments and some Neogene Conglomerates and clastics; it has never been buried deeply enough to reach the necessary level of thermal maturity for the generation of commercial quantities of hydrocarbons. The reason for the slightly higher level of thermal maturation of the organic matter in the Jajarm area relative to Shahpassand (see Chapter 4) is probably a gradual eastwards increase in the thickness of the sediments overlying the Shemshak Formation.

To the north and northeast of the exposed region the Shemshak Formation is buried under younger sediments. Beneath the south eastern corner of the Caspian Sea and the Dasht-e Gorgan, more than 4,000m of Neogene marine strata (mainly Pliocene: Akchagyl Formation) overlie the Mesozoic rocks (NIOC, 1978), and northeast of the town of Gonbad-e Kavous, drilling has shown that burial depth of the Shemshak Formation is over 5,000m (Madani, 1977). Towards the northeast, where the thick Cretaceous deposits of the Kopet Dagh overlap the eastern extension of the Alborz, the Shemshak Formation may be buried even deeper. South of the Gorgan uplift (see Sect. I.3.3.1) the Shemshak Formation, which immediately overlies the Precambrian metamorphic rocks, is buried beneath the massive Lar limestones (Middle Jurassic) and Upper Cretaceous and Neogene sediments: the overburden is 2,000-3,000m thick.

Afshar-Harb (1979) discussed the temperature gradient of the Gorgan area based on exploration well data (Fig. II.6.1). He noted that the temperature gradient is relatively low down to a depth of about 3,000m (1°C per 60-70m), but that it increases sharply beyond this depth to a rate of 1°C per 29m. Using these

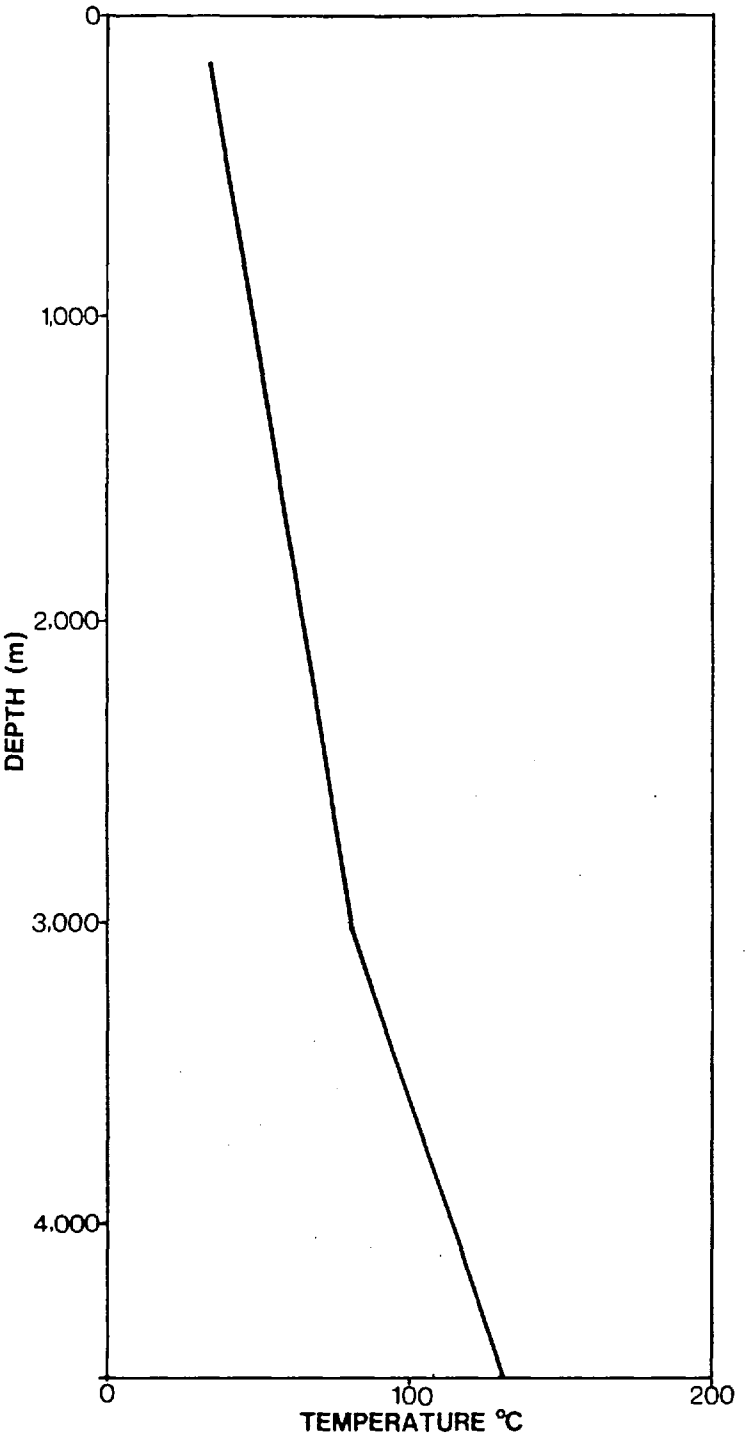


Fig. II.6.1 - Temperature gradient in the Gorgan area (after Afshar Harb, 1979).

data, we may estimate that the Shemshak Formation, in the Dasht-e Gorgan and Southeast Caspian Sea region, where its average depth of burial is 3,000 to 4,000m, has reached a temperature in the range of 80-125°C. At this temperature, the source rocks should have reached the principal stage of oil formation. Consequently, in the whole area north of the Eastern Alborz, the Shemshak Formation might have generated hydrocarbons, most likely wet-gas.

6.1 Evaluation of the Shemshak Formation in the Eastern Alborz

Assuming that the Shemshak Formation is continuously present under the whole area of Dasht-e Gorgan, its northern extension in southern Russia, and the southeastern corner of the Caspian Sea (north of the Gorgan High), the areal extent would be about 30,000 km^2. This area covers the entire region north of the Eastern Alborz mountains from the town of Sari eastwards to the village of Minudasht. The average thickness of the Formation, from the measured sections, is about 1700m which indicates about 5.1×10^{13} cubic metres of sediments. Assuming an average density of 2.5×10^3 kg/m^3, approximately 1.27×10^{14} tons of the Formation are available in the area.

The average organic carbon content of the Formation is 5.9% (see Sect. II.3.2) which represents about 6.9% organic matter if the convertibility factor of 1.18 is used (Table I.2.2). Thus, the organic content of the Formation in this region totals about 8.8×10^{12} tons. According to the pyrolytical analysis results, the average convertibility of this organic matter to hydrocarbons is about 34 percent (see Sect. II.3.5). Thus a quantity of about 2.9×10^{12} tons of kerogen could have converted to hydrocarbons if the Formation has undergone sufficient thermal maturation.

The Shemshak Formation, as a source rock, is probably responsible for the oil seeps on top of the anticlinal structures in the area south of the Gorgan Uplift (Gill, personal comm.), and also for the oil fields near the eastern coast of the Caspian

Sea in Russian Turkmanistan. The subsurface temperature (depth of burial) increases towards the east and if the Formation continuous with similar characteristics underneath the Kopet Dagh basin enormous amounts of gas condensates could have been generated from it.

Unlike the Central Alborz, the sedimentary rocks in the Dasht-e Gorgan and Southeastern Caspian region have not been highly disturbed by orogenic movements. Thick intervals of carbonates, particularly of Cretaceous age, could have accommodated the hydrocarbons generated from the underlying Shemshak Formation. The Lower and Upper Sandstone Members of the Formation itself could act as suitable reservoir bodies, because of their considerable thickness and high porosity (see Chapter I.4). Any large amounts of hydrocarbons would be expected to have been generated relatively recently, after the deposition of the Neogene sediments, when the depth of burial (temperature) had reached the required level. Thus, any structures due to the Tertiary tectonism would have predated hydrocarbon migration and would form prospective traps.

Under these favourable conditions, the Dasht-e Gorgan and Southeastern Caspian region should be regarded as prospective for oil and gas, eventhough no positive data about the degree of maturation of the source rocks and their regional extent are available. A more extensive investigation of the Shemshak Formation, as a potential source rock, and a study of the possible reservoir rocks in the area could be profitable.

The outline of a future exploration programme for the area is suggested to be:

i) Analyses should be made on the material from the wells already drilled in the area provided that these confirm the conclusions of this thesis, then:

ii) Seismic survey should lead to the drilling of further exploration wells in the Dasht-e Gorgan and Southeast Caspian area. Core specimens should be taken from suitable intervals

and a more precise knowledge of the temperature gradient obtained.
iii) Geochemical analysis of the cored Shemshak Formation and other source intervals, as well as investigation of potential reservoirs by means of wire-line logging and petrological studies. Preparation of a basin evaluation map.
iv) This could justify detailed seismic survey of the area to locate additional drilling targets.

CHAPTER 7

CONCENTRATION OF URANIUM IN RELATION TO ORGANIC MATTER DISTRIBUTION

7.1 Introduction

In general concentrated uranium deposits are mainly in Precambrian rocks (Bowie et al., 1971), although other sources in younger permeable sedimentary rocks, such as sandstones have also been reported (Nininger, 1956). Some of the most common comounds of uranium, particularly its sexivalent compounds, are highly soluble in aqueous solutions (Gabelman, 1977). Thus, the ground water can mobilise uranium from uraniferous sources and carry it in dilute solutions. The precipitation of uranium from solution is believed to occur in a wide variety of environments where reducing conditions prevail, probably due to the relative insolubility of its common tetravalent compounds (Gabelman, 1977). This means that, for example in shales, a highly reducing environment may be prerequisite to the concentration of uranium.

Organic matter in sediments is believed to function as a reducimg agent for the precipitation of uranium. Moore (1954) noted that in nature, it is commonly associated with carbonaceous material and he suggested that some uranium deposits may have been fromed over a long period of time by extraction from dilute ground water solutions. Moore's laboratory experiments showed that low-rank coals are extremely effective in extracting the uranium form compounds such as uranyl sulphates or uranyl carbonates in solution.

The possible role of the sedimentary organic matter in the fixation of uranium has been a controversial subject. Breger and Deul (1959) found a direct relationship between uranium and carbonaceous material separated from the shales of the Dakota sandstone, Colorado. However, Cameron and Allan (1973), who analysed lake sediments of northern Canada, concluded that organic matter has not seriously influenced the distribution

of uranium; and Gabelman (1976) stated that , despite the well-known ability of carbon to fix mobile uranium, well-studied coals and oils were found to represent insignificant resources.

Substantial evidence has been adduced by many authors that humic organic matter is a reducing agent in the fixation of uranium. Andreyev and Chumachenko (1964) mentioned that organic matter participates indirectly in the reduction of uranium, and that the degree of reduction depends on the kind of organic matter and the activity of the medium. They concluded that the most effective reducing agents in a broad PH range are peat, kerogen, wood and cellulose. Plant debris are the commonest organic associates of uranium, so that plant tissues and the products of their oxidation are considered to be the most effective reducing agents of uranium in nature (Haji-Vassiliou and Kerr, 1973).

Although the role and effectiveness of plant debris or other organic matter in the fixation of mobile uranium have been discussed by many authors, the factor of availability of mobile uranium has often been ignored. Uranium is an element which requires a combination of favourable conditions for its economic concentration. For example the abundance of suitable organic matter (plant debris and coal) must be accompanied by a continuous flow of ground water, with uranium compounds in solution, through the sediments over a relatively long period of time. To achieve this a source of uranium exposed to the ground water is required, and the water must flow through the sediments at a suitable rate which will be dependent upon their permeability.

7.2 Present Study

A gamma ray survey was carried out during the geological

field work in the area studied* using a portable gamma ray scintillometer model GR-101A. The radiation levels of the rocks were recorded and compared with the background level in a counts per second (CPS) scale (the ratemeter was calibrated in CPS). Some samples with relatively high levels of radiation were collected for further geochemical analysis.

South of the village of Tilabad (see Geological Map A, loose) towards Khoshyeilaq and beyond, Devonian sediments are extensively exposed and basic igneous rocks (basalt) are present, sometimes with a typical columnar appearance. The radiation background of the area and the radioactivity of rocks, as expected from basic igneous rocks, are very low (about 50 CPS). Some local yellow horizons (possibly sulphuric or phosphatic compounds), which are wedge shaped secondary deposits in the lower part of this succession, give a higher radiation count (about 3 to 4 times the background). The Carboniferous, Permian and Triassic rocks all gave very low radiation counts (about 35-50 CPS). The most prospective sequence for radioactive mineral deposits is probably the deltaic Shemshak Formation: its radiation background is higher than that of the other formations in the area (about 100-140 CPS).

The Shemshak Formation represents favourable conditions for the deposition of uranium compounds. These include a high content of plant remains and humic organic matter, extensive black carbonaceous shales, several coal seams, and a moderate permeability. Throughout the Formation, the dark carbonaceous shales with some coaly horizons show a higher radiation level. The highest gamma counts recorded from the basal shale layers of the sequence near Shahpassand are about 6-7 times the background. Similar levels were obtained at Jajarm, showing the regional

* Uranium exploration activities have started recently in Iran by the AEOI, although no work has yet been done in the Eastern Alborz region.

extension of this interval.

The principal radioelements, in order of their decreasing abundance, are potassium (K^{40}), thorium and uranium (Gabelman, 1977). The gamma radiation recorded in the survey could have been due to any of these, although especially in shales potassium is the most abundant. To clarify the matter, some of the Shemshak Formation samples were analysed by neutron activation technique for their uranium content.

7.3 Experimental

The delayed neutron technique was used to determine the uranium content of the analysed samples. This method is known to be sensitive, very rapid, non-destructive and accurate for the determination of fissionable nuclides, such as the isotopes of uranium and thorium. Sensitivities of less than 10^{-7} gram for uranium and 10^{-6} gram for thorium are attainable (Amiel, 1962). In this method the delayed neutrons emitted due to the decay of the fission products of uranium and thorium are detected, shortly after fission has been induced by exposing the samples to the intense neutron flux inside a nuclear reactor. Detailed description of the technique is given by Amiel (1962) and Gale (1967).

In this study samples were analysed in the University of London Reactor Centre as follows: One gram of each pulverised rock sample was weighed with an accuracy of 0.0001 gram in a uranium free polyethene capsule (15mm diameter, 30mm long) and then sealed. Each sample was then loaded into a pneumatic transfer tube and irradiated at the reactor core (2.3×10^{12} N/cm^2.sec thermal flux, 1.1×10^{12} N/cm^2 sec fast flux) at its full power (100 kW) for 60 seconds. A slight disturbance of the neutron flux occurs when the sample reaches the reactor core, and causes a slight decrease of about 2% in the reactor power; this was compensated by the controller in the first few seconds

and in practice does not affect the overall activation of the sample. After irradiation, the sample was automatically removed from the reactor core and dropped into a 3 - MX135 BF_3 counter unit. A 20 sec. preselected delay time was allowed when the sample came to rest in the counter unit, after which the scalers were started automatically by the timer. Counting was carried out for 60 sec. by a unit of the Harwell 2,000 series.

The background of the counting assembly varies slightly, depending on environmental conditions. A few background measurements were made at the beginning, in the middle and at the end of the working hours. The variation of background during a day was within an acceptable range of a few CPM. A pure alluminum sample was run before and after analysis to check the effect of gamma radiation on the detector. The gamma ray interference was found to be negligible. A piece of natural uranium plate (323.0 microgram) in a similar capsule to the rock samples was used for standard recording before and after running each batch of samples. The uranium content of the rock samples was calculated on the basis of the mean value of these two standards. As the samples were irradiated in a mixed neutron flux, the effect of the activity due to thorium needed to be examined. A piece of thorium plate weighing about 80 times the uranium standard specimen was used. The effect of the activity due to thorium was observed to be 86 times smaller than that of uranium. In practice, the interference due to the possible presence of thorium is negligible for rocks of the Shemshak Formation type. Three blank measurements were also recorded after each standard run and their average was used in calculations.

The formula used for calculation of the uranium content is:

$$U\ (ppm) = \frac{C_i - C_b}{C_s \times W_i} \qquad (1)$$

where:

U (ppm) = The uranium content of the sample in parts per million.

C_i = Counts per minute for sample i.
C_b = Average blank CPM.
C_s = Average CPM per microgram of standard uranium.
W_i = Weight of the analysed sample in grams.

For this study the W_i factor can be omitted as the weights of all samples were exactly 1 gram. Then:

$$U\ (ppm) = \frac{C_i - C_b}{C_s} \qquad (2)$$

C_s for each batch of samples is calculated by:

$$C_s = \frac{1}{2}\left(\frac{C_u - C_b}{W_u} + \frac{C'_u - C'_b}{W_u}\right) \qquad (3)$$

C_u = CPM of the first standard recording.
C'_u = CPM of the second standard recording.
C_b = Average blank CPM recorded with the first standard run.
C'_b = Average blank CPM recorded with the second standard run.
W_u = Weight of the standard uranium in microgram.

74 samples were analysed for their uranium content and the results are shown in Table II.7.1.

7.4 Results and Interpretation

The majority of samples analysed for their uranium content were from the Shemshak Formation, because it is probably the most favourable succession for the concentration of uranium in the region studied. The average uranium content of these sediments is 5.43 ppm in the Shahpassand area, while in the Jajarm region the average is 3.61 ppm. As discussed in previous chapter, the concentration of carbonaceous matter and plant remains is also higher in the former, which can suggest some sort of connection between the two. The delay neutron analysis showed that the basal shale interval of the Formation, both near Shahpassand and at Jajarm, has the highest concentration of uranium (59 ppm at

Table II.7.1 - The uranium content of the Shemshak Formation specimens.

Sample No.	CPM	U ppm
Shahpassand area		
122	563	2.11
124	6807	50.97
125	7839	59.05
129	961	5.23
133	702	3.20
138	1277	7.70
142	683	3.05
149	703	3.21
150	737	3.47
152	583	2.27
157	706	3.23
161	747	3.55
162	412	0.93
166	783	3.83
169	628	2.62
171	755	3.62
173	346	0.41
174	581	2.25
177	872	4.53
179	1074	6.11
184	983	5.40
191	879	4.59
196	648	2.78
197	680	3.03
203	860	4.44
207	686	3.08
208	749	3.57
212	345	0.41
213	384	0.71
218	876	4.47
220	929	4.89
222	915	4.78
224	830	4.11
228	789	3.78
232	749	3.46
233	707	3.13
236	744	3.42
238	734	3.34
242	797	3.84
245	733	3.34
249	740	3.39
251	568	2.03
253	545	1.84
254	772	3.65
256	887	4.56
257	786	3.76
259	724	3.27
260	544	1.84
261	821	4.04
262	643	2.62
265	970	5.22
271	951	5.07
276	909	4.73
282	1053	5.88
285	961	5.15
Average		5.43
Jajarm area		
325	531	1.86
326	2296	15.67
327	698	3.17
330	707	3.24
333	729	3.41
336	762	3.67
339	574	2.20
343	726	3.39
344	726	3.39
346	525	1.82
350	751	3.58
354	649	2.79
355	636	2.68
356	663	2.90
257	709	3.26
360	682	3.04
361	777	3.69
365	771	3.74
367	426	1.04
Average		3.61
Total Average		4.97

Shahpassand and 15.67 at Jajarm). It is noteworthy that the field monitoring of the gamma ray emission had shown similar results. It can therefore be concluded that the gamma ray emission of the sediments is mainly due to uranium.

Uranium content is said to increase directly with increasing percentages of carbon in many shales (McKelvey in Nininger, 1956). A plot of the uranium content versus total organic carbon of the analysed samples is shown in Figure II.7.1. As is indicated from this Figure, hardly any relationship exists between the two factors, and the concentration of uranium is generally low if compared with other uraniferous carbonaceous shales (e.g. shales of south Dakota in the United States having up to 0.2% uranium, McKelvey in Nininger, 1956). Therefore, one can conclude that, although the facies of the Shemshak Formation is favourable to the concentration of uranium, the absence of economic deposits is probably due to the lack of mobile uranium circulating in the sediments. The Shemshak Formation in the localities studied consists dominantly of terrestrial deposits transported from the south (see Chapter I.5) but, as far as is known, no fundamental source of uranium was available in the pre-Jurassic rocks or even in the pre-Cretaceous (when the Alborz Ranges started to rise), in that direction. However, even with the scarcity or possible absence of mobile uranium, the Shemshak Formation still contains traces. It is suggested that this uranium was deposited in the sediments together with the plant remains, since certain land plants are known to concentrate uranium, sometimes in sufficient quantity to be of value in prospecting for ore deposits. The relatively high concentration of uranium in the basal shale interval is presumably related to the Upper Triassic unconformity (see Chapter I.4, Stratigraphy) and its underlying soil horizon.

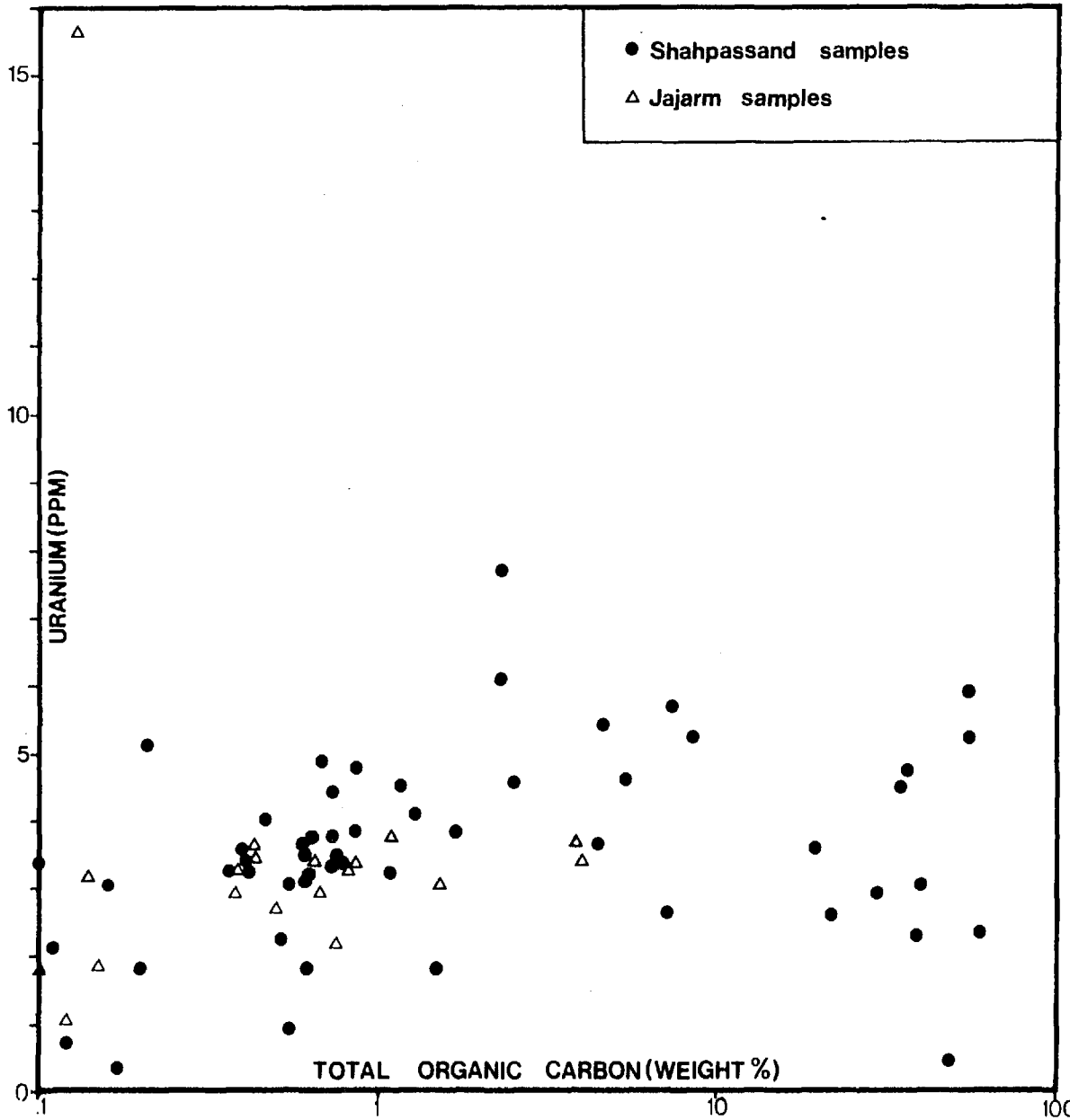


Fig. II.7.1 - Uranium content - total organic carbon (C_T) cross-plot of the Shemshak Fm. in the Eastern Alborz region.

7.5 Conclusions

The gamma radiation of the Shemshak Formation is mainly due to uranium.

Although the uranium content and the total organic carbon show hardly any relationship, some sort of connection exists between the amount of uranium and humic plant matter.

It is suggested that the uranium content of the Shemshak Formation originated from the plant remains originally deposited with the sediments.

The Upper Triassic unconformity and its associated soil deposits may have been responsible for a relatively high concentration of uranium in the basal shale interval of the Formation.

REFERENCES

Afshar-Harb, A., 1979, The stratigraphy, tectonic and petroleum geology of the Kopet Dagh region, Northern Iran: Unpub. Ph.D. thesis, Univ. London, 316 p.

Albrecht, P., Vandenbrouck, M., and Mandengue, M., 1976, Geochemical studies on the organic matter from the Douala Basin (Cameroon) - I. Evolution of the extractable organic matter and the formation of petroleum: Geochim. Cosmochim. Acta, V. 40, No. 7, p. 791-799.

Allan, J. and Douglas, A.G., 1977, Variations in the content and distribution of n-alkanes in a series of carboniferous vitrinites and sporinites of bituminous rank: Geochim. Cosmochim. Acta, V. 41, No. 9, p. 1223-1230.

Allenbach, P., 1966, Geologie und petrographie des Damavand und seiner Umgebung (Zentral-Elburz), Iran: Mitt. Geol. Inst. E.T.H, Univ. Zurich, n.s., V. 63, 144 p.

Amiel, S., 1962, Analytical applications of delayed neutron emission in fissionable elements: Analyt. Chem. V. 34, No. 13, p. 1683-1692.

Amit, O., 1978, Organochemical evaluation of Gevar'am shales (Lower Cretaceous), Israel, as possible oil source rock: A.A.P.G. Bull., V. 62, No. 5, p. 827-836.

Andreev, P.F., Bogomolov, A.I., Dobryanskii, A.F., Kartsev, A.A., 1958, Transformation of petroleum in nature (in Russian), Leningrad: Gestoptekhizdat 416 p.; Engl. transl. Int. Ser. Monogr. Earth Sci., 1968, V. 29, New York: Pergamon Press.

Andreyev, P.F. and Chumachenko, A.P., 1964, Reduction of uranium by natural organic substances: Geochem. Internat., No. 1, p. 3-7.

Assereto, R., 1966, The Jurassic Shemshak Formation in Central Elburz (Iran): Riv. Ital. Paleont., V. 72, No. 4, p. 1133-1182.

———, Barnard, P.D.W. and Fantini Sestini, N., 1968, Jurassic stratigraphy of the Central Elburz (Iran): Riv. Ital. Paleont., V. 74, No. 1, p. 3-21.

Badgley, P.C., 1959, Structural methods for the exploration geology: Harper and Brothers, Publishers, New York, 280 p.

Baker, D.R., 1962, Organic geochemistry of Cherokee Group in Southern Kansas and Northeastern Oklahoma: A.A.P.G. Bull., V. 46, p. 1621-1642.

Barker, C., 1974, Pyrolysis techniques for source rock evaluation: A.A.P.G. Bull., V. 58, No. 11, p. 2349-2361.

Barnard, P.D.W., 1967, The geology of the upper Djadjerud and Lar Valleys (North Iran): Riv. Ital. Paleont. Strat., V. 73, No. 2, p. 539-587.

Biederman, JR., E.W., 1969, Significance of High-Wax oils with respect to genesis of petroleum; commentary: A.A.P.G. Bull., V. 53, No. 7, p. 1500-1502.

Bitterli, P., 1963, Aspects of the genesis of bituminous rock sequences: Geol. en Mijnbouw, V. 42, No. 6, p. 183-201.

Blatt, H., Middleton, G., and Murray, R., 1972, Origin of sedimentary rocks: Prentice-Hall, New Jersey, 634 p.

Bowie, S.H.U., Davies, M. and Ostle, D., 1971, Uranium prospecting handbook: Inst. Min. Metal., London.

Bozorgnia, F., 1973, Paleozoic foraminiferal biostratigraphy of central and east Alborz Mountains, Iran: Nat. Iranian Oil Co., Geological Labs., Pub. No. 4.

Bray, E.E., and Evans, E.D., 1961, Distribution of n-paraffins as a clue to recognition of source beds: Geochim. Cosmochim. Acta, V. 22, No. 1, p. 2-15.

———, 1965, Hydrocarbon in non-reservoir-rock source beds: A.A.P.G. Bull., V. 49, No. 3, p. 248-257.

Berger, I.A. and Deul, M., 1959, Association of uranium with carbonaceous materials, with special reference to Temple Mountain Region: U.S. Geol. Survey Prof. Paper 320, p. 139-149.

Brooks, J. and Thusu, B., 1977, Oil-source rock identification and characterisation of the Jurassic sediments in the Northern North-Sea: Chem. Geol., V. 20, No. 4, p. 283-294.

Brooks, J., 1978, The role of geochemistry in petroleum exploration: British Nat. Oil Corp., Report No. 254/78/04 (unpub.).

Cameron, E.M. and Allan, R.J., 1973, Distribution of uranium in the crust of the northwestern Canadian Shield as shown by lake-sediment analysis: Jour. Geochem. Expl., V. 2, No. 3, p. 237-250.

Cannan, J., 1974, Time-temperature relation in oil genesis: A.A.P.G. Bull., V. 58, No. 12, p. 2516-2521.

Claypool, G.E., Love, A.H. and Maughan, E.K., 1978, Organic geochemistry, incipient metamorphism, and oil generation in Black Shale Member of Phosphoria Formation, Western Interior United States: A.A.P.G. Bull., V. 62, No. 1, p. 98-120.

Claypool, G.E. and Reed, P.R., 1976, Thermal-analysis technique for source-rock evaluation; Quantitative estimate of organic richness and effects of lithologic variation: A.A.P.G. Bull., V. 60, No. 4, p. 608-626.

Combaz, A., 1971, Thermal degradation of sporopollenin and genesis of hydrocarbons, in: Sporopollenin, J.Brooks, P.R. Grant, M.D. Muir, P. Van Gijzel and G. Shaw Eds., p. 621-653.

Correia, M., 1971, Diagenesis of sporopollenin and other comparable organic substances; application to hydrocarbon research, in: Sporopollenin, J. Brooks, P.R. Grant, M.D. Muir, P. Van Gijzel and G. Shaw Eds., p. 569-620.

Crimes, T.P., 1970, The significance of trace fossils in sedimentology, stratigraphy and palaeoecology with examples from Lower Palaeozoic strata in: Trace fossils, T.P. Crimes and J.C. Harper Eds.; Geol. Jour. Spec. Issue, No. 3, p. 101-126.

Dark, W.A., McFadden, W.H. and Bradford, D.L., 1977, Fractionation of coal liquids by HPLC with structural characterisation by LC-MS: Jour. of Chromat. Sci., V. 15, No. 10 p. 454-460.

Davies, R.A., 1978, A petroleum source rock study of a Kimmeridgian section in Dorsetshire, England: Unpub. Ph.D. thesis, Univ. London, 419 p.

Davies, R.G., Jones, C.R., Hamzepour, B. and Clark, G.C., 1972, Geology of the Masuleh Sheet, 1:100,000, Northwest Iran: Geol. Survey of Iran, Rept. No. 24, 110 p.

Degens, E.T. and Reuter, H.J., 1962, Analytical techniques in the field of organic geochemistry in: Advance in Organic Geochemistry, 1964, U. Colombo and G.D. Hobs Eds., p. 377-402.

Demaison, G.J. and Shibaoka, M., 1975, Contribution of the study of hydrocarbon generation from hydrogen-poor kerogen: 9th World Pet. Congr. Proc., V. 2, Geol., p. 195-197.

Dott, R.H. and Reynolds, M.J., 1969, Sourcebook for petroleum geology: A.A.P.G. Memoir 5.

Douglas, A.G. and Henderson, W., 1972, Some aspects of gas chromatography applied to geology in: Gas Chromatography Proc. Intern. Symp., 1971, V. 9, p. 247-260.

Dow, W.G., 1978, Petroleum source beds on continental slope and rises: A.A.P.G. Bull., V. 62, No. 9, p. 1584-1606.

———, 1977, Kerogen studies and geological interpretations: Jour. Geochem. Expl., V. 7, No. 2, p. 79-99.

Dunton, M.L. and Hunt, J.M., 1962, Distribution of low molecular-weight hydrocarbons in recent and ancient sediments: A.A.P.G. Bull., V. 46, No. 12, p. 2246-2248.

Durand, B. and Espitalié, J., 1976, Geochemical studies on the organic matter from the Douala Basin (Cameroon) - II. Evolution of kerogen: Geochim. Cosmochim. Acta, V. 40, No. 7, p. 801-808.

Eisma, E. and Jurg, J.W., 1967, Fundamental aspects of the diagenesis of organic matter and the formation of hydrocarbons: 7th World Pet. Congr. Proc., V. 2, p. 61-72.

Erdman, J.G., 1975, Relations controlling oil and gas generation in sedimentary basins: 9th World Pet. Congr. Proc., V. 2, p. 139-148.

Espitalié, J., Laporte, J.L., Madec, M., Marquis, F., Leplat, P., Paulet, J., Boutefeu, A., 1978, Rapid method for source rock characterisation and for evaluating their petroleum potential and their degree of evolution: Inst. Fr. Pét., LABOFINA S.A., Ref. 26447, 33 p.

Espitalié, J., Madec, M., Tissot, B., Mennig, J.J., Laplat, P., 1977, Source rock charactersation method for petroleum exploration: Offshore Tech. Conf. 2935, p. 439-442.

Ettre, L.S. and McFadden, W.H., 1969, Ancilary techniques of gas chromatography: Wiley-Interscience, 395 p.

Falcon, N.L., 1974, Southern Iran; Zagros Mountains in Mesozoic-Cenozoic orogenic belts, data for orogenic studies: Geol. Soc. London Spec. Pub. No. 4, p. 199-211.

———, 1967, The geology of the north-east margin of the Arabian basement shield: Advan. Sci., Sept. 1967, p. 31-42.

Fantini Sestini, N., 1966, Upper Liassic molluscs from Shemshak Formation: Riv. Ital. Paleont. Strat., V. 72, No. 3, p. 795-854.

Frankenberg, D. and Giles, R.T., 1970, Acid treatment of organic materials and the removal of calcium carbonate: Jour. Sed. Pet., V. 40, No. 3, p. 1046-1048.

Fuller, J.G.C.M., 1975, Jurassic source-rock potential and hydrocarbon correlation, North Sea in: Jurassic Northern North Sea symposium, 1975, K.G. Finsta and R.C. Selley, Eds., p. JNNSS/11/1-18.

Fuloria, R.C., 1967, Source rocks and criteria for their recognition: A.A.P.G. Bull., V. 51, No. 6, p. 842-848.

Gabelman, J.W., 1977, Migration of uranium and thorium-exploration significance: A.A.P.G. Studies in Geology, No. 3.

———, 1976, Expectation from uranium exploration: A.A.P.G. Bull., V. 60, No. 11, p. 1993-2004.

Gale, N.H., 1967, Development of delayed neutron technique as rapid and precise method for determination of uranium and thorium at trace levels in rocks and minerals, with applications to isotope geochronology in: Radioactive dating and methods of low-level counting (Vienna), I.A.E.A., p. 431-452.

Gansser, A., 1969, The large earthquakes of Iran and their geological frame: Eclogae. Geol. Helv., V. 62/2, p. 443-466.

———, 1955, New aspects of the geology in Central Iran: 4th World Pet. Congr. Proc., Rome, Sec. I/A/5, paper 2, p. 279-300.

——— and Huber, H., 1962, Geological observation in the Central Elburz, Iran: Schwei. Mine. Petr. Mitt., V. 42, No. 2, p. 583-630.

Gill, W.D., 1978, Petroleum source rock and the origin of oil and gas in Iran, Pakistan and the North Sea: Iranian Pet. Inst. Bull., No. 69, Tehran, Iran.

———, 1962, Geology in the search for oil: Inaugural lecture in I.C., London Univ., p. 129-142.

———, 1953, Construction of geological sections of folds with steep limb athenuation: A.A.P.G. Bull., V. 37, p. 2389-2406.

Giraud, A., 1970, Application of pyrolysis and gas chromatography to geochemical characterisation of kerogen in sedimentary rocks: A.A.P.G. Bull., V. 54, No. 3, p. 439-455.

Gransch, J.A., Eisma, E., 1966, Characterisation of the insoluble organic matter of sediments by pyrolysis in: Advances in organic geochemistry, 1970, G.D. Hobson and G.C. Speers, Eds., 3rd Int. Congr. Proc., Oxford: Pengamon Press, p. 407-426.

Gray, J. and Boucot, A.J., 1975, Colour changes in pollen and spores; A Review: Geol. Soc. Am. Bull., V. 86, p. 1019-1033.

Guiochon, G. and Pommier, C., 1973, Gas chromatography in inorganics and organometallics: Ann. Arbor. Science Publishers Inc., 332 p.

Gutjahr, C.C.M., 1966, Carbonsiation measurements of pollen grains and spores and their application: L. Geol. Med., V. 38, p. 1-29.

Haji-Vassiliou, A. and Kerr, P.F., 1973, Analytic data on nature of urano-organic deposits: A.A.P.G. Bull., V. 57, No. 7, p. 1291-1296.

Harwood, R.J., 1977, Oil and gas generation by laboratory pyrolysis of kerogen: A.A.P.G. Bull., V. 61, No. 12, p. 2082-2102.

Heckel, P.H., 1972, Recognition of ancient shallow marine environments: Soc. Econ. Palaeont. Miner., Spec. Pub., No. 16, Tulsa, p. 226-286.

Hedberg, H.D., 1968, Significance of High-Wax oils with respect to genesis of petroleum: A.A.P.G. Bull., V. 52, No. 5, p. 736-750.

———, 1967, Geologic controls on petroleum genesis: 7th World Pet. Congr. Proc., V. 2, p. 3-11.

———, 1964, Geologic aspects of origin of petroleum: A.A.P.G. Bull., V. 48, No. 11, p. 1755- 1803.

Hobson, G.D. and Tiratsoo, E.N., 1975, Introduction to petroleum geology: Beaconsfield, Scientific Press, 300 p.

Hobson, G.D., 1959, Some fundamentals of petroleum geology: Oxford University Press, London-New york-Toronto.

Hood, A., Gutjahr, C.C.M. and Heacock, R.L., 1975, Organic metamorphism and the generation of petroleum: A.A.P.G. Bull., V. 59, No. 6, p. 986-996.

Huckriede, R., Kürsten, M. and Venzlaff, H., 1962, Zur geologie des gebietes zwischen Kerman und Sagand (Iran): Geol. Jahrb., Beihft., V. 51, p. 197.

Hunt, J.M., 1977, Distribution of carbon as hydrocarbon and asphaltic compounds in sedimentary rocks: A.A.P.G. Bull., V. 61, No. 1, p. 100-104.

———, 1975, Geochemistry of petroleum: A.A.P.G. Continuing Education Lecture Series, A.A.P.G. Spec. Pub.

——— and Jamieson, G.W., 1956, Oil and organic matter in source rocks of petroleum: A.A.P.G. Bull., V. 40, No. 3, p. 477-488.

Ishiwatari, R., Ishiwatari, M., Kaplan, I.R. and Rohrback, B.G., 1976, Thermal alteration of young kerogen in relation to petroleum genesis: Nature, V. 264, p. 347-349.

———, ———, Rohrback, B.G. and Kaplan, I.R., 1977, Thermal alteration experiments on organic matter from recent marine sediments in relation to petroleum genesis: Geochim. Cosmochim. Acta, V. 41, No. 6, p. 815-828.

———, Rohrback, B.G. and Kaplan, I.R., 1978, Hydrocarbon generation by thermal alteration of kerogen from different sediments: A.A.P.G. Bull., V. 62, No. 4, p. 687-692.

James, G.A. and Wynd, J.G., 1965, Stratigraphic nomencature of Iranian Oil Consortium Agreement area: A.A.P.G. Bull., V. 49, No. 12, p. 2182-2245.

Kaiser, R., 1963, Gas phase chromatography: English translation of chromatographie in der gasphase by P.H. Scott, V. III.

Kartsev, A.A., Vassoevich, N.B., Geodekian, A.A., Neruchev, S.G. and Sokolov, V.A., 1971, The principal stage in the formation of petroleum: 8th World Pet. Congr. Proc., V. 2, p. 3-11.

Koons, C.B., Jamieson, G.W. and Ciereszko, L.S., 1965, Normal alkane distributions in marine organisms; possible significance to petroleum origin: A.A.P.G. Bull., V. 49, No. 3, p. 301-316.

Krevelen, D.W. Van, 1961, Coal: Amsterdam; Elsvier.

Laplante, R.E., 1974, Hydrocarbon generation in Gulf Coast Tertiary sediments: A.A.P.G. Bull., V. 58, No. 7, p. 1281-1289.

Larter, S. and Douglas, A.G., 1977, Low-molecular-weight aromatic hydrocarbons in coal maceral pyrolysates as indicators of diagenesis and organic matter type in: Environmental biochemistry and geomicrobiology, W.E. Krumbien, Ed., V. 1, Chapt. 30, p. 373-386.

Lijmbach, G.W.M., 1975, On the origin of petroleum: 9th World Pet. Congr. Proc., V. 2, p. 357-369.

Littlewood, A.B., 1970, Gas chromatography, 2nd ed: Academic Press, 546 p.

Lorenz, C., 1964, Die geologie des oberden Karadj-Tales (Zentral-Elburz), Iran: Zurich Univ. Thesis, 113 p. (in German with English abs.).

Madani, M., 1977, A study of the sedimentology, stratigraphy and regional geology of the Jurassic rocks of Eastern Kopet Dagh, N.E.Iran: Unpub. Ph.D. thesis, London Univ., 246 p.

Moore, G.W., 1954, Extraction of uranium from aqueous solution by coal and some other materials: Econ. Geol., V. 49, No. 6, p. 652-658.

McInnes, W., Dowling, D.B. and Leach, W.W. (Eds.), 1913, The coal resources of the world: Morang and Co., Limited, Toronto, Canada, 3 volumes, 1266 p.

McIver, R.D., 1967, Composition of kerogen-clue to its role in the origin of petroleum: 7the World Pet. Congr. Proc., V. 2, p. 25-36.

National Geographical Institude of Iran, Topographic maps of Gorgan, Mayamey and Gonbad: Serial No.s K.551, Sheets NJ 40-13 and NJ 40-14.

National Iranian Oil Company; Exploration and Production Affairs, (1978): Geological Maps and Sections of Iran.

Nininger, R.D., 1956, Exploration for nuclear raw materials: McMillan and Co. Limited, 293 p.

Peters, K.E., Ishiwatari, R. and Kaplan, I.R., 1977, Colour of kerogen as index of organic maturity: A.A.P.G. Bull., V. 61, No. 4, p. 504-510.

Pettijhon, F.J. and Potter, P.E., 1964, Atlas and glossary of primary sedimentary structures: Springer-Verlag, New York, 370 p.

———, ——— and Siever, R., 1972, Sand and sandstone: Springer-Verlag, Berlin. Heidelberg. New York, 618 p.

Phillippi, G.T., 1977, Proteins as a possible source material of low molecular weight petroleum hydrocarbons: Geochim. Cosmochim. Acta, V. 41, No. 8, p. 1083-1086.

———, 1974, The influence of marine and terrestrial source material on the composition of petroleum: Geochim. Cosmochim. Acta, V. 38, No. 6, p. 947-966.

———, 1965, On the depth, time and mechanism of petroleum generation: Geochim. Cosmochim. Acta, V. 29, No. 9, p. 1021-1049.

Powell, T.G., 1978, An assessment of the hydrocarbon source rock potential of the Canadian Arctic Islands: Geol. Surv. Can., paper 78-12.

———, Douglas, A.G. and Allan, J., 1976, Variations in the type and distribution of organic matter in some Carboniferous sediments from Northern England: Chem. Geol., V. 18, No. 2, p. 137-148.

———, and McKirdy, D.M., 1973, Relationship between ratio of pristane to phytane, crude oil composition and geological environment in Australia: Nature Phys. Sci., V. 243, No. 123, p. 37-39.

———, 1975, Geochemical studies related to the occurrence of oil and gas in the Dampier sub-basin, Western Australia: Jour. Geochem. Expl., V. 4, No. 4, p. 441-466.

Potter, P.E. and Pettijohn, F.J., 1963, Paleocurrents and basin analysis: Springer-Verlag, Berlin. Gottingen. Heidelberg, 296 p.

Purcell, L.P., Rashid, M.A. and Hardy, I.A., 1979, Geochemical characteristics of sedimentary rocks in Scotian basin: A.A.P.G. Bull., V. 63, No. 1, p. 87-105.

Rainwater, E.H., 1963, The environmental control of oil and gas occurrence in terrigenous clastic rocks: Gulf Coast Assoc. Geol. Soc. Trans., V. 13, p. 79-94.

Rashid, M.A., 1979, Pristane-phytane ratios in relation to source and diagenesis of ancient sediments from the Labrador Shelf: Chem. Geol., V. 25, No. 1/2, p. 109-122.

Reed, K.J., 1969, Environment of deposition of source beds of High-Wax oil: A.A.P.G. Bull., V. 53, No. 7, p. 1502-1506.

Reineck, H.E. and Singh, I.B., 1973, Depositional sedimentary environments with reference to terrigenous clastics: Springer-Verlag, Berlin. Heidelberg. New York.

Ronov, A.B., 1958, Organic carbon in sedimentary rocks in relation to presence of petroleum: Translation in Geochem. No. 5, p. 510-536.

Scalan, R.S. and Smith, J.E., 1970, An improved measure of the odd-even predominance in the normal alkanes of sediment extracts and petroleum: Geochim. Cosmochim. Acta, V. 34, p. 611-620.

Seilacher, A., 1964, Biogenic sedimentary structures in: Approaches to paleoecology, J. Imbrie and N. Newell, Eds: John Wieley and Sons, Inc., New York, p. 296-316.

Selley, R.C., 1976, An introduction to sedimentalogy: Academic Press, London, 408 p.

———, 1970, Ancient sedimentary environments: Chapman and Hall, London, 237 p.

Şengör, A.M.C., 1979, Mid-Mesozoic closure of Premo-Triassic Tethys and its implications: Nature, V. 279, P. 590-593.

Seyed-Emami, K., 1967, Zur ammoniten-fauna und stratigraphie der Badamu-Kalke bei Kerman, Iran: Inaugural Dissertation, Munich.

Shibaoka, M., Saxby, J.D. and Taylor, G.H., 1978, Hydrocarbon generation in Gippsland basin, Australia-Comparison with Cooper basin, Australia: A.A.P.G. Bull., V. 62, No. 7, p. 1151-1158.

Shirley, M.L. and Ragsdale, J.A., 1966, Deltas in their geologic framework: Houston Geol. Soc., 251 p.

Staplin, F.L., 1969, Sedimentary organic matter, organic metamorphism and oil and gas occurrence: Can. Pet. Geol. Bull., V. 17, p. 47-66.

Steiger, R., 1966, Die geologie der West-Firuzkuh-area , (ZentralElburz/Iran): Mitt. Geol. Inst. E.T.H., Univ. Zurich, n.s., V. 68, 145 p.

Stevens, N.P., 1956, Origin of petroleum - A review: A.A.P.G. Bull., V. 40, No. 1, p. 51-61.

Stöcklin, J., 1974, Northern Iran; Alborz Mountains. in: Mesozoic-Cenozoic orogenic belts, data for orogenic studies: Geol. Soc. London Spec. Pub., No. 4, p. 213-234.

———, 1974, Possible ancient continental margins in Iran. in: The geology of continetal margins, 1974, C.A. Burk and C.L. Drake, Eds., p. 873-887.

———, 1971, Stratigraphic lexicon of Iran, Part 1 - Central, North and East Iran: Geol. Surv. Iran, Report No. 18, 338 p.

———, 1968, Structural history and tectonics of Iran; A Review: A.A.P.G. Bull., V. 52, No. 7, p. 1229-1258.

Stock, R. and Rice, C.B.F., 1974, Chromatographic methods, 3rd ed: Chapman and Hall and Science Paperbacks, 383 p.

Stoneley, R., 1974, Evolution of the continental margins bounding a former southern Tethys, in: The geology of continental margins, 1974, C.A. Burk and C.L. Drake, Eds., p. 889-903.

———, 1969, Sedimentary thicknesses in orogenic belts, in: Time and place in orogeny, P.E. Kent, G.E. Satterthwaite, A.M. Spencer, Eds: Geol. Soc. London, Spec. Pub. No. 3, p. 215-238.

Strakhov, N.M., 1962, Principles of lithogenesis. Moscow: Izdat. Akad. Nauk SSSR (in Russian), Transl. Consult. Bur. and Edinburgh and London: Oliver and Boyd, I, 1967; II, 1969.

Süssli, P.E., 1976, The geology of the Lower Haraz Valley area, Central Alborz (Iran): Geol. Surv. Iran, Report No. 38.

Takin, M., 1972, Iranian geology and continental drift in the Middle East: Nature, V. 235, No. 5334, p. 147-150.

Tchalenko, J.S., Ambraseys, N.N., Berberian, M., Iranmanesh, M.H., Mohajer-Ashjai, A., Bailly, M. and Arsovsky, M., 1974, Materials for the study of seismotectonics of Iran: Geol. Surv. Iran, Report No. 29, p. 127-138.

Tissot, B.P., Durand, B., Espitalié, J. and Combaz, A., 1974, Influence of nature of organic matter in formation of petroleum: A.A.P.G. Bull., V. 58, No. 3, p. 499-506.

——— and Welte, D.H., 1978, Petroleum formation and occurrence-A new approach to oil and gas exploration: Springer-Verlag, Berlin. Heidelberg. New York, 538 p.

Twenhofel, W.H. and Tyler, S.A., 1941, Methods of study of sediments: McGraw-Hill Book Company Inc., New York, 183 p.

Vandenbroucke, M., Albrecht, P. and Durand, B., 1976, Geochemical studies on the organic matter from the Douala basin (Cameroon)-III, comparison with the Early Toarcian shales, Paris basin, France: Geochim. Cosmochim. Acta, V. 40, No. 10, p. 1241-1249.

Vassoyevich, N.B., Korchagina, Yu.I., Lopatin, N.V. and Chernyshev, V.V., 1969, Principal phase of oil formation: Vestnik Mosk. Univ. No. 6, p. 3-27, English translation in Int. Geol. Rev., 1970, V. 12, No. 11, p. 1276-1296.

Waples, D.W., 1979, Simple method for oil source bed evaluation: A.A.P.G. Bull., V. 63, No. 2, p. 239-244.

PERSONAL COMMUNICATIONS

Afshar-Harb, A., Chief Geologist of Nat. Iranian Oil Co: Geological Div., N.I.O.C., P.O. Box 1516, Tehran, Iran.

Donovan, D.T., Professor of Geology: Univ. Coll., London Univ., London, England.

Gill, W.D., Emeritus professor of Petroleum Geology and consultant: Imp. Coll., London Univ., London, England.

Kinghorn, R.R.F., Lecturer of Petroleum Geology: Imp. Coll., London Univ., London, England.

Micropalaeontology Section, Univ. Coll., London Univ., London, England.

Selley, R.C., Reader of Petroleum Geology and consultant: Imp. Coll., London Univ., London, England.

Solli, H., Post-Doc. research, Organic Geochemictry Section, Univ. Newcastle-Upon-Tyne, Newcastle, England.

Stoneley, R., Professor of Petroleum Geology: Imp. Coll., London Univ., London, England.

FOSSILS LOCALITY

Locality	Section	Fossils collected
λ_1	Qoznavi Section (Fig. I.4.3)	Fig. I.5.10 D
λ_2	"	Fig. I.5.10 A,B and C
λ_3	"	Fig. I.5.11 D,F,H,I and L Fig. I.4.11 A and B
λ_4	"	Fig. I.5.11 A,B and G
λ_5	"	Fig. I.5.11 C,E and J
λ_6	"	Fig. I.4.1 A,B, and C
λ_7	Rudbar Section (Fig. I.4.4)	Fig. I.5.11 M
λ_8	"	Fig. I.5.11 N
λ_9	Nargess-Chall Section (Geological Map A)	Fig. I.5.11 O
λ_{10}	"	Fig. I.5.11 R
λ_{11}	"	Fig. I.5.11 P and Q
λ_{12}	Jajarm Section (Fig. I.4.5)	Fig. I.5.13 G
λ_{13}	"	Fig. I.5.13 C and F
λ_{14}	"	Fig. I.5.14 D
λ_{15}	"	Fig. I.5.13 A and B
λ_{16}	"	Fig. I.5.12 A,B,C and D Fig. I.5.13 E

KEY TO STRATIGRAPHIC COLUMNS DESCRIPTION

Lst: limestone
Sh: shale
Sst: sandstone
Stst: siltstone
Mudst: mudstone
ironst: ironstone
cgl: conglomerate
cglc: conglomeratic
microcgl: microconglomerate
gr: grey
gn: green
br: brown
bk: black
d.: dark
l.: light
vf: very fine
f: fine
m: medium
c: coarse
g: grained
argill: argillaceous
calc: calcareous
sl.calc: slightly calcareous
ferr: ferruginous
mica: micaceous
lam: laminated
cem: cemented
carb: carbonaceous
foss: fossiliferous
mass: massive
med bdd: medium bedded
thin bdd: thin bedded
org rich: organic rich
x bd: cross bedding
gd bd: graded bedding
current bd: current bedding
S to N: south to north
rdd: rounded
i.o.nods: iron oxide nodules
diam: diameter
concr: concretion
mod: moderate
@: porosity

FIGURE 2.4.4

STRATIGRAPHIC COLUMN
OF
BOREHOLE
SECTION

Scale 1:10,000

LOCATION MAP

Scale 1:50,000

F4.M3

DESCRIPTION

PALAEONTOLOGY

TRIASSIC

JURASSIC

ALTERNATING SHALE & SANDSTONE

LOWER SANDSTONE

CHANNEL SAND

COMPLEX

SHALE

SANDSTONE

CENTRAL ALBORZ
(After Assereto, 1966)

EASTERN ALBORZ

Rudbar

Qoznavi

Type-section

Jajarm

200m
100
0

FORMATION
SHEMSHAK
1
2
3
4
5
6
ELIKAH FM

sandstone
calcareous sandstone
shale
siltstone, mudstone
marl
chalk
conglomerate
orthoquartzite
limestone
qoquina limestone
ironstone
covered

iron oxide nodules
haematite balls
chert
concretion
plant fossils
Trunks, branches & other plant remains

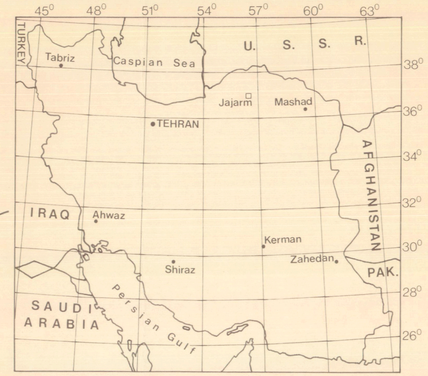
C carbonaceous matter
ammonites
belemnites
lamelli
gastropods
corals
U burrows
worm tracks
foraminiferas
cross bedding
channels
graded bedding
ripple marks
scour and fill structure
load cast
lamination
cone in cone structure

FIG. I.4.6 Lithostratigraphic correlation chart of the Shemshak Formation in the Eastern and Central Alborz.

Geological Map 'B'
JAJARM AREA

Scale 1 : 50,000

0 1 2 3 4 5 Km.



- Q — Alluvium
- Q — Alluvial fan, gravel fan
- QL — Loess
- J-K — Upper Jurassic-Cretaceous — Chaman Bid-Mozduran Fms.
- Jb — Middle Jurassic — Bashkalateh Fm.
- Js — Lower-Middle Jurassic — Shemshak Fm.
- Tr — Triassic — Elika Fm.
- P — Permian
- Pz — Palaeozoic
- Major fault
- Minor fault
- Anticlinal axis
- Synclinal axis
- Dip: Steep, Medium, Gentle, Horizontal
- Formation boundary
- Formation and alluvium boundary
- Main road
- Minor road
- Drainage
- Qanat system
- Town, village
- Section
- Centre of aerial photograph
- Farmland

Photogeological interpretation of Palaeozoic rocks confirmed by field checking by the author and Dr. A. Afshar Harb.

F.K.Rad, 1979

FIGURE 2.4.3

STRATIGRAPHIC COLUMN OF OOZNAVI SECTION

LOCATION MAP

Scale 1:1,000

Scale 1:50,000

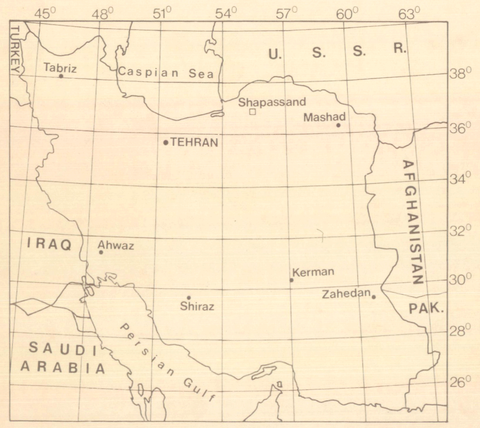
P.F. No.

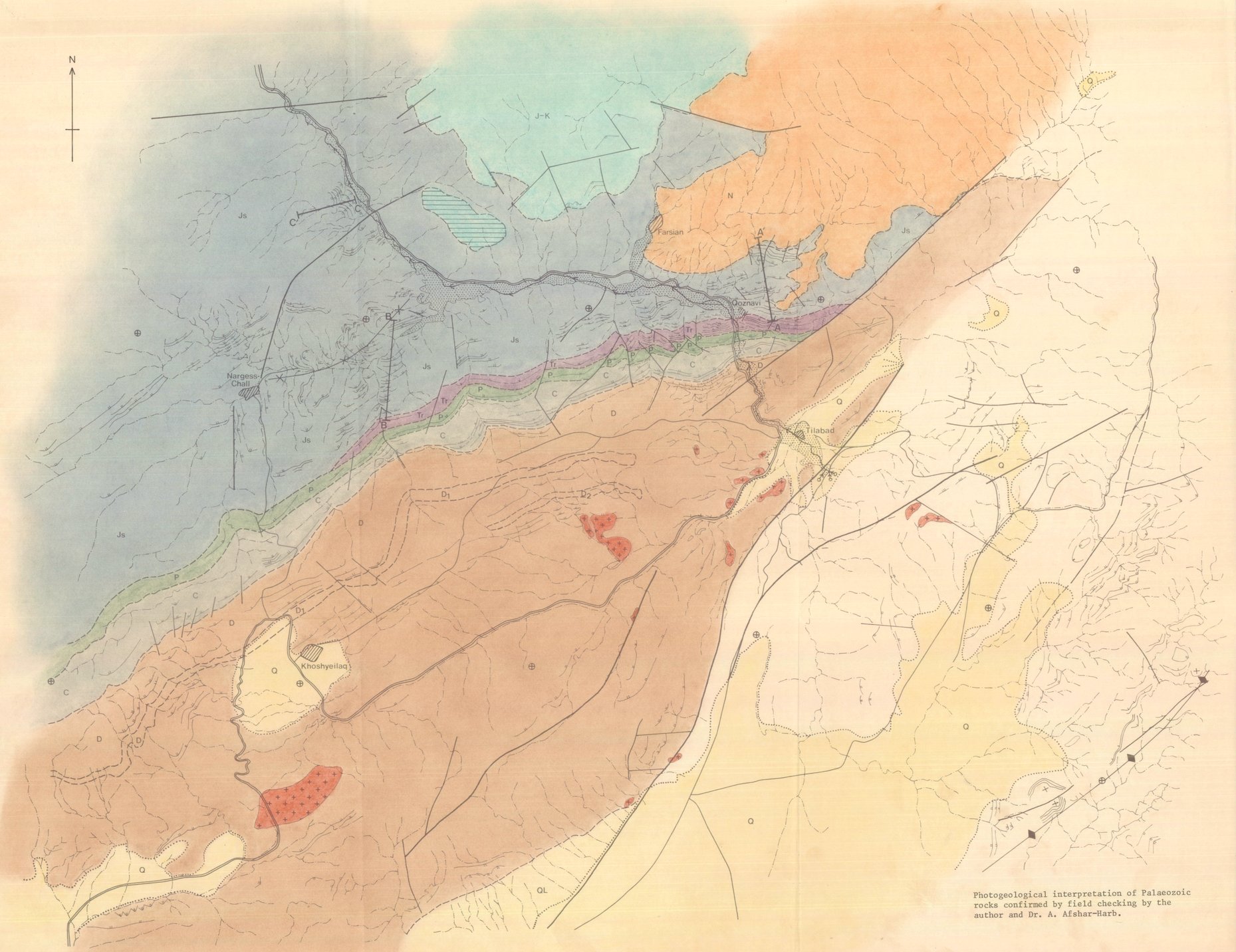
| | | |

Geological Map 'A'
SHAHPASSAND AREA

Scale 1 : 50,000

0 1 2 3 4 5 Km.





Photogeological interpretation of Palaeozoic rocks confirmed by field checking by the author and Dr. A. Afshar-Harb.

- Q — Alluvium
- Q — Alluvial fan, gravel fan
- QL — Loess
- N — Neogene
- J-K — Jurassic–Cretaceous (Dalichai Lar Fms.)
- Js — Lower-Middle Jurassic (Shemshak Fm.)
- Tr — Triassic (Elika Fm.)
- P — Permian (Dorud-Rutch Fms.)
- C — Carboniferous
- D — Devonian
- Basalt
- Major fault
- Minor fault
- Anticlinal axis
- Synclinal axis
- Dip: Steep, Medium, Gentle, Horizontal
- Landslide
- Formation boundary
- Formation and alluvium boundary
- Main road
- Minor road
- Drainage
- River
- Spring
- River bank
- Town, village
- Section
- Centre of aerial photograph

F.K.Rad, 1979

FIGURE 2.4.5

STRATIGRAPHIC COLUMN OF JAJARM SECTION

LOCATION MAP

Scale 1:50,000

Scale 1:1000

Y.K. RAO

SYSTEM	SERIES	GROUP	FORMATION	MEMBER	DESCRIPTION	PALAEONTOLOGY
TRIASSIC	ELIKAH (?N)	ALTERNATING SHALE & SANDSTONE				
JURASSIC	MIDDLE	LOWER	UPPER	CHANNEL SAND COMPLEXES	CARBONACEOUS SEQUENCE	KHANDAL	BASIN KALATEH			

